

EVALUATION OF GROUND HEAVE PREDICTION METHODS

By

GANG HUANG

**Bachelor of Science
Wuhan University of Hydraulic
and Electric Engineering
Wuhan, P.R. China
1982**

**Master of Science
Wuhan University of Hydraulic
and Electric Engineering
Wuhan, P.R. China
1984**

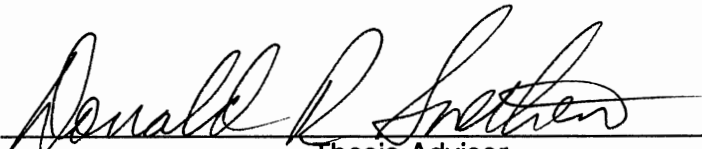
**Submitted to the Faculty of the Graduate College
of the Oklahoma State University
in partial fulfillment of the requirements
for the Degree of
DOCTOR OF PHILOSOPHY
December, 1992**

19920 H874e

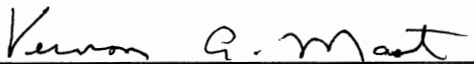
Thesis
19920
H874e

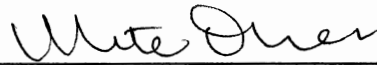
EVALUATION OF GROUND HEAVE PREDICTION METHODS

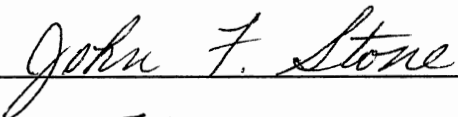
Thesis Approved:

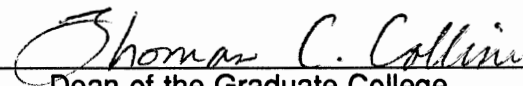


Thesis Adviser









Dean of the Graduate College

**To my wife, Fengshia,
for her encouragement and
patience during
this study**

ACKNOWLEDGMENTS

The author expresses his sincere appreciation and gratitude to Dr. D. R. Snethen, Thesis Adviser and Chairman of the Advisory Committee, for his guidance and support throughout the graduate studies.

The author is also grateful to Dr. J. F. Stone, Dr. M. Oner, and Dr. V. A. Mast, committee members, for their valuable instruction and advice during this research program.

The author extends his gratitude to the School of Civil Engineering for its financial support and assistance which made this study possible; and to the Oklahoma Department of Transportation for conducting field surveying and sampling and providing survey data which were essential to this study.

Finally, the author is indebted to Ms. Charly Fries for her assistance in editing and formatting the final manuscript.

TABLE OF CONTENTS

Chapter	Page
I. INTRODUCTION	1
1.1 General	1
1.2 Purpose and Scope of Study	2
II. LITERATURE REVIEW	3
2.1 Clay Mineralogy	3
2.2 Clay-Water Interaction	11
2.3 Soil Suction Concept	18
2.4 Soil Suction Measurement	22
2.5 Heave Prediction Methods	32
III. SITE INVESTIGATION	52
3.1 Site Description	52
3.2 Sampling	59
3.3 Initial Soil Conditions	63
3.4 Elevation Study	71
IV. MEASUREMENT OF SUCTION INDEX AND VOLUMETRIC PARAMETERS	73
4.1 Soil Suction Methods	73
4.2 Oedometer Swell Index	83
V. HEAVE PREDICTION RESULTS	87
5.1 Soil Suction Methods	87
5.2 Oedometer Swell Methods	94
VI. DISCUSSION	97
6.1 Accuracy	97
6.2 Ease of Use and Time of Application	101
6.3 Influence of Sample Size on Core Shrinkage Test	102
VII. CONCLUSIONS AND RECOMMENDATIONS	105
7.1 Conclusions	105
7.2 Recommendations	107

Chapter	Page
SELECTED REFERENCES	109
APPENDIX A - INITIAL SOIL CONDITIONS AND SOIL PROPERTIES	113
APPENDIX B - SOIL SUCTION, CLOD SHRINKAGE, AND CORE SHRINKAGE TEST RESULTS	119
APPENDIX C - ELEVATION SURVEY DATA AND SITE PLAN	178

LIST OF TABLES

Table	Page
2.1. Definitions of Suction	23
2.2. Common Laboratory Suction Measurement Methods	33
3.1. Temperature and Precipitation	57
3.2. Identification and Description of Soils	58
3.3. Characteristics of Sampling Tube	60
4.1. Suction Index for Different Soil Layers	74
4.2. Suction Index Ratio and Shrinkage Limit	80
4.3. Instability Index at Various Depths	82
4.4. Suction Compression Index	83
4.5. Constant Volume Swell Pressure and Swell Index	86
4.6. Overburden Swell Test Results	86
5.1. Physical and Engineering Properties of Soil	89
5.2. Heave Prediction Using Snethen and Johnson's Method	90
5.3. Heave Prediction Using Nelson and Hamberg's Method	92
5.4. Heave Prediction Using Mitchell's Method	93
5.5. Heave Prediction Using Mckeen's Method	94
5.6. Heave Prediction Using Fredlund's Method	96
5.7. Heave Prediction Using the Swell Method	96
6.1. Comparison of the Accuracy of the Various Prediction Methods	98
6.2. Effect of Overburden on Mitchell's Method	98

Table	Page
A.1. Initial Soil Conditions	114
A.2. Atterberg Limits	115
B.1. Suction Test Results	120
B.2. Clod and Core Shrinkage Test Results	136
C.1. Elevation of Center Line for Northbound Lane	179

LIST OF FIGURES

Figure	Page
2.1. Schematic Diagram of Tetrahedral Sheet	4
2.2. Schematic Diagram of Octahedral Sheet	5
2.3. General Categorization of Clay Minerals	6
2.4. Structure of Kaolinite	8
2.5. Structure of Montmorillonite	9
2.6. Structure of Illite	10
2.7. Location of Common Clay Minerals on Casagrande's Plasticity Chart	12
2.8. Relative Dimensions of Common Clay Minerals	13
2.9. Distribution of Ions Near Particle Surface	15
2.10. Density of Adsorbed Water	16
2.11. Soil Water System for Clay Particles	21
2.12. Placement of Filter Papers for Different Suction Measurements	25
2.13. Calibration of Filter Paper	26
2.14. A Peltier Thermocouple Psychrometer	28
2.15. Pressure Plate for High Suction Measurement	31
2.16. Soil Suction Vs. Water Content Relationship	36
2.17. Specific Volume Vs. Water Content Relationship	37
2.18. Idealized Moisture Boundary Profile	39
2.19. Representative Clod Shrinkage Curves	41
2.20. Linear Strain Vs. Moisture Content Relationship	43
2.21. Chart for γ_n Prediction	45

Figure	Page
2.22. Stress History by Drying and Wetting	47
2.23. Typical Constant Volume Oedometer Swell Test Results	49
2.24. Stress Paths Representing Swelling of Soil	51
3.1. Location of Sampling Site	53
3.2. Photographs Taken at the Site	54
3.3. General Geology of Garvin County, Oklahoma	56
3.4. Position of Six Sampling Boreholes	61
3.5. Sampling Equipment	62
3.6. Water Content Profile	65
3.7. Soil Suction Vs. Depth	67
3.8. Void Ratio Profile	69
3.9. Grain Size Distribution	70
3.10. Plasticity Chart for Identifying Mineral Types	72
4.1. Suction Vs. Water Content	75
4.2. Specific Volume Vs. Water Content	76
4.3. Clod Shrinkage Curve	78
4.4. Core Shrinkage Curve	81
4.5. Constant Volume Swell Pressure Curve	85
5.1. Initial and Final Soil Suction Profile	88
6.1. Effect of Sample Size on Ratio $\Delta\varepsilon_v/\Delta\omega$	103
6.2. Effect of Sample Size on Heave Prediction	104
A.1. Grain Size Distribution (Hole 3, 0.5-1.5 ft)	117
A.2. Grain Size Distribution (Hole 1, 5.0-5.5 ft)	118
B.1. Suction Vs. Water Content	122
B.2. Specific Volume Vs. Water Content	129

Figure	Page
B.3. Clod and Core Shrinkage Curves	138
C.1. Site Plan and Profile of Surveying Section	180

CHAPTER I

INTRODUCTION

1.1 General

Expansive soils were recognized in a previous NSF study as being one of the six most damaging natural hazards in the United States. Currently in third place behind riverine flooding and hurricane wind/storm surge damage, expansive soils will probably be surpassed by only hurricane wind/storm surge by the year 2000. Wiggins et al. (1978) indicate that mitigation studies could reduce as much as 35% of the damage associated with expansive soils. Mitigation studies refer to those studies which provide the profession with a better understanding of the problem and the factors which influence it. For example, reduction of volume change can be achieved through preconstruction treatment or adequate structural design of the foundation, both of which rely on an accurate estimate of the potential volume change.

Clay soils with a potential for shrinking or swelling are located throughout the United States, as well as many parts of the world, as evidenced by the participants in the six international conferences which have been held on the topic of expansive soils since 1969. Naturally occurring expansive soils are generally unsaturated. In a macro sense, the soils are usually shattered, i.e, fissured, with open filled joints. The soil mineralogy consists of a certain amount of montmorillonite and/or illite. The soil exhibits high strength and low compressibility in most natural conditions. When moisture content of the soil increases, volume of the soil mass increases. The driving force behind this volume change is soil moisture retention force or soil suction. Because of its greater sensitivity to volume change in comparison to moisture content, soil suction has been shown to be a more sensitive and accurate indicator of

potential swell, as well as a more reliable parameter for estimating volume change (Fredlund, 1983; Johnson and Snethen, 1978; Snethen, 1980). Soil suction is a measure of the tendency of the soil to undergo a change in moisture content and is directly related to the volume change characteristics of expansive soils. As the moisture content increases, the soil suction decreases and the soil swells. Heave prediction by soil suction test may involve the measurement of soil suction over the moisture contents in the range of shrinkage limit to plastic limit (Hamberg, 1985; Johnson and Snethen, 1978; Mitchell and Avalle, 1984).

During the last three decades, dozens of methods were developed for predicting ground heave. Based on the required input data, all heave prediction methods can be utilized in one of three approaches: soil suction approach, empirical correlation approach, and oedometer swell approach. Selection of a method may depend first on the accuracy and reliability of the method and then on simplicity of the method and importance of the project. Little work has been done to evaluate the accuracy of different prediction methods and factors most influencing these methods. Study of accuracy and reliability helps to choose a prediction method with more confidence. Many prediction methods, especially for the soil suction approach, are actually very similar. Using different testing procedures and sample dimensions, the prediction output yields quite different results. It may be necessary to specify testing procedures and sample dimensions according to extensive parametric studies.

1.2 Purpose and Scope of Study

The primary objective of this investigation was to evaluate the accuracy of six different heave prediction methods; four of them use the soil suction approach, and the others use the oedometer swell approach. The accuracy of the prediction methods was assessed based on comparisons with actual field measurements, while the ease of use and time required for testing was evaluated based on comparisons with one another. In addition, the effect of sample size for clod/core shrinkage tests on the predicted heave was studied.

CHAPTER II

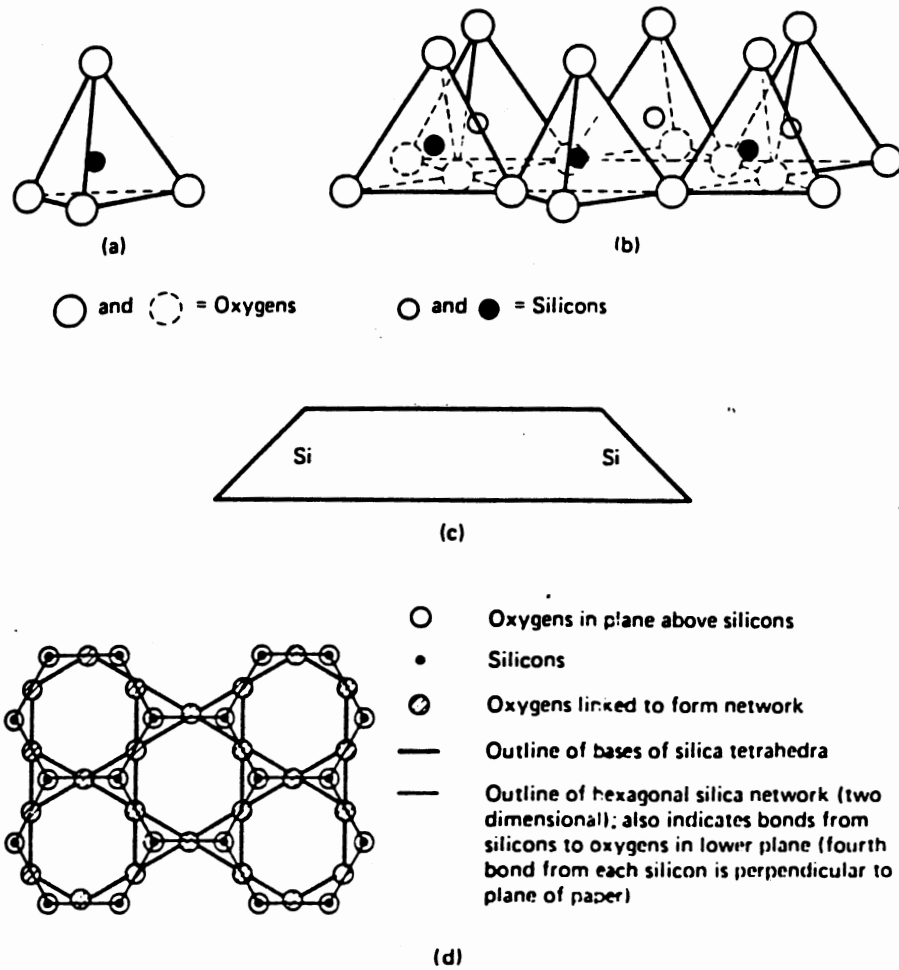
LITERATURE REVIEW

2.1 Clay Mineralogy

Natural clay soils are generally composites of different combinations of several clay minerals, such as kaolinite, illite, montmorillonite, etc. These clay minerals are tiny crystalline substances with particle sizes in the range of 10^{-6} mm to 1 μ m, and are generally referred to as colloids. Unlike sands and silts, the grain size distribution of clays has almost no influence on the engineering behavior whereas colloidal properties such as adsorption of water due to the large specific surface area of the particles dominate the performance of the clay soils (Grim, 1953; Hillel, 1980; Yong and Warkentin, 1966)

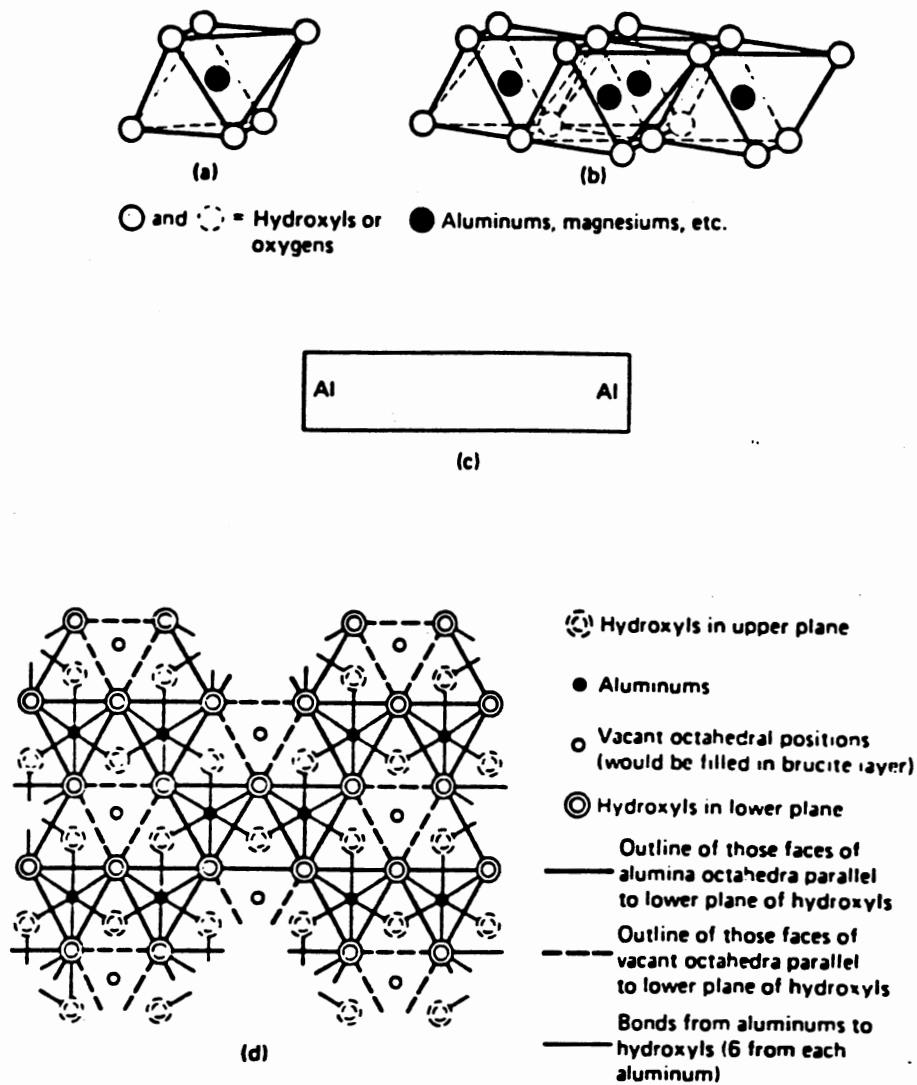
Clay minerals are formed by chemical weathering of certain rock forming minerals, i.e., decomposition of the primary minerals and their recombination into new ones. Chemically, clay minerals are hydrous alumino-silicates plus other metallic ions. Typical alumino-silicate clay minerals exist as layered microcrystals, composed of two fundamental structural units: the silicon-oxygen tetrahedron and the aluminum-oxygen or hydroxyl octahedron unit. The units are bonded together into "sheets." Stacking of these sheets, along with different bonding and different metallic ions in the crystal lattice, define the different clay minerals. Understanding the structure and function of clay minerals helps define the micro-scale mechanisms of shrink and swell behavior of expansive soils.

The silicon-oxygen tetrahedron unit (Figure 2.1) consists of a silicon cation, Si^{4+} , surrounded by four oxygen atoms which are at the corner of a tetrahedron with equal distance to the silicon cation. The oxygen atoms at the base of tetrahedron are



- (a) Single Silica Tetrahedron
 (b) Isometric View of the Tetrahedral or Silica Sheet
 (c) Schematic Representation of the Silica Sheet
 (d) Top View of the Silica Sheet

Figure 2.1. Schematic Diagram of Tetrahedral Sheet
 [Holtz and Kovacs, 1981]



- (a) Single Aluminum (or Magnesium) Octahedron
 (b) Isometric View of the Octahedral Sheet
 (c) Schematic Representation of the Aluminum (or Magnesium) Sheet
 (d) Top View of the Silica Sheet

Figure 2.2. Schematic Diagram of Octahedral Sheet
 [Holtz and Kovacs, 1981]

shared by two silicon cations of adjacent units. Such a sharing pattern results in a sheet that has hexagonal holes as shown in Figure 2.1.d.

The aluminum-oxygen/hydroxyl octahedron unit (Figure 2.2) consists of an aluminum (magnesium, iron, or other) cation, Al^{3+} , surrounded by six oxygen atoms or hydroxyls which are at the corner of an octahedron. Each oxygen or hydroxyl is shared by two aluminum (magnesium, etc.) cations. This leads to a sheet structure shown in Figure 2.2.d. Different cations in the octahedral sheet form different clay minerals. However, not all octahedrons necessarily contain a cation. When only two-thirds of the possible cation positions are filled with aluminum and all anions are hydroxyls, the mineral is called gibbsite. Minerals with only two-thirds of the octahedral positions filled are usually termed dioctahedral. When all positions are occupied by magnesium instead of aluminum, the mineral is called brucite. Minerals with all positions filled are usually termed trioctahedral. The different stacking pattern of these two basic sheets (tetrahedral and octahedral) with certain cations in the sheets and between the layers account for different clay minerals.

Depending upon the arrangement of the above mentioned basic sheets and cations present, the clay minerals are generally categorized into two main groups: structured and amorphous. The structured group can be further divided into 1:1 (two-layer) and 2:1 (three-layer) type. The 2:1 type minerals are subdivided into expanding and nonexpanding minerals (Hillel, 1980). This is shown in Figure 2.3.

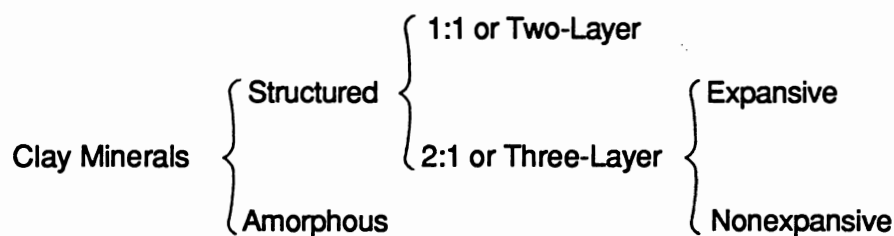
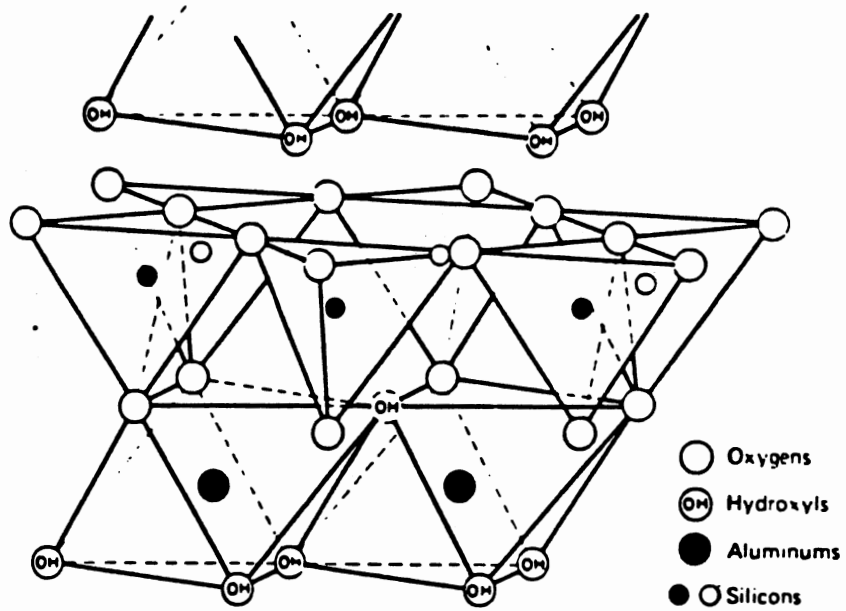


Figure 2.3. General Categorization of Clay Minerals

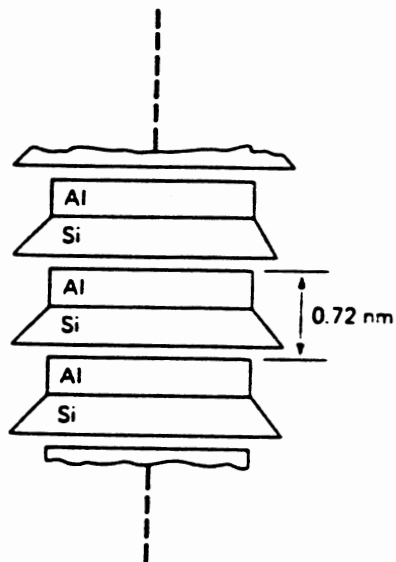
For the purpose of distinguishing expanding and nonexpanding clay minerals, it is sufficient to describe only a few common minerals found in clay soils. Among these, kaolinite, montmorillonite, and illite would be typical. Kaolinite consists of alternating layers of silica and alumina sheet (1:1 or two-layer type). The layers are held together by hydrogen bonding between hydroxyls from the alumina sheet and oxygens from the silica sheet (Figure 2.4). Such bonding is very strong, preventing water entering into the basic layers and allowing many layers to build up to make a rather large crystal. A typical kaolinite crystal may be 70 to 100 layers thick. Due to the relative large particle size and low specific surface area, i.e., total surface area of particles per unit mass, kaolinite shows less plasticity and swelling than most other clay minerals.

Montmorillonite is made of repeating layers of an alumina sheet (gibbsite) sandwiched by two silica sheets (2:1 or three-layer type). Since the bonding between the silica sheets is weak and isomorphous, substitution of aluminum with magnesium or iron in the octahedral sheet occurs, and water and exchangeable ions enter easily between layers (Figure 2.5), pushing the layers farther apart. As a result, the specific surface increases several times. Because of the extremely small particle sizes and unbalanced charge in the octahedral sheet, montmorillonite shows a distinctive swelling/ shrinking behavior. Upon wetting, montmorillonite clays may swell several times its dry volume and when dried they tend to shrink and crack. Usually, such dry soils are very hard.

Illite is also a 2:1 type (three-layer) mineral with repeating layers of an alumina sheet in the middle and silica sheet at both top and bottom, very similar to montmorillonite; but the layers are bonded together with potassium cations (Figure 2.6). The potassium cations are almost exactly fitted into the hexagonal hole (formed by the silica tetrahedral sheets) due to the relatively high density negative charges induced from isomorphous substitution of aluminum ions for silicon ions in the tetrahedral sheets. Such a tight bonding between layers prevents the expansion of

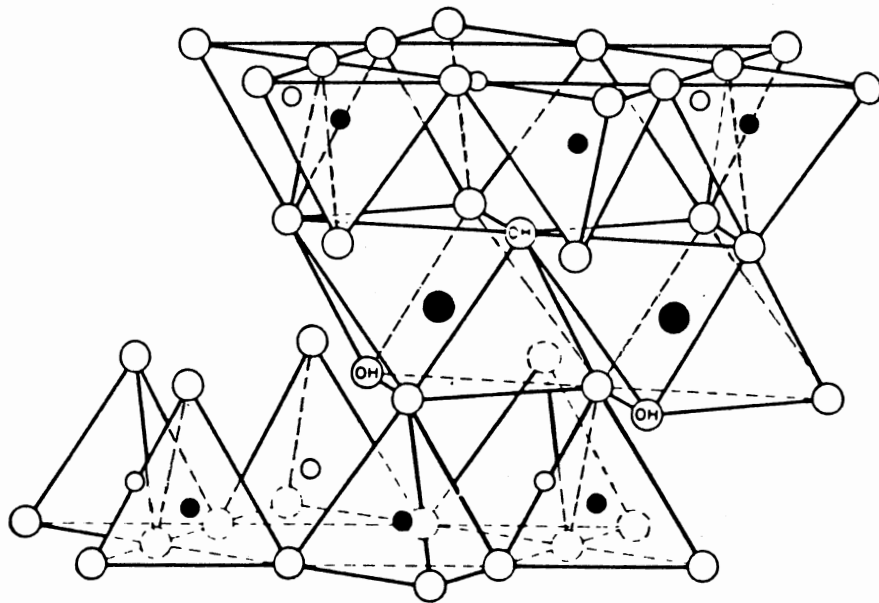


(a) Atomic Structure of Kaolinite [Grim, 1959]

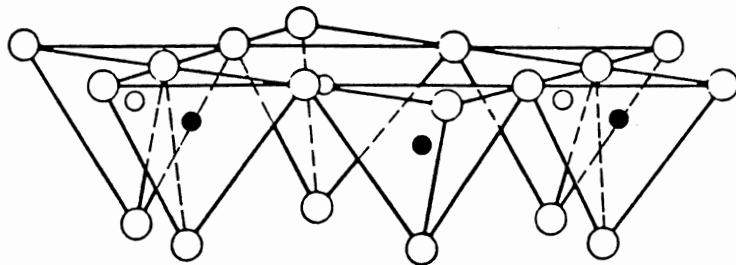


(b) Symbolic Structure of Kaolinite [Lambe, 1953]

Figure 2.4. Structure of Kaolinite

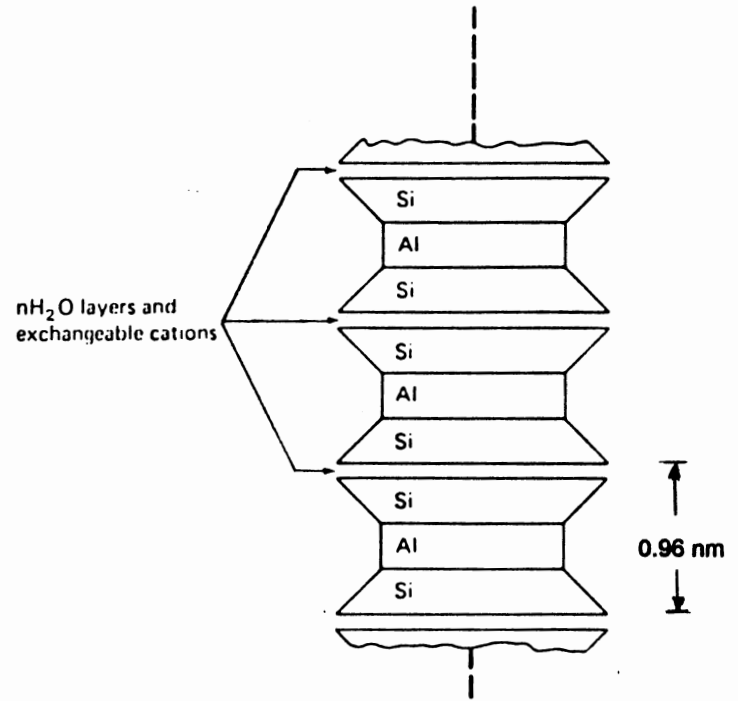


nH₂O layers and exchangeable cations



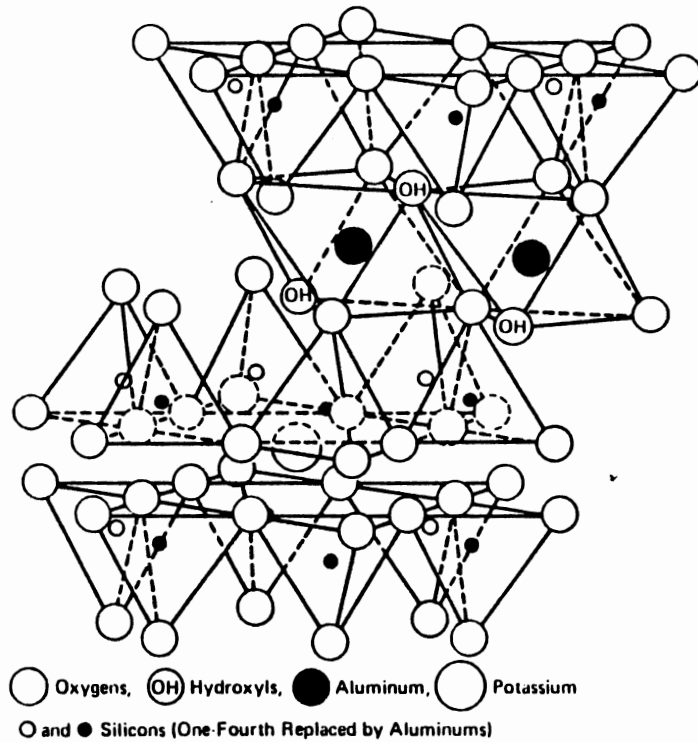
- Oxygens ○ OH Hydroxyls ● Aluminum, iron, magnesium
- and ● Silicon, occasionally aluminum

(a) Atomic Structure [Grim, 1959]

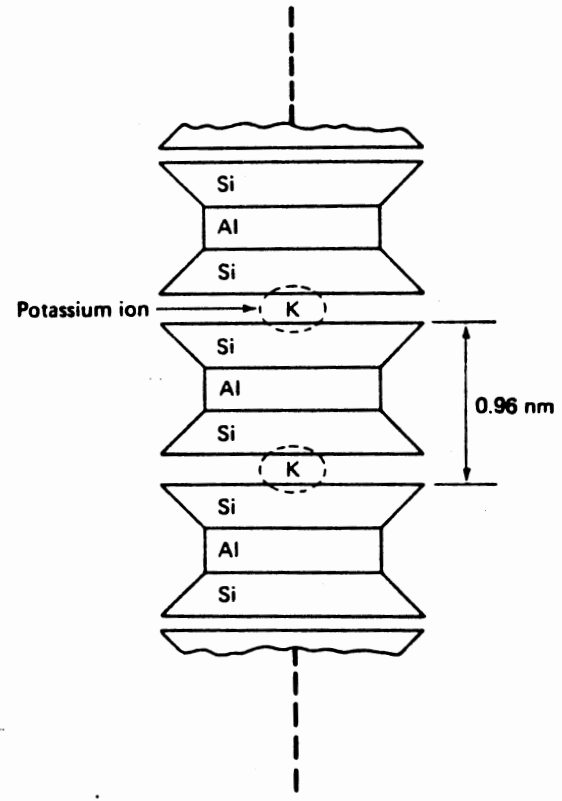


(b) Symbolic Structure [Lambe, 1953]

Figure 2.5. Structure of Montmorillonite



(a) Atomic Structure [Grim, 1959]



(b) Symbolic Structure [Lambe, 1953]

Figure 2.6. Structure of Illite

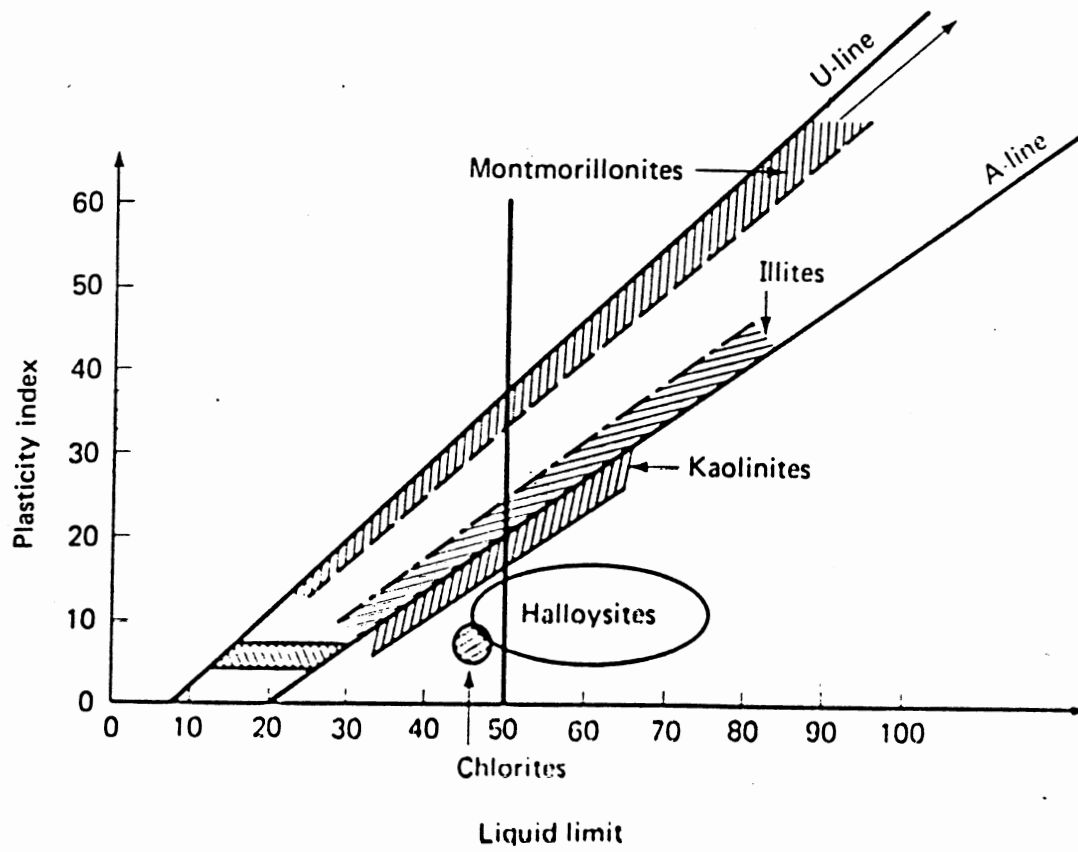
the entire lattice and makes illite much less expansive than montmorillonite. The engineering behavior of illite is between kaolinite and montmorillonite.

In most cases, natural clay soils consist of more than one mineral type. They are often the complex mixture of several different minerals. Furthermore, the internal structure is not the same as previously described idealized minerals. Mixed or interstratified internal structures are very common. Therefore, clay minerals are often composite minerals such as illite-montmorillonite, chlorite-illite, etc. Sometimes these minerals are loosely termed bravaisite (Hillel, 1980).




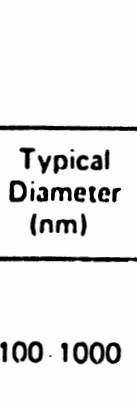
Identification of different clay minerals usually involves using X-ray diffraction, differential thermal analysis (DTA), or electron microscopy transmission and scanning. These methods are rather sophisticated and quantitative analysis is not possible. Use of Atterberg Limits to identify clay minerals was suggested by Casagrande (1948). A plasticity chart for clay mineral identification was developed by Holtz and Kovacs (Figure 2.7). From an engineering point of view, this method gives about the same information as the more sophisticated analyses (Holtz and Kovacs, 1981). Different zones in such plasticity charts indicate the behavior of a soil within a zone is controlled by the corresponding mineral type. It does not necessarily mean the soils are 100% of the labeled mineral.

2.2 Clay-Water Interaction

Clays are very small plate-shaped or tubular particles with large specific surfaces (Figure 2.8). Because of their size, unbalanced electrical charge, and crystalline structures, clays tend to actively react with water. In nature, clay particles appear to be hydrated; that is, water molecules are electrically attracted toward the surface of the clay particles, forming several layers of water envelopes around the particles called double-layer water. It is this characteristic of double-layer water that determines shrink/swell potential, plasticity, and cohesion of clays (Holtz and Kovacs, 1981; Snethen et al., 1975). The innermost layer of double-layer water is often called



2.7. Location of Common Clay Minerals on Casagrande's Plasticity Chart [Holtz and Kovacs, 1981]

Edge View	Typical Thickness (nm)	Typical Diameter (nm)	Specific Surface (km ² /kg)
 Montmorillonite	3	100-1000	0.8
 Illite	30	10 000	0.08
 Chlorite	30	10 000	0.08
 Kaolinite	50-2000	300-4000	0.015

2.8. Relative Dimensions of Common Clay Minerals
[Yong and Warkentin, 1975]

adsorbed water because of very strong bonding between the water and a clay particle.

The distribution of ions near a clay particle surface is illustrated in Figure 2.9. Based on the Gouy-Chapman theory, the effective thickness of the diffuse double layer may be expressed as:

$$z = \frac{1}{e v} \sqrt{\frac{\epsilon k T}{8\pi n_0}} \quad (2.1)$$

where

- z = the characteristic length or thickness;
- e = unit charge of an electron, 4.77×10^{-10} esu;
- ϵ = dielectric constant;
- k = Boltzmann constant, 1.38×10^{-6} erg/K;
- v = valency of the ions;
- n_0 = concentration of the ions in the bulk solution in ions/cm³; and
- T = temperature, K.

The cations surrounding a clay particle generally exist in two layers, the Stern layer and the diffuse layer. On one hand, cations within the Stern layer are those that adhere to the clay particle surface. There is a general agreement among many investigators that water in this layer has significant different structure and physio-chemical properties from "free" water. The mutual attraction force between negatively charged clay surface and water molecules contributes to the change in structure of the adsorbed water. Because of highly-oriented ionic packing, density and viscosity of adsorbed water can be much higher than free water. Figure 2.10 demonstrates such a phenomenon. Adsorbed water is usually considered as part of clay mineral. On the other hand, cations within the diffuse layer gradually decrease in concentration and the water eventually becomes "free" water as distance from the particle surface increases.

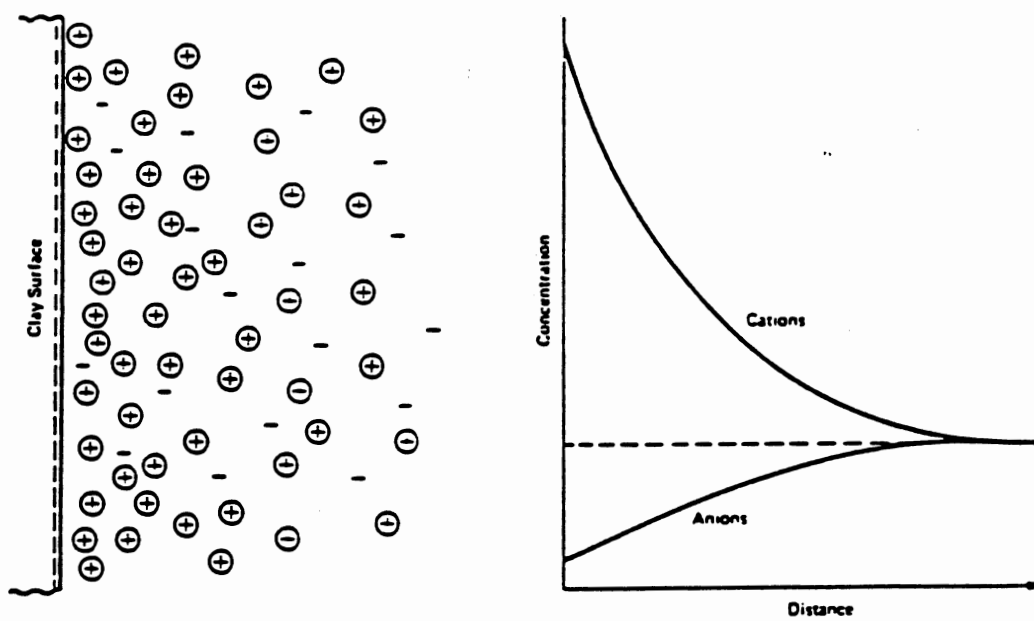


Figure 2.9. Distribution of Ions Near Particle Surface
[Mitchell, 1976]

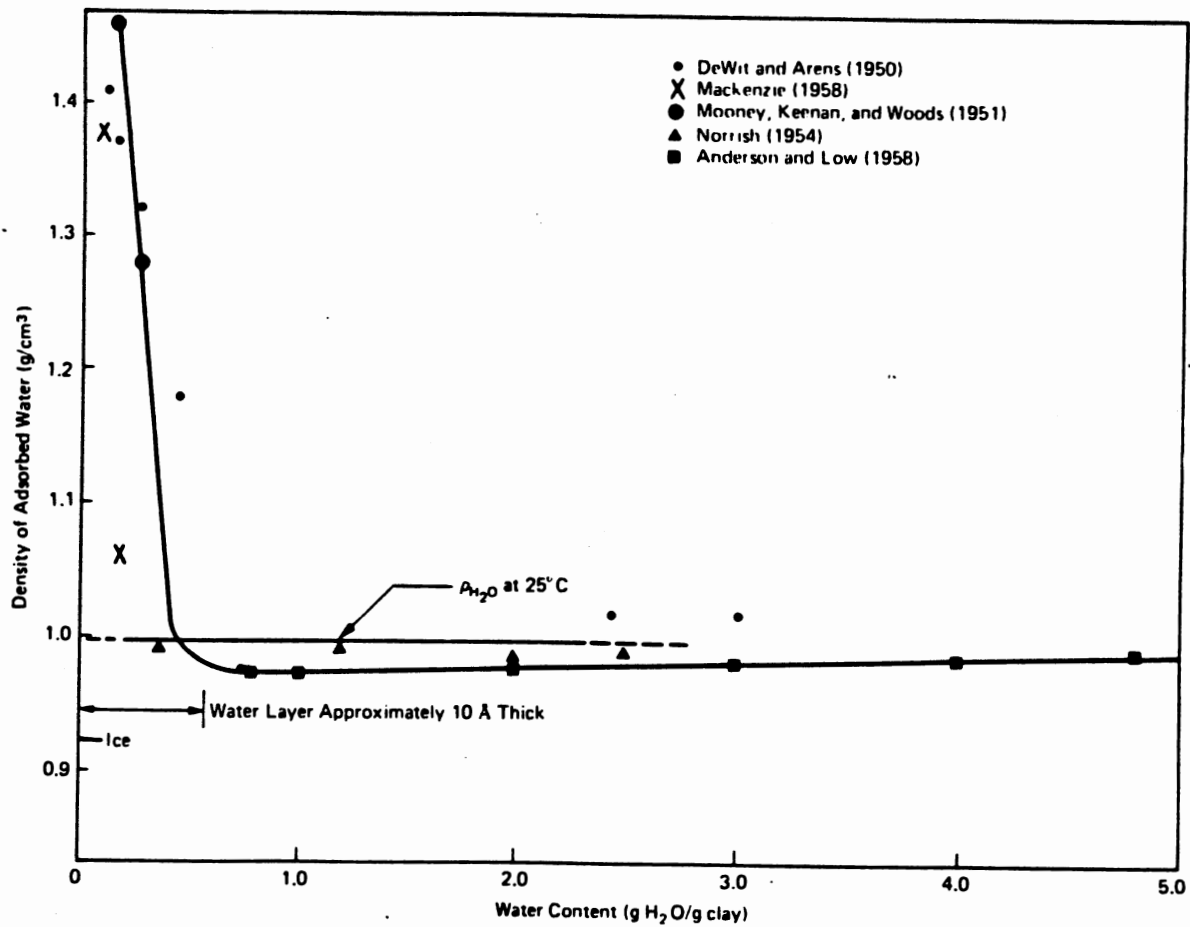


Figure 2.10. Density of Adsorbed Water [Martin, 1960]

The balance of ionic distribution between the Stern layer and diffuse layer is due to the twofold tendencies (Hillel, 1980): (1) the electrostatic attraction between the clay particle surface and cations that are pulled toward the surface to keep the minimum energy level, and (2) the kinetic motion of the water molecules which pushes the adsorbed cations outward to seek the same concentration within the whole solution phase.

All clays show some degree of swelling when they are in contact with water. Highly expansive clays differ from other clays in that they continue swelling to high moisture contents. Montmorillonite soils, for example, exhibit much higher expansivity than kaolinite and illite clays because of atomic structure and large specific surface areas, resulting in the thicker double-layer water around the particle and between the layer spaces. The types of exchangeable ions also play an important role in clay swelling process. The ions increase in size when hydrated. The smaller the ion is, the greater the amount of hydration the ion undergoes and thus the larger volume change is likely to occur. The common ions in a clay water system, in order of increasing ionic radii, are sodium (Na), magnesium (Mg), and potassium (K). This is why the sodium-montmorillonite clay soils experience higher expansivity than calcium-montmorillonite clay soils. Also, montmorillonite clays showing high volume change do so because of repulsion resulting from diffuse ion-layer interpenetration which depends on the distance between clay particles. A uniform distribution of the exchangeable ions between two clay particles occurs when the particles are less than 15 Å apart. In this case there is a net attraction between particles. As water is introduced into soil, water molecules adsorbed on the clay surface will force adjacent particles apart. When the distance of two particles reaches about 15 Å, two diffuse ion layers are formed, one associated with each surface. In this case there is a net repulsion. Soils with kaolinite and/or illite minerals exhibit much less volume change since the interpenetration of ions are not available (Yong and Warkentin, 1966; Snethen et al., 1975).

Microscale mechanisms of shrink/swell expansive soils, such as clay mineral type, clay-water interaction, etc., are only useful for qualitative analysis, since the influence of the different components on volume change is difficult to separate. Also, exact measurements for the type and amount of different clay minerals are impossible. Because of all these, the physical and/or mechanical properties of soils that reflect the microscale mechanisms of expansive soils are used for engineering purposes (Hamberg, 1985; Holtz and Kovacs, 1981).

2.3 Soil Suction Concept

Soil suction is an energy term that describes the state of water in the soil. According to classical physics, bodies in nature contain two kinds of energy: kinetic and potential. Kinetic energy is generally negligible due to very slow movement of water in the soil, especially in unsaturated soil whereas potential energy becomes the key factor in determining the internal condition with regard to change in mode of a soil water system (Hillel, 1980). The more quantitative definition of the soil suction states that suction is a negative gage pressure which represents the interaction between soil particles and water. The concept of soil suction should not be confused with pore water pressure since the latter is normally associated with the density of water, distance from groundwater surface, and surface tension forces (McKeen, 1981).

The total soil suction indicates the potential of absorbing pore liquid to satisfy the water deficit of the soil and volumetric swell tendency. Because of this, it can be used to characterize the effect of moisture on the volume and strength properties of soils (Snethen, 1980; Johnson, 1973; Olson and Langfelder, 1965).

The total soil suction represents all microscale mechanisms including clay particle attraction, cation hydration, and osmotic repulsion. It can be alternatively defined as the free energy present in soil water with respect to a pool of pure water located outside the soil at the same elevation. In other words, the free energy difference is the work that is done to draw the pure water into the soil by countering

the friction, resisting the flow of water, and expanding the lattice of soil. Soil composition (type and amount of clay mineral) and the cation environment determine the impact of the dissipation of free energy on the physical properties of the soil (Snethen, Johnson, and Patrick, 1977).

Based on the energy concept, the total soil suction can be determined by using the following formula:

$$h^o = \frac{1.058 R T}{v} \times \ln \left(\frac{p}{p_o} \right) \quad (2.2)$$

where

- h^o = total soil suction;
- R = ideal gas constant, 82.06 cc-atm/K;
- T = absolute temperature, K;
- p = vapor pressure of the pore water in the soil;
- p_o = vapor pressure of free pure water;
- p/p_o = relative humidity; and
- v = volume of a mole of liquid water, 18.02 cc/mole.

The superscript "o" after total suction, h , indicates the soil is not subject to any confining pressure (Hillel, 1980; Snethen, 1980). Several factors affect the total soil suction; these include moisture content, applied external pressure, gravity, temperature, mineralogy and texture of soil particles, soil fabric, and the amount of soluble matter in the soil water (Johnson, 1978; Motan, 1981). Because of different intrinsic characteristics of the above described factors, total soil suction is generally divided into two components—matrix suction and osmotic suction. This is expressed as

$$h^o = h_m^o + h_s^o \quad (2.3)$$

where h_m^o is the matrix suction, and h_s^o is the osmotic suction. Since the matrix suction is a negative pressure it is sometimes called capillary potential. Other names for

matrix suction may appear in the literature as matrix potential, soil-water suction, and soil-moisture retention force. These terms are used interchangeably by geotechnical engineers and soil physicists. The matrix suction results from the capillary and adsorptive forces due to the soil matrix, which are two of the three major microscale mechanisms causing swelling of a soil. This is illustrated in Figure 2.11.

In coarse-grained soils with relatively large particle size, the surface tension effect accounts for practically all of the matrix suction whereas the surface attractive forces for water and cations are negligible because of low specific surfaces. However, in clayey soils with colloidal size the characteristic of water around the soil particles (both adsorbed and capillary water) is very much controlled by the electric double layer and the exchangeable cations present. Generally, the two effects (adsorptive and capillary) cannot be easily separated, and are dependent on one another in most clayey soils.

The matrix suction is the function of moisture content and external load. The effect of air pressure within a soil matrix has shown little significance on the matrix suction. The osmotic suction represents the effect of solutes, soluble salts for instance, in soil water on thermodynamic properties of soil water system. The difference in the type and concentration of the solutes between pore water and free water (from outside sources) leads to an osmotic imbalance such that physical changes in soil structure may occur through water moving in or out of the pore spaces. Moisture content and external load do not affect the osmotic suction (Hillel, 1980; Snethen, 1980).

Using thermodynamic formulation (free energy per unit volume), the osmotic suction can be expressed as

$$h_s^o = \frac{1.058 R T}{V} \ln \left(\frac{p_s}{p_o} \right) \quad (2.4)$$

where h_s is the osmotic pressure, and p_s is the vapor pressure of soil water.

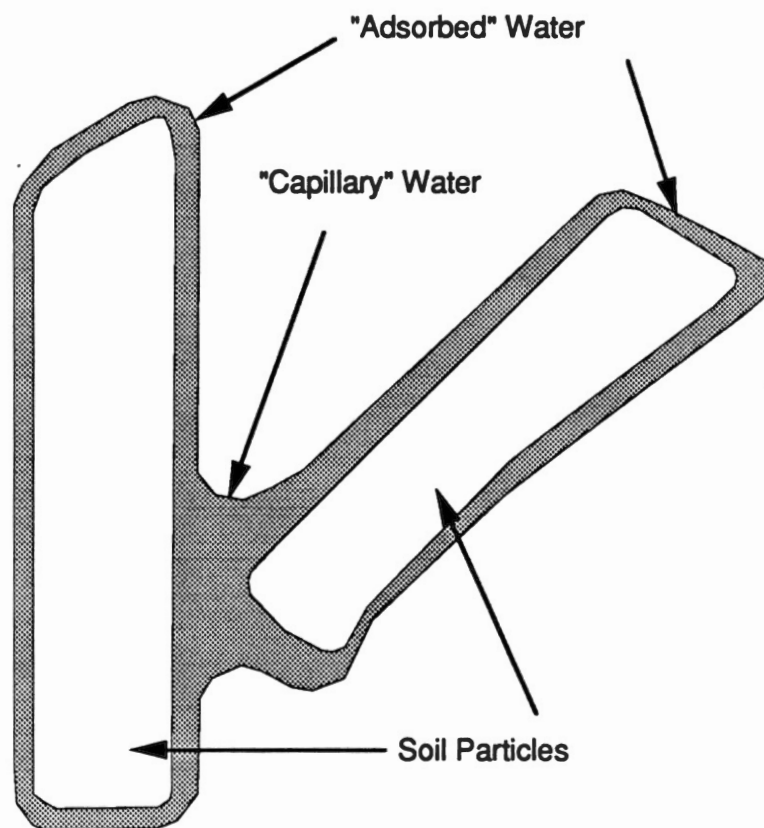


Figure 2.11. Soil Water System for Clay Particles
[Hillel, 1980]

It is often assumed that osmotic suction accounts for no swell when compared to the effect of matrix suction. This assumption is valid for most engineering problems since (1) many soils do not contain a high concentration of solutes, and (2) liquid flow in the soil is not affected significantly by the presence of solutes in the soil water (McKeen, 1981; Hillel, 1980; Snethen, 1980; Johnson, 1978; Snethen, Johnson, and Patrick, 1977). Detailed definitions of total soil suction, matrix suction, and osmotic suction are summarized in Table 2.1.

2.4 Soil Suction Measurement

Measuring soil suction is generally based on two principles, i.e., capillarity and vapor pressure reduction. Methods that measure the sum of capillary pressure and adsorptive forces within the soil include the pressure plate and tensiometer. Because of its limited measuring range (matrix suction less than one atmosphere), the tensiometer is not appropriate for expansive soil study. On the other hand, methods that measure the equilibrium vapor pressure of soil water include the thermocouple psychrometer and filter paper methods, which are useful for obtaining total soil suction.

2.4.1 Filter Paper Method

It was first discovered by agricultural soil scientists that papers can be used to estimate the soil attraction for water as indirect soil suction sensors (Hansen, 1926). Since then different papers have been used for this purpose and the accuracy of the method had been improved by numerous studies (Gardner, 1937; Gradmann, 1934; Stocker, 1930).

From the late sixties the filter paper method has been used extensively and routinely by the Water Resources Division of the U.S. Geological Survey (USGS) (McQueen and Miller, 1968). It was not until the late seventies that the method was applied for the study of expansive soils and finally adopted by ASTM as a standard

TABLE 2.1
DEFINITIONS OF SUCTION

Term	Symbol	Definition	Illustration
Total Suction	τ	The negative gage pressure, relative to the external gas pressure* on the soil water, to which a pool of pure water must be subjected in order to be in equilibrium through a semipermeable (permeable to water molecules only) membrane with the soil water.	<p>The illustration consists of three vertically stacked diagrams. Each diagram shows two chambers separated by a vertical barrier. The top chamber is labeled 'PURE WATER' and the bottom chamber is labeled 'SOIL WATER' or 'SOLUTION OF SOIL WATER'. 1. Top diagram: A 'SEMIPERMEABLE MEMBRANE' separates the chambers. The top chamber is open to air. The total suction is indicated as $\tau = \tau_b + \tau_m$. 2. Middle diagram: A 'SEMIPERMEABLE MEMBRANE' separates the chambers. The top chamber is open to air. The suction is indicated as τ_b. 3. Bottom diagram: A porous permeable wall separates the chambers. The suction is indicated as τ_m. A note at the bottom states 'NO PASSAGE OF WATER THROUGH MEMBRANES AT EQUILIBRIUM'. A vertical arrow on the left side of the diagrams points downwards and is labeled 'INCREASING SUCTION'.</p>
Osmotic (Solute) Suction	τ_b	The negative gage pressure to which a pool of pure water must be subjected in order to be in equilibrium through a semipermeable membrane with a pool containing a solution identical in composition with the soil water.	
Matrix (Soil Water) Suction	τ_m	The negative gage pressure, relative to the external gas pressure* on the soil water, to which a solution identical in composition with the soil water must be subjected in order to be in equilibrium through a porous permeable wall with the soil water.	

Source: L. D. Johnson and W. R. Stroman, *Analysis of Behavior of Expansive Soil Foundations*, U.S.A.E. Waterways Experiment Station, Vicksburg, MS, June 1976.

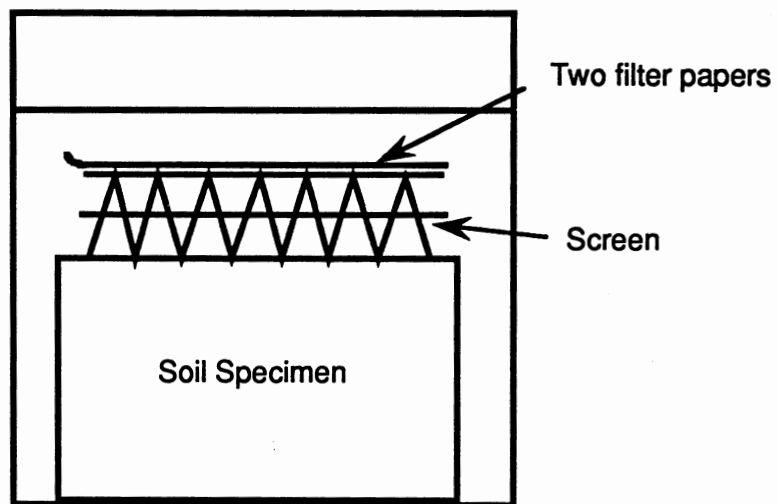
*The magnitude of the matrix suction is reduced by the magnitude of the external gas pressure. The osmotic suction is determined by the concentration of soluble salts in the pore water and can be given by $\tau_b = RT/v_w \log_e P/P_o$, where R is the universal gas constant, T is absolute temperature, v_w is volume of a mole of liquid water, P is vapor pressure of the pore-water extract, and P_o is vapor pressure of free pure water.

test method (ASTM, 1990; McKeen, 1981, 1976; Snethen and Johnson, 1980; McKeen and Hamberg, 1980; McKeen and Nielson, 1978).

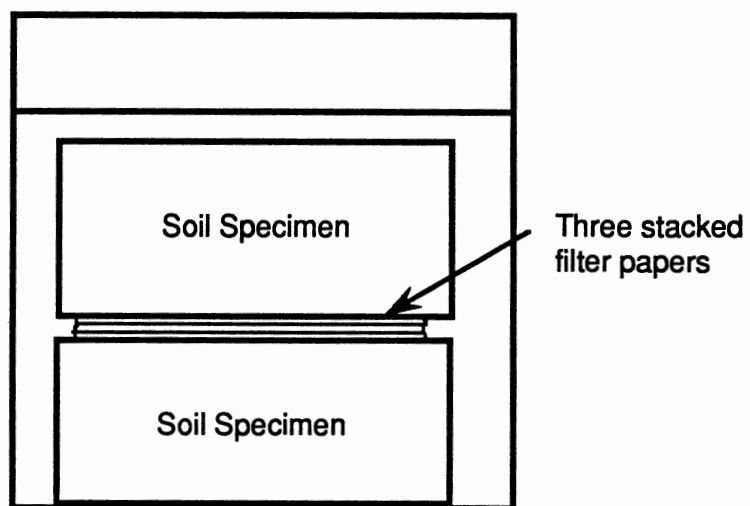
The procedure involves measuring moisture contents of the filter papers which are placed in an air-tight container with a soil sample. It takes a minimum of seven days to equilibrate the vapor pressure or moisture retention between the paper and soil sample, during which time the container must be placed in an insulated chest to avoid large temperature variations. Whatman No. 42 and Schleicher No. 589 filter papers are commonly recommended and are both commercially available.

The measurement of the total soil suction or matrix suction depends on the placement of filter papers within the container. This is illustrated in Figure 2.12. For total soil suction determination, filter papers are not allowed to be in direct contact with soil samples. As a result, osmotic suction is eliminated and moisture is transferred only through diffusion processes. Screen wire is often used for this purpose (Figure 2.12a). For matrix suction determination, filter papers must be in contact with the soil sample in order to minimize the difference in osmotic concentration between filter papers and the sample. However, most expansive soils in nature exist at high suction levels beyond the range of capillary water so that flow of liquid from soil pores to the filter paper could not be accomplished through capillary action. Therefore, the method actually measures total soil suction instead of matrix suction (Hamberg, 1985; McKeen, 1981).

Calibration of filter papers is required for converting moisture content of filter paper to the corresponding soil suction level. It involves using salt solutions of known concentration (known suction) such as reagent grade potassium chloride or sodium chloride as the measuring object to establish the relationship between moisture content of the filter paper and suction level of the solution. The calibration curves of Whatman No. 42 filter paper and Schleicher and Schuell No. 589 filter paper are shown in Figure 2.13; they become two segments of straight lines. The upper segment indicates moisture retained as films adsorbed to particle surfaces



(a) Total Suction



(b) Matrix Suction

Figure 2.12. Placement of Filter Papers for Different Suction Measurements

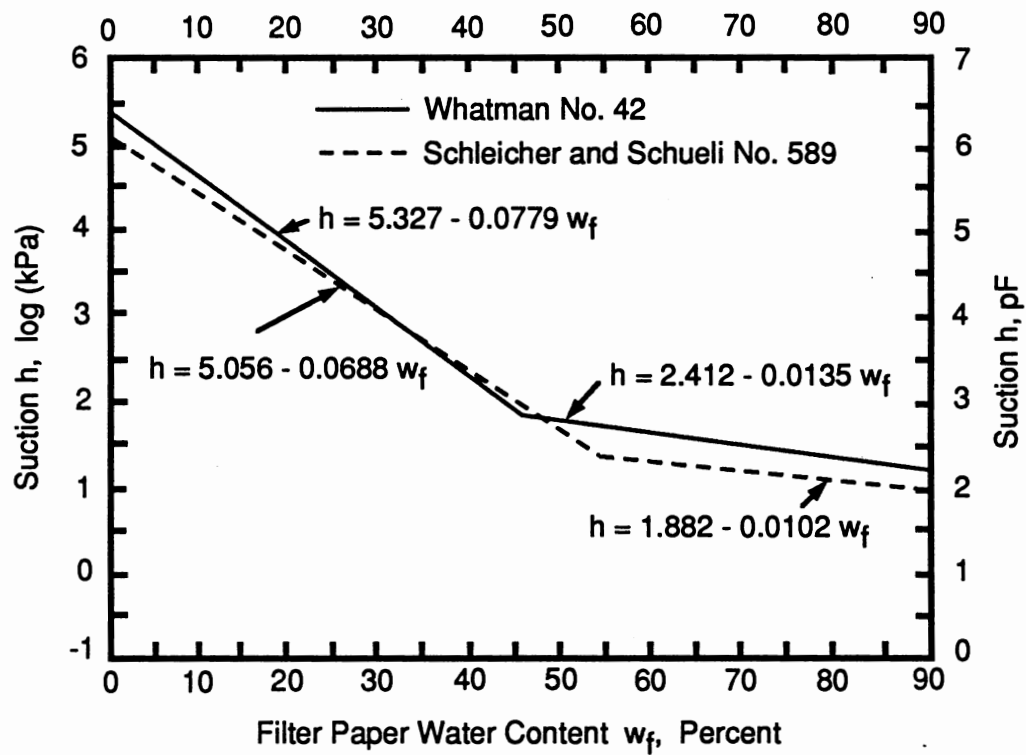


Figure 2.13. Calibration of Filter Paper

while the lower segment represents moisture retained by capillary action (McQueen and Miller, 1974).

The key for successful measurement of soil suction by this method is minimizing the time of transferring filter papers during moisture content determination. Also, condensation may sometimes occur inside the container because of very wet soil or a significant difference in temperature between the soil sample and the environment. Accidentally touching of the filter papers to the side of the container can cause an erroneous result. Therefore, care must be exercised in order to keep the predescribed influences to a minimum. Detailed testing procedures can be found elsewhere (ASTM, 1990; Hamberg, 1985; McKeen, 1981).

Comparison between the filter paper method and the thermocouple psychrometer showed that under the same condition of soil sample and equilibrium time, both methods yield the approximately same result in the suction range of 150 to 6000 kPa (McKeen, 1981).

2.4.2 Thermocouple Psychrometer Method

Based on the fact that the potential of soil moisture is the same as the potential of water vapor in the ambient air at equilibrium state, total soil suction can be inferred from the vapor potential assuming equilibrium thermal condition and negligible gravitational effect (Hillel, 1980). A thermocouple psychrometer is a device following this concept. It indicates the relative humidity of the soil water system and actually measures the difference in the temperature registered by a wet bulb and a dry bulb thermometer which is discussed in the following paragraphs.

A psychrometer, as shown in Figure 2.14, consists of two thermometers; one is kept wet and the other dry. Evaporation cools down the wet bulb of the thermometer and decreases its temperature. The temperature difference between the wet bulb and the dry bulb is a measure of the atmosphere dryness, which is called the wet bulb depression. Relative humidity is defined as the ratio of partial pressure of water

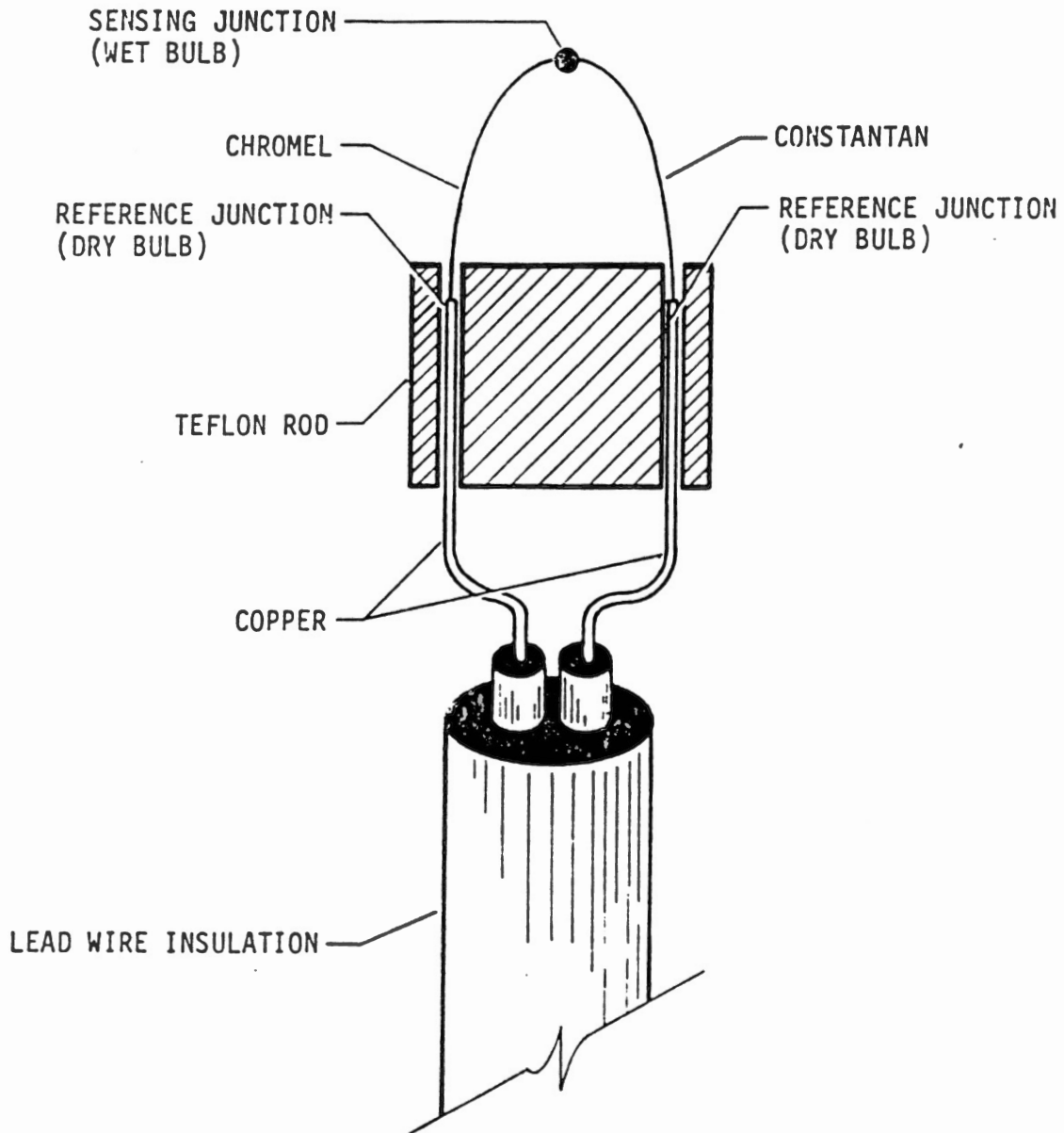


Figure 2.14. A Peltier Thermocouple Psychrometer
[McKeen, 1981]

vapor in the air to equilibrium partial pressure of vapor in vapor-saturated air at the same temperature.

Two principles of thermoelectricity are involved: the Peltier and Seebeck effects. According to the Peltier effect, cooling of the junction occurs when a small current is passed through a thermocouple sensing junction (wet bulb) in the proper direction. At the same time, heating of the reference junction (dry bulb) occurs with an exactly equal amount. The cooling and heating process will continue until the temperature of the sensing junction reaches the dew point. Water will then start to condense on the junction. This results in a temperature decrease in the sensing junction and a temperature increase in the reference junction. According to the Seebeck effect, a current will flow around a loop of two dissimilar metals as long as there is a temperature difference between the two junctions. Soil suction is related with relative humidity by Equation (2.2):

$$h^o = \frac{1.058 RT}{V} \ln \left(\frac{p}{p^o} \right) \quad (2.5)$$

The thermocouple psychrometer test procedure includes preparing several undisturbed soil cubes, 1.5 in. in dimension. Moisture contents of the samples should be modified to fit the field condition of moisture variation so that the whole range of soil suction versus moisture content relation can be defined. Such a relation is often called the soil-moisture characteristic curve. The samples are then sealed in separate containers. A thermocouple psychrometer is placed in the container through a rubber stopper that seals the container. The containers are kept in a polystyrene chest in order to equilibrate in a stable temperature environment. Approximately 48 hours is needed for equilibrium.

The thermocouple psychrometer voltage output values (millivolts and microvolts) are measured and are then converted to temperature ($^{\circ}\text{C}$) and soil suction by the calibration curve:

$$T (^{\circ}\text{C}) = \frac{\text{Output (millivolts)}}{0.0395 \text{ millivolts}/^{\circ}\text{C}} \quad (2.6)$$

$$E_{25} = \frac{E_t}{0.325 + 0.027 T} \quad (2.7)$$

where E_{25} is the microvolt output at 25°C (calibration temperature), E_t is the microvolt output at measuring temperature (°C), and T is the measured temperature.

Calibration is essential and is made over standard salt solutions, such as potassium chloride. A range of relative humidity can be obtained by varying concentrations of the salt solution. A typical linear relationship between soil suction and microvolt output at 25°C, E_{25} is

$$h^0 = m \cdot E_{25} - n \quad (2.8)$$

where m and n are constants. Detailed information about testing procedure and calibration are reported by McKeen (1981), Snethen (1989, 1979), Riggle (1978), and Meyn and White (1972). The instrument is not practical at low suction levels but can be quite useful considerably beyond the suction range of the tensiometer. It is most often used in research and is commercially available (Hillel, 1980).

2.4.3 Pressure Plate

The pressure plate method is one that directly measures the pressure difference between the chamber air pressure and the pressure within the porous plate which is generally at atmospheric pressure (Figure 2.15). As the soil sample is placed on the porous plate, it tends to extract the water due to the negative pore pressure within unsaturated soils in general. The chamber pressure is continuously increased until equilibrium is reached. The chamber pressure at that point is considered to be the matrix suction.

Successive suction values as well as moisture content at each suction can be determined by this method (Hillel, 1980). The maximum soil suction which can be measured by the pressure plate is dependent on the air entry value of the porous

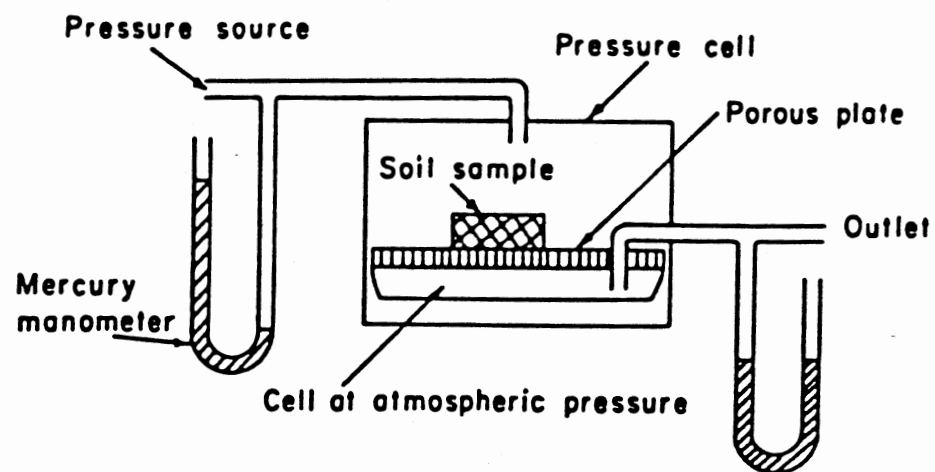


Figure 2.15. Pressure Plate for High Suction Measurement
[Hillel, 1980]

plate and the design of the chamber. The air entry value represents the maximum air pressure that can be applied to a saturated plate without causing cavitation.

Cellulose acetate membranes may be used as a porous plate, resulting in the air entry value above 150,000 kPa. In this case, the device is often called the pressure membrane (Hillel, 1980; Lytton, 1969; Richard, 1947). The problems associated with measurement of suction for expansive soils are controversial between ideal assumptions and actual field conditions.

The assumption made for the pressure plate to work is that all air voids within the soil matrix are interconnected. Evidence shows (Bocking and Fredlund, 1980; Barden and Pavlakis, 1971) that unsaturated soils contain significant amounts of occluded air for degree of saturation beyond 85%. Other practical shortcomings include long response time due to the deformation of the sample, air diffusion under high pressure, etc. (Fredlund and Morgenstern, 1973; Johnson, 1973; Bishop and Hinkel, 1962). For comparison purposes, the three previously described soil suction measuring methods are summarized in Table 2.2.

2.5 Heave Prediction Methods

There are three categories of prediction methods: empirical, soil suction, and oedometer methods. Empirical methods use soil classification parameters, i.e., Atterberg limits, plasticity index, and percent clay. These methods are highly dependent on local experience and have limited application in design. Soil suction methods, on the other hand, involve measurement of soil suction with respect to change in moisture content, often called the soil-moisture characteristic curve. Several investigators (Hamberg and Nelson, 1984; Mitchell, 1984; McKeen, 1980; Snethen, 1980) report different approaches, and associated heave prediction methods, which can be categorized as soil suction methods.

The basic difference among the different soil suction methods is the way the following terms are defined: soil suction index, suction index ratio, instability index, or suction compression index. These different terms refer to the soil suction

TABLE 2.2
COMMON LABORATORY SUCTION MEASUREMENT METHODS

Test Method	Suction Component(s)	Range (kPa)	Advantages	Disadvantages
Thermocouple Psychrometers (TCPs)	Total	300 to 10 ⁶ (±10) Lab* (±50) Field	Field and laboratory applications Convenient range for most soils Fairly inexpensive equipment commercially available	Temperature calibration required Not applicable in moist soils Requires 2 to 7 days equilibration time
Filter Paper Sensors	Total	0 to 10 ⁶ (±10) [‡]	Measures full range of suction Very inexpensive No specialized equipment required Simple procedure	Requires 7-day equilibration time Care required for moist soils to prevent saturation of sensors
Pressure Membranes (Axis Translation Technique)	Matrix	0 to 155,500	Can develop continuous moisture/suction relationship for single sample Measures matrix suction stress state variable directly Commercially available	Conceptual and measurement problems of axis-translation technique (see text) Wetting-drying hysteresis Requires 2- to 10-day equilibration time for each moisture-section measurement Requires expensive equipment More appropriate for coarse-grained soils
Membrane Oedometers	Total [¶] Matrix Osmotic [¶]	0 to 4000 10 to 10000 0 to 40000	Can control stress state variable simultaneously Australian model measures suction components separately	Requires specialized equipment Not available commercially
Tensiometers and Pressure Plates	Matrix	0 to 100	Measures matrix suction stress state variable directly Commercially available	Low suction range applicable in moist soils only

*TCP accuracy estimated from reported calibration data (Brown and van Haveren, 1972).

‡Filter paper accuracy is comparable with TCP accuracy in 150 to 6000 kPa range (McKeen, 1981).

¶Australian type only (Aitchison and Martin, 1973; Fargher et al., 1979).

parameter that relates unit volume change or linear extensibility to the soil suction change or moisture content change within the range of field conditions.

Oedometer methods use consolidometers to directly measure the one-dimensional heave upon saturation of a soil specimen from its natural moisture state. Depending on the loading procedure, several methods are developed such as free swell, overburden swell, and constant volume swell. Fredlund (1980, 1983) showed that the constant volume swell test or swell pressure test was more realistic than the other oedometer methods. The following sections describe the basic theory and procedures for four soil suction methods and the constant volume oedometer swell method evaluated in this study.

2.5.1 Snethen and Johnson's method

Heave is induced by suction change within the active zone. When an expansive soil is wetted after a dry season, its soil suction level decreases and the volume of soil increases. Based on this concept, the unit heave may be expressed as

$$\frac{\Delta H}{H} = \frac{C_t}{1 + e_o} [\log(h_o) - \log(h_f + \alpha \cdot \sigma_f)] \quad (2.9)$$

where

- C_t = suction index, equal to $\alpha \cdot G_s/100B$;
- $\log(h_o)$ = $A - B \cdot w$ = matrix soil suction without surcharge pressure, kPa (tsf), and A and B are constant from soil suction versus moisture content relationship;
- α = compressibility index;
- h_f = final matrix soil suction, kPa (tsf); and
- σ_f = final applied pressure (sum of overburden and external load), kPa (tsf).

The initial matrix suction can be measured by the thermocouple psychrometer or filter paper methods. Soil moisture characteristic curves are established by determining the soil suction value at different moisture content, i.e., several soil

specimens are dried or wetted for different lengths of time so that the field moisture condition is modified.

Hysteresis was not evidenced for the soil-moisture characteristic curves using the thermocouple psychrometer method (Snethen, 1979, 1980). The process of drying or wetting the test specimens from the natural moisture condition instead of completely air drying and then saturating may inhibit the hysteretic phenomenon.

The parameters A and B can be determined from the soil-moisture characteristic curve (Figure 2.16). A is the soil suction value (logarithmic scale) at zero moisture content; B is the slope of soil suction versus moisture content curve that is defined by

$$\log(h) = A - B \cdot w \quad (2.10)$$

The compressibility factor, α , is the slope of specific volume, $(1 + e)/G_s$, versus the moisture content curve (Figure 2.17). An empirical relationship between the plasticity index and the compressibility factor is also available (Russam, 1961):

$$\alpha = \begin{cases} 0 & PI \leq 5 \\ 0.0275 \cdot PI - 0.125 & 5 \leq PI \leq 40 \\ 1 & PI \leq 40 \end{cases} \quad (2.11)$$

The suction index, C_t , reflects the change of volume with respect to soil suction changes. The initial soil suction, h_0 , is measured during the suction test and the final suction profile can be assumed as one of four suggestions (Fredlund, 1983; Johnson, 1978, 1977, 1976; Richards, 1976; Russam, 1965, 1961; Snethen, 1980):

1. Zero throughout the depth of active zone
2. Linearly increasing with depth through the active zone
3. Saturated water content profile
4. Constant at some equilibrium value.

Assumption (1) is extremely conservative because soil suction in the field will probably never be reduced to zero for the entire profile. However, using this assumption suggests the upper limit of the field heave. Assumption (2) is also conservative but to a lesser degree than assumption (1). Assumption (3) may be the

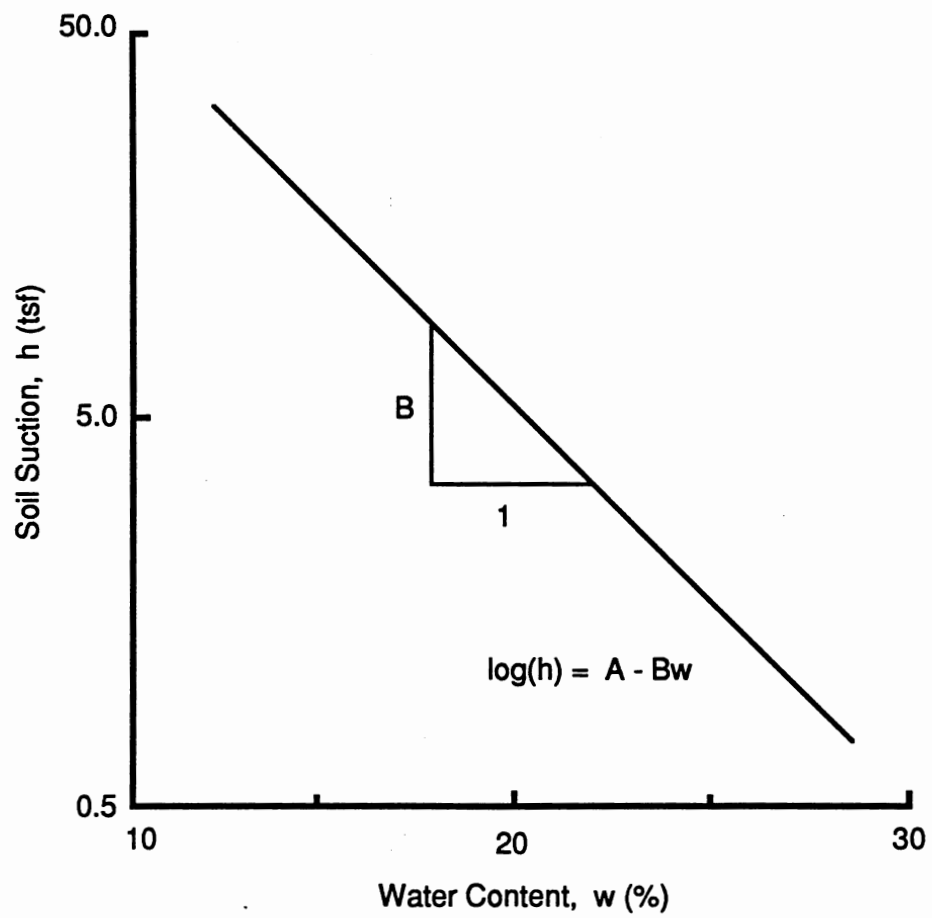


Figure 2.16. Soil Suction Vs. Water Content Relationship

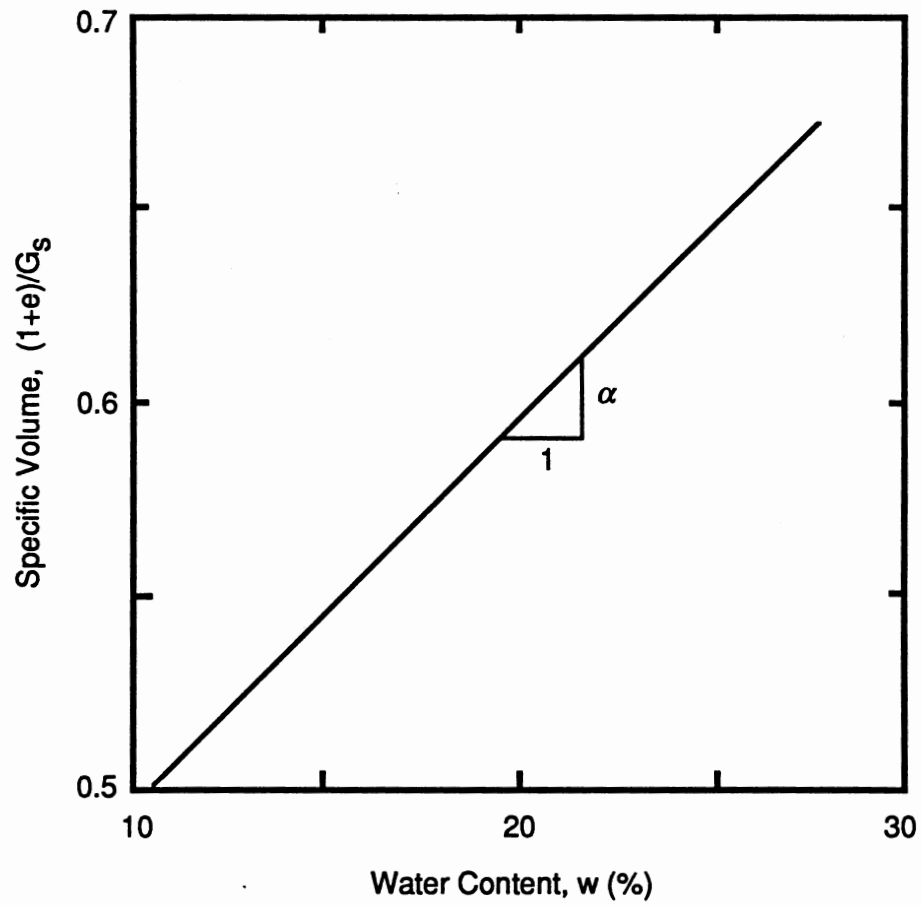


Figure 2.17. Specific Volume Vs. Water Content Relationship

most realistic assumption since the soil suction is calculated from the calculated saturation moisture content (Equation 2.10) instead of a relatively arbitrary hypothesis. Assumption (4) applies to the situation where a more or less stable soil suction profile has been reached because of the type of surface covers, i.e., buildings, pavements, etc. Such a suction profile depends on the local climate and soil type. In addition, the final soil suction profile must be monitored for similar soil and climate conditions to properly use assumption (4).

Another very important factor which affects the estimate of ground heave is the depth of the active zone. In general, the depth of the active zone is not the same as the depth of seasonal moisture variation. Because clay soils respond slowly to changes in moisture content caused by changes in climate, the depth of seasonal moisture variation is usually smaller than that of the active zone. There is no detailed procedure for estimating depth of the active zone at this stage. However, suggested "rules of thumb" exist (Snethen, 1980, 1979).

2.5.2 Nelson and Hamberg's Method

Heave is related to soil suction change and soil suction is dependent on the moisture content of the soil; therefore, heave may be predicted by estimating or measuring changes in moisture content. The amount of heave is expressed as:

$$\Delta H = \sum_i \frac{H_i}{1 + e_o} (C_w \cdot \Delta \omega_i) \quad (2.12)$$

where H_i is the thickness of the i th layer, C_w is the suction index ratio, and $\Delta \omega$ is the moisture content change.

Long-term field monitoring of moisture content is preferred in order to develop the upper and lower boundaries of the moisture content profile. However, such measurement data are often not available. An idealized moisture boundary profile was suggested for typical western clay shales (Figure 2.18). It indicates that volume changes occur mainly in the moisture content range from the shrinkage limit to the plastic limit.

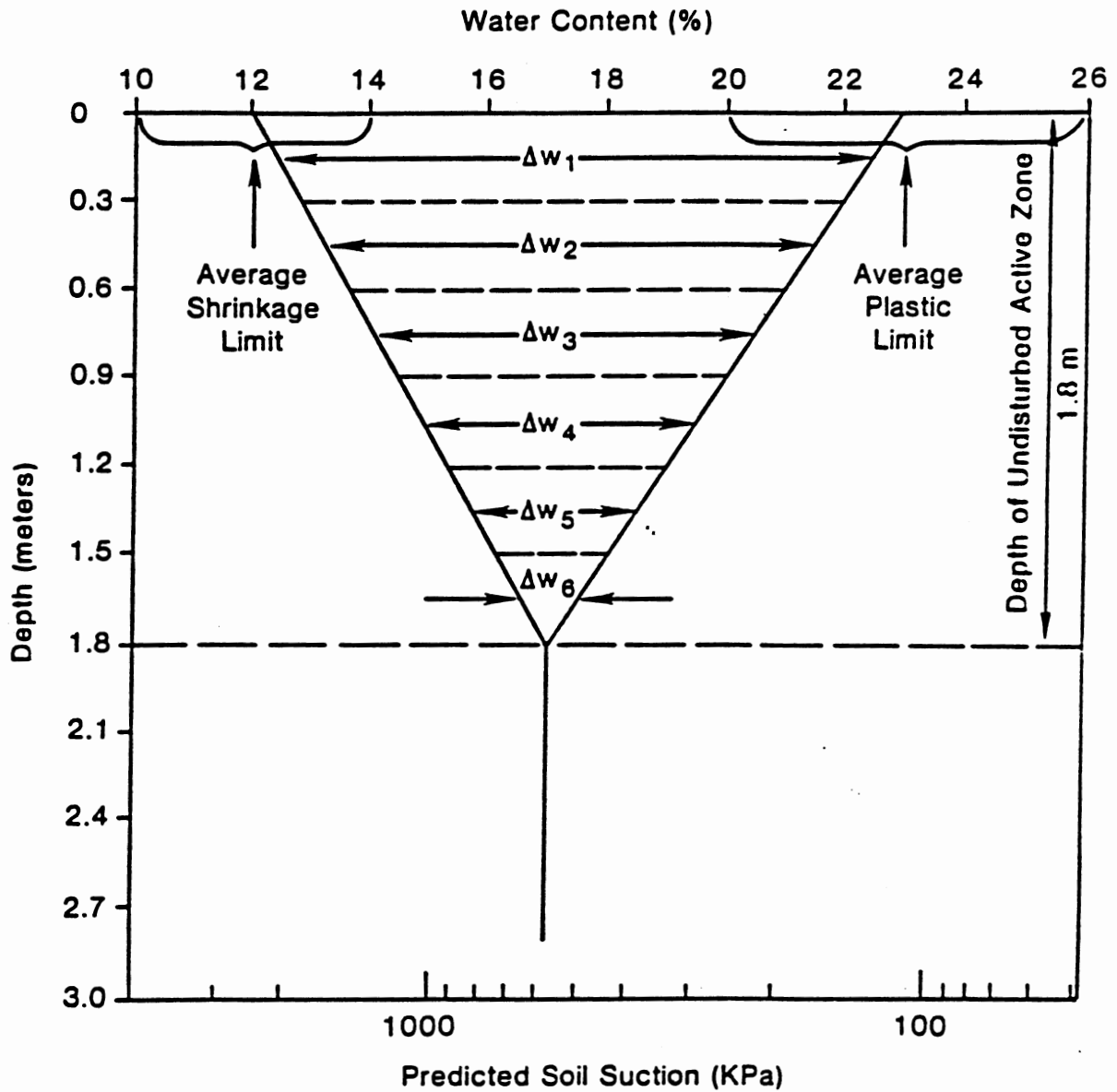


Figure 2.18. Idealized Moisture Boundary Profile
[Hamberg, 1985]

If the final soil suction profile is available instead of the moisture content change profile, the following equation may be used (Hamberg, 1985):

$$\Delta H = \sum_i \frac{H_i}{1 + e_o} [C_h \cdot \log(h)]_i \quad (2.13)$$

where C_h is the suction index with respect to void ratio, equal to $C_w \cdot D_h$, in which D_h is the suction index with respect to moisture content and is defined in the following expression:

$$w = A' - [D_h \cdot \log(h)] \quad (2.14)$$

The suction index ratio, C_w , is measured by the CLOD test which is a modified COLE (the coefficient of linear extensibility) test. In general terms, the CLOD test procedure involves preparing soil samples with a variety of moisture contents. After the initial soil suction measurements, the samples are coated with a waterproof resin. A suitable resin is Dow Saran F310, which dissolves readily in acetone or methyl ethyl ketone. Once the resin is dried, the volume of the sample is determined by weighing a saran-coated soil clod in air and in water, based on Archimedes' principle, so bulk density can be obtained. Dry density of the sample is determined after oven drying the sample for approximately 48 hours. Unit volume change $\Delta V/V_o$ is plotted against moisture content to determine a shrinkage curve. Typical shrinkage curves are shown in Figure 2.19. The suction index ratio, C_w , is then determined by calculating the slope of volumetric strain versus the moisture content curve as follows:

$$C'_w = \frac{\Delta V / V_o}{\Delta \omega} = \frac{\Delta V / V_o}{\omega_o - \omega_{sh}} \quad (2.15)$$

$$C_w = C'_w (1 + e_o) \quad (2.16)$$

where C_w is the suction index ratio in terms of volumetric strain, ω_o is the initial moisture content, and ω_{sh} is the shrinkage limit based on clod shrinkage tests. The suction index with respect to moisture content, D_h , can be determined by calculating

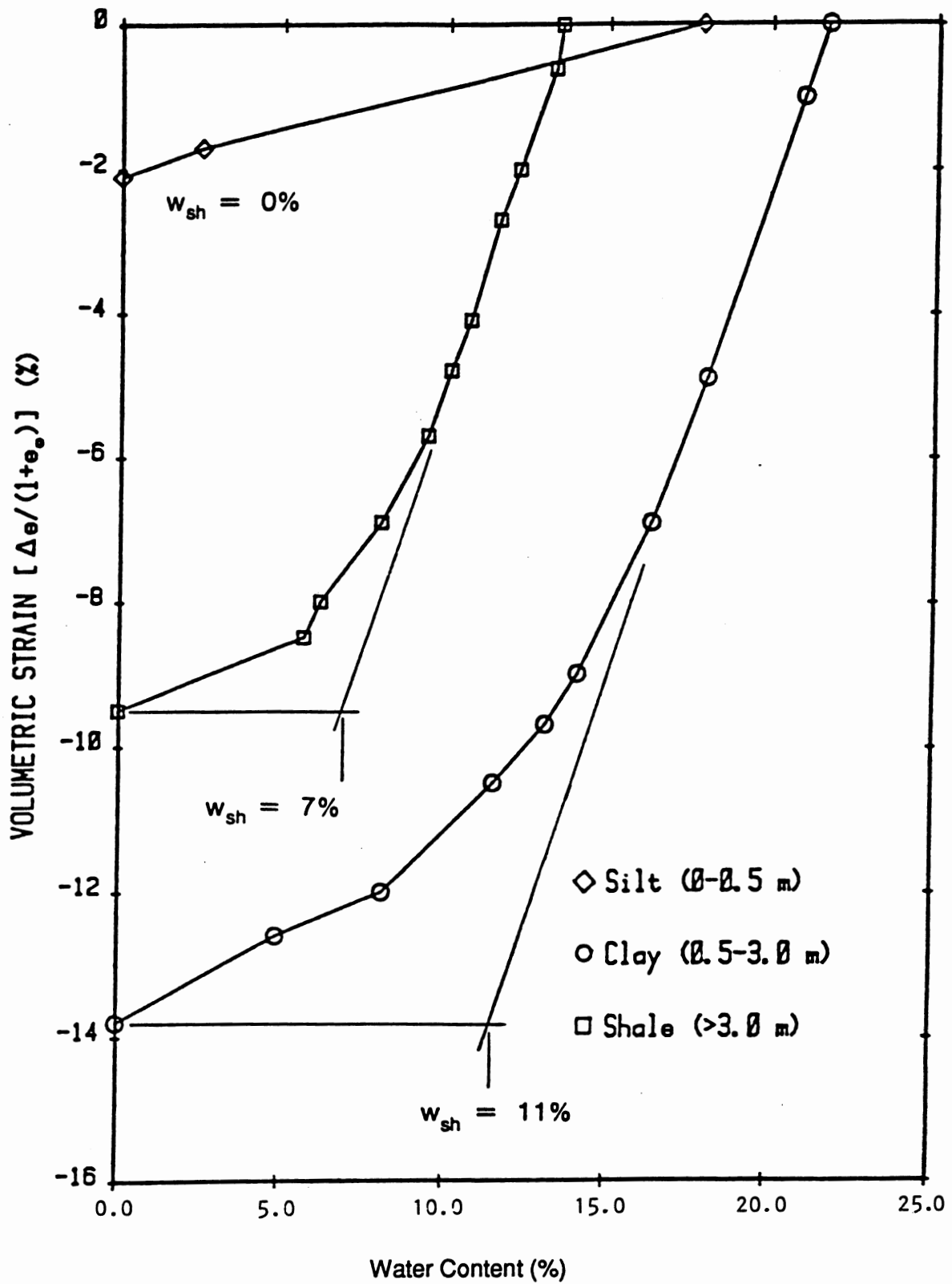


Figure 2.19. Representative Clod Shrinkage Curves
[Hamborg, 1985]

the slope of moisture content versus the soil suction (logarithmic scale) curve. Actual ground heave may be adjusted depending on the confinement situation:

$$\Delta H_{\text{act}} = f \cdot \Delta H_{\text{pred}} \quad (2.17)$$

where f is the correction factor, 0.33 to 1.0. The lower limit, 0.33, refers to the ground surface condition of fissuring and cracking while the upper limit refers to no cracking condition.

2.5.3 Mitchell's Method

Based upon experimental observations (Aitchison and Woodburn, 1969; Aitchison, 1970; Lytton and Woodburn, 1973), it is assumed that vertical strain of the expansive soil is linearly proportional to soil suction. Therefore, ground heave can be expressed as

$$\Delta H = \Sigma (I_{\text{pt}} \cdot \Delta u \cdot H_i) \quad (2.18)$$

where I_{pt} is the instability index, and Δu is the soil suction change. The value of the instability index is obtained by a test called the core shrinkage test (Fargher and Stevens, 1973; Aitchison and Peter, 1973). It involves the measurement of linear strain versus moisture content relationship, $\Delta \varepsilon_v / \Delta w$, and the moisture characteristic, $c = (\Delta w / \Delta u)$, of an unconfined, undisturbed core sample. The moisture characteristic reflects the gains and losses of soil moisture with respect to change in soil suction.

The undisturbed core samples from different depths in the active zone are needed for establishing a linear strain versus a moisture content profile. The specimen is air dried for a period of two days, during which time the length and mass of the shrinkage core are measured frequently. It is then oven dried to obtain the moisture content. Figure 2.20 (Mitchell, 1984) shows the typical results of this measurement.

The instability index is calculated as the slope of linear dimension change versus moisture content, $\Delta \varepsilon_v / \Delta w$, times the moisture characteristic, c ; that is,

$$I_{\text{pt}} = \frac{\Delta \varepsilon_v}{\Delta w} C \quad (2.19)$$

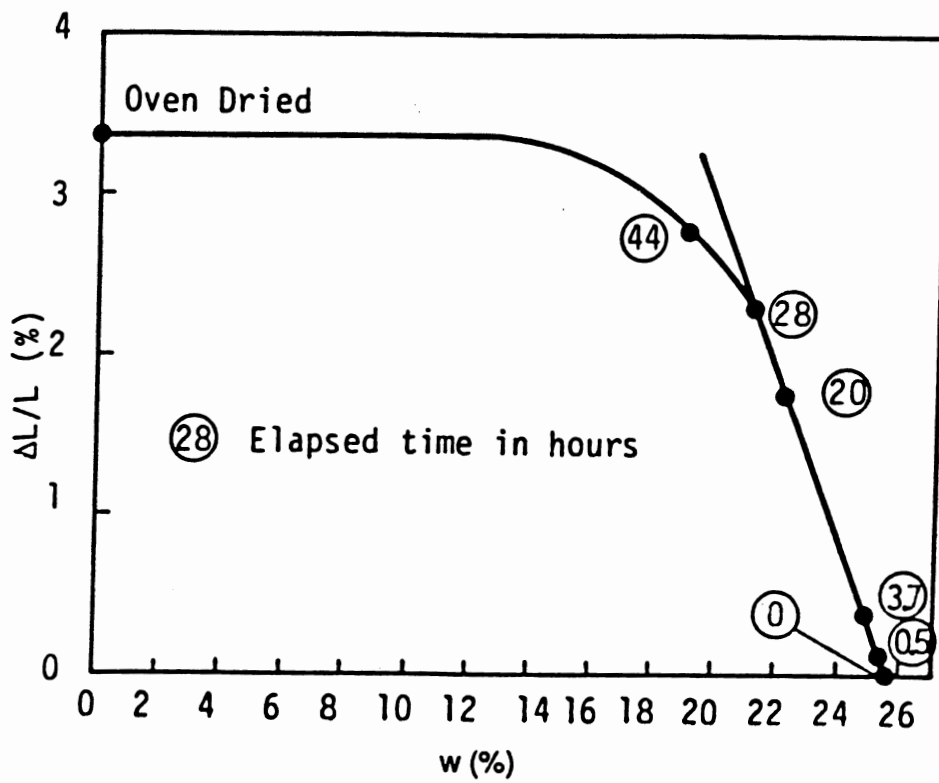


Figure 2.20. Linear Strain Vs. Moisture Content Relationship [Mitchell, 1984]

The moisture characteristic, c , is determined directly through the soil suction test using the thermocouple psychrometer or filter paper methods. Mitchell's method also requires suction change profiles which in most cases are not available. Actual application of this method involves the assumption of the final soil suction profile. It was reported (Mitchell and Avalle, 1984) that both shrinking and swelling can be analyzed by using the instability index.

2.5.4 McKeen's Method

The total heave is related to soil suction change by a parameter called the suction compression index and is expressed as

$$\Delta V / V_0 = \sum_i \gamma_h \cdot \log \left(\frac{h_f}{h_0} \right) \quad (2.20)$$

where $\Delta V / V_0$ is the soil volume change, γ_h is the suction compression index, and h_f , h_0 are the final and initial weighted suctions.

The original version of Equation (2.20) was developed by Lytton for expansive soil classification purposes (McKeen and Nielsen, 1978). The suction compression index is determined by COLE or CLOD tests. However, two empirical correlations for estimating the suction compression index were developed and experimental data showed a consistent relationship between the measured and predicted heave using the empirical methods. One of the methods requires input data of soil activity (A_c) and cation exchange activity (CEAc), which can be calculated from the plasticity index (P.I.), percentage of clay, and cation exchange capacity (CEC) as follows:

$$A_c = \frac{\text{P.I.}}{\% \text{ Clay}} \quad (2.21)$$

$$\text{CEAc} = \frac{\text{CEC}}{\% \text{ Clay}} \quad (2.22)$$

The suction compression index, γ_h , for a soil with 100% clay can be determined from Figure 2.21. For a soil with a percentage of clay less than 100, which is a

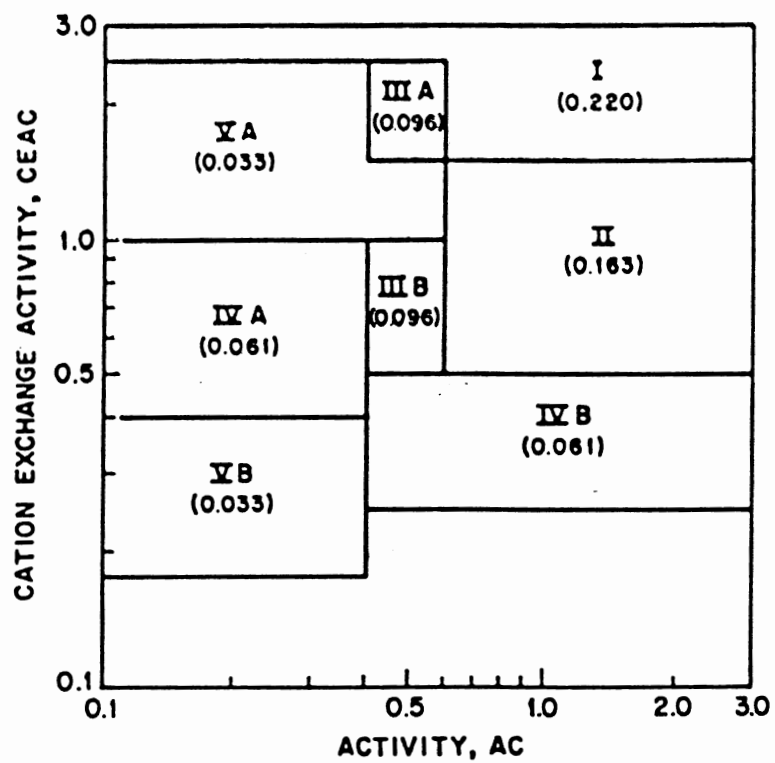


Figure 2.21. Chart for γ_h Prediction [McKeen, 1980]

general case, the suction compression index must be multiplied by percentage of clay; that is,

$$\gamma_h = (\gamma_h)_{100} \cdot (\% \text{ Clay}) \quad (2.23)$$

The cation exchange capacity can be determined by different procedures used in agricultural laboratories. The other empirical correlation is established between the suction compression index and percentage of clay:

$$\gamma_h = \begin{cases} 0.00179(C) - 0.041, & \text{high activity, } 40 < C < 70 \\ 0.00057(C) - 0.00057, & \text{low activity, } 25 < C < 70 \end{cases} \quad (2.24)$$

where C is the percentage of clay.

2.5.5 Fredlund's Method

In-situ behavior of a soil is highly dependent on stress levels. Since a soil consists of three phases (solid, water, and air), three types of stresses are generally involved: total stress, σ ; pore-water pressure, u_w ; and pore-air pressure, u_a . Of these stresses, combination variables $(\sigma - u_a)$ and $(u_a - u_w)$ are independent and proven to be satisfactory to describe in-situ stress states for unsaturated soils (Fredlund and Morgenstern, 1977). The $(\sigma - u_a)$ term is often referred to as the "net total" stress and the $(u_a - u_w)$ term is referred to as the matric suction.

Use of these independent stress variables for the analysis of shrinking and swelling soils is most convenient because the environmental effect can be separated from the loading effect. The environmental effect represents mainly the wetting and drying process due to climatic variation, and includes other factors that contribute to the process such as grass, trees, and pavement. This wetting and drying process is independent of external loading and is reflected in the matric suction level. The drying process (evaporation or evapotranspiration) increases the matric suction level, whereas the wetting process (infiltration) decreases the suction level (see Figure 2.22). The loading effect represents houses, buildings, and other structures that change the net total stress of the subsoils.

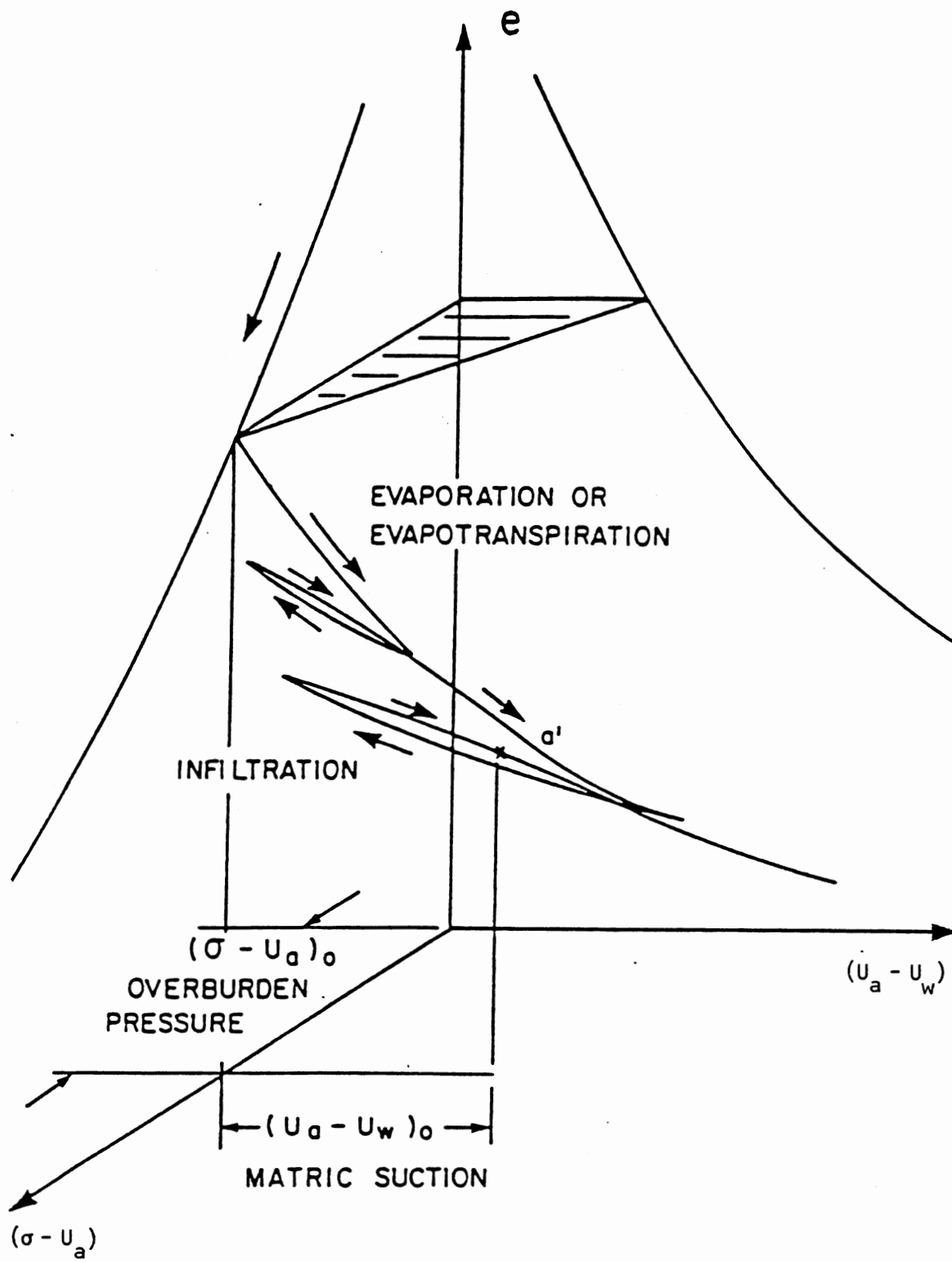


Figure 2.22. Stress History by Drying and Wetting [Fredlund, 1983]

There is no method currently available to measure the matric suction during oedometer swell tests. Assumptions must be made in order to obtain expansive soil properties from oedometer tests. Fredlund (1983) suggested that matric suction can be eliminated by immersion of the sample in water. As a result, total stress changes reflect swelling behavior of the soil. The constant volume oedometer method is based on this concept and is discussed in the following paragraphs.

The constant volume oedometer method is a consolidation test run in such a way that after the equivalent overburden pressure is applied the specimen is inundated. The soil will try to swell because of a decrease in soil suction; however, a small increment of load is applied intermittently so that volume change of the specimen will not take place. The pressure at which no more swelling potential occurs is called the "uncorrected" swelling pressure. The sample is then loaded and unloaded with the conventional consolidation test procedure (see Figure 2.23). Many investigations (Johnson and Snethen, 1978; Fredlund, 1983; Sayed and Rabbaa, 1986) indicate that the "uncorrected" swelling pressure by this method is too low. A recent procedure suggested by Fredlund (1983) accounts for sampling disturbance of the swell pressure specimen. Basically, the procedure involves the deduction of compressibility of the apparatus from the actual deformation measurement and correction of swelling pressure for sampling disturbance by the modified Casagrande graphical method. The corrected swelling pressure showed accurate prediction of heave on expansive soils.

Once the swelling pressure is determined, the total heave can be calculated by using the following equation:

$$\Delta H = C_s \frac{H}{1 + e_o} \log \left(\frac{p_f}{p_o} \right) \quad (2.25)$$

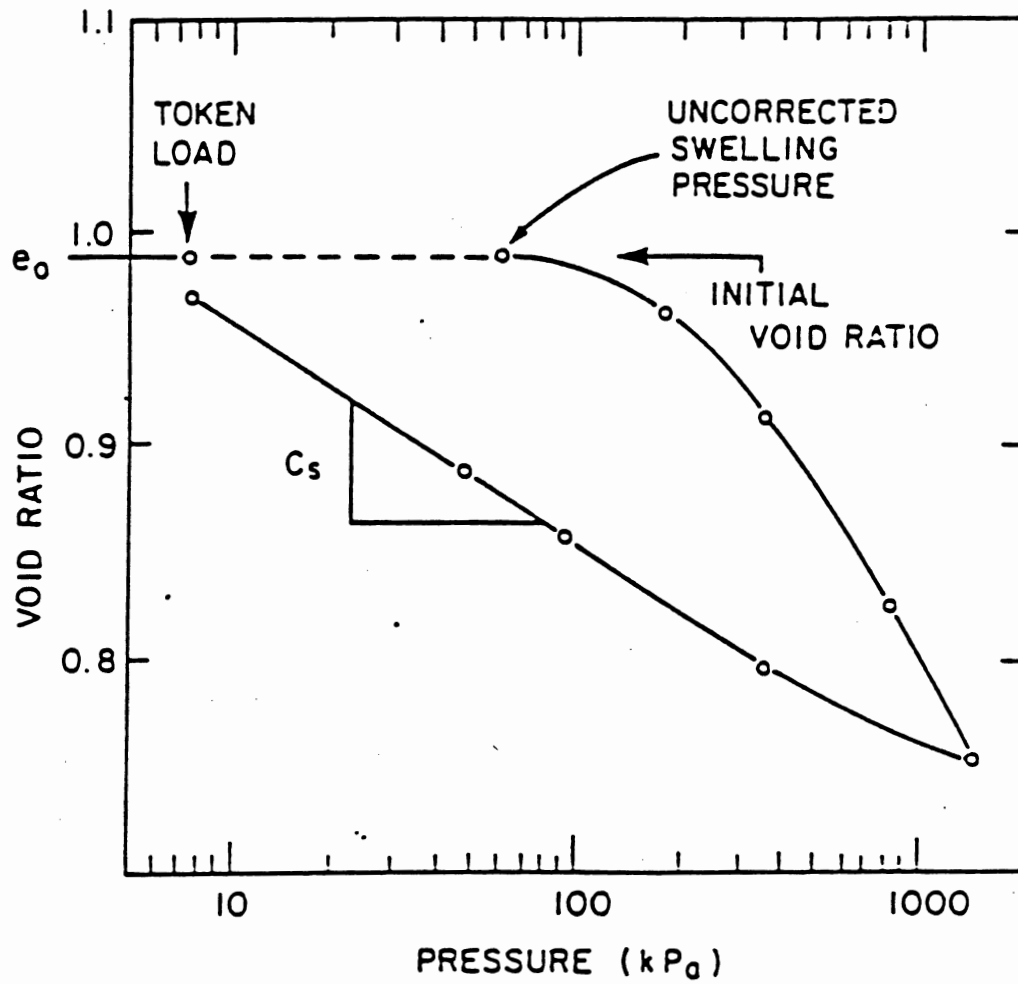


Figure 2.23. Typical Constant Volume Oedometer Swell Test Results [Fredlund, 1983]

where p_f is the final stress state, $\sigma + \Delta\sigma - u_{wf}$; p_0 is the initial stress state, equal to the corrected swelling pressure, p_s ; and C_s is the slope from the rebound curve of oedometer tests.

The concept of the constant volume oedometer method is based on the assumption that in-situ suction is transferred onto the saturated effective stress plane within the constant volume plane. The stress paths of the in-situ and consolidation testing situation are shown in Figure 2.24. The transferred stress is called the "matric suction equivalent" and is generally less than the in-situ matric suction (Hamberg, 1985).

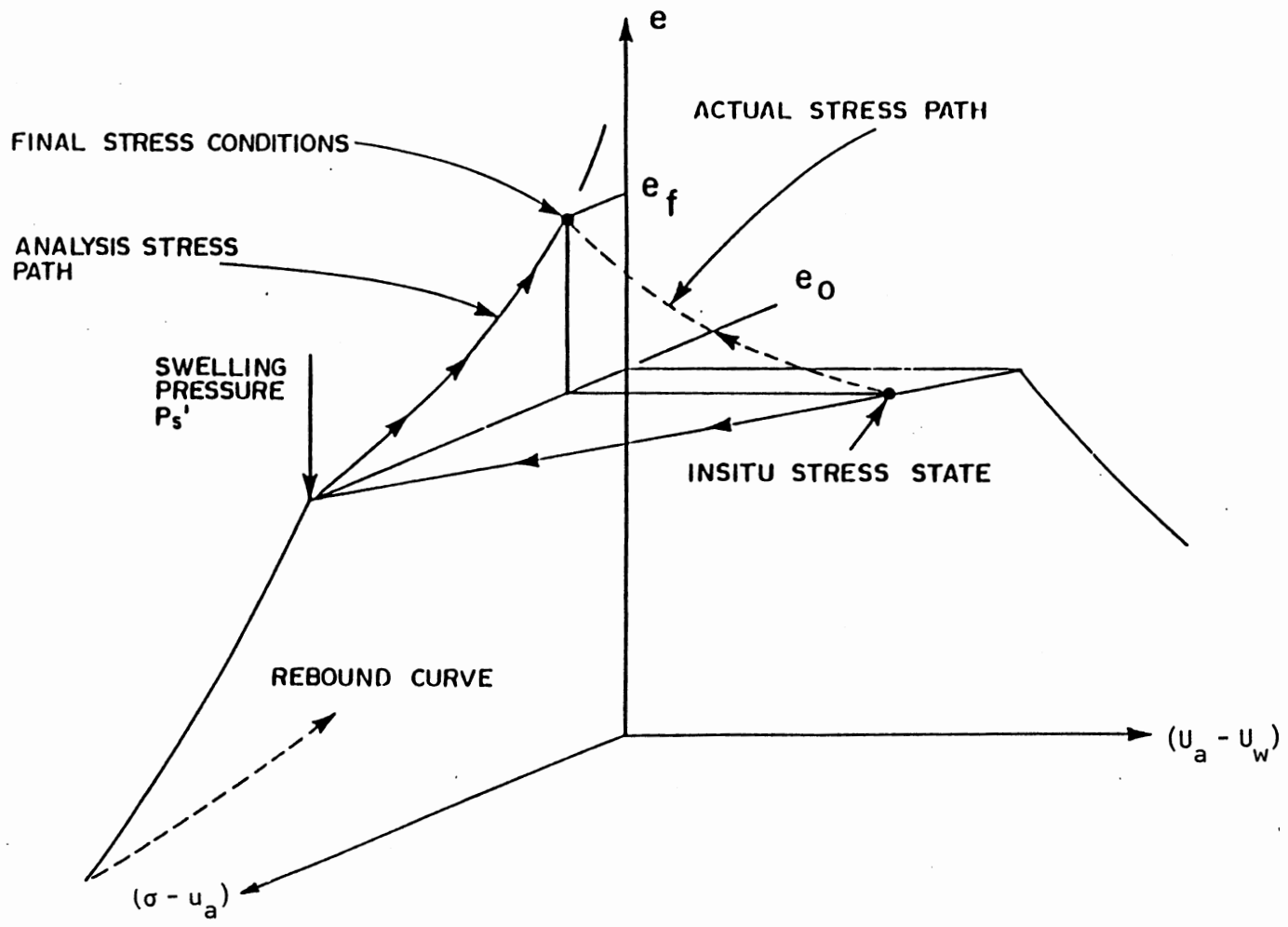


Figure 2.24. Stress Paths Representing Swelling of Soil [Fredlund, 1983]

CHAPTER III

SITE INVESTIGATION

3.1 Site Description

3.1.1 Location and Site History

Location. The soil investigated in this study was sampled from the site near Wynnewood in southern Oklahoma, approximately 8 miles south of Pauls Valley, Oklahoma (Garvin County). The site is located approximately 100 ft southeast of the I-35 and SH 17A junction. Samples were taken from the east verge slope of the northbound lane of I-35 (600 ft west of NE corner of section 29, T2N, R1E) (Figure 3.1).

Site Description. The sampling site is located in an at-grade section. Drainage is in a southerly direction on a moderate slope. The surrounding area has a complete grass cover with a sparse tree cover along both sides of the freeway (Figure 3.2). The pavement was badly damaged during the past 20 years.

3.1.2 Site Geology

The sampling site is located in the South Great Plain section of the Great Plains Physiographic Province. Samples were taken in the Pontotoc Group of the Permian-Pennsylvanian System which consists of interstratified limestone and shale with sandstone and coal (Hicks, 1956; Patrick and Snethen, 1976). The shales in the Pennsylvanian System may contain mixed layer illite-montmorillonite minerals. Argillaceous rocks of the Pennsylvanian age in Oklahoma are covered by the Permian System. Permian Red Beds are widespread in this area. The overall lithology of the Permian is mixed. Compositionally "Red Bed" is one of the two

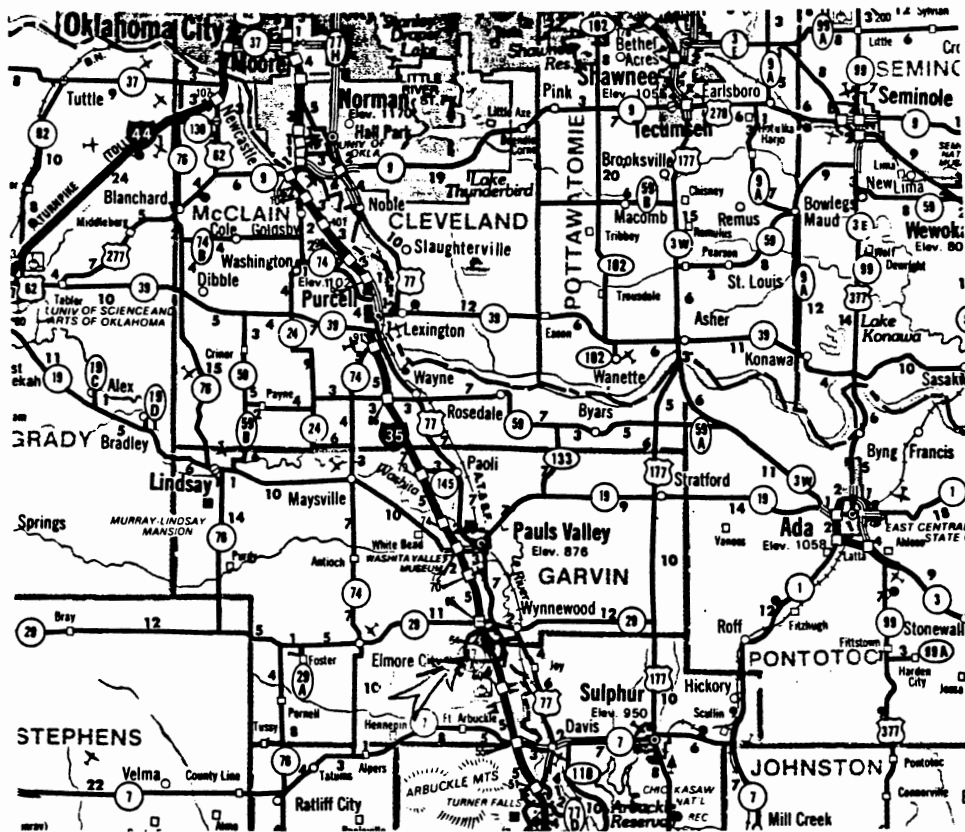


Figure 3.1. Location of Sampling Site

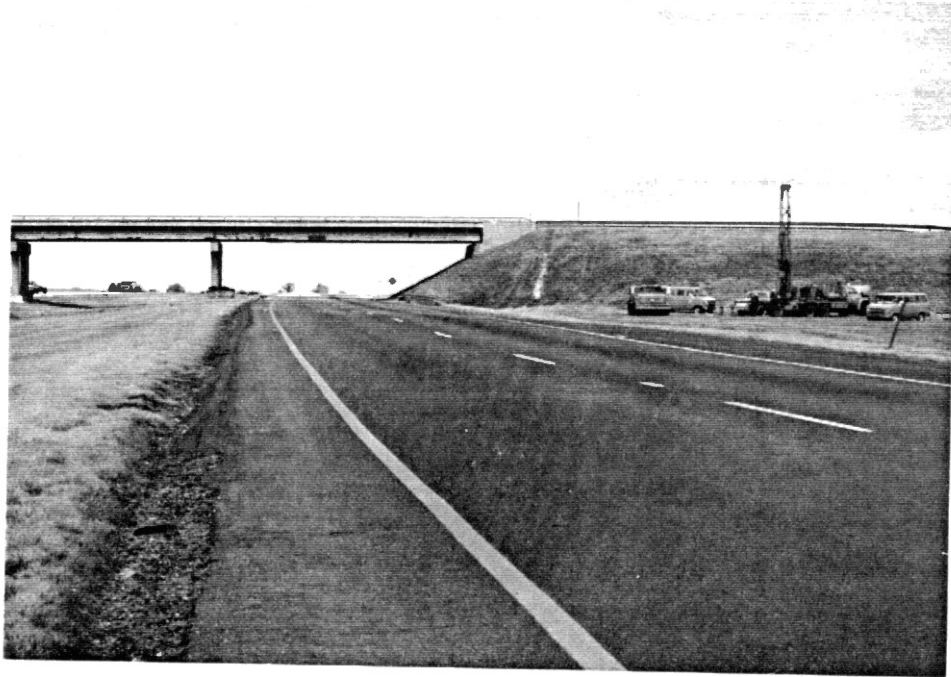


Figure 3.2. Photographs Taken at the Site

predominant associations and consists of red shale, sandstone carbonate, and evaporite.

The surface layer is the Wellington formation, Leonardian series, which is about 500 feet thick and consists of interbedded red shales and red, grey, or black shaly sandstones. The formation is overlain by the Garber sandstone and the Hennessey shale and underlain by a series of red beds, arkosic sandstones, limestones, and limestone conglomerates of the Stratford formation. Drainage is into the Washita River which flows generally southeastward across Garvin County (Yong,1960). The geological formation of the soil in Garvin County, Oklahoma, is shown in Figure 3.3 based on the Soil Survey (1985) presentation, which is modified from Hart (1974).

3.1.3 Description of Climate

The climate of Oklahoma is a mostly continental type. Warm, moist air moving northward from the Gulf of Mexico exerts much influence at times, particularly over the southern and more eastern sections of the state where, as a result, humidity and cloudiness are generally greater and precipitation is considerably heavier than in the western and northern sections. Summers are long and occasionally very hot. Winters are shorter and less rigorous than those of the more northern Plains states. Periods of extreme cold are infrequent.

Based on the weather data recorded at Pauls Valley in the period 1951 to 1977, the average temperature is 45°F and the average daily minimum temperature is 32°F in winter. The average temperature in summer is 82°F and the average daily maximum temperature is 95°F.

The total annual precipitation is 33 in. Of this, 21 in., or 63%, usually falls in April through September. In 2 years out of 10, the rainfall in April through September is less than 9 in. The average relative humidity in mid-afternoon is about 50%. Humidity is higher at night, and the average at dawn is about 80%. The prevailing wind is from the south-southwest. Average wind speed is highest, 15 mph, in spring. Detailed information about temperature and precipitation is listed in Table 3.1.

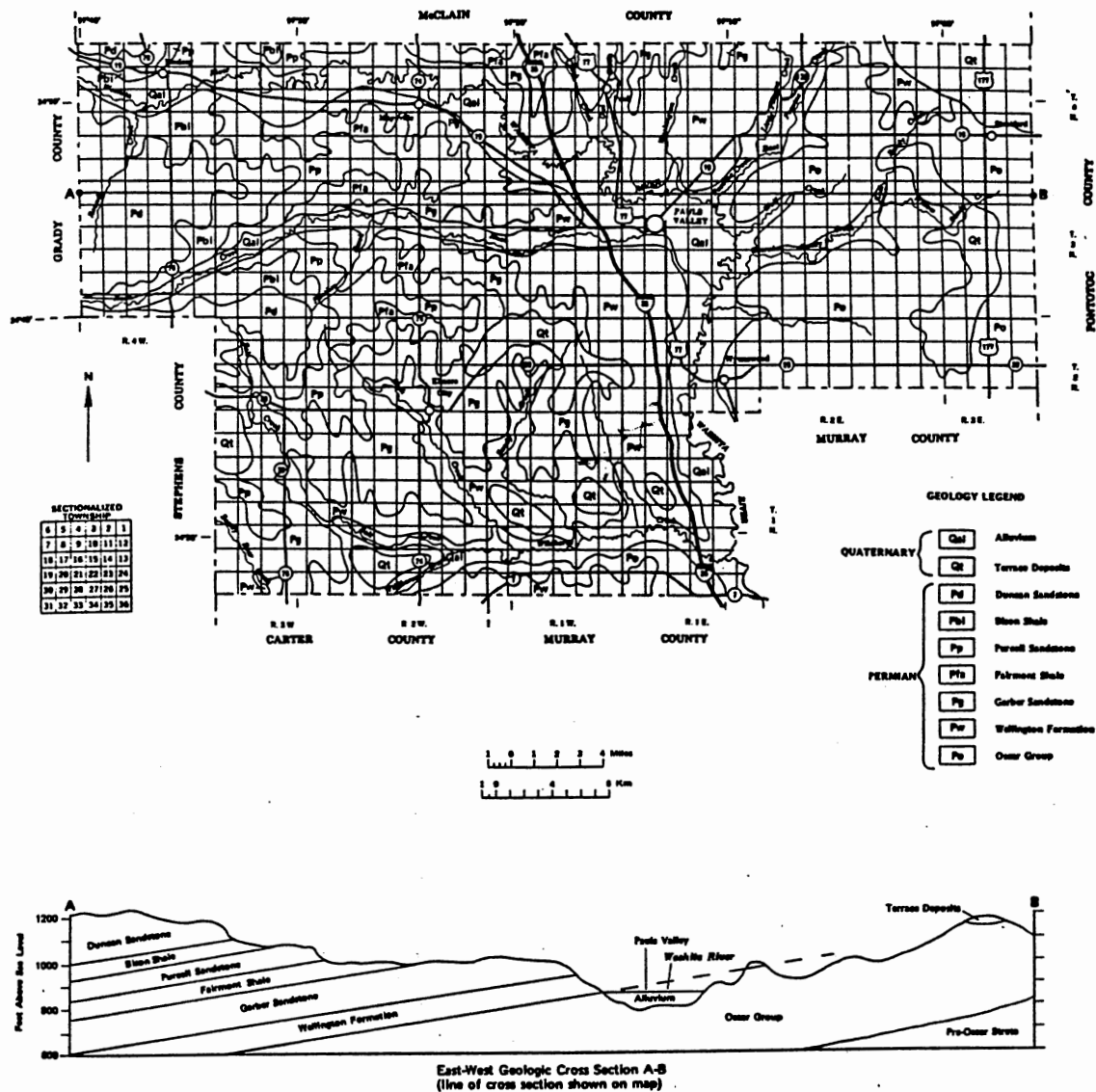


Figure 3.3. General Geology of Garvin County, Oklahoma

TABLE 3.1
TEMPERATURE AND PRECIPITATION*

Month	Temperature						Precipitation				
	Average Daily Maximum (°F)	Average Daily Minimum (°F)	Average (°F)	2 Years in 10 Will Have—		Average Number of Growing Degree Days [‡]	Average (In)	2 Years in 10 Will Have—		Average Number of Days With 0.10 in. or More	Average Snowfall (In)
				Maximum Temperature Higher Than— (°F)	Maximum Temperature Lower Than— (°F)			Less Than— (In)	More Than— (In)		
Jan.	51.9	27.6	39.8	77	2	21	1.29	0.25	2.09	3	2.5
Feb.	58.1	32.2	45.2	82	11	52	1.46	0.68	2.10	4	1.8
Mar.	65.7	39.6	52.6	91	16	192	2.30	0.97	3.37	5	1.1
Apr.	75.9	50.7	63.3	94	27	399	3.52	1.72	4.98	6	0.0
May	83.1	59.3	71.2	97	40	657	5.22	2.54	7.41	7	0.0
June	91.2	67.7	79.5	102	51	885	3.18	1.37	4.64	5	0.0
July	96.3	71.5	83.9	107	57	1051	2.46	0.99	3.65	4	0.0
Aug.	96.1	70.0	83.1	107	57	1026	2.46	0.81	3.77	4	0.0
Sept.	88.0	62.7	75.4	103	42	762	3.85	1.27	5.92	5	0.0
Oct.	77.5	51.0	64.3	95	30	443	3.72	0.96	5.92	5	0.0
Nov.	64.0	38.9	51.4	84	17	127	2.07	0.53	3.31	4	0.3
Dec.	54.4	30.8	42.6	77	7	21	1.72	0.58	2.63	3	2.2
Year	75.2	50.2	62.7	109	0	5636	33.25	25.77	40.73	55	7.9

*Based on data recorded in the period 1951-1977 at Pauls Valley, Oklahoma.

‡A growing degree day is a unit of heat available for plant growth. It can be calculated by adding the maximum and minimum daily temperatures, dividing the sum by 2, and subtracting the temperature below which growth is minimal for the principal crops in the area (50°F).

3.1.4 Soil Profile

Soil Survey. Based on the information from the *Soil Survey of Garvin County, Oklahoma* (1985), the soil taken from the sampling site is categorized as Bethany Series which consists of deep, well drained, slowly permeable soils on broad smooth ridge tops of uplands with very gentle slope (0 to 3%). These soils formed in material weathered from alluvium under a cover of tall prairie grasses. The A1 horizon (0 to 10 in.) is generally dark to very dark greyish brown moist silt loam with many fine roots. It is slightly acid. The B1 horizon (10 to 20 in.) is dark greyish brown moist clay loam or silty clay loam with moderate fine subangular blocky structure. The B2 horizon (20 to 60 in.) is dark brown to pale brown mottled with reddish or yellowish brown, firm to hard moist clay, neutral to moderately alkaline. The B3 horizon (60 to 80 in.) is reddish yellow mottled with pale brown, firm to hard, moist silty clay loam.

Sample Description. According to ASTM D2488-84, the soil is mainly tan, moist, firm clay down to the depth of 2 meters (6.7 ft) with the top 15 cm (0.6 ft) being sandy silt. Soil color then turns to brown mottled with tan and gradually changes to grey mottled with brown with soil texture and moisture being the same to the depth of 2.7 m (8.7 ft). Beyond that the soil is identified as reddish brown, moist, firm silty clay or clay. Information of soil description and identification can be found in Table 3.2.

TABLE 3.2

IDENTIFICATION AND DESCRIPTION OF SOILS

Depth (Ft)	Description	Soil Type
0.0 to 0.5	Dark Brown, Moist, Soft	Sandy Silt
0.5 to 6.5	Tan, Moist, Firm	Clay
6.5 to 9.0	Brown, Moist, Firm	Clay
9.0 to 11.0	Reddish Brown, Moist, Firm	Clay

3.2 Sampling

For almost any geotechnical project, subsurface exploration is essential to define soil profiles within a construction site. Information of soil layer variation and ground-water elevation is very useful for geotechnical engineers to foresee the potential problems that may be posed on a structure to be built on such soil. The sampling techniques are the basic component for good exploration.

The proper interpretation of exploration data is extremely beneficial for light structures, such as highway pavement and residential construction, built on expansive soils. The difficulties of sampling undisturbed expansive soil may be listed as variation of consistency, wide range of moisture content and structural discontinuities, particularly in the upper layer, such as fissures, cracks, and bedding planes. Because of all these field-related problems, different sampling techniques must be employed to keep the sample disturbance minimal.

Depending on the nature of the soil properties that are to be determined in laboratory, appropriate sampling technique may be applied. For example, auger borings are often used to obtain information for classification purpose. These include specific gravity, grain size distribution, Atterberg Limits, etc. Disturbed samples from auger borings are adequate for those tests. Undisturbed samples, on the other hand, are required for soil suction, oedometer swell, and swell pressure tests. Push tube samplers are often used for this purpose. The expansive soil samples should be taken in the driest season of the year in order to predict the maximum possible heave towards saturation of the soil.

According to *Climatological Data, Oklahoma* (1991), precipitation in February and March, 1991, was well below normal and less than 30% of the total for the same period of the previous year. During February 7 to March 16, 1991, there was no precipitation reported at the Pauls Valley weather station, which is about 9 miles from the sampling site. Average maximum daily temperature in March, 1991, was 69.4°F; the highest temperature recorded was 92°F on March 5, 1991. Samples were taken

on March 7, 1991. Based on the information, the samples represent low moisture conditions for the soil in the field. Six boreholes were drilled and relative position and distance reference to Hole No. 1 (hand auger) are shown in Figure 3.4.

3.2.1 Undisturbed Soil Sampling

The undisturbed soil samples in this study were taken by pushing thin-wall seamless steel sampling tubes into the ground with a hydraulic ram mounted on a mobile drilling rig (Figure 3.5). The samples were obtained by the Oklahoma Department of Transportation (ODOT). The sampling tubes which were used are described in Table 3.3.

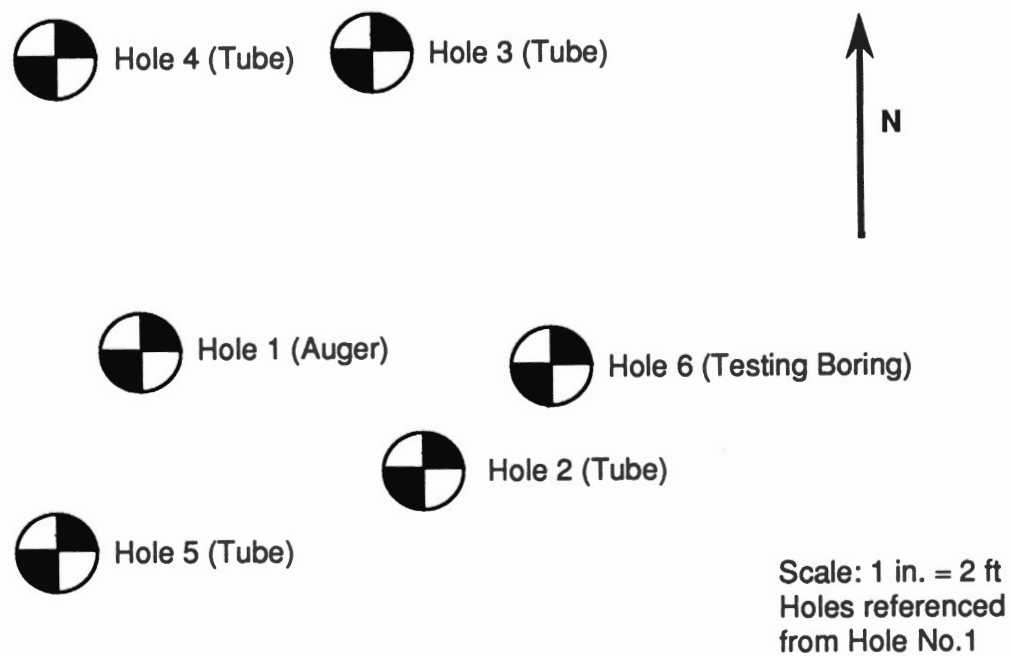
TABLE 3.3
CHARACTERISTICS OF
SAMPLING TUBE

Dimension	Size (In.)
Outside Diameter	3.00
Inside Diameter	2.86
Wall Thickness	0.07
Length	16.00
Sample Length	4.2 to 9.6

The samples were sealed at the both ends of the push tube with aluminum foil and plastic caps so that the moisture loss was negligible. They were taken on March 7, 1991, and shipped to the Civil Engineering Soils Laboratory at Oklahoma State University (OSU). During March 18-21, 1991, the samples were extruded, waxed



(a)



(b)

Figure 3.4. Position of Six Sampling Boreholes

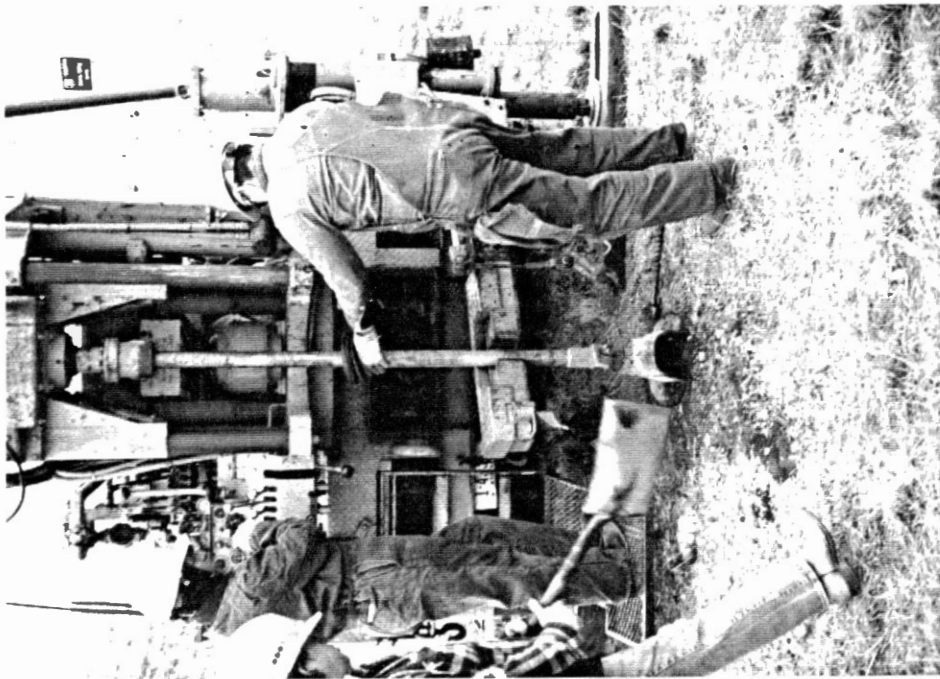
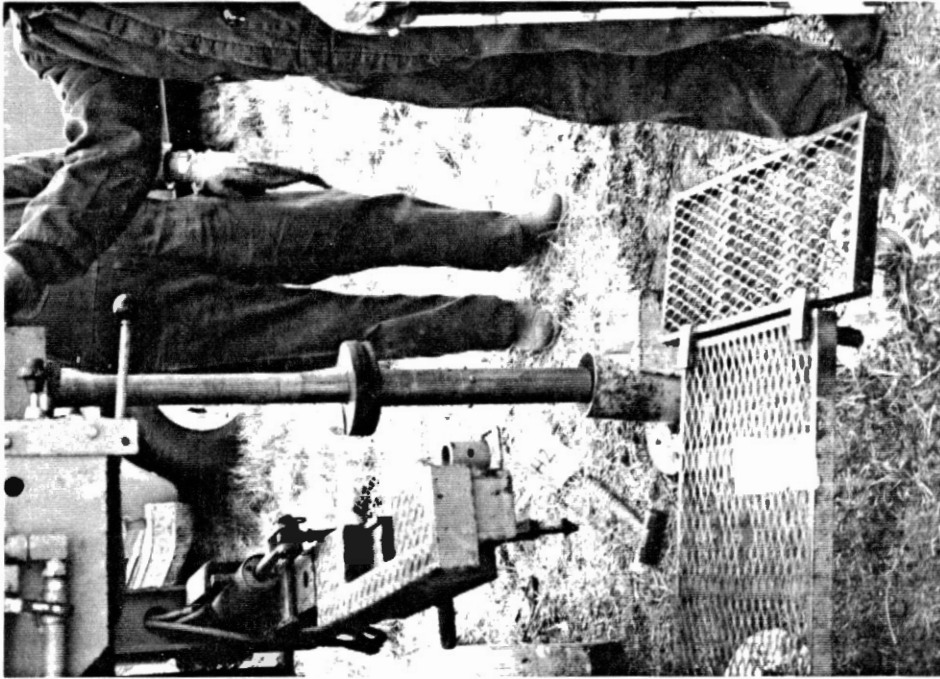


Figure 3.5. Sampling Equipment

and stored within 100% relative humidity room. The initial moisture contents of the samples were determined during this process. Drilling fluid was not used during the sampling so that moisture contents of the samples were representative of the field situation at the time of sampling.

Sampling disturbance is unavoidable due to the friction between the sampler and the soil and the stress relief after the sample is extruded from the tube. The friction may be reduced by keeping the sampler straight as well as applying a light coat of lubricant on the inner surface of the sampling tube. However, stress relief of the soil is difficult to minimize and as a result volume change may occur because of particle reorientation of the sample. The suggestions for restricting this type of disturbance is cutting the soil sample directly from the sampler or using a sampler consisting of a series of rings (Snethen et al., 1975). In the case of soil suction measurement in this study, specimens were cut immediately upon the extrusion of samples from the push tube. However, specimens for oedometer tests were stored after sample extrusion. Information on the effects of storing samples of expansive soil prior to testing is extremely limited and requires further clarification.

3.2.2 Disturbed Soil Sampling

A hand auger boring was used to collect disturbed samples for borehole No. 1. Disturbed samples were also taken from boreholes No. 2 through No. 5. The soils were then sealed in 1.75-mil Ziploc bags and transported along with the undisturbed samples to the Oklahoma State University Soils Laboratory. The samples were taken between undisturbed samples at a variety of depths through the profiles down to 11 ft. The natural water contents of the samples were determined immediately after they arrived at the OSU Soils Laboratory.

3.3 Initial Soil Conditions

Natural soil conditions at the time of sampling were important input data for all heave prediction methods. The moisture content and soil suction determine the amount of swell that will occur as the assumed final conditions are reached. Soil

properties such as void ratio and dry density influence the amount of swelling. The following sections present the test data describing the initial soil conditions that were used for all calculations involved in the different heave prediction methods.

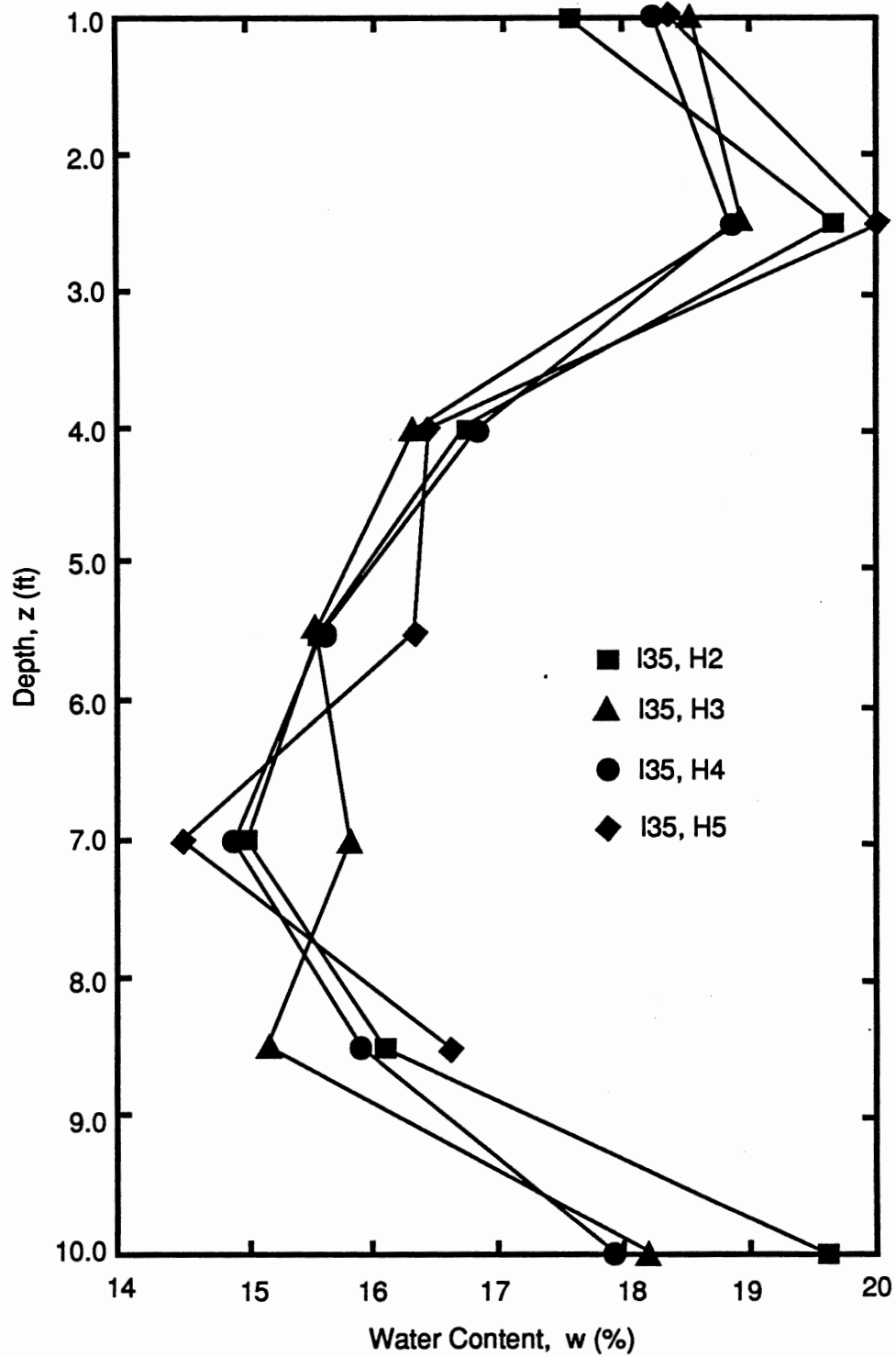
3.3.1 Moisture Content Profile

Soil moisture contents were taken from both undisturbed and disturbed samples for boreholes No. 2 through No. 5, and from hand auger samples for borehole No.1. The initial moisture content profile established from the moisture content determination is in very good agreement across all boreholes and between undisturbed and disturbed samples. This along with the description and identification of the soils (Table 3.2) indicates uniform distribution of soil layers with depth. The moisture content profile from hand auger samples (borehole No. 1) matched the other profiles very well for the top 6.5 ft of soil but shows wetter conditions below 6.5 ft. The moisture content profiles from undisturbed and disturbed samples are shown in Figure 3.6. The tabulated results can be found in Table A-1 of Appendix A.

It was observed during sampling that water was encountered at a depth of approximately 10 ft. This is reflected from the moisture content profile of undisturbed samples. The moisture content increases dramatically from 9 to 10 ft. This is not shown in the moisture content profile of disturbed samples since the soil was not collected below 9 ft.

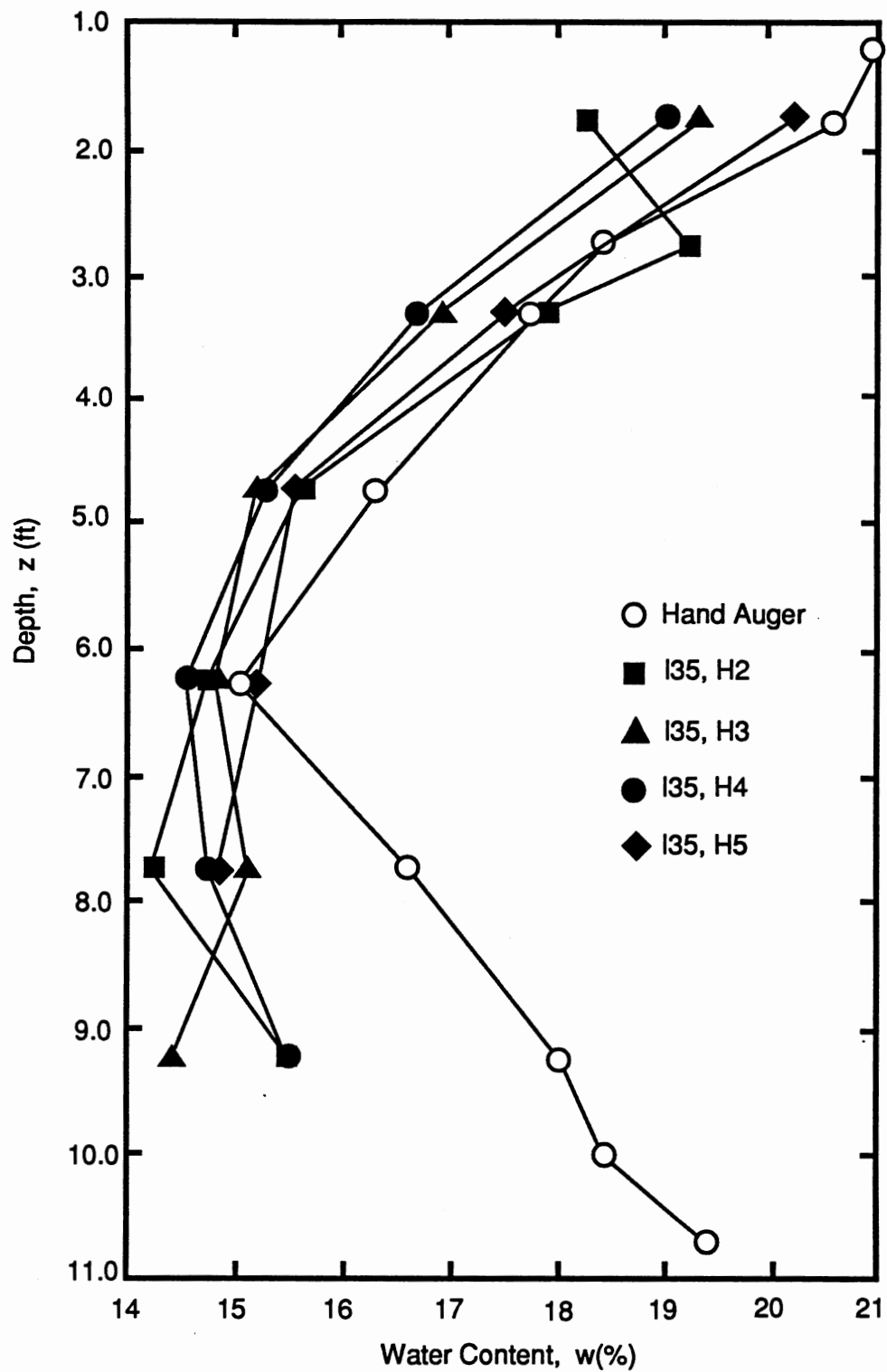
3.3.2 Soil Suction Profile

The initial soil suction was measured for undisturbed samples from boreholes No. 2 through No. 5 by the filter paper method following the procedure outlined by the ASTM Standards (1990). As can be seen in Figure 3.7, soil suction measurements tend to be scattered from hole to hole. This is expected because soil suction is much more sensitive to the condition of the sample than moisture content. Similar trends were also reported by other investigators (Hamberg, 1985; McKeen, 1981; Snethen, 1980). The tabulated soil suction results can be found in Table A-1 of Appendix A.



(a) From Undisturbed Samples

Figure 3.6. Water Content Profile



(b) From Disturbed Samples

Figure 3.6. Continued

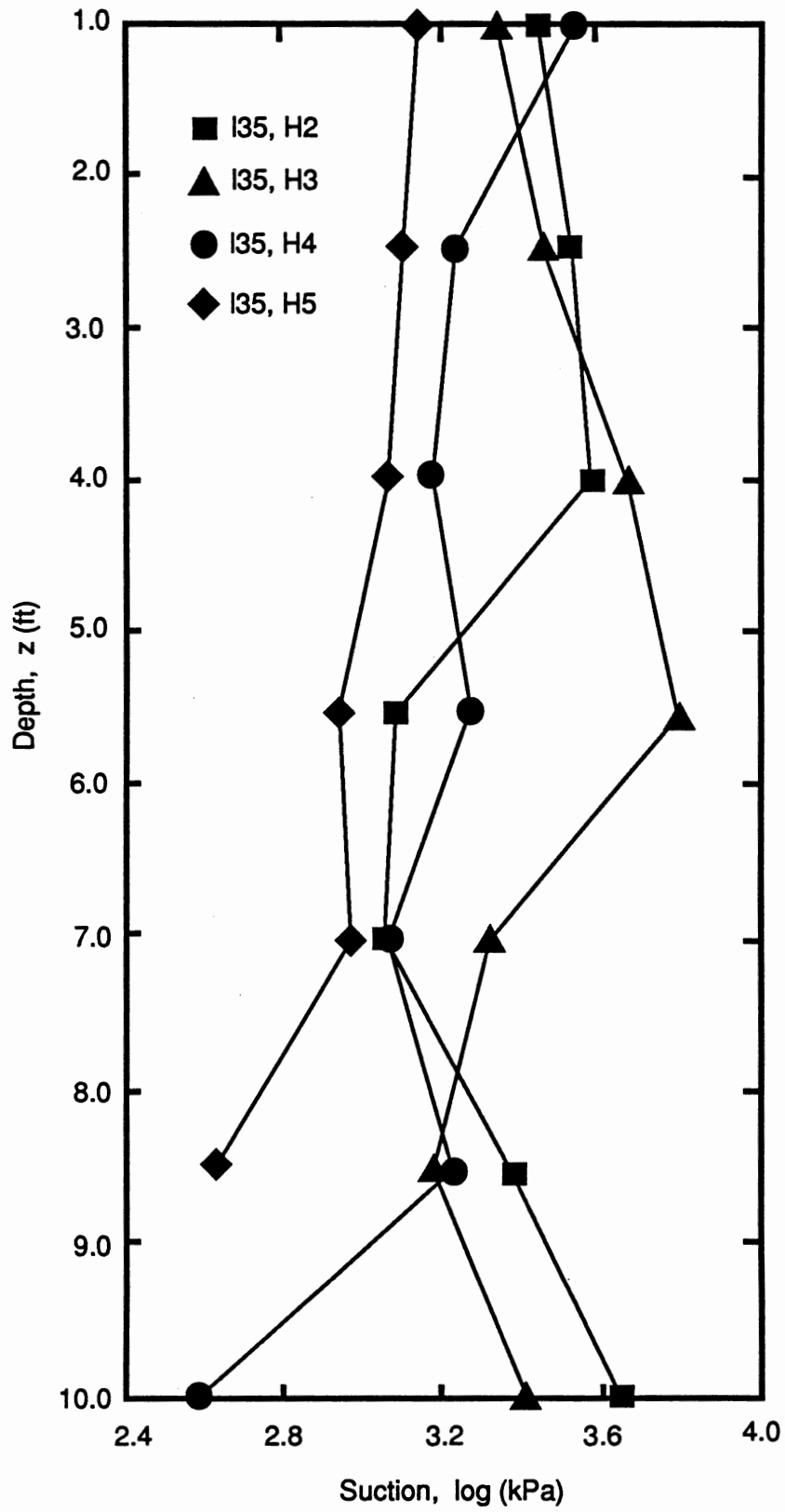


Figure 3.7. Soil Suction Vs. Depth (Undisturbed Samples)

3.3.3 Soil Properties

Soil Densities. Wet densities of the soils were measured from extruded push tube samples during the sample extrusion process and also determined from oedometer samples during the swell tests. Dry densities from both procedures were in the range of 110 to 120 pcf which is relatively high for dry density of clay soils. In general, the amount of volume change of a soil is affected by its dry density. High values of dry density indicate increasing swelling potential because of particle interaction induced by close packing of the soil particles (Snethen et al., 1975). Soil dry densities are summarized in Table A-1 of Appendix A.

Specific Gravity. Hand auger (borehole No. 1) samples were used to determine the specific gravity of the soil with depth, using ASTM Standard procedures (ASTM, 1991). The specific gravity increases with depth in a range from 2.73 to 2.79.

Void Ratio. Void ratio calculations were based on measured dry densities and specific gravities. The void ratio in the top layer (0.5 to 1.5 ft) was about 0.6 and gradually decreased with depth. The average void ratio profile for the four holes is shown in Figure 3.8.

3.3.4 Soil Characteristics

Grain Size Distribution. By visual examination the majority of the soil particles were fines. The hydrometer analysis was used to determine the silt and clay proportions. A typical grain size distribution curve is shown in Figure 3.9. The percentage of soil passing No. 200 sieve for the entire profile is greater than 50%. Clay percentages varied from 31 to 42%.

Atterberg Limits. Liquid limits were in the upper 40s for the top 3 feet of soil and gradually decreased with depth. It increased significantly at a depth of 10 ft; this along with soil identification and description indicates a change in soil characteristics at that depth. The plastic limit was approximately 16% for the top layer and gradually decreased to 11% at a depth of 10 ft; it increased below 10 ft. The Plasticity Index follows the same trend; that is, approximately 34 for the top layer and decreased to

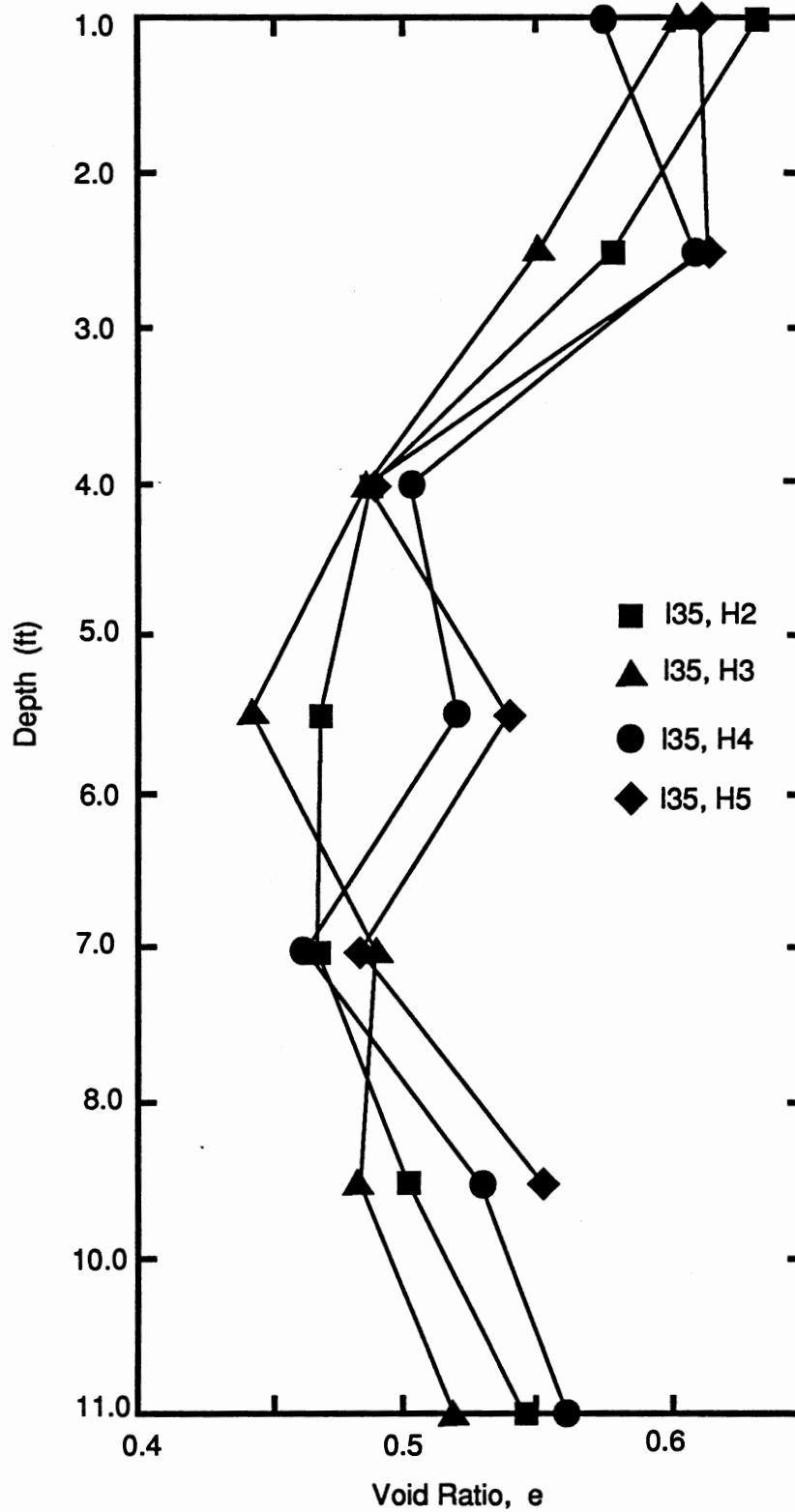


Figure 3.8. Void Ratio Profile (Undisturbed Samples)

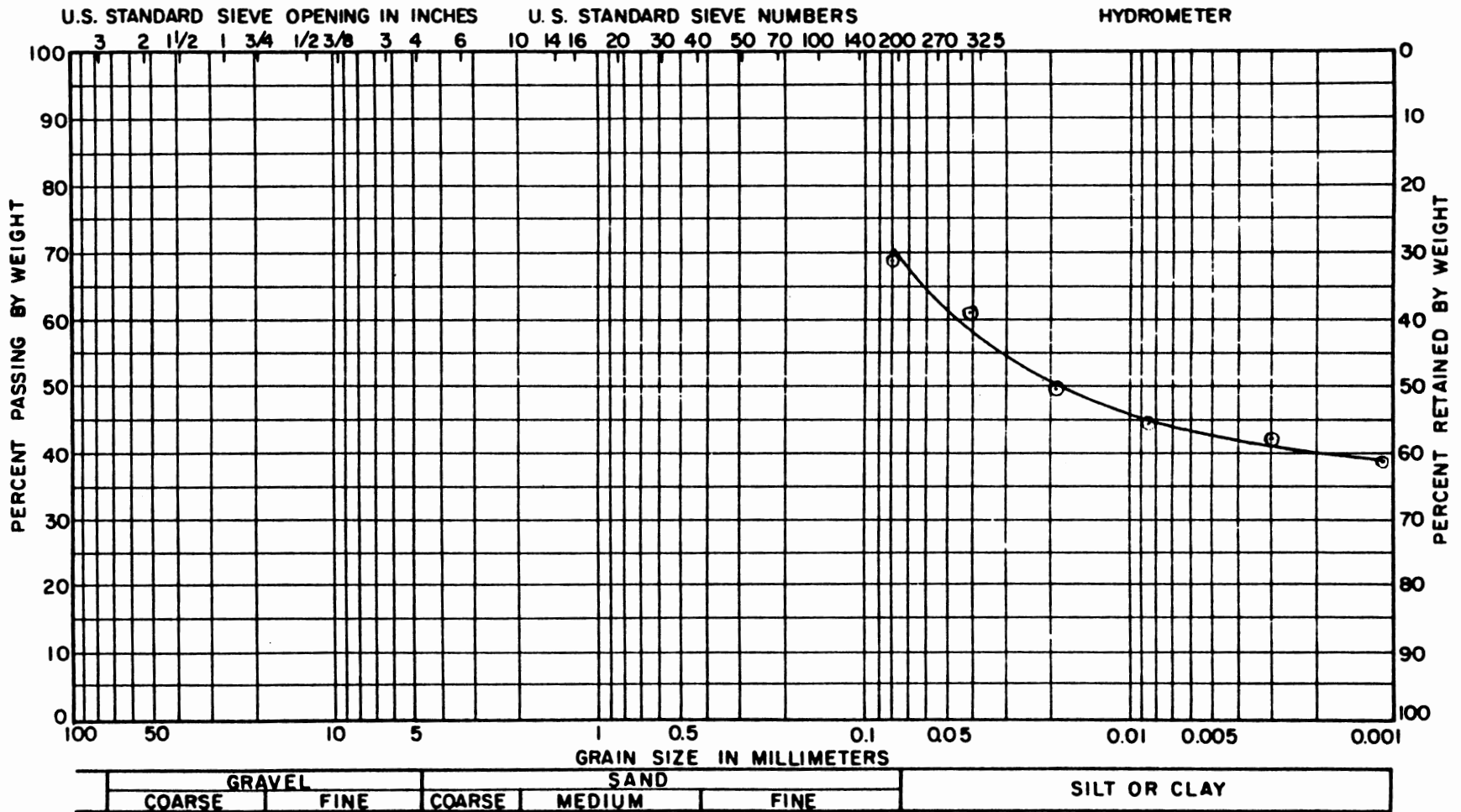


Figure 3.9. Grain Size Distribution (I-35, H1, 1.8-2.2 Ft)

13 at a depth of 10 ft. The Bar Linear Shrinkage results showed the percentage linear shrinkage was 14% for the top soil layer and decreased with depth through the profile. Based on Atterberg Limits results, the top 3- to 4-ft layer of the soil was expected to exhibit the predominant swelling potential for the study site. Data points were plotted on a plasticity chart for determining the type of clay mineral. As shown in Figure 3.10, the clay portion of the soil is predominantly montmorillonite. Complete information on Atterberg Limits, Plasticity Index, and Bar Linear Shrinkage are presented in Table A-2 of Appendix A.

Soil Classifications. Both the Unified Soil Classification System (USCS) and AASHTO methods were used. The soil is classified as clay with low plasticity (CL) by the USCS system. However, for the top 3-ft layer, data points plotted on a plasticity chart (Figure 3.10) are near the boundary line between low- (CL) and high-plasticity (CH) clays. In one case (1.8 to 2.2 ft) the soil was classified as high plasticity clay. This indicates the higher plasticity and activity of the top layer soil than the lower layer. Using the AASHTO system, the soil is classified as A-7-6(20) for the top 4-ft layer and A-6(7) for lower soil layers. Soil classifications by both methods are summarized in Table A-3 of Appendix A.

3.4 Elevation Study

The vertical differential deformation of the roadway along a 60-meter (200 ft) section was determined using a field level survey. The total differential heave along the section was 9.1 centimeters (3.6 in.). This was taken as the reference for various heave prediction methods. True field heave may be the elevation difference between the wet and dry seasons. Because of limited survey data, actual field heave was not able to be determined. The differential heave, however, represents the ground heave due to variation of the ground moisture profile.

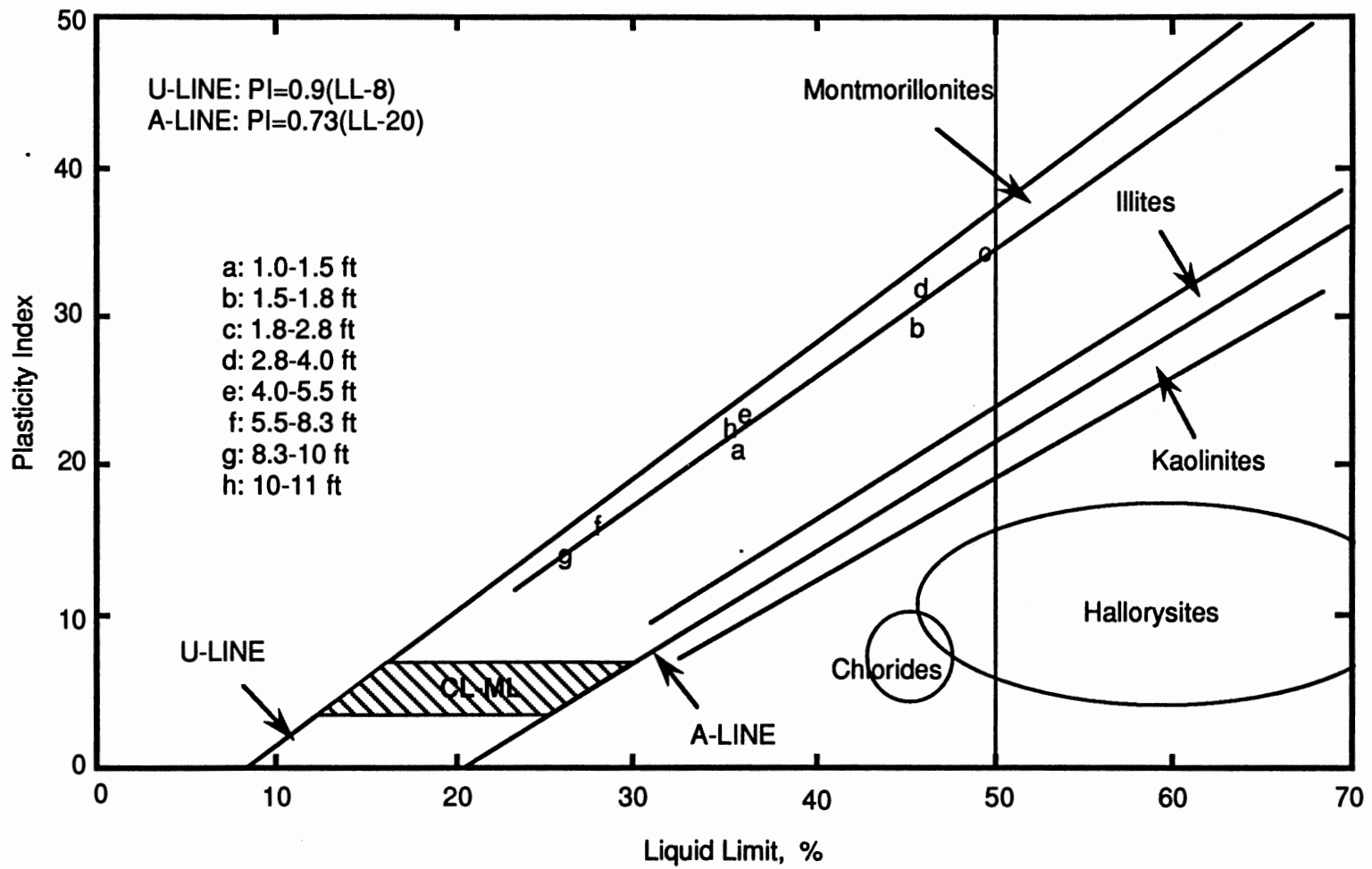


Figure 3.10. Plasticity Chart for Identifying Mineral Types

CHAPTER IV

MEASUREMENT OF SUCTION INDEX AND VOLUMETRIC PARAMETERS

4.1 Soil Suction Methods

Soil suction index is a critical factor in soil suction heave prediction methods that controls the magnitude of volume change corresponding to soil suction change or moisture content change. The suction indices were measured using three different methods (Johnson and Snethen, 1978; Nelson and Hamberg, 1980; Mitchell, 1984). The detailed procedures used in this study were as close to the original methods as possible based on research provided by the various authors. The following section presents the test results and discusses any differences between the procedures used here and the original procedures given by the authors.

4.1.1 Suction Index

Suction index is the term used in Snethen and Johnson's method. It involves the measurement of the slope of soil suction (logarithmic scale) versus moisture content curve and the slope of specific volume versus moisture content curve.

Shelby tube samples were cut into eight 2.5 centimeter (1.0 in.) thick slices; two were tested at the natural moisture content, three were wetted by adding different amounts of water, and the other three were air dried for varying periods of time so that moisture conditions were varied from dry to wet. The test procedure followed the ASTM (1990) Standard for Measurement of Soil Suction by Filter Paper Method.

Following the soil suction measurements, soil samples were coated with wax and weighed in air and water to determine their bulk densities. The actual moisture

contents were then determined. Figure 4.1 shows a typical suction versus moisture content relationship. The complete set of curves for samples from borehole No. 3 at different depths can be found in Figure B-1 of Appendix B.

Specific volume data points were plotted versus moisture content to determine the compressibility factor, α , as shown in a typical curve presented in Figure 4.2. The complete set of curves can be found in Figure B-2 of Appendix B. The complete test results are summarized in Table B-1 of Appendix B.

Parameters A and B were determined from the soil suction versus moisture content curves. The compressibility factor, α , was determined from the specific volume versus moisture content curves. The suction indexes, C_t , were calculated following Equation (2.9) and are listed in Table 4.1 for different depths.

TABLE 4.1
SUCTION INDEX FOR DIFFERENT SOIL LAYERS

Depth (ft)	A Log (kPa)	B Log (kPa)	α	C_t^* 1/Log (kPa)
0.5-1.5	9.748	0.357	0.570	0.044
2.0-3.0	7.488	0.225	0.960	0.117
3.5-4.5	7.201	0.273	0.830	0.084
5.0-6.0	5.375	0.209	0.860	0.114
6.5-7.5	6.507	0.288	0.820	0.079
8.0-9.0	4.952	0.102	0.840	0.229
9.5-10.5	6.773	0.245	0.880	0.100

$$*C_t = \alpha \cdot G_s/100B.$$

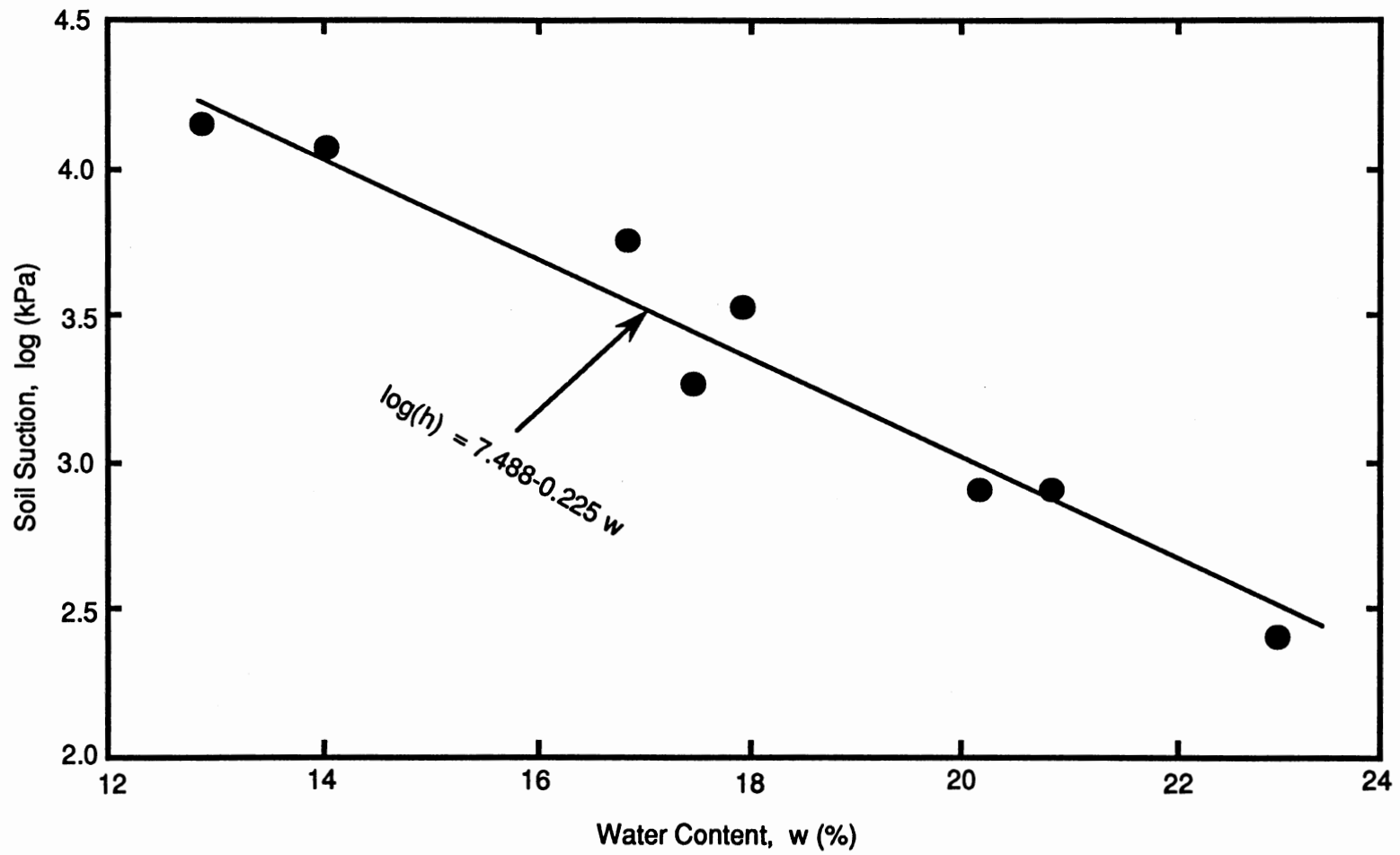


Figure 4.1. Suction Vs. Water Content (I-35, H3, 2.0-3.0 ft)

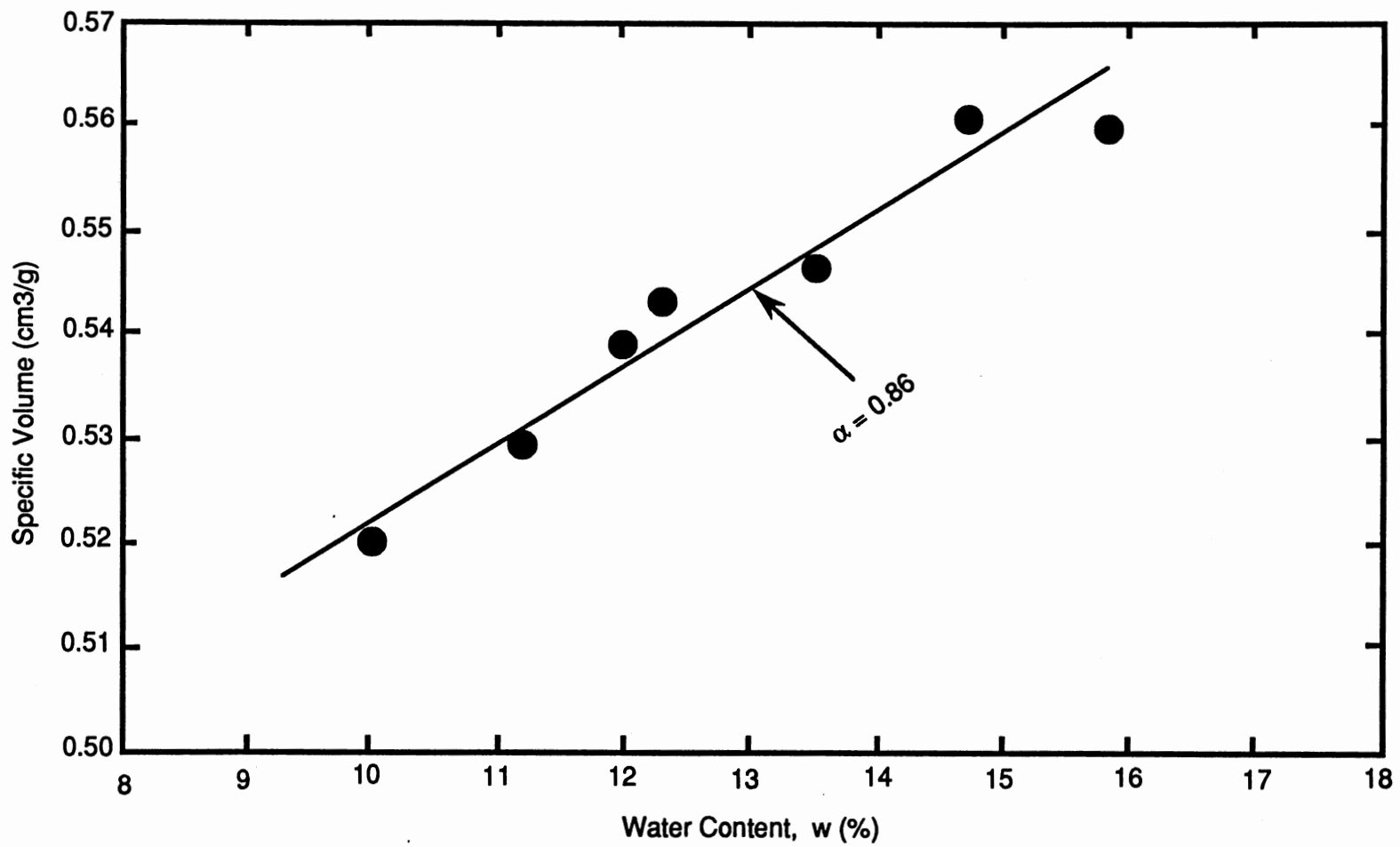


Figure 4.2. Specific Volume Vs. Water Content (I-35, H3, 5.0-6.0 ft)

4.1.2 Suction Index Ratio

The suction index ratio is the term used in Nelson and Hamberg's method. The filter paper method is used to measure the soil suction at different moisture contents, and the Clod Shrinkage Test was used to determine the slope of volumetric strain versus moisture content curve.

The undisturbed core samples were cut into 2.8 centimeter thick slices (5.1 and 10.1 centimeter sizes were also used for studying the sample size effect). The samples were air dried from their original moisture content until the sample reached relative constant volume. During the drying process, weight and volume of the sample were measured for later determination of the relationship between volumetric strain and moisture content. The sample was then oven dried to determine moisture content at different measurement times.

Cross sectional cracks were observed during the air drying process for 5.1 centimeter size samples at 2.0 to 3.0 ft and 3.5 to 4.5 ft layers. Both cross sectional and longitudinal cracks were observed for 10.1 centimeter size samples at all layers, with crack opening being maximum at the 3.5 to 4.5 ft layer and opening size up to 4 millimeters. The cracks were probably due to the nonuniform distribution of stress across the soil specimen induced by difference in temperature inside and outside of the specimen. They were also an indicator of active clay minerals.

The difference in number of cracks and opening sizes between layers at 2.0 to 4.5 ft and other layers is significant, which indicates relatively higher activity of the soil from the 2.0 to 4.5 ft layer than that of other soil layers. Cracks opened at an early stage of the drying process (about 3 to 5 hours after samples were exposed to room temperature, approximately 20°C) and closed slightly as samples were further dried.

A typical clod shrinkage curve is shown in Figure 4.3. The suction index ratio in terms of volumetric strain, C'_w , was calculated as the slope of volumetric strain versus moisture content and the suction index ratio $C_w = C'_w (1 + e_0)$. The suction index with respect to moisture content, D_h , was determined from the soil suction test described

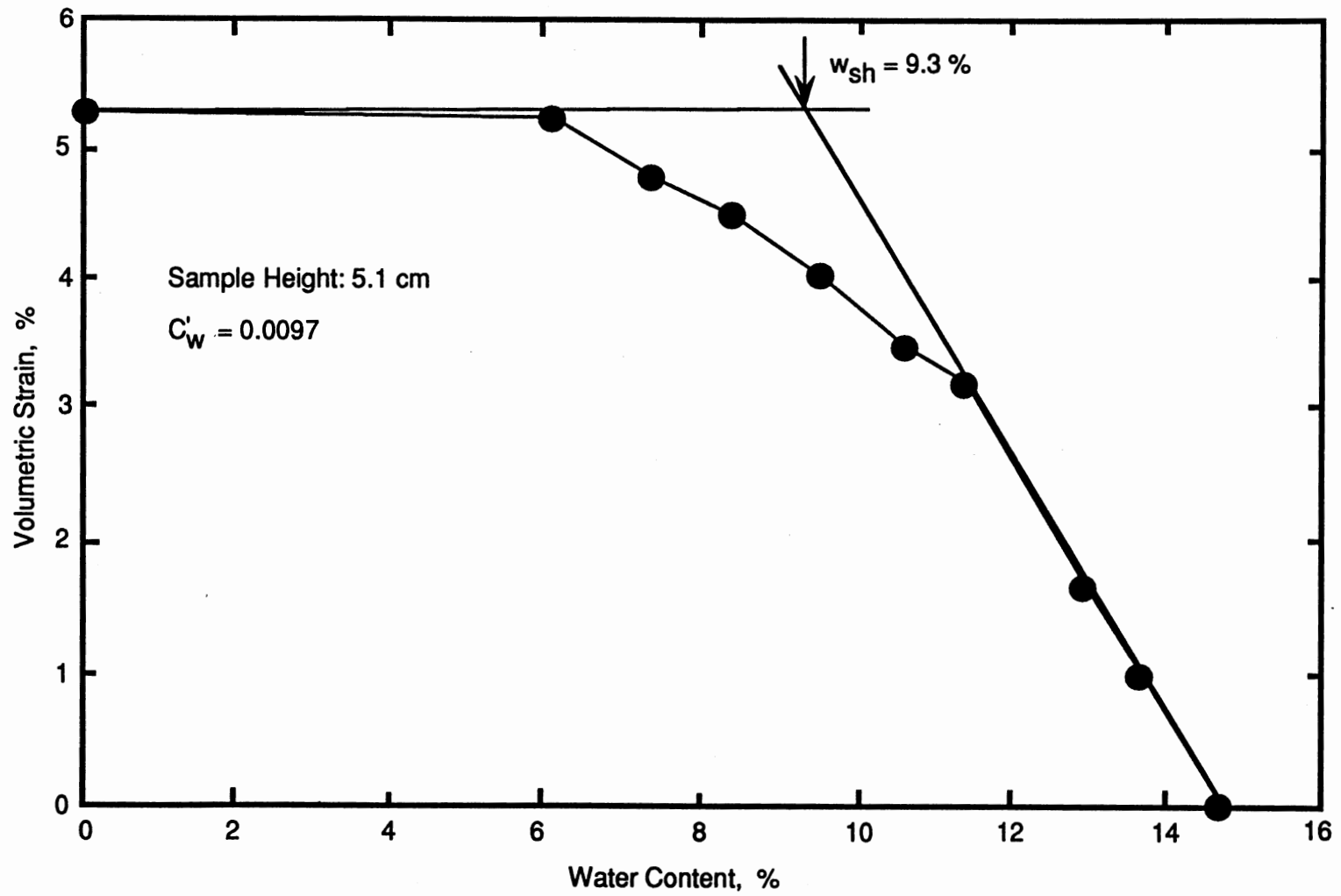


Figure 4.3. Clod Shrinkage Curve (I-35, H2, 5.0-6.0 ft)

previously. By comparing Equations (2.10) and (2.14), it was found that D_h is actually the reciprocal of the parameter B in Snethen and Johnson's method.

The Clod Shrinkage Test conducted in this study was slightly different from Nelson and Hamberg's method due to the availability of equipment. However, the same concept was followed. It was expected that the suction index ratio, C_w , from this testing procedure would be higher than that from Nelson and Hamberg's method. The Clod Shrinkage Test results for different size samples at different depths are summarized in Table B-2 and Figure B-3 (Appendix B). Suction index ratios and shrinkage limits are then determined from volumetric strain versus moisture content curves and presented in Table 4.2. The effect of sample size on the suction index ratio cannot be simply ignored from the Clod Shrinkage Test results. Increasing sample length from 2.8 to 5.1 centimeters may lead to a decrease in the suction index ratio by 50 to 100%. This will be discussed in more detail in Chapter VI.

4.1.3 Instability Index

The instability index is used in Mitchell's method and defined as the ratio of change in linear dimension to the soil suction change. The Core Shrinkage Test was used to measure the instability index. The test procedure was the same as that of the Clod Shrinkage Test except only linear change in height of the sample was measured against weight of the sample during the air drying process. Linear strain was then plotted versus moisture content to determine the slope of $\Delta H/H$ versus the ω relationship, as can be seen from a typical curve in Figure 4.4. Similar to the Clod Shrinkage Test, Core Shrinkage Test results were very much influenced by the sample size.

The moisture characteristic, c , was the same as the suction index with respect to moisture content, D_h , in Nelson and Hamberg's procedure. The complete test results and the set of linear strain versus moisture content curves can be found in Table B-2 and Figure B-3 of Appendix B, respectively. The instability indexes were calculated by using Equation (2.19) and are listed in Table 4.3 for various depths.

TABLE 4.2
SUCTION INDEX RATIO AND SHRINKAGE LIMIT

Depth (ft)	C _w	e ₀	C _w (1+e ₀)	D _h 1/log (kPa)	C _h (C _w D _h)	ω _{sh} (%)
Sample Size: D ₀ = 7.3 cm, H ₀ = 2.8 cm						
0.5-1.5	0.007	0.564	0.010	2.801	0.028	11.0
2.0-3.0	0.022	0.485	0.033	4.444	0.147	13.3
3.5-4.5	0.047	0.498	0.070	3.663	0.257	12.9
5.0-6.0	0.033	0.483	0.048	4.785	0.232	12.0
6.5-7.5	0.033	0.440	0.047	3.472	0.163	12.0
8.0-9.0	0.016	0.478	0.023	9.804	0.229	9.6
9.5-10.5	0.012	0.563	0.018	4.082	0.075	10.3
Sample Size: D ₀ = 7.3 cm, H ₀ = 5.1 cm						
0.5-1.5	0.012	0.575	0.018	2.801	0.052	10.8
2.0-3.0	0.021	0.550	0.033	4.444	0.147	12.3
3.5-4.5	0.024	0.484	0.035	3.663	0.129	11.8
5.0-6.0	0.010	0.462	0.014	4.785	0.068	9.3
6.5-7.5	0.014	0.450	0.020	3.472	0.070	9.5
8.0-9.0	0.008	0.467	0.012	9.804	0.114	7.5
Sample Size: D ₀ = 7.3 cm, H ₀ = 10.1 cm						
0.5-1.5	0.007	0.593	0.011	2.801	0.029	10.1
2.0-3.0	0.020	0.575	0.032	4.444	0.140	11.5
3.5-4.5	0.014	0.474	0.020	3.663	0.075	11.2
5.0-6.0	0.012	0.461	0.017	4.785	0.080	10.7
6.5-7.5	0.010	0.441	0.014	3.472	0.049	10.2
8.0-9.0	0.004	0.491	0.006	9.804	0.054	7.3

Note: Data at 2.0 to 3.0 ft for the 10.1 cm sample were estimated following the general trend.

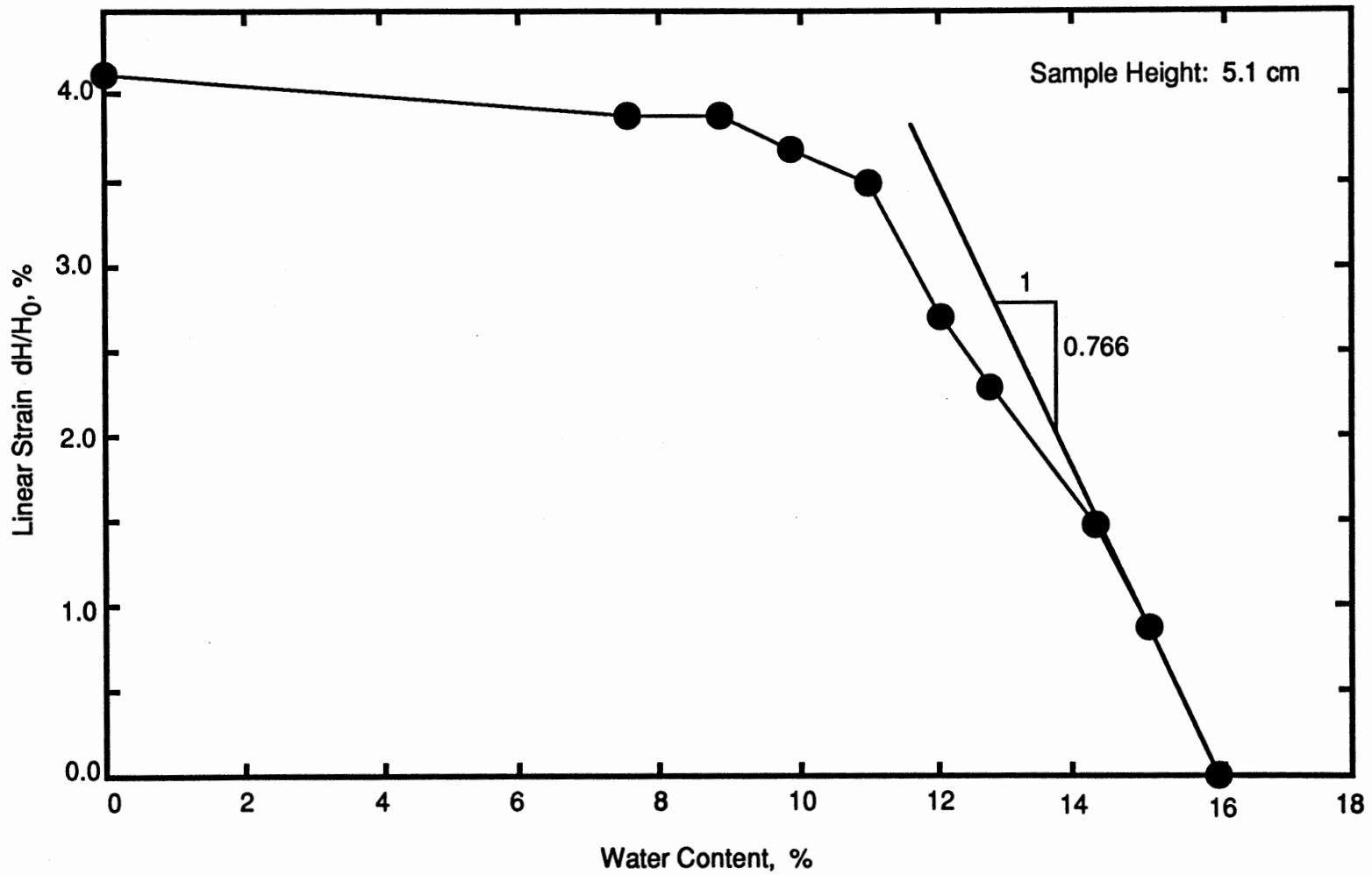


Figure 4.4. Core Shrinkage Curve (I-35, H2, 3.5-4.5 ft)

TABLE 4.3
INSTABILITY INDEX AT VARIOUS DEPTHS

Depth (ft)	$(d\varepsilon_v)/d_w$ (%)	c 1/log (kPa)	l_{pt} ($c \cdot dH/H_0$)
Sample Size: $D_0 = 7.3$ cm, $H_0 = 2$			
0.5-1.5	0.100	2.801	0.280
2.0-3.0	0.530	4.444	2.355
3.5-4.5	2.580	3.663	9.451
5.0-6.0	1.100	4.785	5.264
6.5-7.5	1.610	3.472	5.590
8.0-9.0	0.180	9.804	1.765
9.5-10.5	0.540	4.082	2.204
Sample Size: $D_0 = 7.3$ cm, $H_0 = 5$			
0.5-1.5	0.385	2.801	1.078
2.0-3.0	0.811	4.444	3.604
3.5-4.5	0.766	3.663	2.806
5.0-6.0	0.435	4.785	2.081
6.5-7.5	0.410	3.472	1.424
8.0-9.0	0.333	9.804	3.265
Sample Size: $D_0 = 7.3$ cm, $H_0 = 10$			
0.5-1.5	0.108	2.801	0.303
2.0-3.0	0.840	4.444	3.733
3.5-4.5	0.484	3.663	1.773
5.0-6.0	0.429	4.785	2.051
6.5-7.5	0.368	3.472	1.279
8.0-9.0	0.162	9.804	1.590

Note: The slope of linear strain vs. water content for the 10.1 cm height sample at 2.0-3.0 ft was measured using a 2.5 x 2.5 x 10.5 cm bar-shaped sample.

4.1.4 Suction Compression Index

McKeen's method (Equation 2.24) was used to estimate the suction compression index in this study. Based on the results of clay percentage and Atterberg Limits, the suction compression index, γ_h , is calculated using Equation (2.24) and is listed in Table 4.4.

TABLE 4.4
SUCTION COMPRESSION INDEX

Depth (ft)	P.I. (%)	Clay Activity (%)	P.I./Clay	γ_h
1.0-1.5	21.4	31	0.69	0.017
1.8-2.2	34.4	41	0.84	0.032
3.0-3.5	28.8	38	0.76	0.027
4.0-4.5	24.5	36	0.68	0.020
5.0-5.5	21.2	32	0.66	0.018
5.9-6.7	17.8	32	0.56	0.018
7.2-7.7	16.6	31	0.54	0.017
8.3-8.7	15.3	31	0.49	0.017
9.1-9.4	13.2	31	0.43	0.017
10.1-10.6	21.6	42	0.51	0.023

4.2 Oedometer Swell Method

4.2.1 Constant Volume Swelling Pressure Test

The constant volume swelling pressure tests were used to determine the swelling index, C_s , and initial stress state, p_0 (which is equal to the "corrected" swelling pressure p'_s). A typical constant volume oedometer swell test result is shown in

Figure 4.5 and Table 4.5 presents the swelling index and initial swelling pressure versus depth.

4.2.2 Overburden Swell Test

Overburden oedometer swell tests were also conducted to study the effect of external load on the swelling potential. The test results are summarized in Table 4.6.

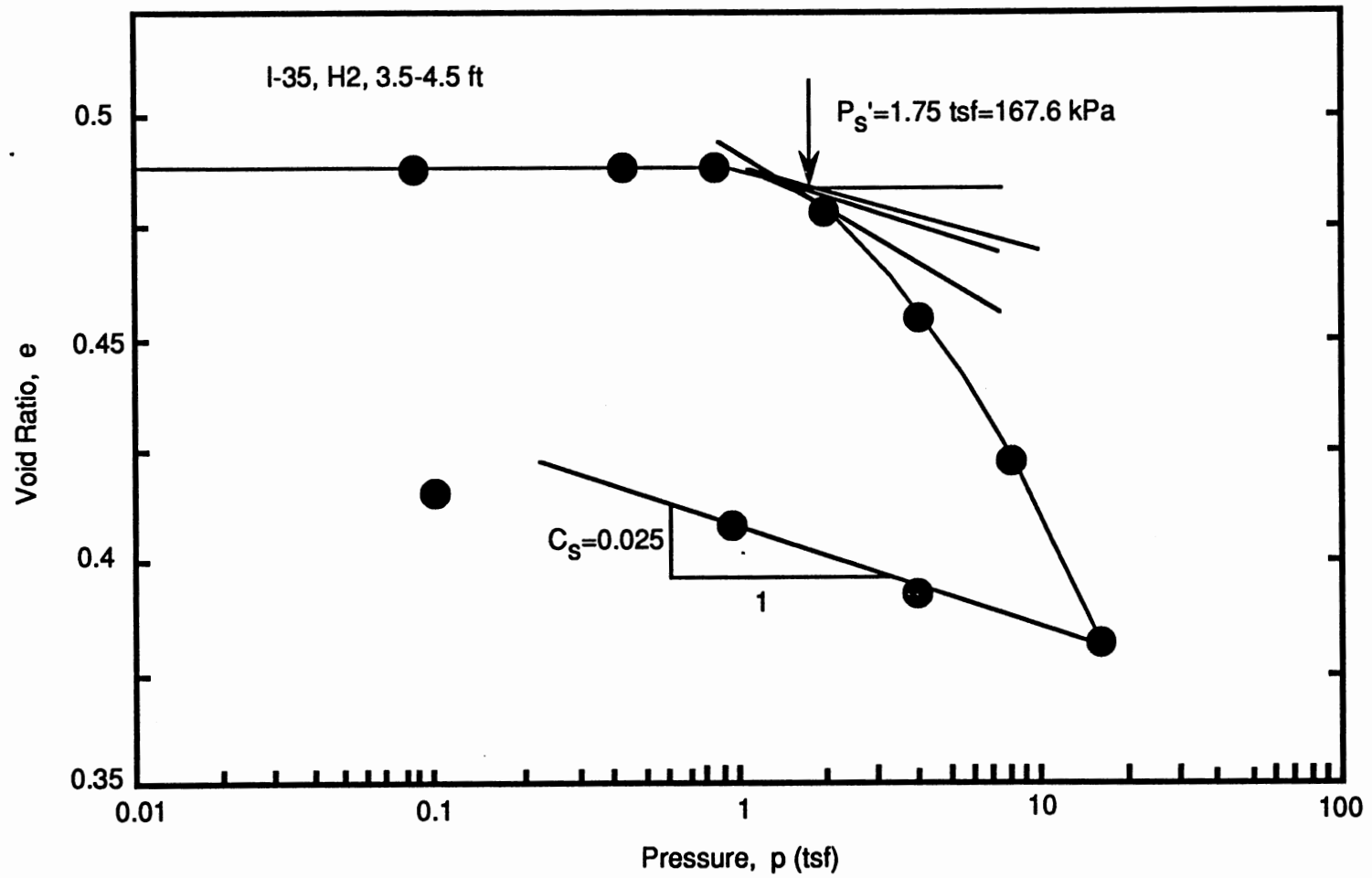


Figure 4.5. Constant Volume Swell Pressure Curve

TABLE 4.5
CONSTANT VOLUME SWELL PRESSURE AND SWELL INDEX

Depth (ft)	p_s (tsf)	p'_s (tsf)	C_s	ω_o (%)	γ_w (pcf)	γ_d (pcf)	e_o	S_o (%)
0.5-1.5	0.00	0.13	0.016	16.3	121.4	104.4	0.644	69
2.0-3.0	0.37	0.84	0.048	19.5	126.0	105.4	0.627	85
3.5-4.5	0.86	1.75	0.025	15.0	132.0	114.8	0.495	83
5.0-6.0	0.21	0.62	0.036	14.8	131.7	114.7	0.496	82
6.5-7.5	0.60	0.83	0.020	14.0	128.2	112.5	0.526	66

Assuming $G_s = 2.75$.

TABLE 4.6
OVERBURDEN SWELL TEST RESULTS (SAMPLE I-35, H5)

Depth (ft)	ω (%)	γ_w (pcf)	γ_d (pcf)	e_o	S (%)	p_o (tsf)	$\Delta H/H$ (%)
0.5-1.5	17.1	118.6	101.3	0.694	67.7	0.060	0.027
2.0-3.0	20.2	127.9	106.4	0.613	90.7	0.165	0.747
3.5-4.5	16.0	131.0	112.9	0.520	84.7	0.260	0.453
5.0-6.0	14.6	127.9	111.6	0.538	74.7	0.360	-0.107
6.5-7.5	13.5	121.7	107.2	0.600	61.8	0.455	-0.227
8.0-9.0	16.2	124.2	106.9	0.605	73.6	0.546	-0.067

Note: p_o is the overburden pressure during the swell test. Assume $G_s = 2.75$.

CHAPTER V

HEAVE PREDICTION RESULTS

The ground heave was predicted using three different types of methods: soil suction, empirical, and oedometer swell methods. The predictions were based on initial soil suction profiles at the time of sampling and assumed final suction profiles. The active zone depth was taken as 7.75 ft, which was estimated using observed characteristics of the moisture profile. Since the samples were taken during the dry season of the year, the predicted heave likely represents the maximum heave considering the seasonal change.

5.1 Soil Suction Methods

Heave prediction using soil suction methods in this study include Snethen and Johnson's, Nelson and Hamberg's, Mitchell's, and McKeen's methods. Three final soil suction profiles were assumed to study the effect of final suction on the maximum heave prediction:

1. Zero suction throughout the depth of active zone
2. Suction linearly increasing with depth through the active zone
3. Suction based on saturated water content profile.

The initial and assumed final suction profiles are shown in Figure 5.1.

5.1.1 Snethen and Johnson's Method

Maximum ground heave was predicted based on the measured initial and assumed final soil suction profiles. The following formula was used to calculate the heave:

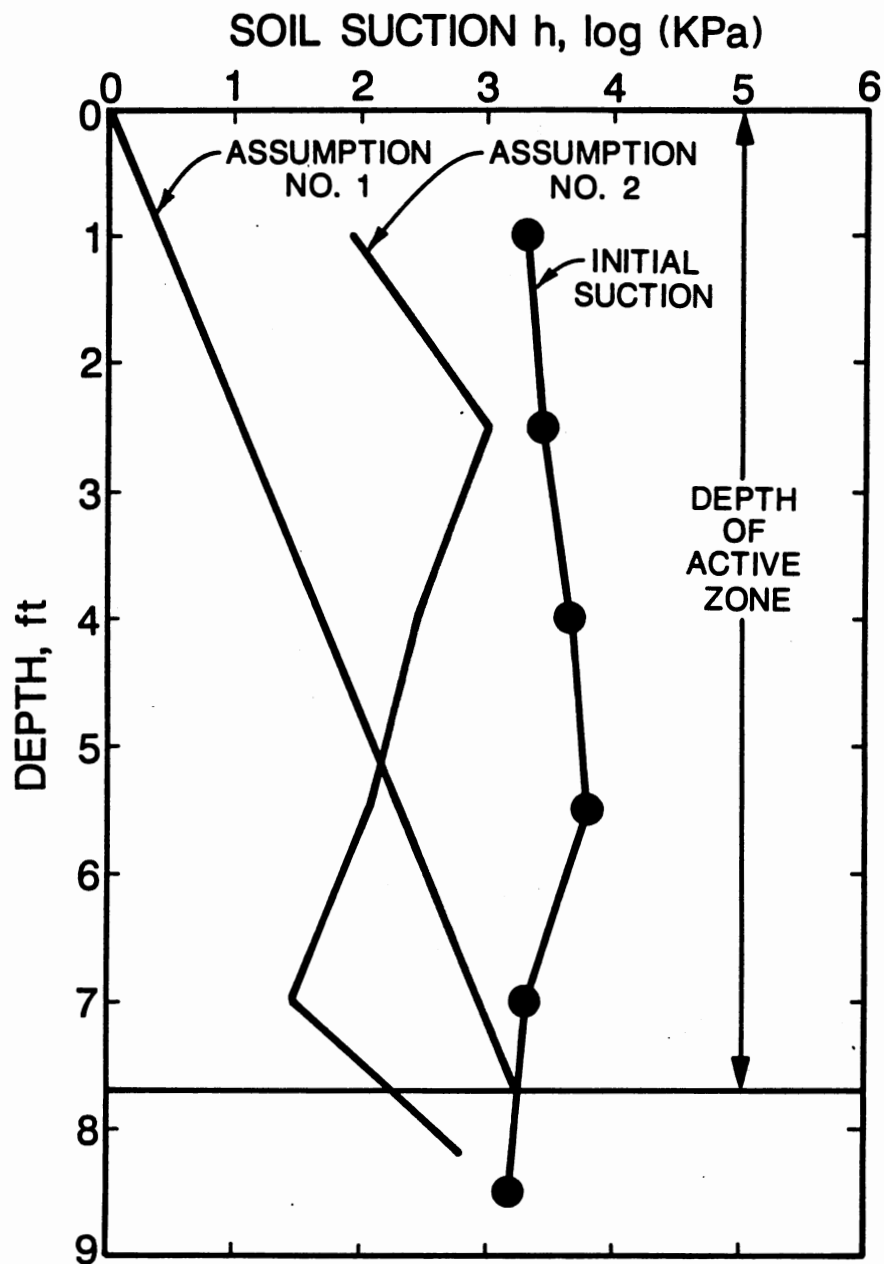


Figure 5.1. Initial and Final Soil Suction Profile

$$\Delta H = \sum_i \frac{C_\tau}{1+e_o} H_i [\log(h_o) - \log(h_f + \alpha \cdot \sigma_f)]_i \quad (5.1)$$

where

- C_τ = suction index, equal to $\alpha \cdot G_s / 100B$;
 h_o, h_f = initial and final soil suction, respectively;
 α = compressibility index; and
 σ_f = overburden pressure.

The initial soil suction was taken as $(A - B \cdot \omega_o)$ based on the measured soil suction versus moisture content relationship. For assumed final soil suction profiles (1), (2), and (3), the maximum heave is 6.0, 2.6, and 0.7 in., respectively (see Table 5.1).

TABLE 5.1
PHYSICAL AND ENGINEERING
PROPERTIES OF SOIL

Depth (ft)	e_o	C_τ	A	B	ω_o (%)	h_o (kPa)	α	σ_v (kPa)
0.60-1.75	0.600	0.044	9.748	0.357	18.5	1995	0.57	6.96
1.75-3.25	0.546	0.117	7.488	0.225	18.9	2692	0.96	15.78
3.25-4.76	0.479	0.084	7.201	0.273	16.3	4467	0.83	25.88
4.75-6.25	0.438	0.114	5.375	0.209	15.6	6026	0.86	36.52
6.25-7.75	0.485	0.079	6.057	0.288	15.8	1995	0.82	45.24

Since A and B parameters are somewhat arbitrary with regard to data interpretation, measured initial soil suction profile was an alternative for prediction

calculation. Using the actual measured initial soil suction profile directly, the maximum heave is 11.4, 7.9, and 6.1 in. with respect to the final suction profile assumptions (1), (2), and (3) (see Table 5.2).

TABLE 5.2
HEAVE PREDICTION USING SNETHEN AND JOHNSON'S METHOD

Sample Depth (ft)	Final Suction Assumption			Predicted Percent Swell and Heave (In.)					
	1	2	3	No. 1		No. 2		No. 3	
				Swell	Heave	Swell	Heave	Swell	Heave
Using $h_0 = A - Bw_0$									
0.60-1.75	0	2	79	7.0	1.0	6.5	0.9	3.4	0.5
1.75-3.25	0	11	1000	15.6	2.8	13.8	2.5	1.7	0.3
3.25-4.75	0	46	269	8.1	1.5	5.2	0.9	1.6	0.3
4.75-6.25	0	200	107	4.9	0.9	-2.0	-0.4	-0.2	0
6.25-7.75	0	871	28	-0.3	-0.1	-7.7	-1.4	-1.6	-0.3
				6.0		2.6		0.7	
Using Measured h_0									
0.60-1.75	0	2	79	7.4	1.0	6.9	1.0	3.8	0.5
1.75-3.25	0	11	1000	17.0	3.1	15.2	2.7	3.2	0.6
3.25-4.75	0	46	269	13.2	2.4	10.3	1.9	6.7	1.2
4.75-6.25	0	200	107	18.1	3.3	11.2	2.0	13.0	2.3
6.26-7.75	0	871	28	9.2	1.7	1.8	0.3	7.9	1.4
				11.4		7.9		6.1	

5.1.2 Nelson and Hamberg's Method

Ground heave was calculated using the following equation:

$$\Delta H = \Sigma [C_h \cdot H / (1 + e) \cdot \log (h_o/h_f)]_i \quad (5.2)$$

where C_h is the suction index with respect to void ratio; and h_o , h_f are the initial and final suction profiles, respectively. The actual measured initial soil suction profile was used along with assumed final suction profiles. Assumption No. 1 (zero throughout the depth of active zone) was changed to 1 kPa throughout the depth instead of zero because of the logarithmic function in the equation.

Three different sample sizes were used to determine the suction index with respect to void ratio, C_h , as described in Chapter IV. Therefore, heave predictions were made using the suction index measured from all three sample sizes. The summarized results are shown in Table 5.3.

5.1.3 Mitchell's Method

The following equation was used to predict the ground heave:

$$\Delta H = \Sigma [I_{pt} \cdot H \cdot \log (h_o/h_f)]_i \quad (5.3)$$

where I_{pt} is the instability index, and h_o , h_f are the initial and final suction profiles, respectively. Like Nelson and Hamberg's method, the actual measured initial soil suction profile was used. The assumed final soil suction profile for assumption No. 1 was modified to a value of 1 kPa (instead of zero) throughout the depth of active zone because of logarithmic function. Prediction of heave was based on the instability index determined from three different sample sizes. The effect of the sample size on heave prediction will be discussed in Chapter VI. Table 5.4 summarizes the predicted heave for three different sample sizes.

5.1.4 McKeen's Method

An empirical correlation between the suction compression index, γ_h , and percent clay and P.I. was used. Total heave was then predicted using the following equation:

$$\Delta H = \Sigma [\gamma_h \cdot H \cdot \log (h_o/h_f)]_i \quad (5.4)$$

where γ_h is the suction compression index, and h_o , h_f are the final and initial soil suction. Based on the measured initial soil suction profile and three assumed final

TABLE 5.3
HEAVE PREDICTION USING NELSON
AND HAMBERG'S METHOD

Depth (ft)	e_0	C_h	h_0 (kPa)	Final Suction h_f (kPa)			Predicted Percentage of Swell/Heave (Inch)					
				1	2	3	No. 1 Swell Heave (%)		No. 2 Swell Heave (&)		No. 3 Swell Heave (&)	
Sample Height: 2.8cm												
0.60-1.75	0.564	0.028	1995	1	200	1000	5.9	0.8	5.4	0.7	2.5	0.3
1.75-3.25	0.485	0.147	2692	1	11	1000	34.0	6.1	23.6	4.3	4.3	0.8
3.25-4.75	0.498	0.257	4467	1	46	269	62.6	11.3	34.1	6.1	20.9	3.8
4.75-6.25	0.483	0.232	6026	1	200	107	59.1	10.6	23.1	4.2	27.4	4.9
6.25-7.75	0.440	0.163	1995	1	871	28	37.4	6.7	4.1	0.7	21.0	3.8
							35.6		16.0		13.6	
Sample Height: 5.1 cm												
0.60-1.75	0.575	0.052	1995	1	2	79	10.9	1.5	9.9	1.4	4.6	0.6
1.75-3.25	0.550	0.147	2692	1	11	1000	32.5	5.9	22.7	4.1	4.1	0.7
3.25-4.75	0.484	0.129	4467	1	46	269	31.7	5.7	17.3	3.1	10.6	1.9
4.75-6.25	0.462	0.068	6026	1	200	107	17.6	3.2	6.9	1.2	8.1	1.5
6.25-7.75	0.450	0.070	1995	1	871	28	15.9	2.9	1.7	0.3	8.9	1.6
							19.1		10.1		6.4	
Sample Height: 10.1 cm												
0.60-1.75	0.593	0.029	1995	1	2	79	6.0	0.8	5.5	0.8	2.6	0.4
1.75-3.25	0.575	0.140	2692	1	11	1000	30.5	5.5	21.2	3.8	3.8	0.7
3.25-4.75	0.474	0.075	4467	1	46	269	18.6	3.3	10.1	1.8	6.2	1.1
4.75-6.25	0.461	0.080	6026	1	200	107	20.7	3.7	8.1	1.5	9.6	1.7
6.25-7.75	0.441	0.049	1995	1	871	28	11.2	2.0	1.2	0.2	6.3	1.1
							15.4		8.1		5.0	

TABLE 5.4
HEAVE PREDICTION USING MITCHELL'S METHOD

Depth (ft)	l_{pt}	h_0 (kPa)	Final Suction			Predicted Percentage of Swell/Heave (Inch)					
			h_f (kPa)			No. 1		No. 2		No. 3	
			1	2	3	Swell	Heave	Swell	Heave	Swell	Heave
						(%)	(%)	(%)	(%)	(%)	(%)
Sample Height: 2.8 cm											
0.60-1.75	0.280	1995	1	2	79	0.9	0.1	0.8	0.1	0.4	0.1
1.75-3.25	2.355	2692	1	11	1000	8.1	1.5	5.6	1.0	1.0	0.2
3.25-4.75	9.451	4467	1	46	269	34.5	6.2	18.8	3.4	11.5	2.1
4.75-6.25	5.264	6026	1	200	107	19.9	3.6	7.8	1.4	9.2	1.7
6.25-7.75	5.590	1995	1	871	28	18.4	3.3	2.0	0.4	10.4	1.9
						14.7		6.3		5.8	
Sample Height: 5.1 cm											
0.60-1.75	1.120	1995	1	2	79	3.7	0.5	3.4	0.5	1.6	0.2
1.75-3.25	3.817	2692	1	11	1000	13.1	2.4	9.1	1.6	1.6	0.3
3.25-4.75	2.806	4467	1	46	269	10.2	1.8	5.6	1.0	3.4	0.6
4.75-6.25	2.081	6026	1	200	107	7.9	1.4	3.1	0.6	3.6	0.7
6.25-7.75	1.424	1995	1	871	28	4.7	0.8	0.5	0.1	2.6	0.5
						6.9		3.8		2.3	
Sample Height: 10.1 cm											
0.60-1.75	0.303	1995	1	2	79	1.0	0.1	0.9	0.1	0.4	0.1
1.75-3.25	3.733	2692	1	11	1000	12.8	2.3	8.9	1.6	1.6	0.3
3.25-4.75	1.773	4467	1	46	269	6.5	1.2	3.5	0.6	2.2	0.4
4.75-6.25	2.051	6026	1	200	107	7.8	1.4	3.0	0.5	3.6	0.6
6.25-7.75	1.279	1995	1	871	28	4.2	0.8	0.5	0.1	2.4	0.4
						5.8		3.0		1.8	

soil suction profiles, the predicted total heave is 6.4, 3.4, and 2.2 in., respectively (see Table 5.5).

TABLE 5.5
HEAVE PREDICTION USING McKEEN'S METHOD

Depth (ft)	γ_h	h_o (kPa)	Final Suction h_f (kPa)			Predicted Percentage of Swell/Heave (Inch)					
			1	2	3	No. 1 Swell/Heave (%)		No. 2 Swell/Heave (%)		No. 3 Swell/Heave (%)	
0.60-1.75	0.017	1995	1	2	79	5.6	0.8	5.1	0.7	2.4	0.3
1.75-3.25	0.030	2692	1	11	1000	10.3	1.9	7.2	1.3	1.3	0.2
3.25-4.75	0.022	4467	1	46	269	8.0	1.4	4.4	0.8	2.7	0.5
4.75-6.25	0.018	6026	1	200	107	6.8	1.2	2.7	0.5	3.2	0.6
6.25-7.75	0.018	1995	1	871	28	5.9	1.1	0.6	0.1	3.3	0.6
						6.4		3.4		2.2	

5.2 Oedometer Swell Methods

Constant volume oedometer swell pressure and overburden swell methods were used to predict ground heave. Fredlund's procedure was followed for the constant volume oedometer swell pressure method. The overburden swell method was under the condition that overburden pressure corresponding to the depth was used during the swell test.

5.2.1 Constant Volume Oedometer Swell Pressure Method

Using the swelling pressure p'_s and the swelling index C_s by Fredlund's procedure, the heave was predicted by:

$$\Delta H = \Sigma [C_s \cdot H / (1 + e) \cdot \log (p'_s / p_f)]_i \quad (5.5)$$

where C_s is the swelling index; p'_s is the corrected swelling pressure; and p_f is the final stress state, $\sigma_v + \Delta\sigma - u_{wf}$. Assumptions were made that external load was insignificant and the soil subgrade layer was saturated for its final condition. Based on these assumptions, the maximum heave predicted was 1.2 in. Table 5.6 presents necessary calculations.

5.2.2 Overburden Swell Method

Heave was calculated by multiplying thickness of soil layer by percent swell from overburden swell tests. Predicted heave was 0.15 in. (see Table 5.7).

TABLE 5.6
HEAVE PREDICTION USING FREDLUND'S METHOD

Depth (ft)	C_s	e_0	p'_s (tsf)	p_f (tsf)	Swell (%)	Heave (in.)
0.60-1.75	0.016	0.644	0.13	0.03	0.6	0.1
1.75-3.25	0.048	0.627	0.84	0.09	2.9	0.5
3.25-4.75	0.025	0.495	1.75	0.14	1.8	0.3
4.75-6.25	0.036	0.496	0.62	0.19	1.2	0.2
6.25-7.75	0.020	0.526	0.83	0.23	0.7	0.1
						1.2

TABLE 5.7
HEAVE PREDICTION USING THE SWELL METHOD

Depth (ft)	Thickness (ft)	%Swell $\Delta H/H$	Heave (in.)	p_0 (tsf)
0.60-1.75	1.15	0.027	0.00	0.060
1.75-3.25	1.50	0.747	0.13	0.165
3.25-4.75	1.50	0.453	0.08	0.260
4.75-6.25	1.50	-0.107	-0.02	0.360
6.25-7.75	1.50	-0.227	-0.04	0.455
			0.15	

CHAPTER VI

DISCUSSION

The accuracy of the heave prediction methods was evaluated by comparing predicted heave with actual measured field value. The heave prediction methods were also compared with one another to assess the ease of use and the time length of the different procedures.

The influence of sample size on suction index and therefore on heave prediction for Nelson and Hamberg's method and Mitchell's method was investigated. Based on the actual measured heave, the most appropriate sample size for Core Shrinkage tests was determined from the three sample sizes used for the tests. Other factors influencing the heave prediction, such as lateral confinement and overburden load, were also considered.

6.1 Accuracy

Following the definition by Tan and Duncan (1991), accuracy was taken as the predicted heave value divided by the actual measured value. A ratio of unity indicates the most accurate prediction method. A ratio larger than unity represents overestimation of ground heave or a conservative estimate. A ratio less than unity, on the other hand, represents underestimation of ground heave or an unconservative estimate. Table 6.1 shows the accuracy of all heave prediction methods investigated corresponding to the actual measured heave of 9.1 cm (3.6 in.).

Using the final suction profile assumption No. 2, i.e., with suction increasing linearly with depth throughout the active zone, Mitchell's method for the 5.1 cm

TABLE 6.1
COMPARISON OF THE ACCURACY OF THE
VARIOUS PREDICTION METHODS

Prediction Method		Final Suction Assumption					
		No. 1		No. 2		No. 3	
Snethen and Johnson	$h_o = A - B \cdot \omega_o$	1.7	(6.0)	0.7	(2.6)	0.20	(0.7)
	Measured h_o	3.2	(11.4)	2.2	(7.9)	1.70	(6.1)
Nelson and Hamberg	H = 2.8 cm	9.9	(35.6)	4.4	(16.0)	3.80	(13.6)
	H = 5.1 cm	5.3	(19.1)	2.8	(10.1)	1.80	(6.4)
	H = 10.1 cm	4.3	(15.4)	2.3	(8.1)	1.40	(5.0)
Mitchell	H = 2.8 cm	4.1	(14.7)	1.8	(6.3)	1.60	(5.8)
	H = 5.1 cm	1.9	(6.9)	1.1	(3.8)	0.60	(2.3)
	H = 10.1 cm	1.6	(5.8)	0.8	(3.0)	0.50	(1.8)
McKeen		1.8	(6.4)	0.9	(3.4)	0.60	(2.2)
Fredlund						0.30	(1.2)
Overburden Swell						0.04	(0.2)

Note: Numbers in parentheses are predicted heave in inches.

TABLE 6.2
EFFECT OF OVERBURDEN ON MITCHELL'S METHOD
(H = 5.1 cm)

Depth (ft)	α	Stress (kPa)	Predicted Percentage of Swell/Heave (Inch)					
			No. 1		No. 2		No. 3	
			Swell (%)	Heave (%)	Swell (%)	Heave (%)	Swell (%)	Heave (%)
0.60-1.75	0.57	6.96	3.0	0.4	2.8	0.4	1.5	0.2
1.75-3.25	0.96	15.78	8.6	1.5	7.7	1.4	1.6	0.3
3.25-4.75	0.83	25.88	6.5	1.2	5.1	0.9	3.3	0.6
4.75-6.25	0.86	36.52	4.8	0.9	2.9	0.5	3.4	0.6
6.25-7.75	0.82	45.24	2.5	0.4	0.5	0.1	2.1	0.4
			4.4		3.3		2.1	

sample yields the best accuracy among the methods studied, with accuracy equal to 1.1. McKeen's method has an accuracy of 0.9, which underestimates the maximum field heave by 10%. Snethen and Johnson's method has an accuracy of 0.7, which underestimates the maximum field heave by 30%. However, if the measured initial soil suction profile is used, Snethen and Johnson's method gives an accuracy of 2.2 that results in overestimation by 120%. Nelson and Hamberg's method, without considering lateral confinement condition, overestimates the maximum field heave by more than 130%. Both oedometer swell methods, Fredlund's method and the overburden Swell method, underestimate the maximum field heave, with accuracy equal to 0.3 by Fredlund's method and 0.04 by the overburden swell method, respectively.

Different from the other prediction methods, Snethen and Johnson's method takes into account the effect of external loads on heave prediction. For comparison purposes, the effect of overburden pressure by Snethen and Johnson was adapted to Mitchell's method to estimate the percentage of overburden influence on total heave prediction (see Table 6.2). Comparing the results of Table 6.2 with Table 5.4, it was found that overburden pressure reduces the predicted total heave by 9% to 35% for different final suction profile assumptions.

Determinations of parameters A and B from soil suction tests by Snethen and Johnson's method were sometimes difficult since the water content versus the soil suction relationship tends to be scattered, especially for soils in very dry and very wet conditions. As observed in Table 6.1, use of the initial soil suction as $(A - B \cdot \omega)$ and measured suction profile yields significant different heave results.

The maximum predicted heave should be adjusted using the correction factor, f , in order to be compared with the actual measured heave. This is especially important for Nelson and Hamberg's method because volume change (3-D) is measured in the Clod Shrinkage test and is applied to one-dimensional ground heave. This is also true for Snethen and Johnson's method. For Mitchell's method, however, the predicted heave may not need to be adjusted since only linear

dimension is measured during the Core Shrinkage test. The correction factor reflects the field lateral confinement condition. A factor equal to 1.0 represents complete confined lateral movement and the volume change upon wetting is one-dimensional, that is, the same as the total ground heave. A factor equal to 0.33 represents no lateral movement restriction and the volume changes in three directions are equal. Actual field conditions may fall in between the extreme conditions depending on the characteristics of the fissures and cracks near the ground surface.

In this study the damaged pavement showed small cracks possibly caused by lateral expansion of the subgrade soils. The correction factor of 0.67 (average of 1.0 and 0.3) was used to adjust the maximum predicted heave using Nelson and Hamberg's method. The actual heave, therefore, for the 5.1 and 10.1 cm samples using final suction profile assumption No. 2 is 6.8 in. and 5.4 in., respectively, with the accuracy being 1.9 and 1.5. In addition, difference in testing procedures may also be one of the reasons leading to the high predicted heave. The original Clod Shrinkage test described by Nelson and Hamberg was such that the sample clods were coated with Saran during the air drying process while the Clod Shrinkage test conducted in this study was not coated with any material. The coated saran may have some restraint on deformation of soil clods and it was expected to produce a relatively low suction index ratio, C_w , compared with no coating samples. Overburden and other external loads are not considered in Nelson and Hamberg's method. Compared with other prediction methods, this method is the most conservative.

Fredlund's constant volume oedometer swell pressure method underestimates the ground heave by 70% in this investigation. It was found during this study that vertical load, even if it is small, influences the amount of swell noticeably in oedometer swell tests. The swelling pressures were low and difficult to measure with a conventional oedometer device. The swelling index, C_s , was actually the slope of the unloading curve. Conceptually it was dependent on elasticity properties of the soil, not the change of soil moisture. In other words, the oedometer sample was close to saturation after soaking several days and volume increase during unloading

is mainly caused by stress relaxation instead of suction change. Elastic rebound of a soil is normally smaller than the swell caused by suction decreasing.

The accuracy of all heave prediction methods depends not only on how each of them evaluates the swelling index (in general) but also on the initial and final conditions of a soil. Three different assumptions for final soil suction profiles are useful guides when field moisture content or suction profile is not available. Assumption No. 1 is conservative and may not apply to Nelson and Hamberg's, Mitchell's, and McKeen's methods without counting the effect of external loads in final suction profile. Assumption No. 2 becomes the most appropriate one in this study. Combinations of these three assumptions may be suitable for actual field conditions.

6.2 Ease of Use and Time of Application

Determination of initial soil suction requires seven days by the standard filter paper method. This controls the time needed for all the soil suction methods and McKeen's method. Other tests such as the soil suction test for A and B parameter determination, Clod Shrinkage test, Core Shrinkage test, etc., can be finished within seven days while the initial soil suction test is running. Clod Shrinkage and Core Shrinkage tests need continuous measurements of sample dimensions of up to three days. Equipment required by the filter paper method for suction measurement was simple to use and inexpensive. The Clod Shrinkage or Core Shrinkage tests only need basic weight and dimension measuring tools.

Large numbers of soil samples can be tested at the same time for soil suction and Clod Shrinkage tests. The effort spent for all the suction methods are more or less the same with Snethen and Johnson's method requiring the least. McKeen's method needs input of the Plasticity Index (P.I.) or Cation Exchange Capacity and activity of the swelling soil. Fredlund's constant volume swell test runs from ten days to two weeks because of complete consolidation procedure following constant volume swell. The effort may not be extensive because there is no need to spend time reading during the consolidation period. Consolidation equipment is much

more expensive than equipment for the filter paper method, and testing large numbers of samples at the same time is impractical. The overburden swell method takes two days to more than a week, depending upon the time required to reach equilibrium for different soils. Overall, Snethen and Johnson's method and McKeen's method are most favorable concerning the ease of use and the time involved in the whole procedure.

6.3 Influence of Sample Size on Core Shrinkage Test

Study on three different sample sizes (height equal to 2.8, 5.1, and 10.1 cm) showed that the ratio of linear strain to water content, $\Delta\varepsilon_v/\Delta\omega$, from Core Shrinkage tests varied with sample height. It generally decreased as the sample height increased. Using the test results from Table 4.3, the ratio $\Delta\varepsilon_v/\Delta\omega$ is plotted against sample height for different soil sample depths (see Figure 6.1). The results are different for the 2.8 cm samples as compared to the 5.1 and 10.1 cm samples. The reason is probably the nonlinear deformation of shrinkage with respect to initial height of sample. As the sample height passes 5.0 cm, the effect of size becomes negligible.

Such size influence on the heave prediction methods by Nelson and Hamberg, and Mitchell follows the same trend. Figure 6.2 shows the maximum predicted heave for three different sample sizes based on the assumption No. 2 of the final suction profile. It was determined from Mitchell's method that a sample height of 5.5 cm would be the most appropriate sample size for the Core Shrinkage test.

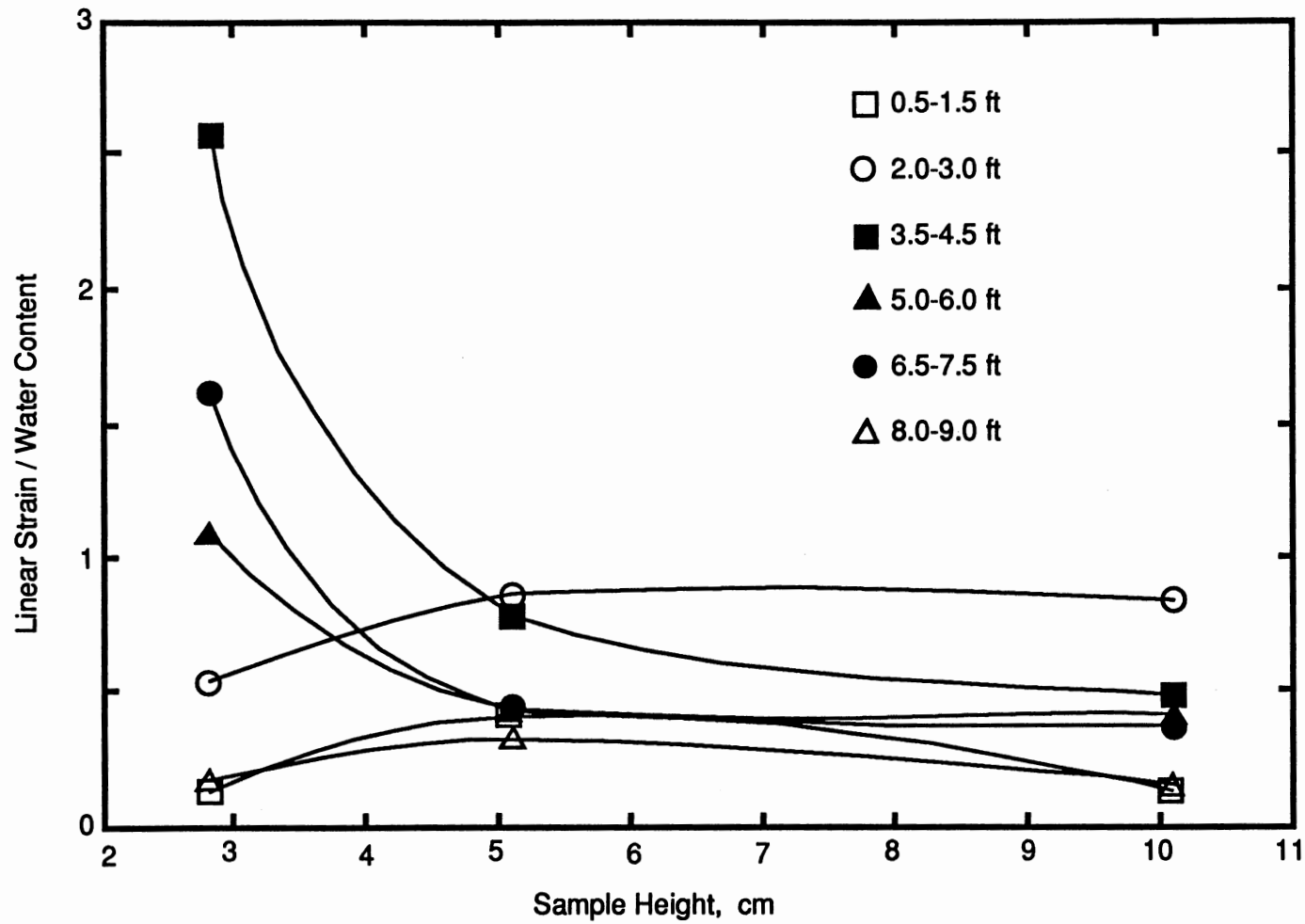


Figure 6.1. Effect of Sample Size on Core Shrinkage Test Results

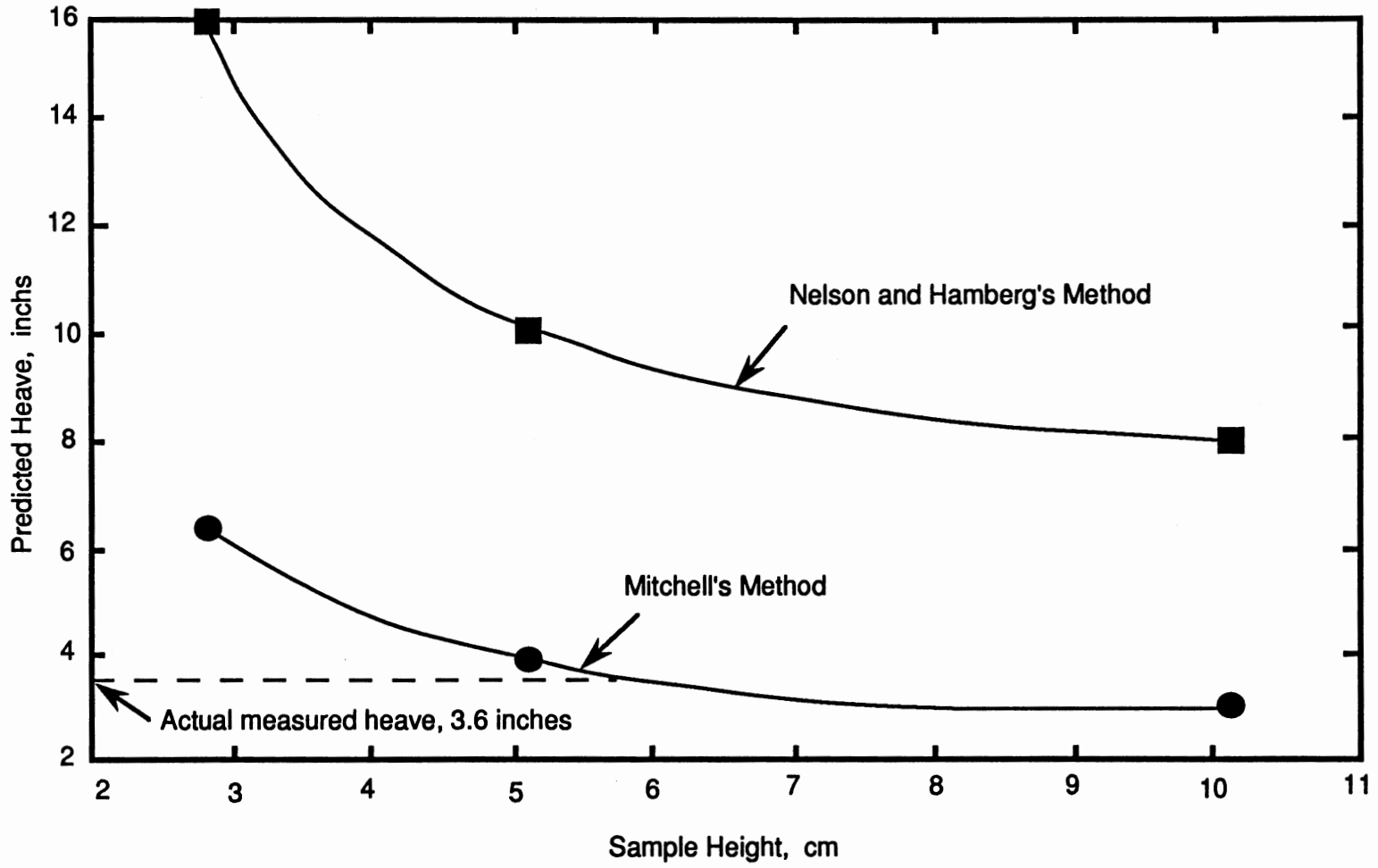


Figure 6.2. Effect of Sample Size on Heave Prediction

CHAPTER VII

CONCLUSIONS AND RECOMMENDATIONS

7.1 Conclusions

Accuracy and efficiency of five ground heave prediction methods were evaluated through comparison between the predicted value and the actual field measurement in one location near Wynnewood, Oklahoma. The major portion of this research was focused on soil suction methods, although oedometer swell methods were also studied. The influence of sample dimension on clod shrinkage and core shrinkage tests was also investigated in detail to find the most appropriate sample size for these two tests.

Based on the experimental data and discussion presented in previous chapters, the following conclusions may be drawn:

1. The heave prediction using soil suction data proved to be the better approach than those using oedometer swell data concerning accuracy and efficiency.
2. Among the soil suction methods, Mitchell's method yields the best accuracy when the final suction profile was assumed to increase linearly with depth throughout the active zone. The method was also easy to use and did not involve expensive equipment and long-time operation.
3. Heave prediction by Nelson and Hamberg's method was too high without considering lateral constraint condition. This method was the most conservative among all the prediction methods studied. A correction factor of 0.56 for a lateral confinement condition was appropriate when the final suction profile assumption No. 3 was used.

4. The predicted heave value using Snethen and Johnson's method was relatively low when the initial suction was calculated from A and B parameters and initial water content, whereas it was high when actual measured initial suction was used. The average of two seemed reasonable when final suction profile assumption No. 3 was used. The difficulty of determining A and B parameters was experienced because of data scattering in suction tests. If the final suction profile No. 2 was used, a confinement correction factor of 0.68 was appropriate for the average predicted heave from two different initial suction methods.
5. Determination of the suction compression index using the correlation developed by McKeen was competitive. The heave predicted using such a method was within an error of 6%. The method reduced the time and effort of testing by more than 50% since Atterberg Limits tests were routine tests for expansive soils and percentage of clay was easy to determine by hydrometer analysis. Final suction profile assumption No. 2 was most favorable for application of McKeen's method. The confinement correction need not be considered in this case.
6. The influence of sample size on clod shrinkage and core shrinkage tests was significant. The experimental data showed that a sample height of at least 5 cm for 7.3 cm core samples was preferred in order to eliminate the influence of sample dimension.
7. Heave predictions using oedometer data were generally low. The heave predicted using Fredlund's method was only one third of actual field measurement. The heave predicted using overburden swell data underestimated actual field measurement by 90%.
8. Overall, the final suction profile following assumption No. 2 was most appropriate, i.e., the soil suction increases linearly with sample depth throughout the active zone. Assumption No.1 was too conservative to use in practice. Assumption No. 3 was realistic conceptually. But because of

uncertainty in interpreting A and B parameters, the error in soil suction calculated from saturated water content was not easy to estimate. The heave predicted using assumption No. 3 for the final suction profile generally gave a lower value than the actual field measurement.

9. Based on Snethen and Johnson's procedure for deduction of external load, the estimate of the overburden effect on Nelson and Hamberg's method as well as Mitchell's method was from 8 to 25% corresponding to different final suction profile assumptions. The overburden effect on heave prediction needs to be considered for Nelson and Hamberg's and Mitchell's methods.

7.2 Recommendations

Evaluation of accuracy and reliability of heave prediction methods needs a large number of input data. Since only one location was chosen in this study, the investigation was considered to be in a preliminary stage. In order to better understand the factors controlling heave prediction methods and gain more confidence about different methods, further research may be recommended as follows:

1. Establish a large database for heave prediction methods so that statistical evaluation of accuracy and reliability of different methods are available. The database should include both laboratory determination of input parameters for prediction methods and field heave measurement.
2. Specification of sample size for clod shrinkage and core shrinkage tests may be needed for a better comparison basis. Based on this study, the core sample with a height of 5.5 cm (2.2 in.) is recommended.
3. Besides suction indexes and swell index, initial and final soil suction profiles are the keys for success in predicting ground heave. Correlation of suction profiles with soil temperature, precipitation, moisture evaporation, and ground water fluctuations should be developed to set realistic boundaries for heave prediction due to seasonal changes.

4. Influence of overburden and external loads on heave predictions needs more attention than the current state of most soil suction methods. It may be accomplished by following Snethen and Johnson's procedure. The alternative is comparison of percent swell from the results of overburden swell and oedometer swell with zero surcharge load. The difference in percentage may be applied to ground heave prediction.
5. Investigate the correction factor for different lateral confinement conditions. A quantitative relation between the correction factor and the ground conditions of the upper layer such as width and depth of cracks, crack spacing, and void ratio will be helpful for accurate prediction.
6. The hysteresis effect on the suction index measurement may be studied by comparing the results obtained from core shrinkage and from core swelling tests. The core swelling test is feasible by spraying core samples with distilled water and placing them in moisture room. Periodical measurement of the sample dimensions and weight is made to establish the relation between volumetric strain and moisture content. Core swelling represents the true field situation.

SELECTED REFERENCES

- Aitchison, G.D., and Woodburn, J.A. "Soil Suction in Foundation Design." *Proc., 7th Int. Conf. on Soil Mech. and Found. Eng.* Vol. 2. Mexico City, Mexico, 1969, pp. 1-9.
- Aitchison, G.D. *The Stability of Lightly Loaded Building Foundations on Clay Soils.* Part 1. Tech. Report No. 26. CSIRO, Div. Appl. Geomech., 1970.
- Aitchison, G.D., and Peter, P. "The Sorption Limit as a Guide to Expansive Properties." *Proc., 3rd Int. Conf. on Expansive Soils*, Haifa, Israel, 1973.
- ASTM Standard Test Method for "Measurement of Soil Potential (Suction) Using Filter Paper." Vol. 04.08. Philadelphia: American Society for Testing and Materials, 1993 (in balloting process).
- Casagrande, A. "Classification and Identification of Soils." *Transactions*, ASCE, Vol. 113 (1948), pp. 901-930.
- Climatological Data, Oklahoma.* Vol. 100. Ashville, NC: National Climate Data Center, U.S. Department of Commerce, 1991.
- Das, B.M. *Advanced Soil Mechanics.* New York: McGraw-Hill, 1983.
- Fargher, P.J., and Stevens, R.L. "Notes on the Design Assumptions and Methods for Grillage Raft Footings." Hosking, Fargher & Oborn Pty. Ltd., Adelaide, Australia, May 1973.
- Fredlund, D.G. "Prediction of Ground Movements in Swelling Clays." *Proc., 31st Annual SMFE Conf.*, Minneapolis, MN, 1983, pp. 44-90.
- Fredlund, D.G., Hasan, J.U., and Filson, H.L. "The Prediction of Total Heave." *Proc., 4th Int. Conf. on Expansive Soils*, Vol. 1, 1980, pp. 1-17.
- Fredlund, D.G. and Morgenstern, N.R. "Stress State Variables for Unsaturated Soils." *J. of Geotech. Engr. Div.*, ASCE, Vol. 103, No. G75 (1977), pp. 447-466.
- Grim, R.E. *Applied Clay Mineralogy.* New York: McGraw-Hill, 1962.
- Grim, R.E. *Clay Mineralogy.* New York: McGraw-Hill, 1953.
- Hamberg, D.J., and Nelson, J.D. "Prediction of Floor Slab Heave." *5th Int. Conf. on Expansive Soils*, Adelaide, South Australia, May 1984, pp. 137-140.
- Hamberg, D.J. "A Simplified Method for Predicting Heave in Expansive Soils." M.S. thesis, Colorado State University, 1985.

- Hicks, C. "Pauls Valley Field." *Petroleum Geology of Southern Oklahoma*. Vol. 1. Tulsa, OK: American Association of Petroleum Geology, 1956, pp. 337-354.
- Hillel, D. *Fundamentals of Soil Physics*. San Diego: Academic Press, 1980.
- Holtz, R.D., and Kovacs, W.D. *An Introduction to Geotechnical Engineering*. Englewood Cliffs, NJ: Prentice-Hall, Inc., 1981.
- Johnson, L.D., and Snethen, D.R. "Prediction of Potential Heave of Swelling Soils." *Geotechnical Testing Journal*, ASTM, Vol.1, No. 3 (Sept. 1978), pp. 117-124.
- Johnson, L.D. *Predicting Potential Heave and Heave With Time in Swelling Foundation Soils*. Technical Report S-78-7. U.S.A.E. Waterways Experiment Station, Vicksburg, MS, Sept. 1978.
- Johnson, L.D. *Evaluation of Laboratory Suction Tests for Prediction of Heave in Foundation Soils*. Technical Report S-77-7. U.S.A.E. Waterways Experiment Station, Vicksburg, MS, Sept. 1977.
- Johnson, L.D., and Stroman, W.R. *Analysis of Behavior of Expansive Soil Foundations*. Technical Report S-76-8. U.S.A.E. Waterways Experiment Station, Vicksburg, MS, June 1976.
- Johnson, L.D. "Influence of Suction on Heave of Expansive Soils." Misc. Paper S-73-17. U.S.A.E. Waterways Experiment Station, Vicksburg, MS, April 1973.
- Lytton, R.L. "The Characterization of Expansive Soils in Engineering." Presentation at the *Symposium on Water Movement and Equilibrium in Swelling Soils*. American Geophysical Union, San Francisco, CA, Dec. 1977.
- Lytton, R.L., and Woodburn, J.A. "Design and Performance of Mat Foundations on Expansive Clay." Vol. 1. *Proc., 3rd Int. Conf. on Expansive Soils*, Haifa, Israel, 1973, p. 301.
- Martin, R.T. "Adsorbed Water on Clay: A Review." *Clays and Clay Minerals*, Vol. 9 (1960), pp. 28-70.
- McKeen, R.G. *Design of Airport Pavements for Expansive Soils*. Report No. DOT/FAA/RD-81-25. Washington, DC: U.S. Dept. of Transportation, 1981.
- McKeen, R.G., and Nielsen, J.P. *Characterization of Expansive Soils for Airport Pavement Design*. Report No. FAA-RD-78-59, Federal Aviation Administration, Washington DC, August, 1978
- McKeen, R.G. "Field Studies of Airport Pavements on Expansive Clay." *4th Int. Conf. on Expansive Soils*. Vol. 1. Denver, CO, June 1980, pp. 242-261.
- Mitchell, P.W., and Avalue, D.L. "A Technique to Predict Expansive Soil Movements." *5th Int. Conf. on Expansive Soils*. Adelaide, South Australia, May 1984, pp. 124-130.
- Motan, E.S. "Influence of Soil Suction on the Behavior of Unsaturated Soils Under Repetitive Loads." Ph.D. dissertation, Univ. of Wisconsin-Madison, 1981.

- Olson, R.E., and Langfelder, L.J. "Pore Water Pressure in Unsaturated Soils." *J. of SMFE, ASCE*, Vol. 91, No. SM4 (1965), pp. 127-150.
- Patrick, D.M., and Snethen, D.R. *An Occurrence and Distribution Survey of Expansive Materials in the United States by Physiographic Areas*. Report No. FHWA-RD-76-82. Washington, DC: Federal Highway Administration, Jan. 1976.
- Richards, B.G. "Design for Australian Conditions." *Towards New Methods in Highway Engineering*. CSIRO Division of Applied Geomechanics Lecture Series No. 31. Australia, 1976.
- Russam, K. "The Prediction of Subgrade Moisture Conditions for Design Purposes." *Moisture Equilibria and Moisture Changes on Soils Beneath Covered Areas*. Butterworth, Australia, 1965, pp. 233-236.
- Russam, K. "Estimation of Subgrade Moisture Distribution." *Transportation and Communication Monthly Review*, Vol. 176 (1961), pp. 151-159.
- Sayed, S.T., and Rabbaa, S.A. "Factors Affecting Behavior of Expansive Soils in the Laboratory and Field—A Review." *Geotech. Engng.*, Vol. 17, No. 1 (1986), pp. 89-108.
- Snethen, D.R. "Characterization of Expansive Soils Using Soil Suction Data." *4th Int. Conf. on Expansive Soils*. Vol. 1. Denver, CO, June 1980, pp. 54-75.
- Snethen, D.R. *An Evaluation of Methodology for Prediction and Minimization of Detrimental Volume Change of Expansive Soils in Highway Subgrades*. Vol I. Report No. FHWA-RD-79-49. Washington, DC: Federal Highway Administration, March 1979.
- Snethen, D.R. *An Evaluation of Methodology for Prediction and Minimization of Detrimental Volume Change of Expansive Soils in Highway Subgrades*. Vol II. Report No. FHWA-RD-79-50. Washington, DC: Federal Highway Administration, March 1979.
- Snethen, D.R. et al. *A Review of Engineering Experiences With Expansive Soils in Highway Subgrades*. Report No. FHWA-RD-75-48. U.S.A.E. Waterways Experiment Station, Vicksburg, MS, 1975.
- Soil Survey of Garvin County Oklahoma*. Washington, DC: U.S. Dept. of Agriculture, 1985.
- Statement of the Review Panel. *Engineering Concepts of Moisture Equilibria and Moisture Changes in Soil Beneath Covered Areas*. G.D. Aitchison, Ed. Australia, 1965, pp. 7-21.
- Tan, C.K., and Duncan, J.M. "Settlement of Footings on Sands—Accuracy and Reliability." *Geotechnical Engineering Congress*. Vol. 1. F.G. McLean, D.A. Campbell, and D.W. Harris, Eds. Geotechnical Special Pub. No. 27, June 10-12, 1991.

Wiggins, J.H, Slossen, J.E., and Krohn, J.P. *Natural Hazards: Earthquake, Landslide, Expansive Soil*. Report prepared for the NSF under Grant No. ERP-75-09998 and No. AEN-74-23993, Oct. 1978.

Wray, W.K. *Measuring Engineering Properties of Soil*. Englewood Cliffs, NJ: Prentice-Hall, Inc., 1986.

Yong, R.N., and Warkentin, B.P. *Introduction to Soil Behavior*. New York: Macmillan, 1966.

Yong, R.T. "Subsurface Geology of East Pauls Valley Area, Garvin County, Oklahoma." M.S. thesis, University of Oklahoma, Norman, OK, 1960.

APPENDIX A .

INITIAL SOIL CONDITIONS AND SOIL PROPERTIES

TABLE A.1
INITIAL SOIL CONDITIONS

Depth (ft)	γ_w (pcf)	ω (%)	γ_d (pcf)	e	Suction log (kPa)	G_s
<u>I-35. H2</u>						
0.5-1.5	123.0	17.5	104.7	0.627	3.41	2.73
2.0-3.0	129.8	19.6	108.5	0.575	3.50	2.74
3.5-4.5	134.9	16.7	115.6	0.484	3.55	2.75
5.0-6.0	135.9	15.6	117.6	0.465	3.06	2.76
6.5-7.5	135.7	15.0	118.0	0.465	3.05	2.77
8.0-9.0	134.4	16.1	115.8	0.499	3.37	2.78
9.5-10.5	134.8	19.6	112.7	0.545	3.65	2.79
<u>I-35. H3</u>						
0.5-1.5	126.2	18.5	106.5	0.600	3.30	2.73
2.0-3.0	131.5	18.9	110.6	0.546	3.43	2.74
3.5-4.5	134.9	16.3	116.0	0.479	3.65	2.75
5.0-6.0	138.5	15.6	119.8	0.437	3.78	2.76
6.5-7.5	134.8	15.8	116.4	0.485	3.30	2.77
8.0-9.0	135.0	15.2	117.2	0.480	3.18	2.78
9.5-10.5	135.7	18.2	114.8	0.516	3.41	2.79
<u>I-35. H4</u>						
0.5-1.5	128.2	18.2	108.5	0.571	3.51	2.73
2.0-3.0	126.5	18.8	106.5	0.606	3.21	2.74
3.5-4.5	133.7	16.8	114.5	0.499	3.16	2.75
5.0-6.0	131.2	15.6	113.5	0.517	3.26	2.76
6.5-7.5	136.0	14.9	118.4	0.460	3.06	2.77
8.0-9.0	131.7	15.9	113.6	0.527	3.21	2.78
9.5-10.5	131.5	17.9	111.5	0.561	2.58	2.79
<u>I-35. H5</u>						
0.5-1.5	125.5	18.3	106.1	0.606	3.10	2.73
2.0-3.0	127.4	20.0	106.2	0.610	3.08	2.74
3.5-4.5	134.7	16.4	115.7	0.483	3.04	2.75
5.0-6.0	130.4	16.3	112.1	0.536	2.93	2.76
6.5-7.5	133.6	14.5	116.7	0.481	2.96	2.77
8.0-9.0	130.6	16.6	112.0	0.549	2.63	2.78

Note: Wet densities were estimated from core samples.

TABLE A.2
 ATTERBERG LIMITS

Depth (ft)	PL (%)	LL (%)	P.I. (%)	B.L. Shrk. (%)	Fine (%)	Clay (%)
<u>I-35. Borehole No. 1</u>						
1.0-1.5	15.9	37.3	21.4	12.6	71	31
1.5-1.8	17.3	44.3	27.0	14.1	74	---
1.8-2.2	16.1	50.5	34.4	13.9	77	41
2.2-2.8	15.9	49.2	33.3	13.4	71	---
2.8-3.0	14.6	45.2	30.6	12.4	69	---
3.0-3.5	14.0	42.8	28.8	12.8	67	38
3.5-4.0	12.7	40.7	28.0	12.5	65	---
4.0-4.5	12.6	37.1	24.5	11.8	63	36
4.5-5.0	12.3	34.9	22.6	10.8	59	---
5.0-5.4	13.2	34.4	21.2	9.3	57	32
5.4-5.9	12.3	30.1	17.8	7.9	55	---
5.9-6.3	12.1	30.0	17.9	9.2	59	32
6.3-6.7	12.4	30.0	17.6	8.9	64	31
6.7-7.2	12.1	29.7	17.6	8.6	63	---
7.2-7.7	12.8	29.4	16.6	8.6	65	31
7.7-8.3	12.0	28.8	16.8	7.9	56	---
8.3-8.7	12.3	27.6	15.3	8.2	58	31
8.7-9.1	12.8	26.3	13.5	6.0	51	---
9.1-9.4	11.3	24.5	13.2	6.6	52	31
9.4-10.1	11.0	26.6	15.6	8.7	57	---
10.1-10.6	14.3	35.9	21.6	4.5	66	42
10.6-11.0	15.0	38.0	23.0	5.9	65	---

TABLE A.3
SOIL CLASSIFICATION BY USCS AND AASHTO

Depth (ft)	LL (%)	P.I. (%)	Fine (%)	Soil Name	
				USCS	AASHTO
<u>Soil Sample: I-35.H3</u>					
1.0-1.5	37.3	21.4	71	CL	A-6 (13)
1.5-1.8	44.3	27.0	74	CL	A-7-6 (19)
1.8-2.2	50.5	34.4	77	CH	A-7-6 (26)
2.2-2.8	49.2	33.3	71	CL	A-7-6 (22)
2.8-3.0	45.2	30.6	69	CL	A-7-6 (19)
3.0-3.5	42.8	28.8	67	CL	A-7-6 (17)
3.5-4.0	40.7	28.0	65	CL	A-7-6 (15)
4.0-4.5	37.1	24.5	63	CL	A-6 (12)
4.5-5.0	34.9	22.6	59	CL	A-6 (10)
5.0-5.4	34.4	21.2	57	CL	A-6 (8)
5.4-5.9	30.1	17.8	55	CL	A-6 (6)
5.9-6.3	30.0	17.9	59	CL	A-6 (7)
6.3-6.7	30.0	17.6	64	CL	A-6 (8)
6.7-7.2	29.7	17.6	63	CL	A-6 (8)
7.2-7.7	29.4	16.6	65	CL	A-6 (8)
7.7-8.3	28.8	16.8	56	CL	A-6 (6)
8.3-8.7	27.6	15.3	58	CL	A-6 (5)
8.7-9.1	26.3	13.5	51	CL	A-6 (3)
9.1-9.4	24.5	13.2	52	CL	A-6 (3)
9.4-10.1	26.6	15.6	57	CL	A-6 (5)
10.1-10.6	35.9	21.6	66	CL	A-6 (11)
10.6-11.0	38.0	23.0	65	CL	A-6 (12)

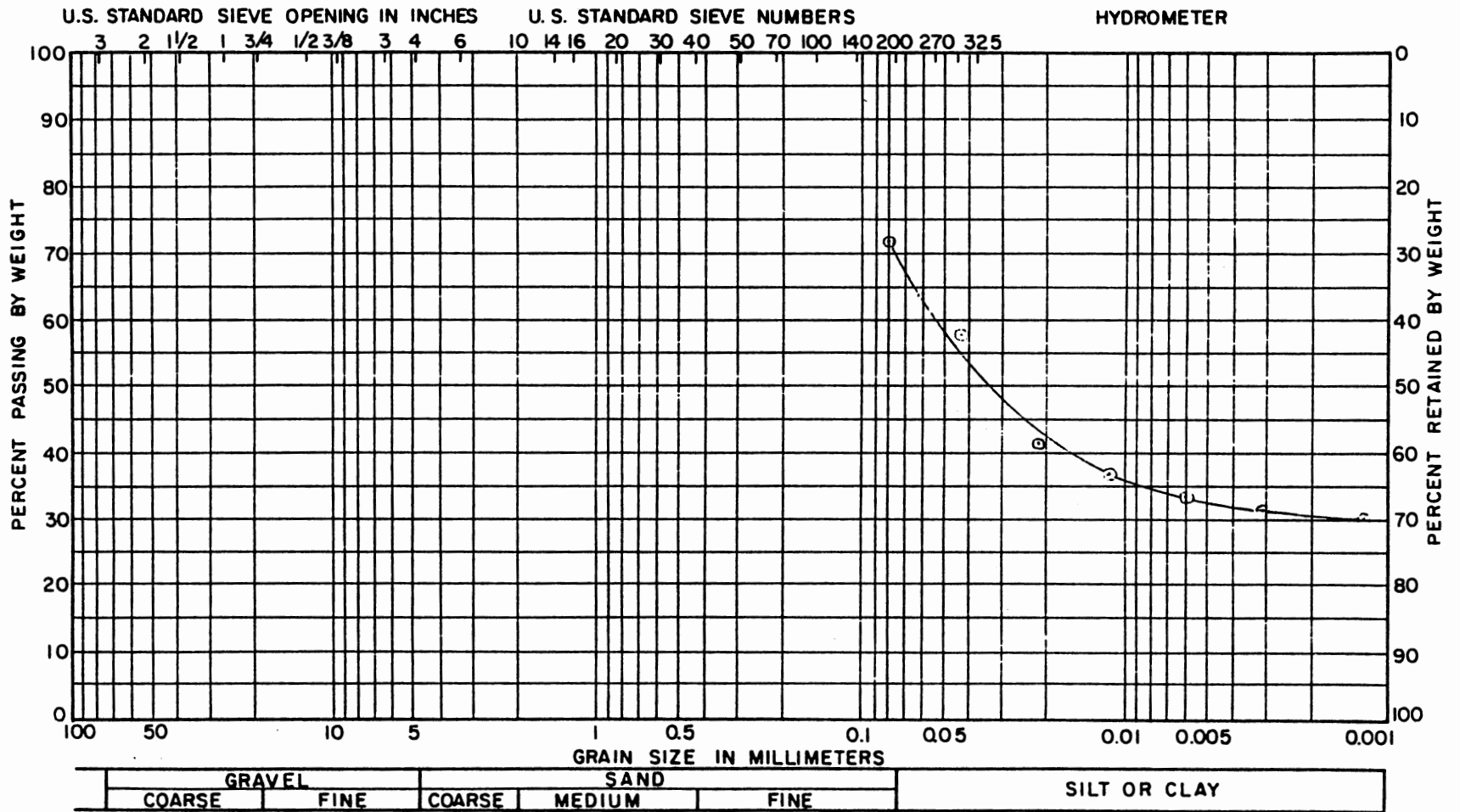


Figure A-1. Grain Size Distribution (Hole 3, 0.5-1.5 ft)

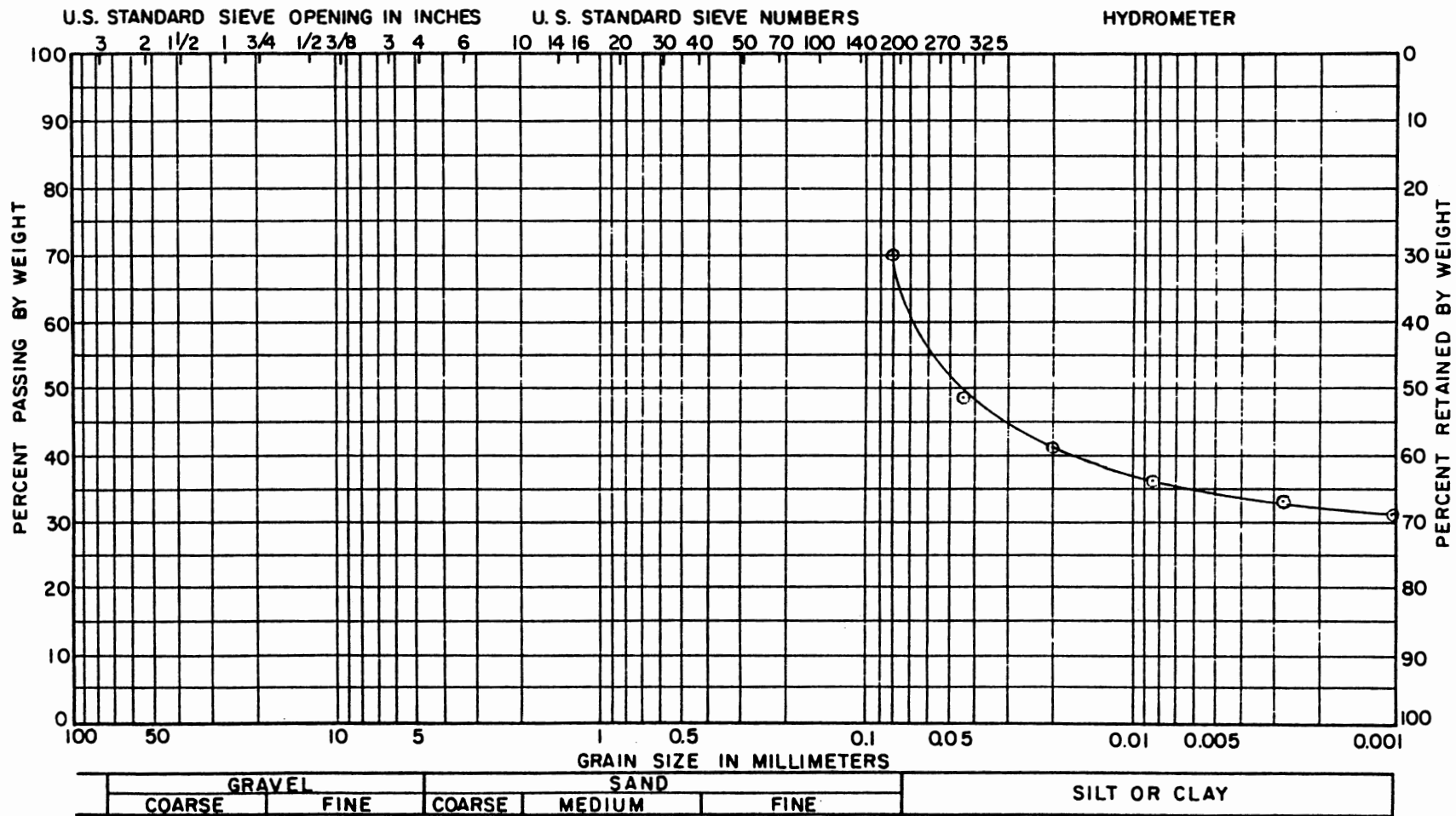


Figure A-2. Grain Size Distribution (Hole 1, 5.0-5.5 ft)

APPENDIX B

**SOIL SUCTION, CLOD SHRINKAGE, AND
CORE SRINKAGE TEST RESULTS**

TABLE B.1
SUCTION TEST RESULTS (I-35, H3)

w (%)	Suction 1 log (kPa)	Suction 2 log (kPa)	Avg. Suction log (kPa)	Vol. Soil (c.cm)	W.D. Soil (gram)	Spec. Vol. (c.cm/g)
<u>Depth: 0.5-1.5 ft</u>						
16.0	2.8686	2.7043	2.7865	94.88	160.83	0.590
16.4	2.4474	2.3779	2.4127	89.76	148.44	0.605
17.4	3.3088	3.2407	3.2748	84.48	138.97	0.608
18.6	3.4789	3.3519	3.4154	78.19	127.56	0.613
18.9	3.2421	3.1808	3.2115	81.90	135.10	0.606
20.3	2.7303	2.3972	2.5638	82.30	130.68	0.630
21.3	2.2291	2.1473	2.1882	88.73	144.20	0.615
22.8	2.7267	2.4899	2.6083	85.98	137.18	0.627
<u>Depth: 2.0-3.0 ft</u>						
12.9	4.1457	4.1375	4.1416	52.38	92.61	0.566
14.1	4.0552	4.0539	4.0546	80.96	152.82	0.530
16.9	3.7719	3.7006	3.7363	67.41	115.64	0.583
17.5	3.2298	3.2684	3.2491	64.29	104.97	0.612
18.0	3.5135	3.5132	3.5134	76.14	127.54	0.597
20.2	2.9777	2.8043	2.8910	60.33	94.84	0.636
20.9	3.0003	2.7829	2.8916	79.03	131.04	0.603
23.0	2.3526	2.4139	2.3833	76.77	124.19	0.618
<u>Depth: 3.5-4.5 ft</u>						
11.0	4.1344	4.1585	4.1465	84.03	165.93	0.506
14.1	4.0507	3.9910	4.0209	61.77	111.16	0.556
15.1	2.8986	2.9693	2.9340	84.06	155.38	0.541
15.5	3.0645	3.0402	3.0524	97.13	176.76	0.550
15.7	3.8814	3.8754	3.8784	75.11	140.84	0.533
16.6	2.1508	2.1338	2.1423	96.97	172.34	0.563
17.5	2.4657	2.3877	2.4267	88.01	156.06	0.564
18.0	2.9710	2.8254	2.8982	82.29	145.82	0.564
<u>Depth: 5.0-6.0 ft</u>						
9.8	3.3702	3.2744	3.3223	108.18	201.08	0.538
10.0	3.7229	3.6855	3.7042	117.00	224.90	0.520
11.2	2.8998	2.7493	2.8246	109.17	206.11	0.530
12.0	2.9735	2.8156	2.8946	100.55	186.42	0.539
12.3	2.9918	2.8121	2.9020	121.64	223.85	0.543
13.5	2.4280	2.3631	2.3956	108.37	198.27	0.547
14.7	2.5425	2.4001	2.4713	110.85	197.58	0.561
15.8	2.1865	1.9890	2.0878	114.50	204.58	0.560

TABLE B.1 (Continued)

w (%)	Suction 1 log (kPa)	Suction 2 log (kPa)	Avg. Suction log (kPa)	Vol. Soil (c.cm)	W.D. Soil (gram)	Spec. Vol. (c.cm/g)
Depth: 6.5-7.5 ft						
9.3	3.6272	3.6985	3.6629	106.44	185.38	0.574
10.2	3.5609	3.4708	3.5159	102.75	176.74	0.581
12.2	2.7900	2.6193	2.7047	109.94	208.50	0.527
13.1	3.3133	3.2538	3.2836	88.01	160.25	0.549
13.2	3.3840	3.1324	3.2582	108.20	201.06	0.538
13.4	3.6928	3.6735	3.6832	129.28	242.46	0.533
14.2	2.5002	2.3031	2.4017	107.88	197.25	0.547
15.6	3.5898	3.3813	3.4856	107.94	193.73	0.557
Depth: 8.0-9.0 ft						
14.4	3.3795	3.3987	3.3891	93.24	169.51	0.550
14.5	3.4505	3.3329	3.3917	82.66	151.47	0.546
15.0	3.3859	3.3524	3.3692	96.30	172.82	0.557
15.3	3.4515	3.3676	3.4096	75.83	134.70	0.563
15.4	3.3540	3.2809	3.3175	76.66	134.92	0.568
15.6	3.6428	3.6219	3.6324	90.28	161.23	0.560
16.6	3.2725	3.1297	3.2011	76.57	137.01	0.559
17.1	3.3295	3.2878	3.3087	79.18	137.99	0.574
Depth: 9.5-10.5 ft						
12.7	3.2969	3.2343	3.2656	97.62	182.13	0.536
13.0	3.3903	3.2804	3.3354	81.06	150.11	0.540
13.1	3.4310	3.3742	3.4026	94.70	175.04	0.541
13.5	3.5967	3.4479	3.5223	84.68	155.37	0.545
14.3	3.3286	3.1774	3.2530	81.29	149.43	0.544
15.0	3.5075	3.3588	3.4332	95.38	177.94	0.536
15.1	3.2652	2.9610	3.1131	76.02	138.21	0.550
15.5	3.3723	3.3769	3.3746	88.20	163.04	0.541

Note: The shaded blocks represent the natural water content condition.

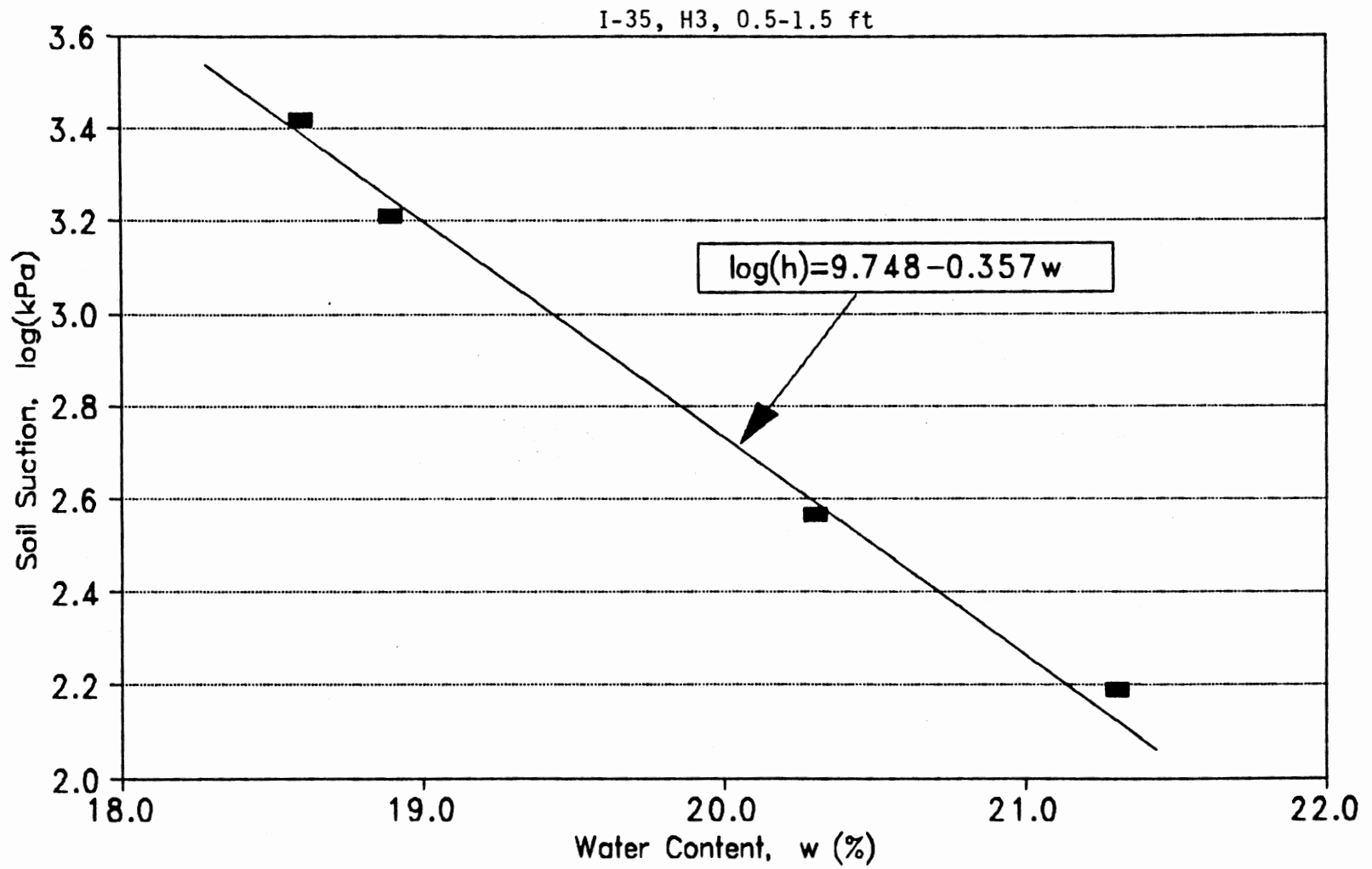


Figure B-1. Suction Vs. Water Content

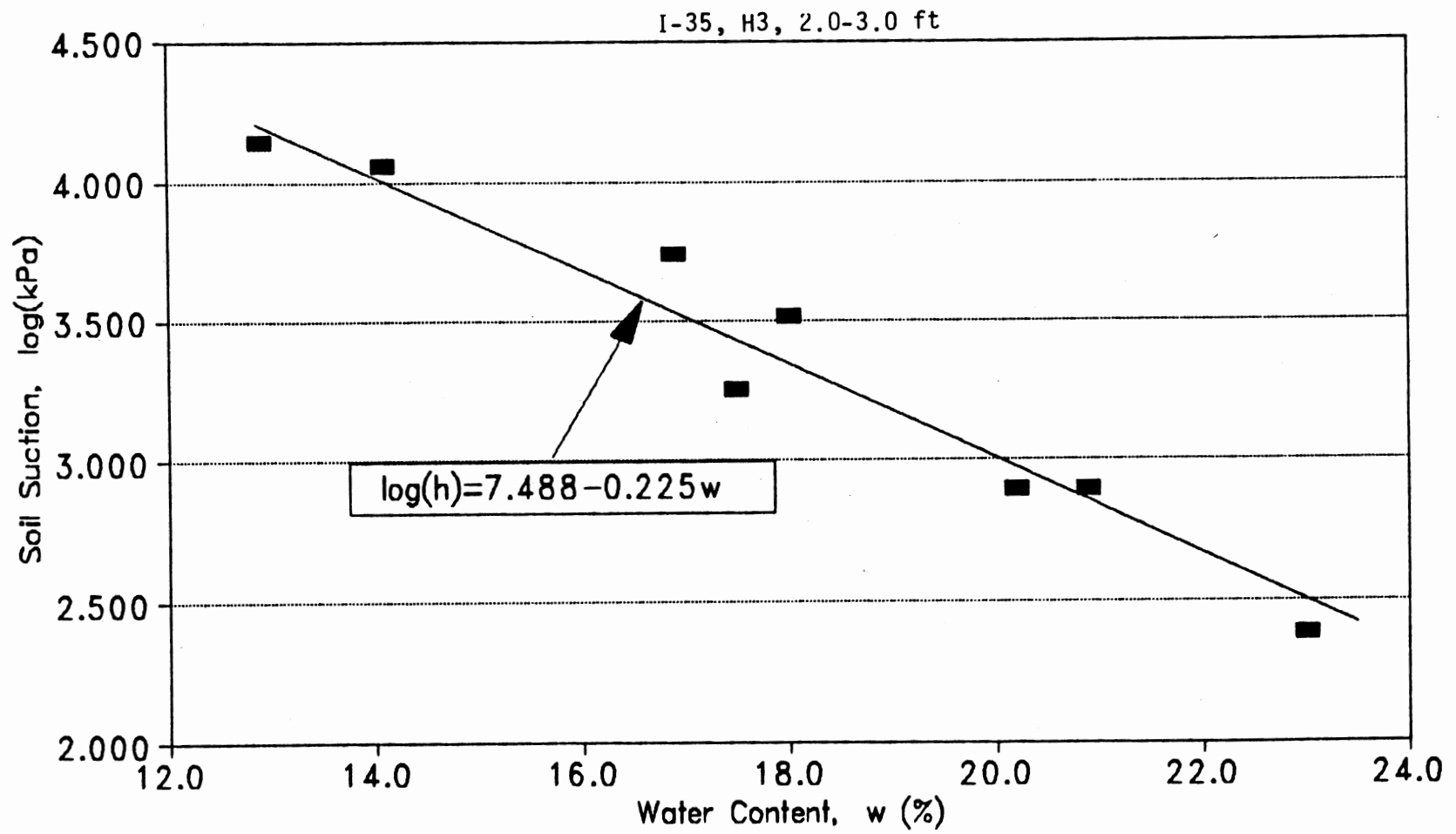


Figure B-1. (Continued)

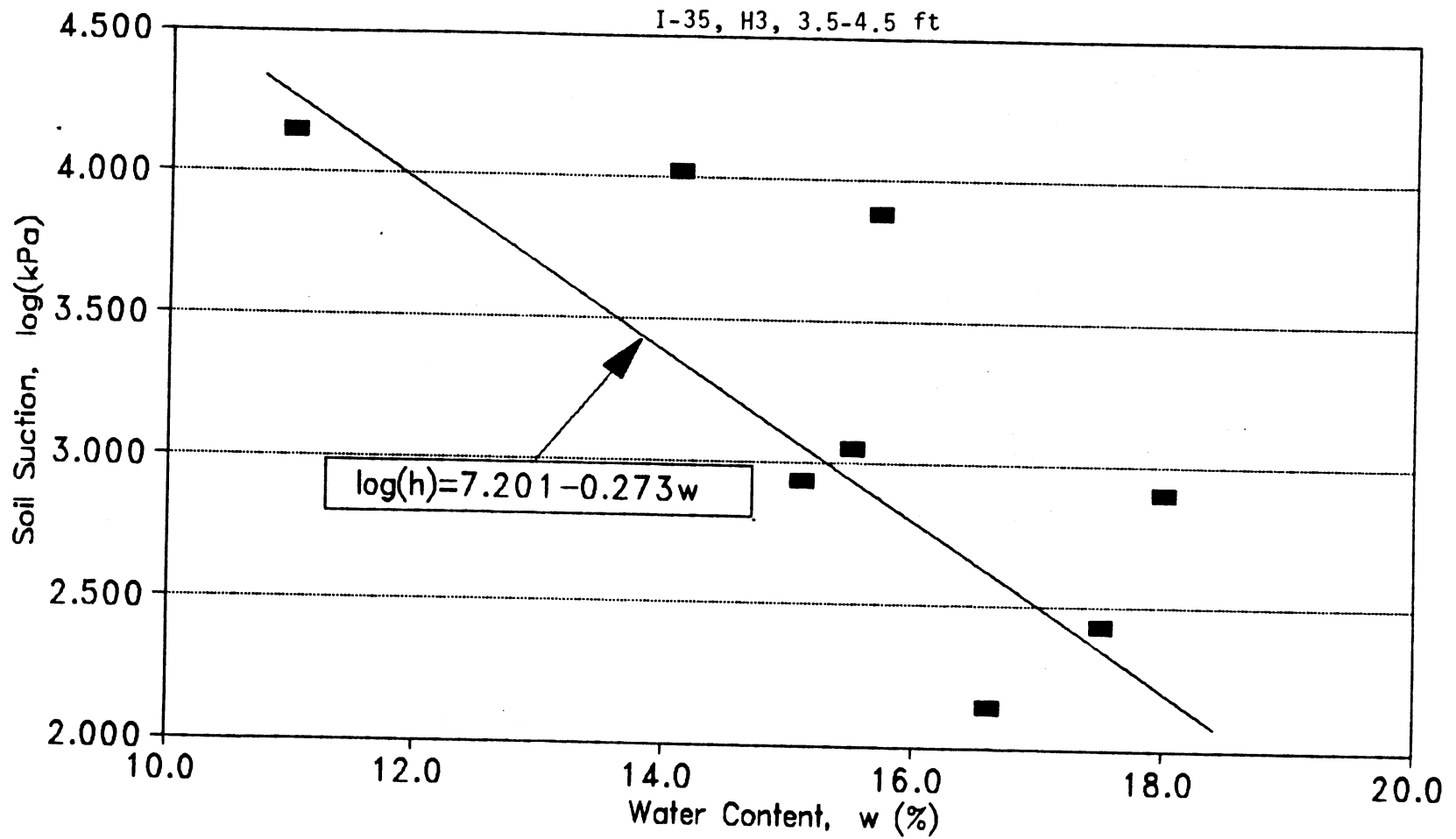


Figure B-1. (Continued)

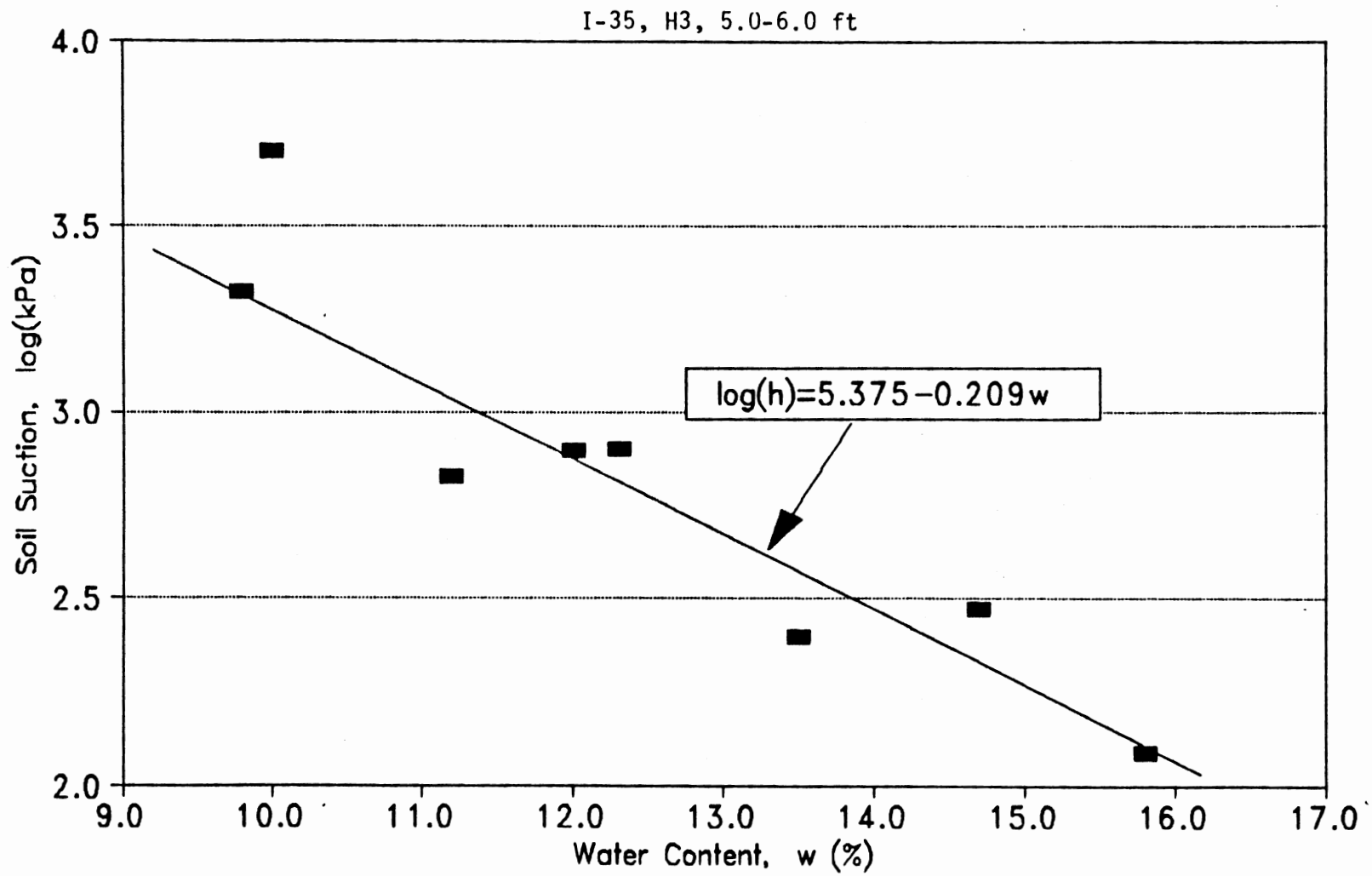


Figure B-1. (Continued)

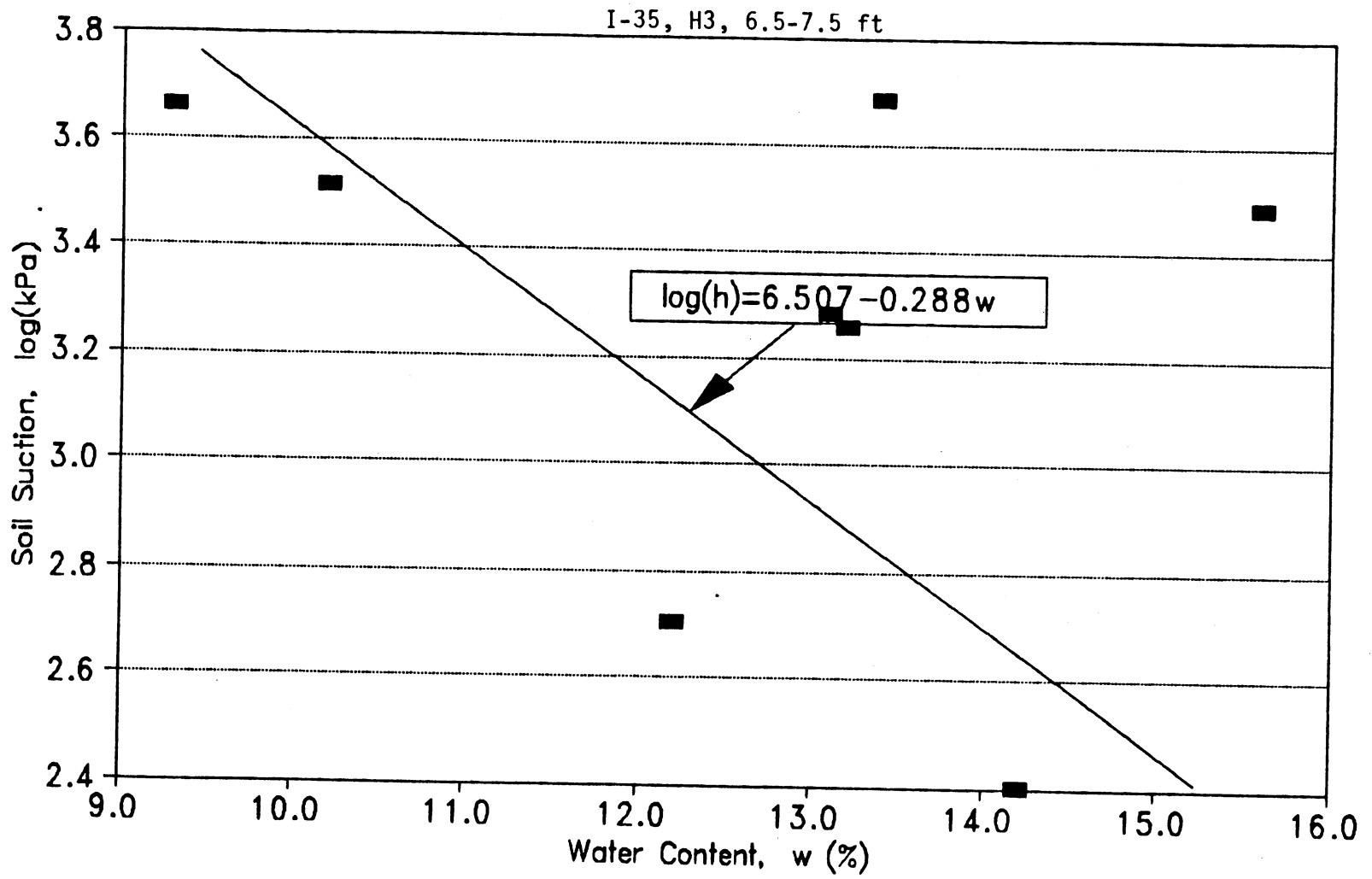


Figure B-1. (Continued)

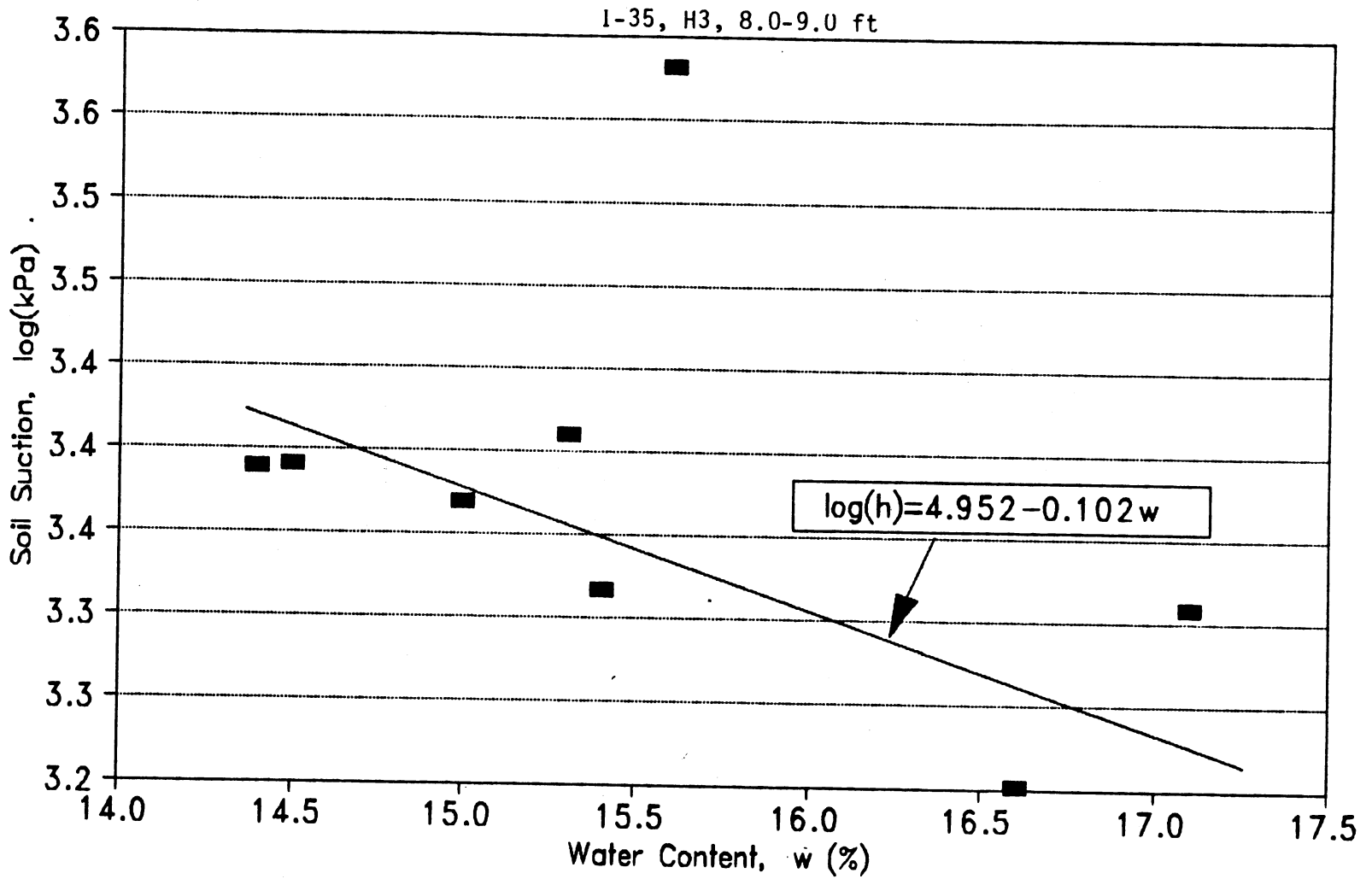


Figure B-1. (Continued)

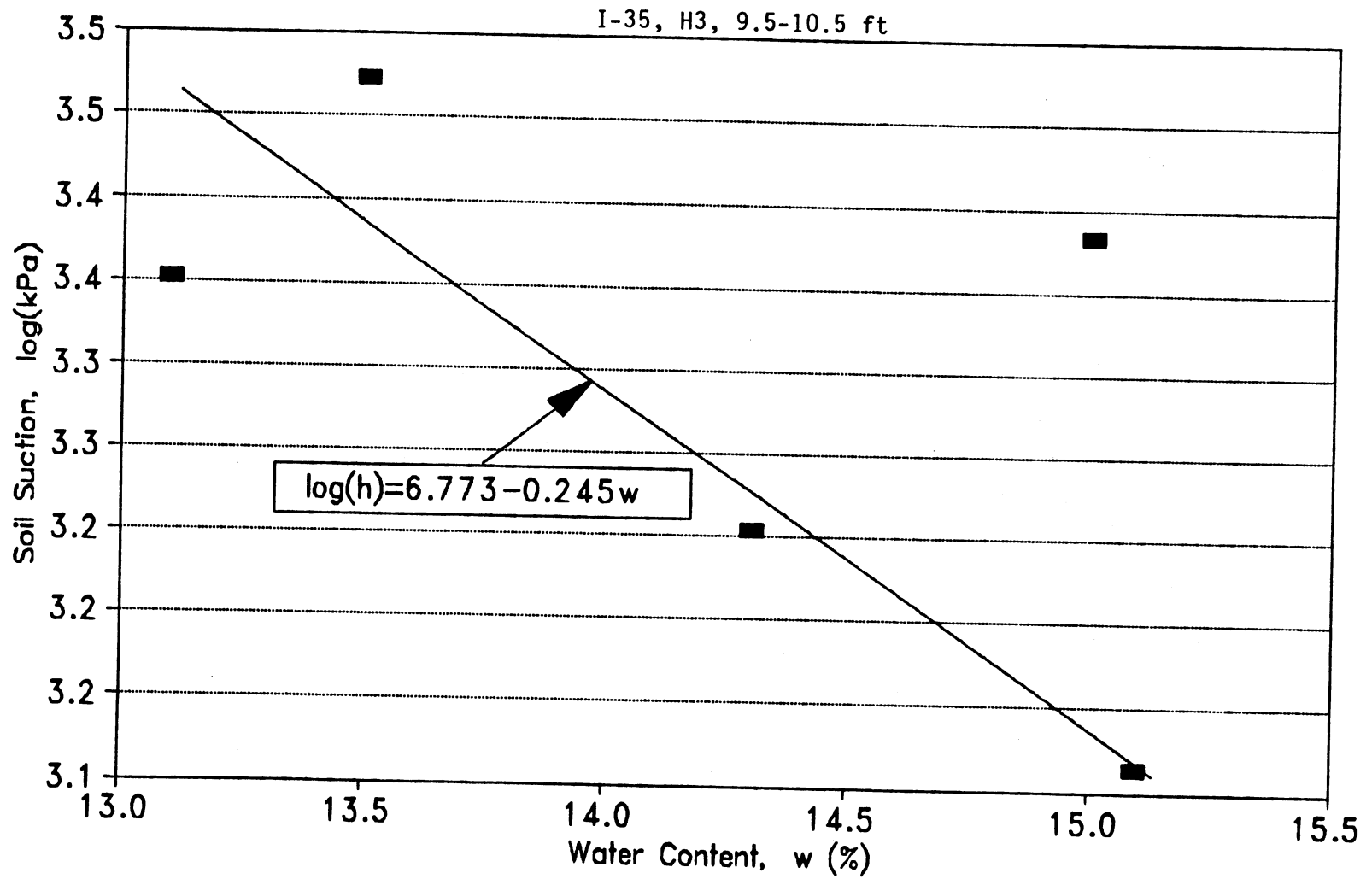


Figure B-1. (Continued)

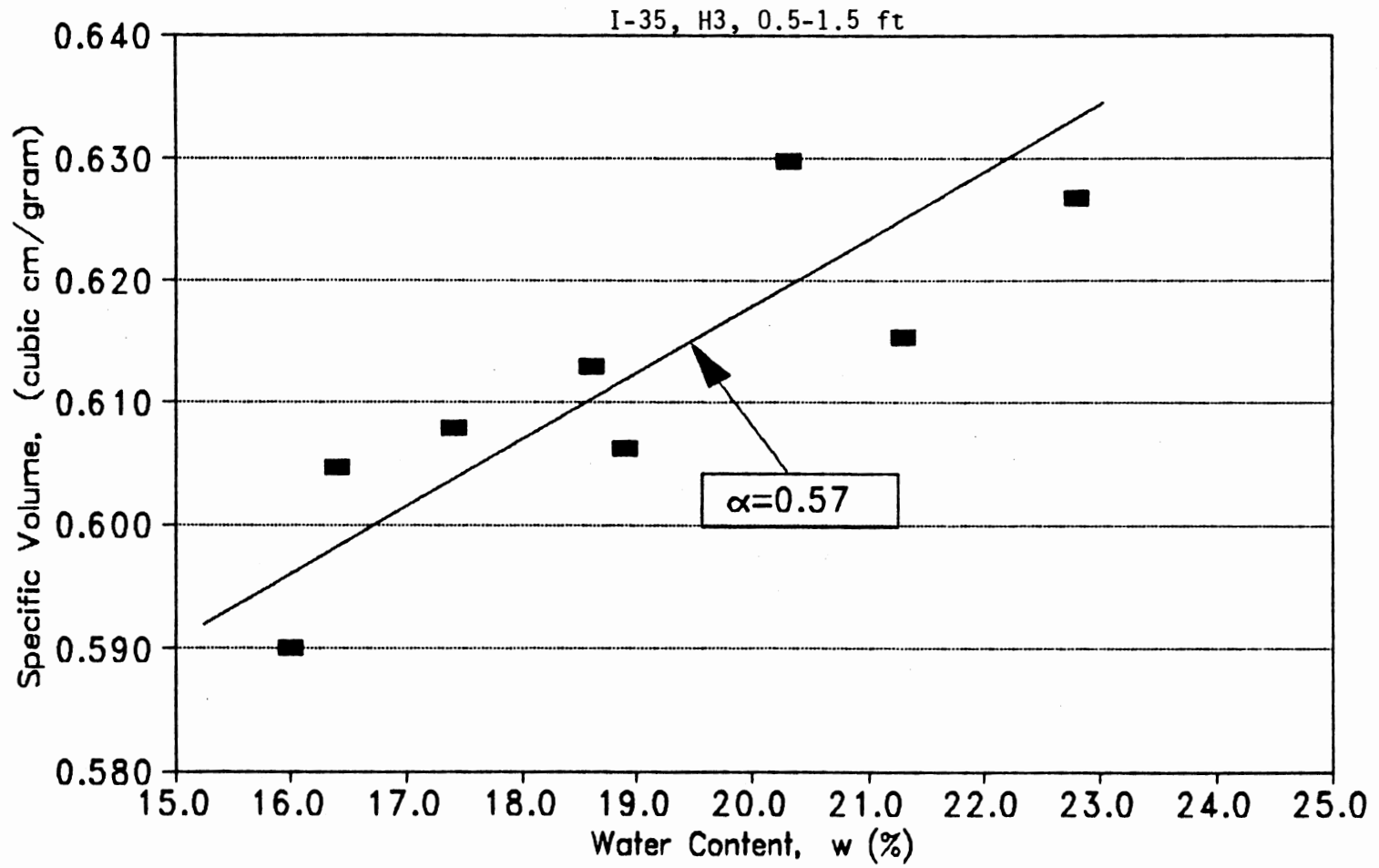


Figure B-2. Specific Volume Vs. Water Content

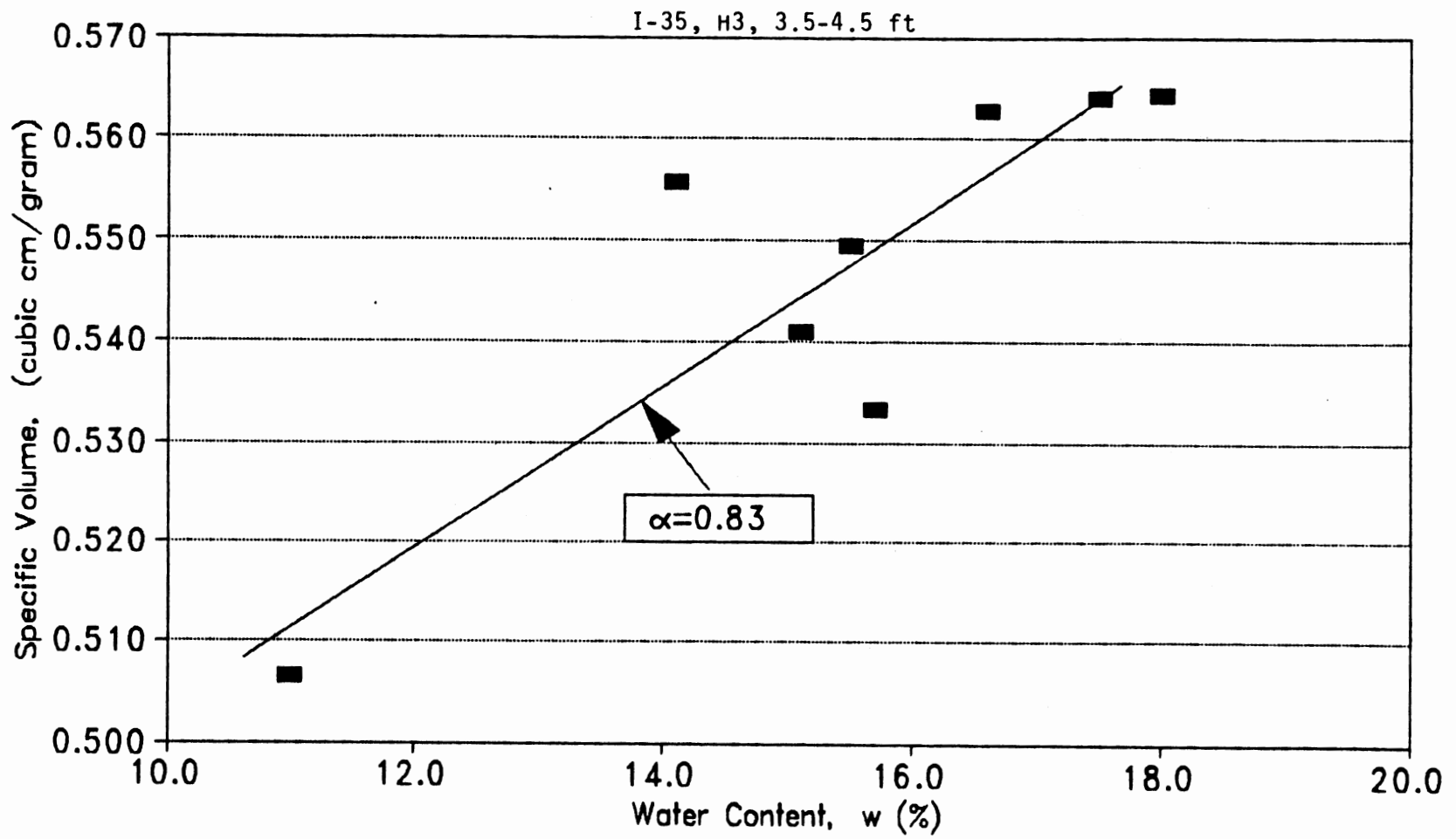


Figure B-2. (Continued)

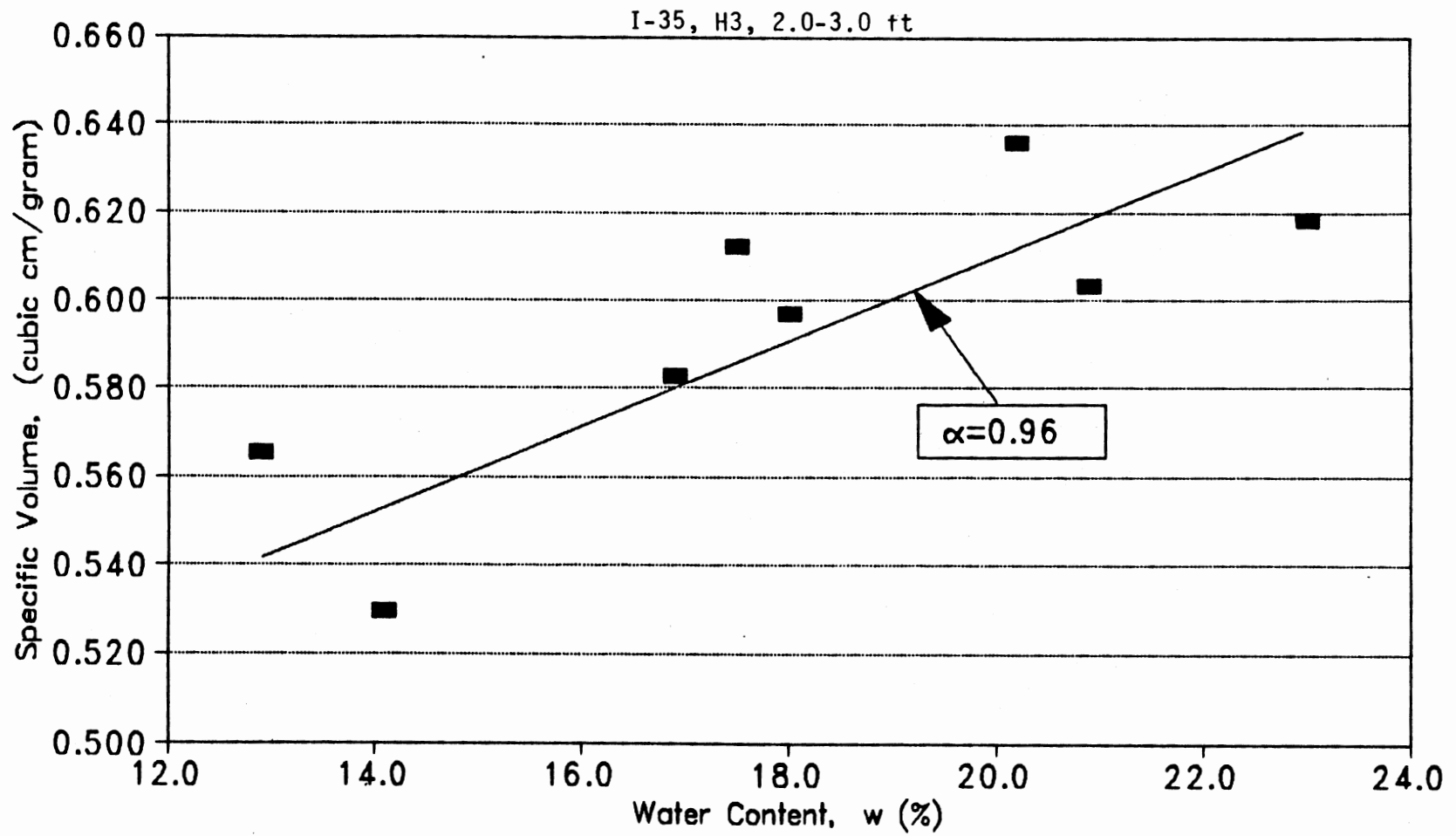


Figure B-2. (Continued)

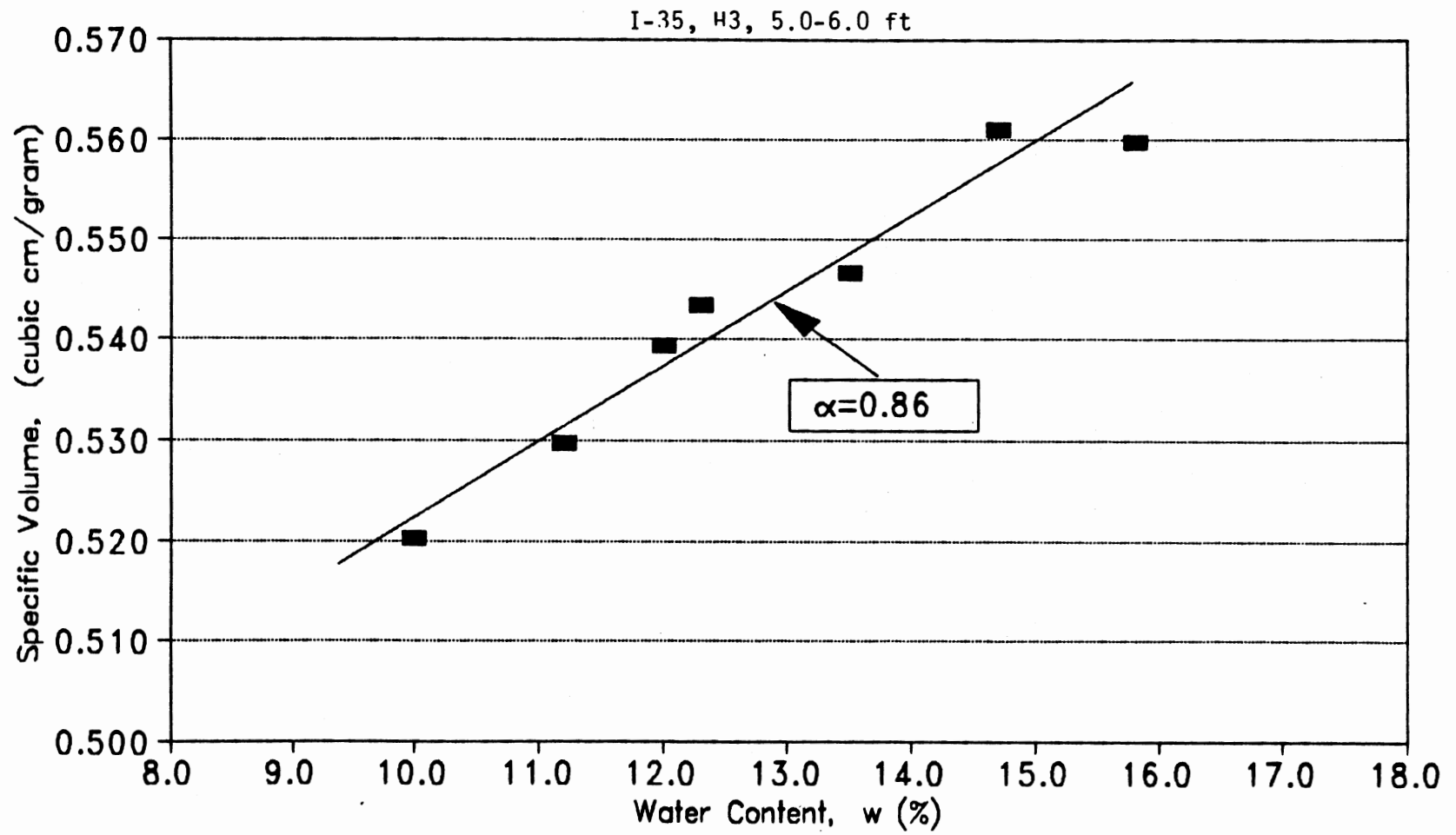


Figure B-2. (Continued)

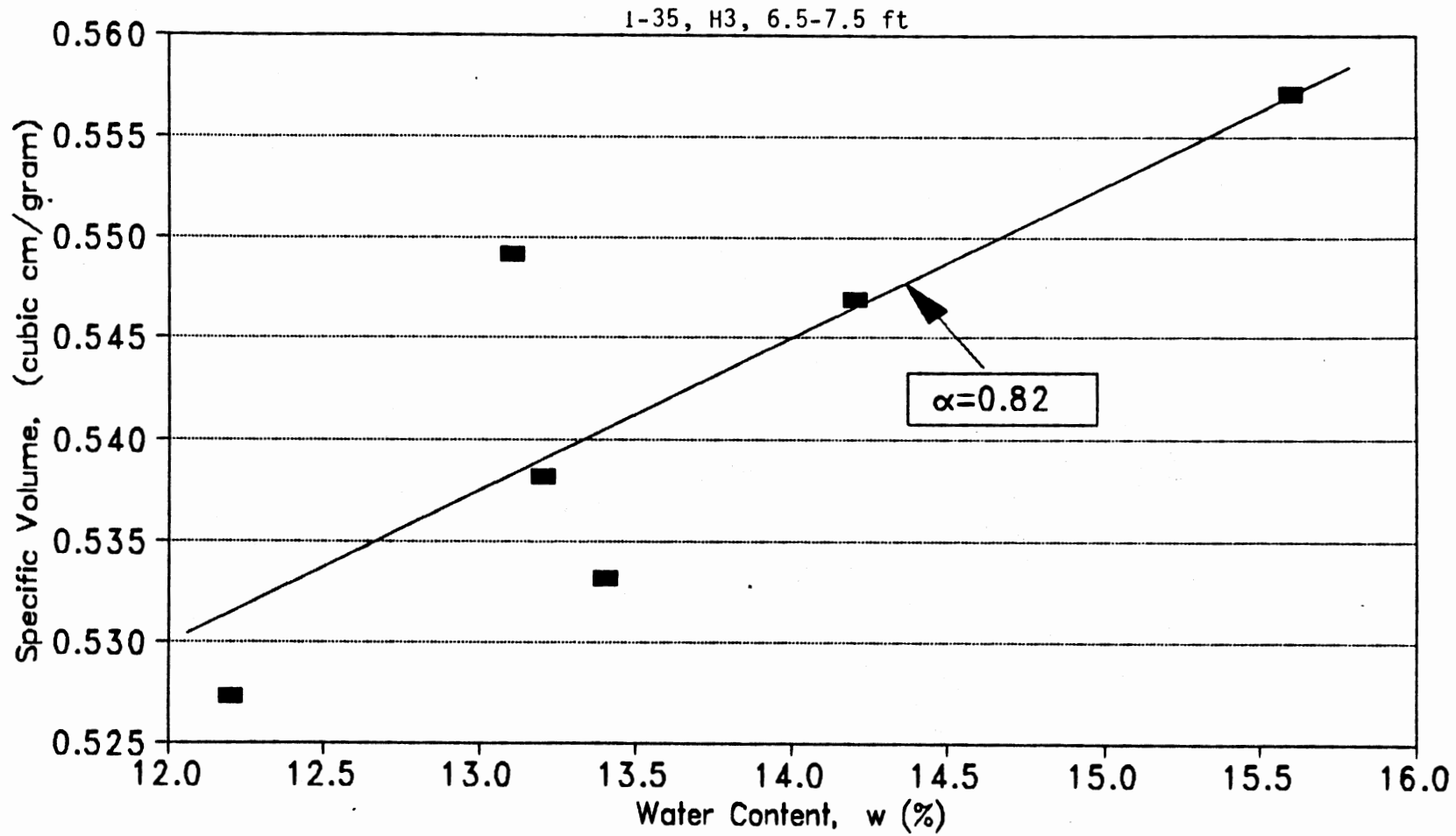


Figure B-2. (Continued)

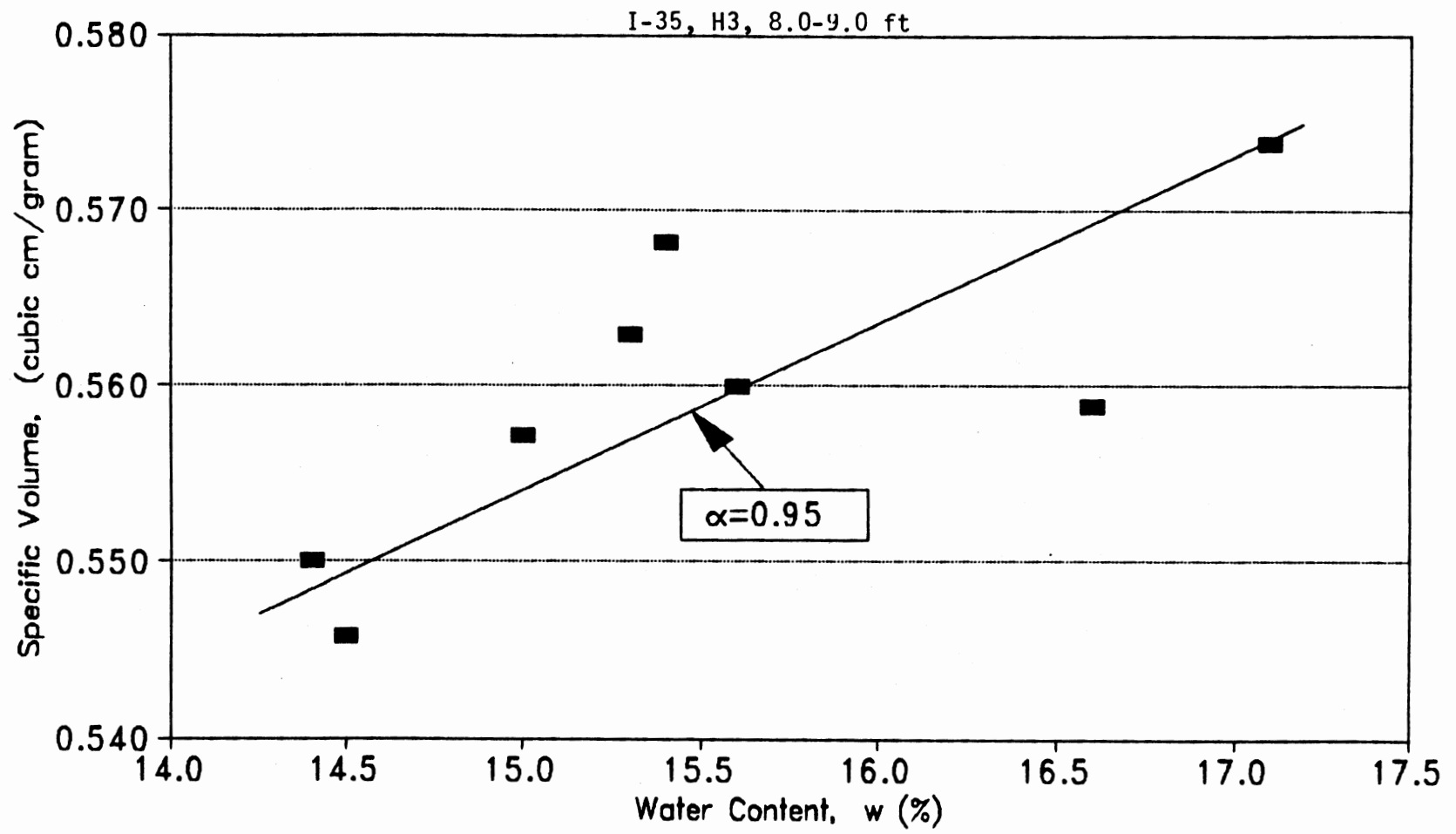


Figure B-2. (Continued)

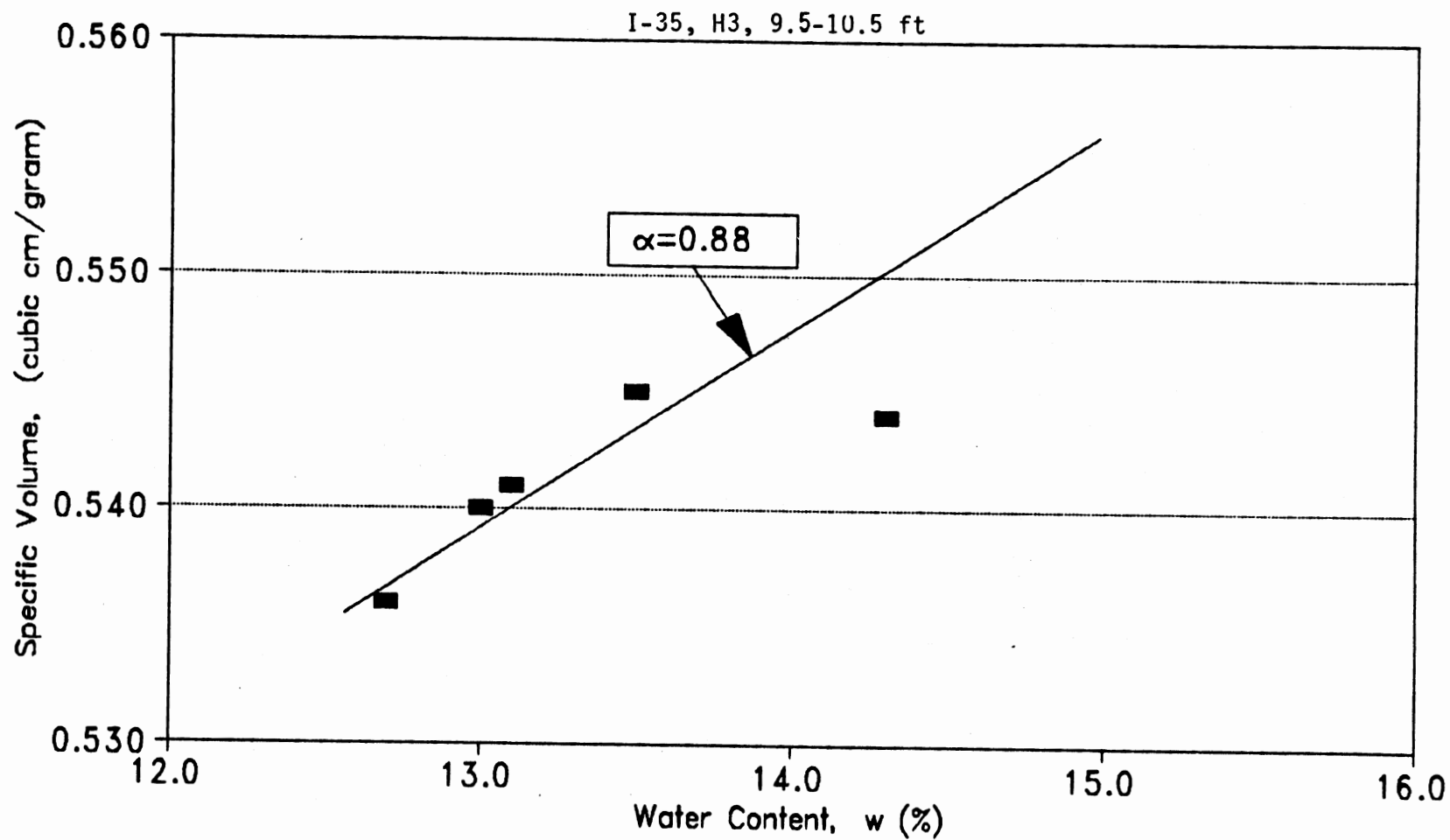


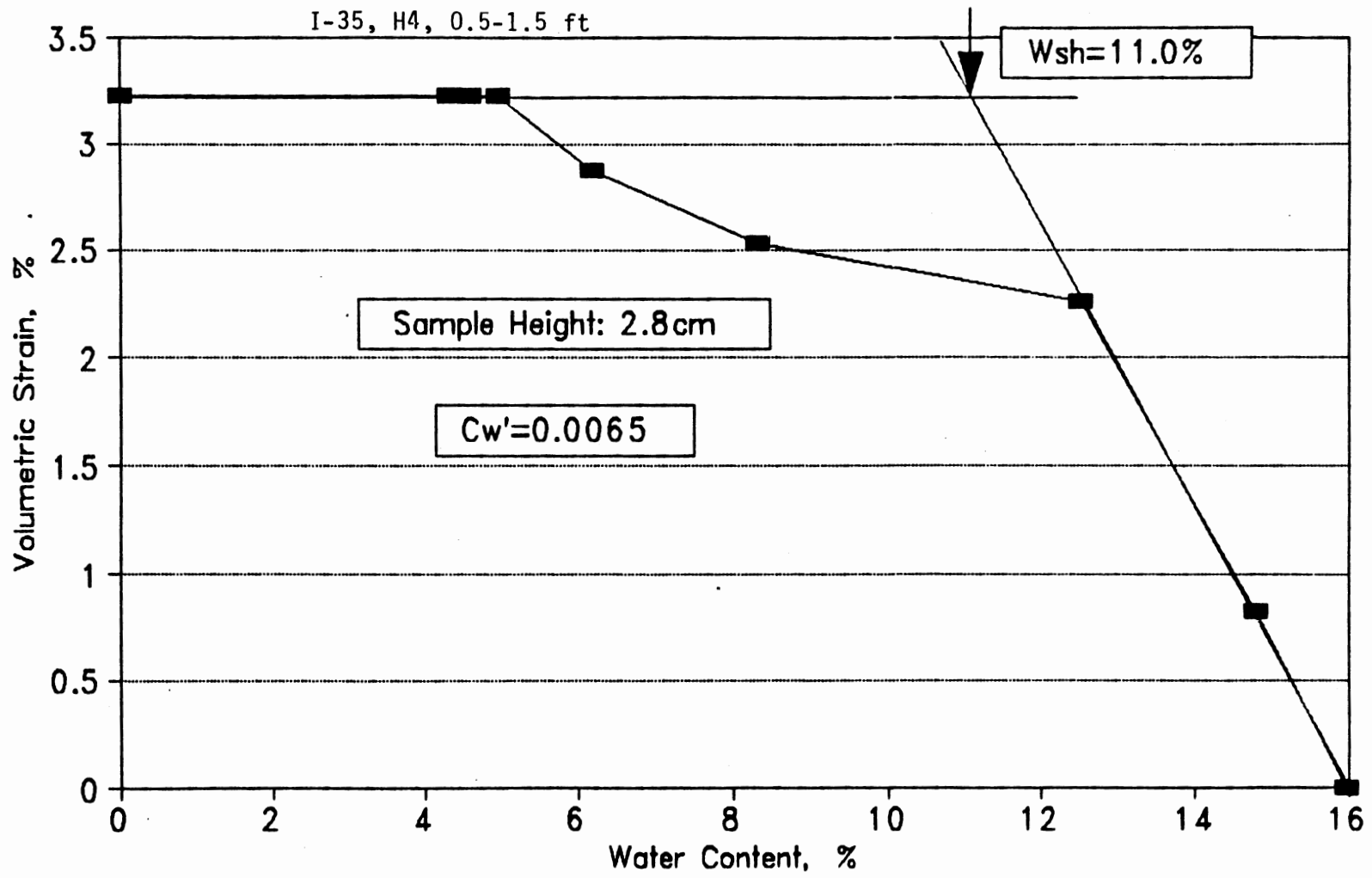
Figure B-2. (Continued)

TABLE B.2
CLOD AND CORE SHRINKAGE TEST RESULTS

W. Weight (grams)	Diameter (cm)	Height (cm)	w (%)	dD/D (%)	dH/H (%)	dV/V (%)
<u>Sample Dimension: Diameter = 7.3 cm, Height = 2.8 cm</u>						
<u>I-35, H2, 0.5-1.5 ft</u>						
238.3	7.28	2.83	16.0	0.00	0.00	0.00
235.9	7.25	2.83	14.8	0.41	0.00	0.82
231.2	7.21	2.82	12.5	0.96	0.35	2.26
222.6	7.20	2.82	8.3	1.10	0.35	2.53
218.2	7.20	2.81	6.2	1.10	0.71	2.88
215.7	7.20	2.80	5.0	1.10	1.06	3.22
214.9	7.20	2.80	4.6	1.10	1.06	3.22
214.4	7.20	2.80	4.3	1.10	1.06	3.22
205.5	7.20	2.80	0.0	1.10	1.06	3.22
<u>I-35, H2, 2.0-3.0 ft</u>						
251.8	7.23	2.78	19.6	0.00	0.00	0.00
249.7	7.15	2.77	18.6	1.11	0.36	2.55
245.6	7.03	2.75	16.7	2.77	1.08	6.48
237.5	6.95	2.67	12.8	3.87	3.96	11.25
232.0	6.93	2.65	10.2	4.15	4.68	12.42
227.5	6.92	2.65	8.1	4.29	4.68	12.68
226.1	6.91	2.64	7.4	4.43	5.04	13.26
225.2	6.89	2.63	7.0	4.70	5.40	14.08
210.5	6.88	2.63	0.0	4.84	5.40	14.33
<u>I-35, H2, 3.5-4.5.0 ft</u>						
232.0	7.30	2.60	16.2	0.00	0.00	0.00
230.4	7.23	2.53	15.4	0.96	2.69	4.55
226.7	7.13	2.45	13.5	2.33	5.77	10.11
219.9	7.08	2.43	10.1	3.01	6.54	12.09
215.9	7.07	2.41	8.1	3.15	7.31	13.06
213.2	7.06	2.40	6.8	3.29	7.69	13.66
212.3	7.05	2.39	6.3	3.42	8.08	14.27
211.6	7.05	2.38	6.0	3.42	8.46	14.62
199.7	7.04	2.38	0.0	3.56	8.46	14.87
<u>I-35, H4, 5.0-6.0 ft</u>						
217.5	7.25	2.48	14.2	0.00	0.00	0.00
215.9	7.20	2.44	13.4	0.69	1.61	2.97
212.1	7.15	2.42	11.4	1.38	2.42	5.09
205.3	7.13	2.41	7.8	1.66	2.82	6.01
200.0	7.11	2.40	5.0	1.93	3.23	6.93
199.5	7.11	2.40	4.8	1.93	3.23	6.93
199.0	7.10	2.40	4.5	2.07	3.23	7.19
190.4	7.10	2.40	0.0	2.07	3.23	7.19

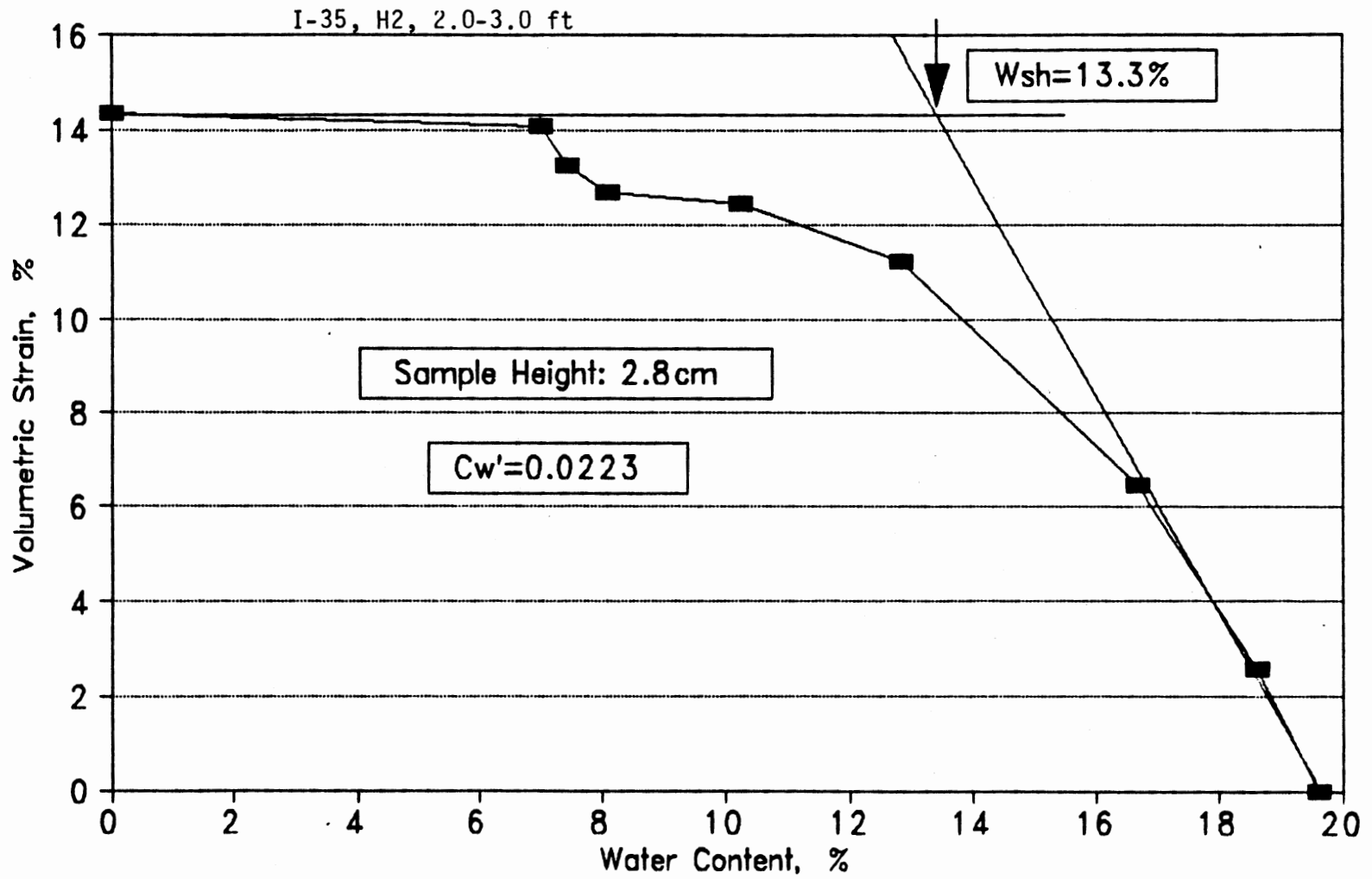
TABLE B.2 (Continued)

W. Weight (grams)	Diameter (cm)	Height (cm)	w (%)	dD/D (%)	dH/H (%)	dV/V (%)
<u>I-35. H3. 6.5-7.5 ft</u>						
256.8	7.25	2.83	14.3	0.00	0.00	0.00
254.0	7.20	2.75	13.1	0.69	2.83	4.16
249.7	7.15	2.74	11.2	1.38	3.18	5.83
242.2	7.15	2.71	7.8	1.38	4.24	6.86
238.2	7.14	2.70	6.1	1.52	4.59	7.47
235.9	7.14	2.70	5.0	1.52	4.59	7.47
235.2	7.14	2.70	4.7	1.52	4.59	7.47
234.7	7.14	2.70	4.5	1.52	4.59	7.47
224.6	7.14	2.70	0.0	1.52	4.59	7.47
<u>I-35. H3. 8.0-9.0 ft</u>						
260.8	7.20	3.05	11.7	0.00	0.00	0.00
258.3	7.15	3.04	10.7	0.69	0.33	1.71
254.4	7.13	3.04	9.0	0.97	0.33	2.26
248.2	7.12	3.03	6.3	1.11	0.66	2.85
245.3	7.11	3.03	5.1	1.25	0.66	3.12
243.7	7.10	3.03	4.4	1.39	0.66	3.40
243.1	7.10	3.03	4.2	1.39	0.66	3.40
242.7	7.10	3.03	4.0	1.39	0.66	3.40
233.4	7.10	3.03	0.0	1.39	0.66	3.40
<u>I-35. H3. 9.5-10.5 ft</u>						
227.6	7.20	2.75	13.9	0.00	0.00	0.00
225.4	7.18	2.73	12.8	0.28	0.73	1.28
221.5	7.17	2.71	10.9	0.42	1.45	2.27
215.0	7.16	2.70	7.6	0.56	1.82	2.91
209.9	7.14	2.69	5.1	0.83	2.18	3.81
209.4	7.14	2.69	4.8	0.83	2.18	3.81
208.9	7.14	2.68	4.6	0.83	2.55	4.16
199.8	7.14	2.68	0.0	0.83	2.55	4.16



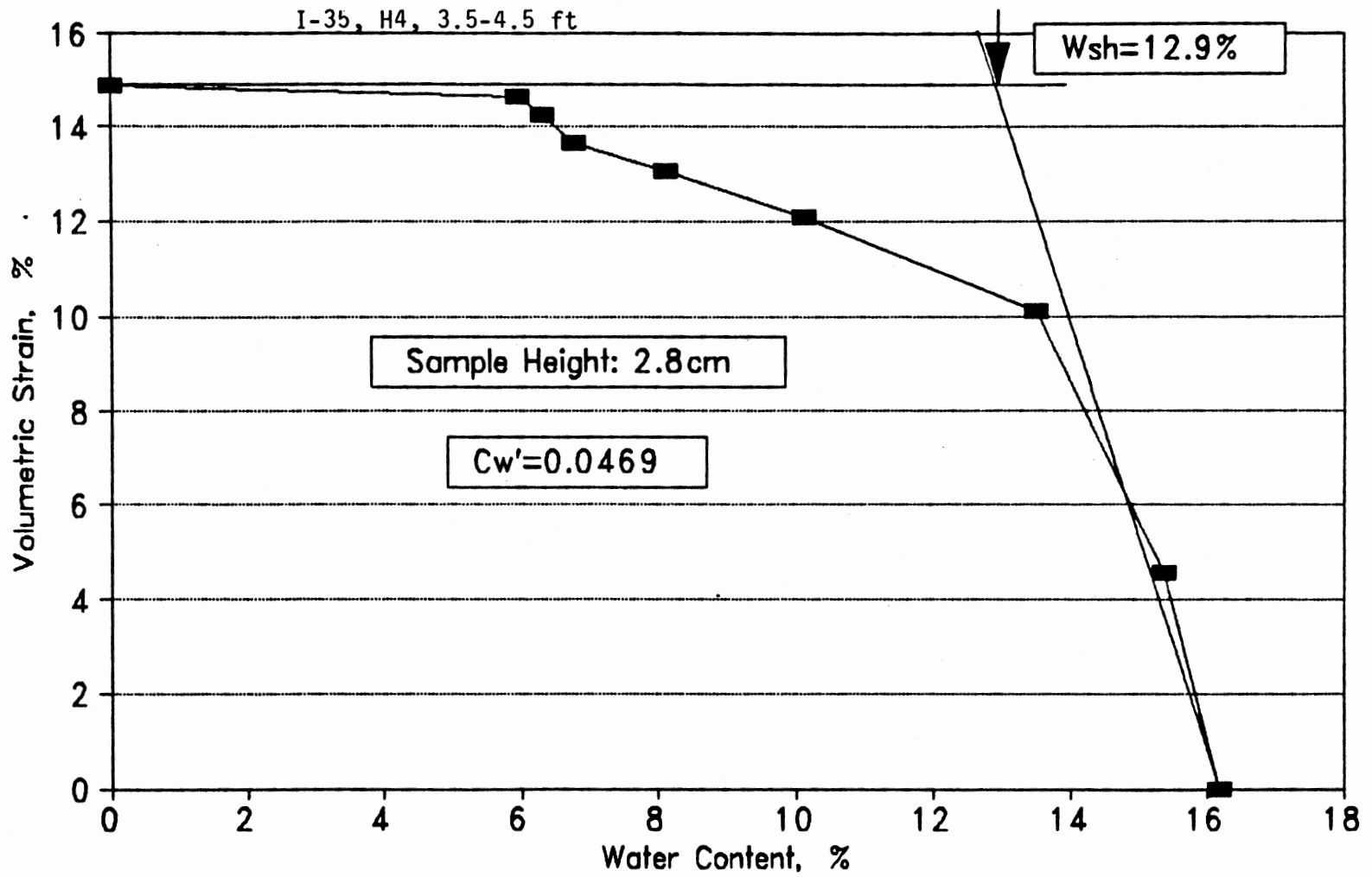
(a) Clod Shrinkage Curve

Figure B-3. Clod and Core Shrinkage Curves



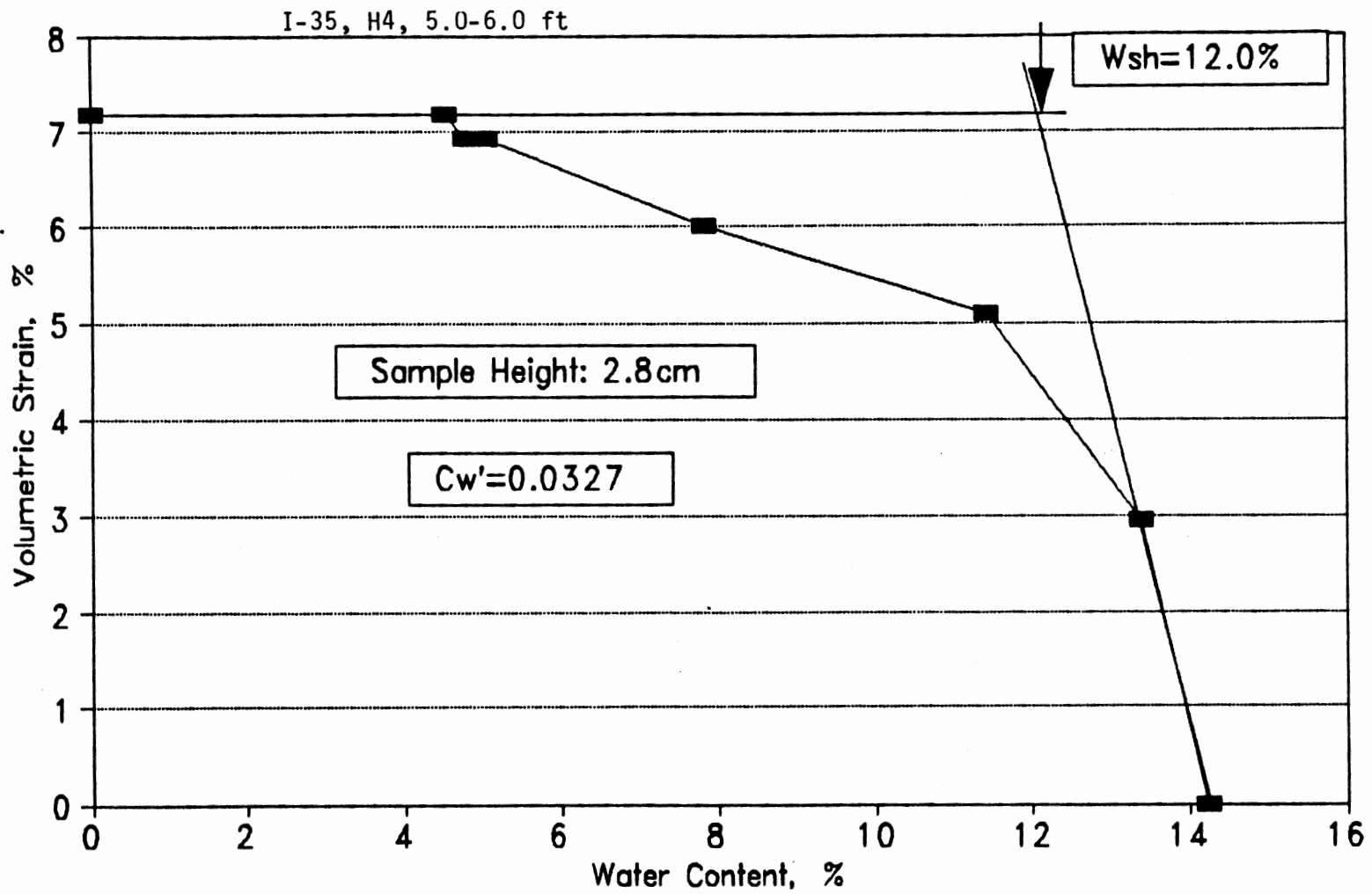
(a) Clod Shrinkage Curve

Figure B-3. (Continued)



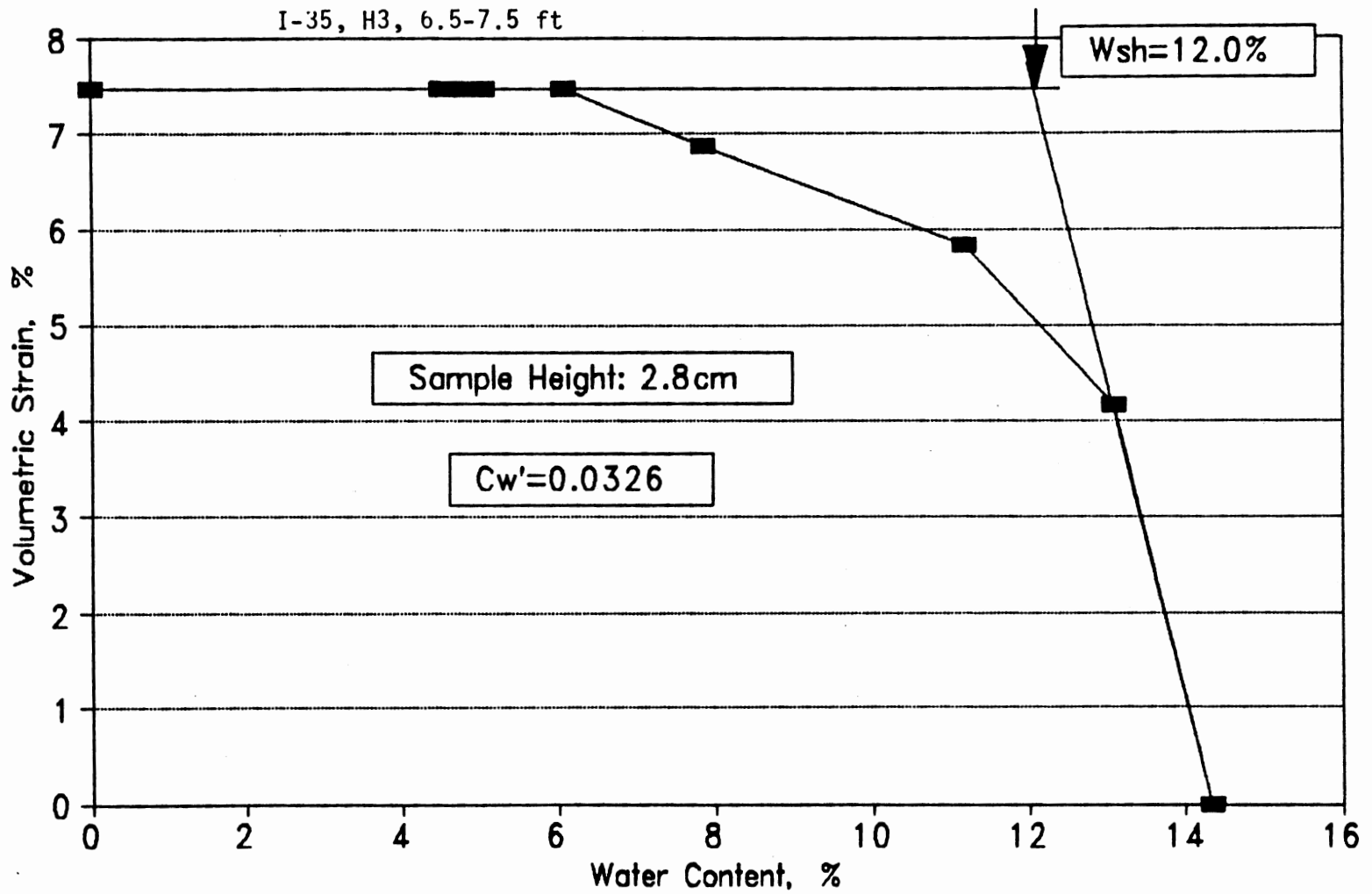
(a) Clod Shrinkage Curve

Figure B-3. (Continued)



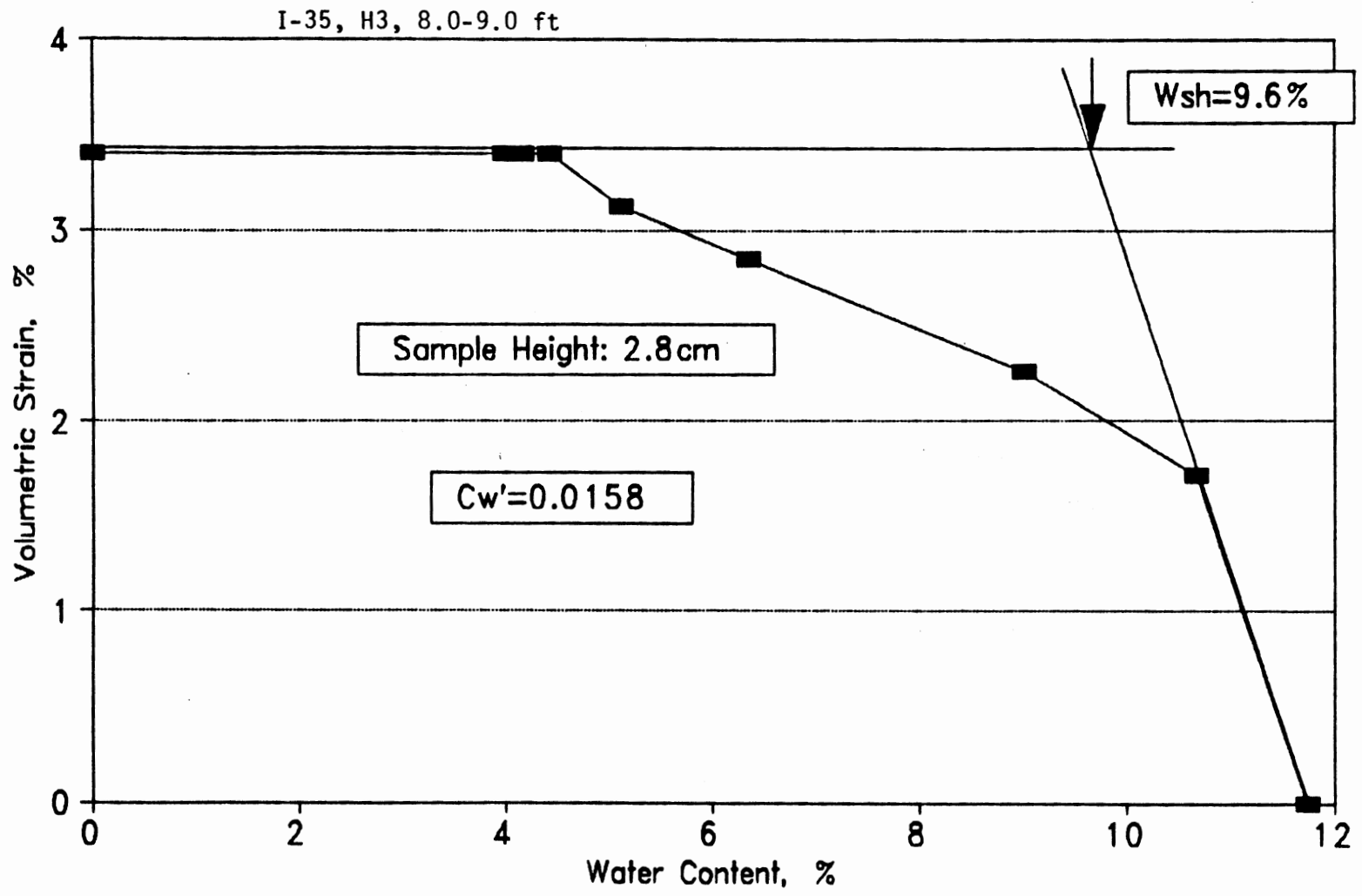
(a) Clod Shrinkage Curve

Figure B-3. (Continued)

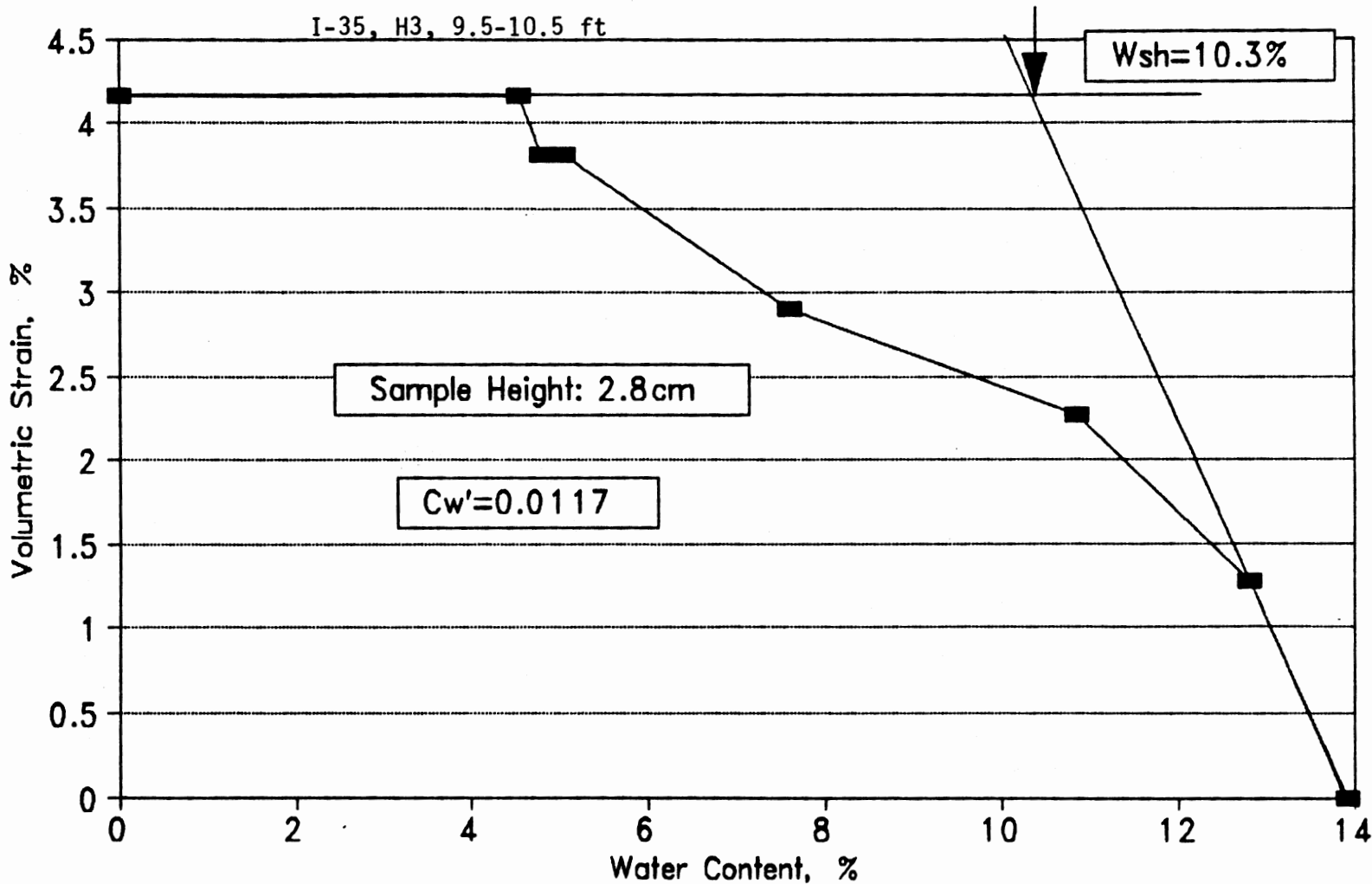


(a) Clod Shrinkage Curve

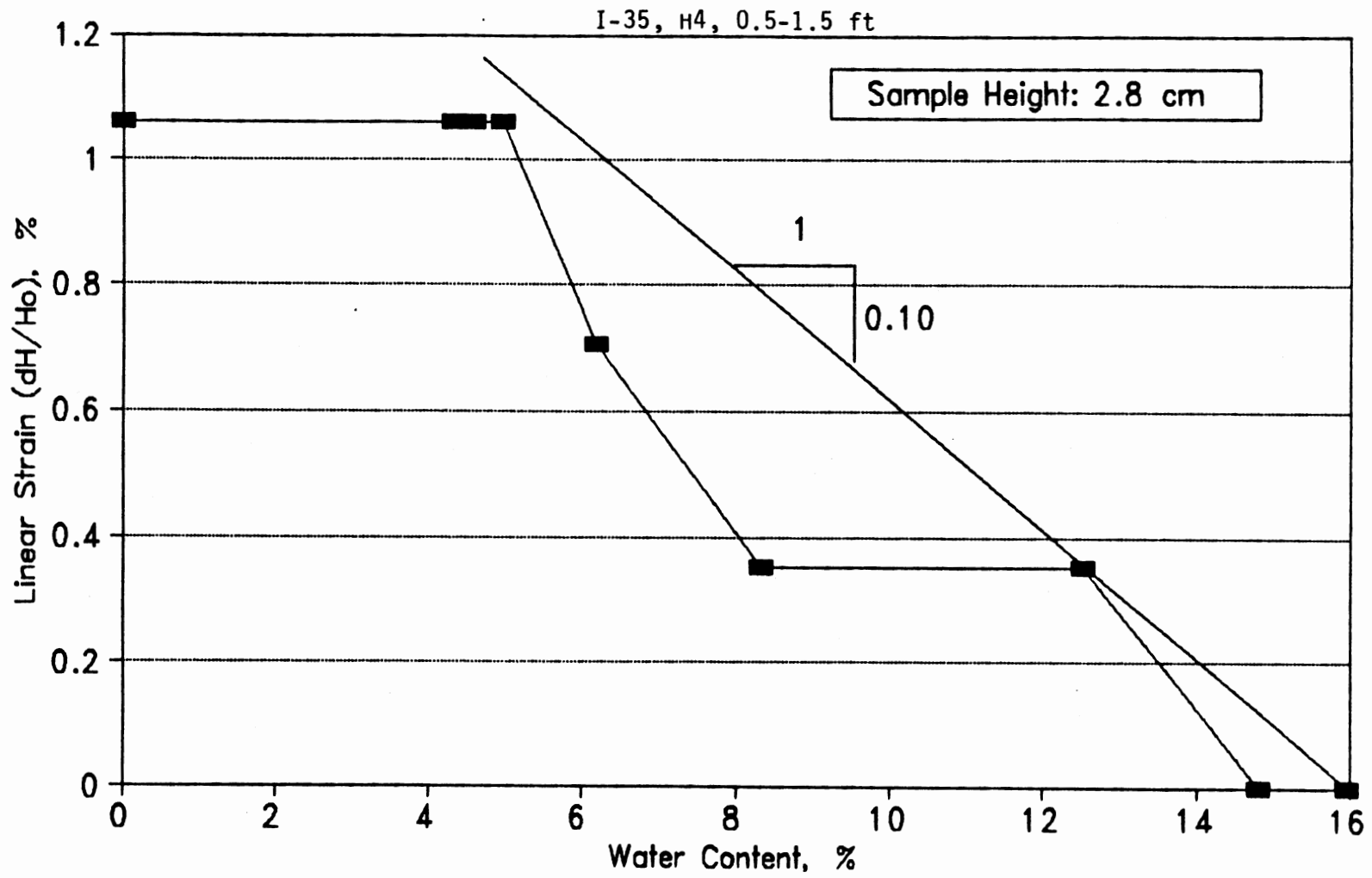
Figure B-3. (Continued)



(a) Clod Shrinkage Curve
 Figure B-3. (Continued)

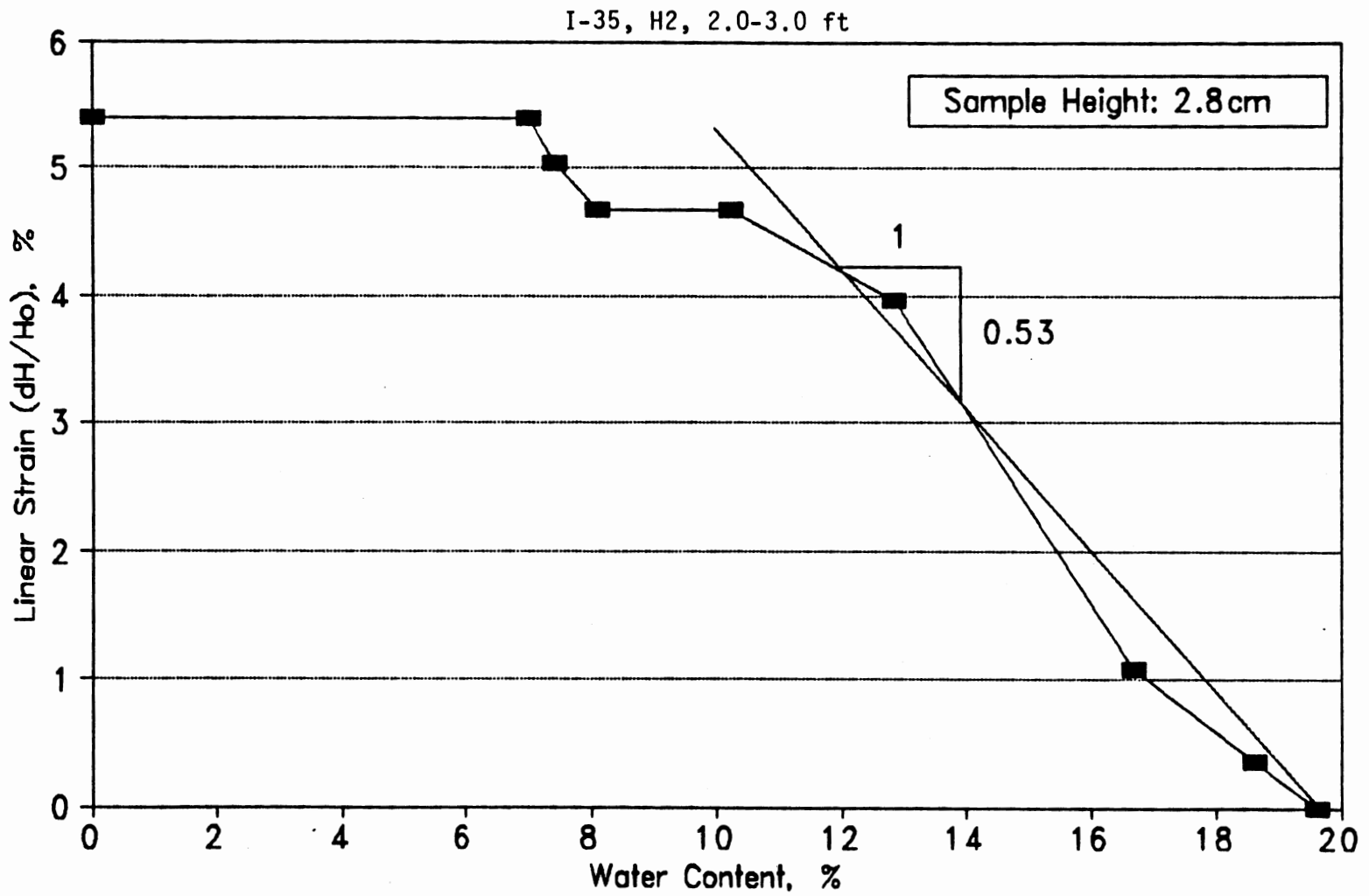


(a) Clod Shrinkage Curve
 Figure B-3. (Continued)



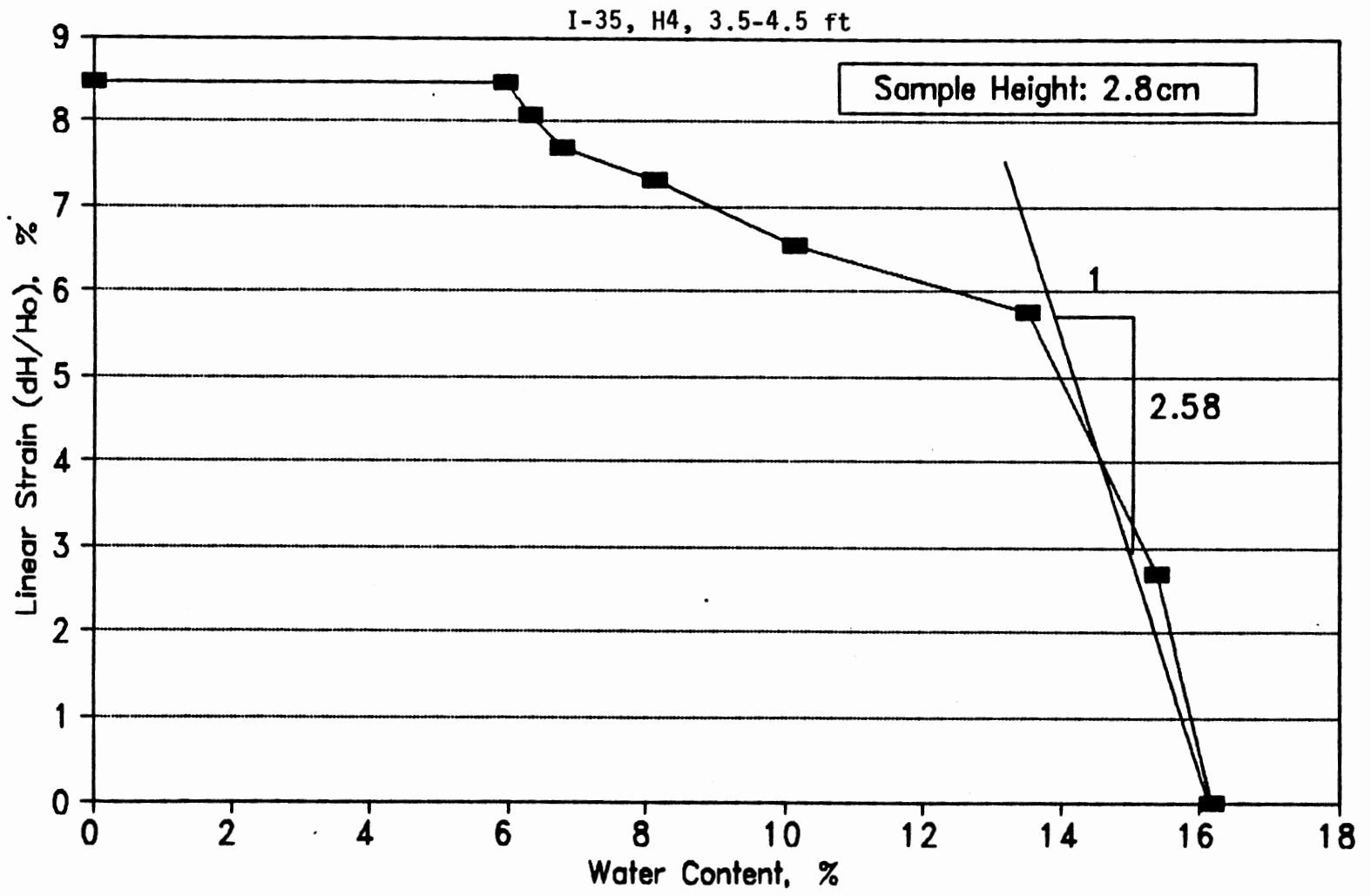
(b) Core Shrinkage Curve

Figure B-3. (Continued)



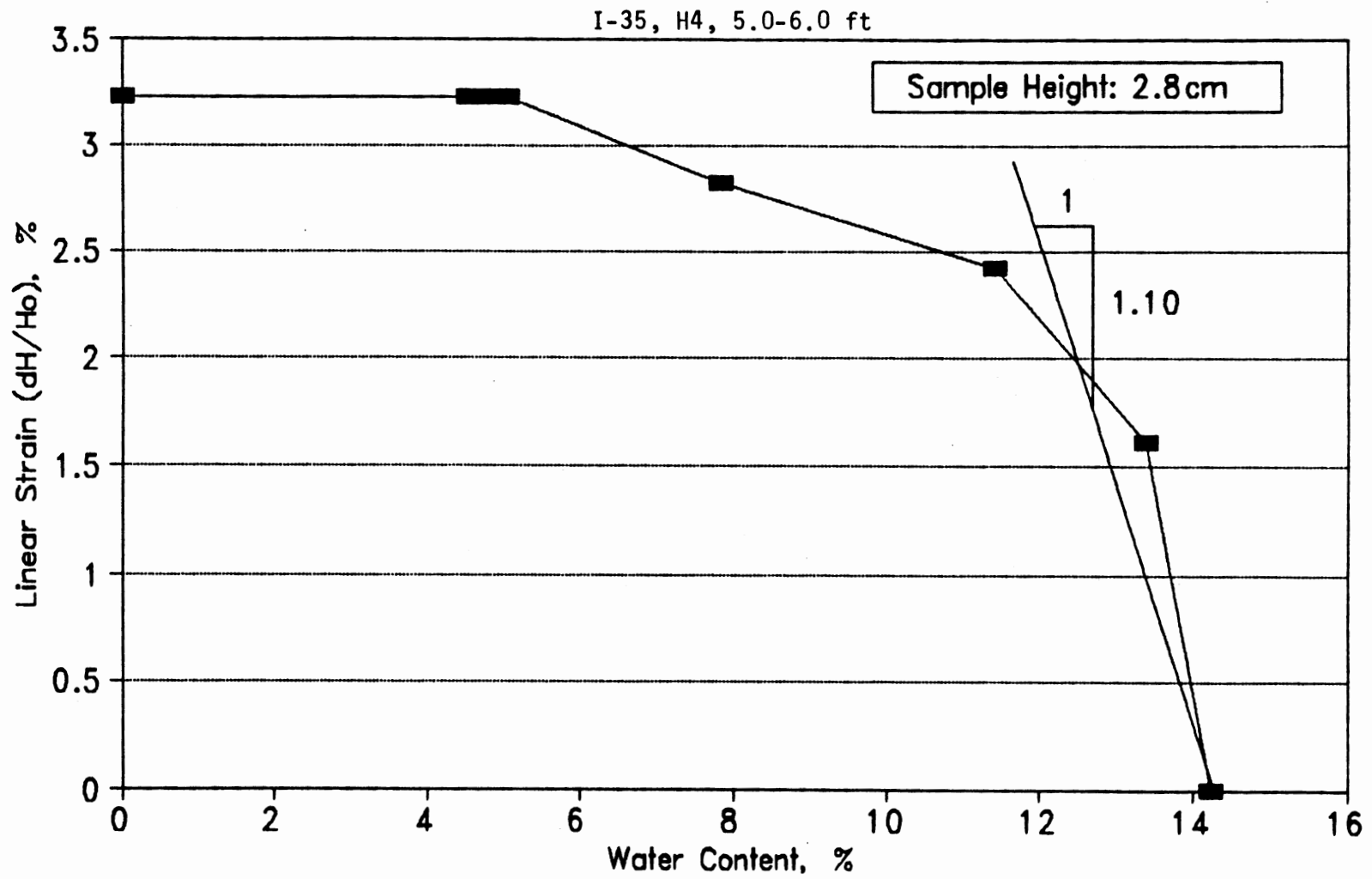
(b) Core Shrinkage Curve

Figure B-3. (Continued)



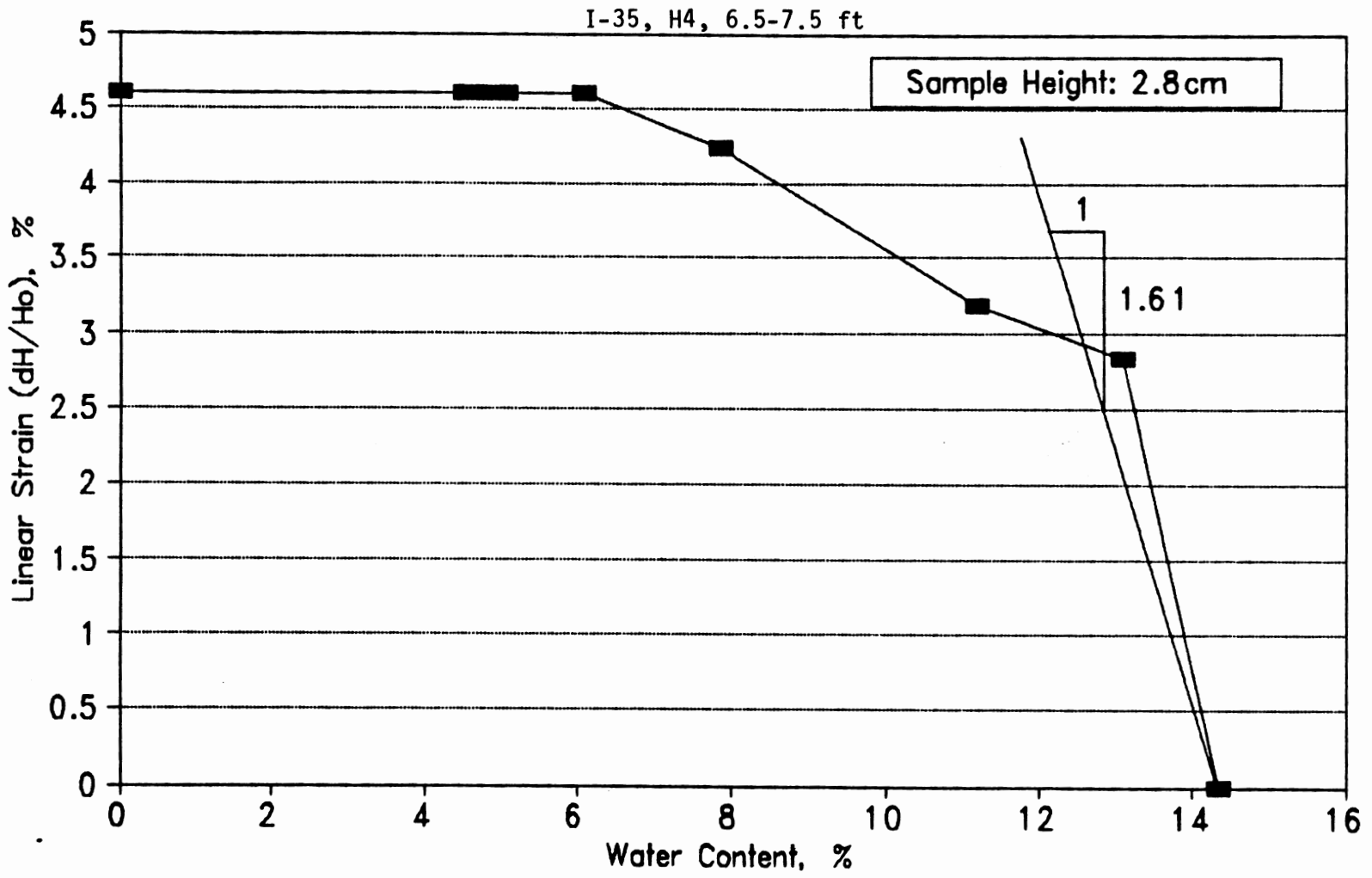
(b) Core Shrinkage Curve

Figure B-3. (Continued)



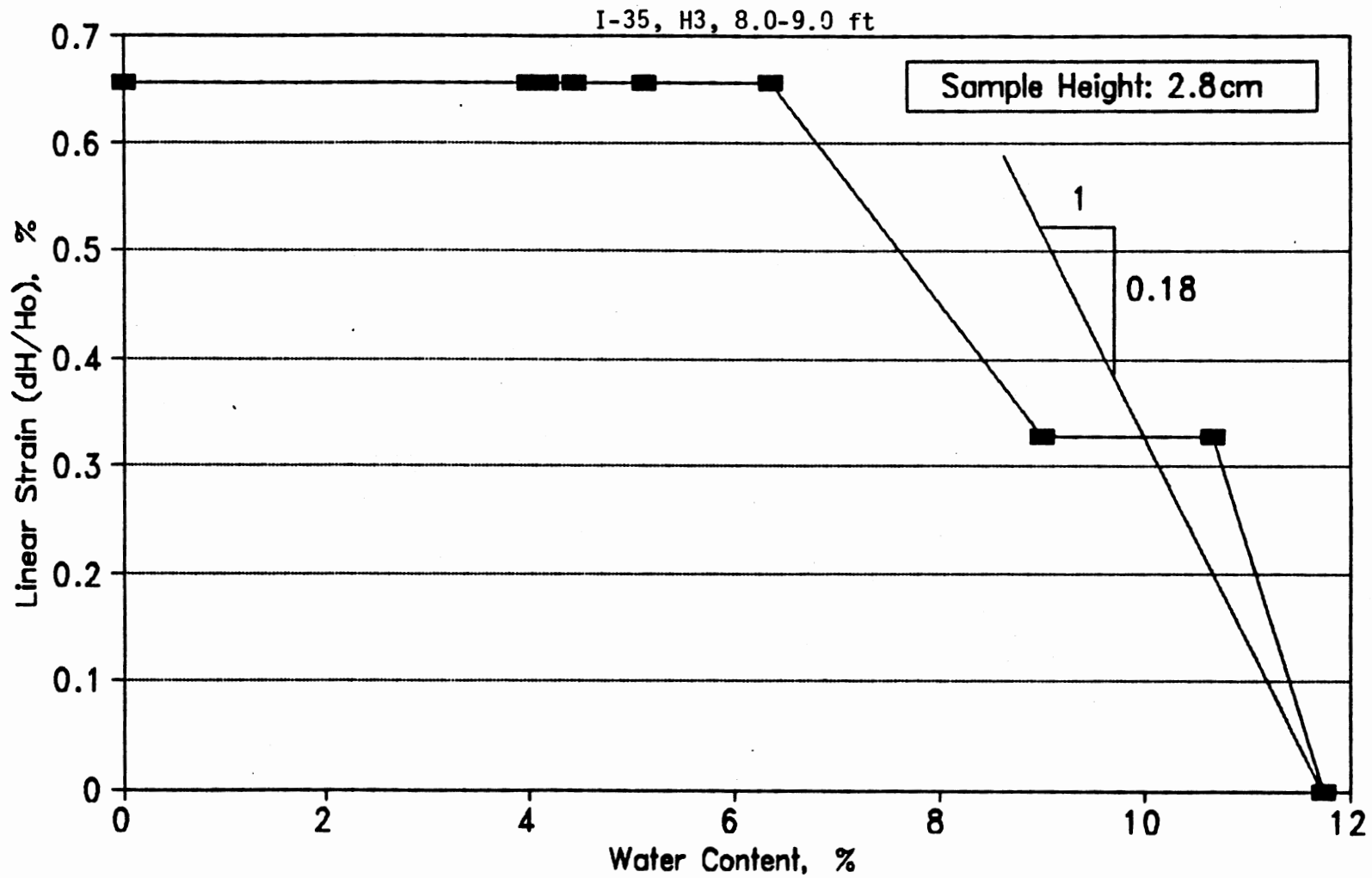
(b) Core Shrinkage Curve

Figure B-3. (Continued)



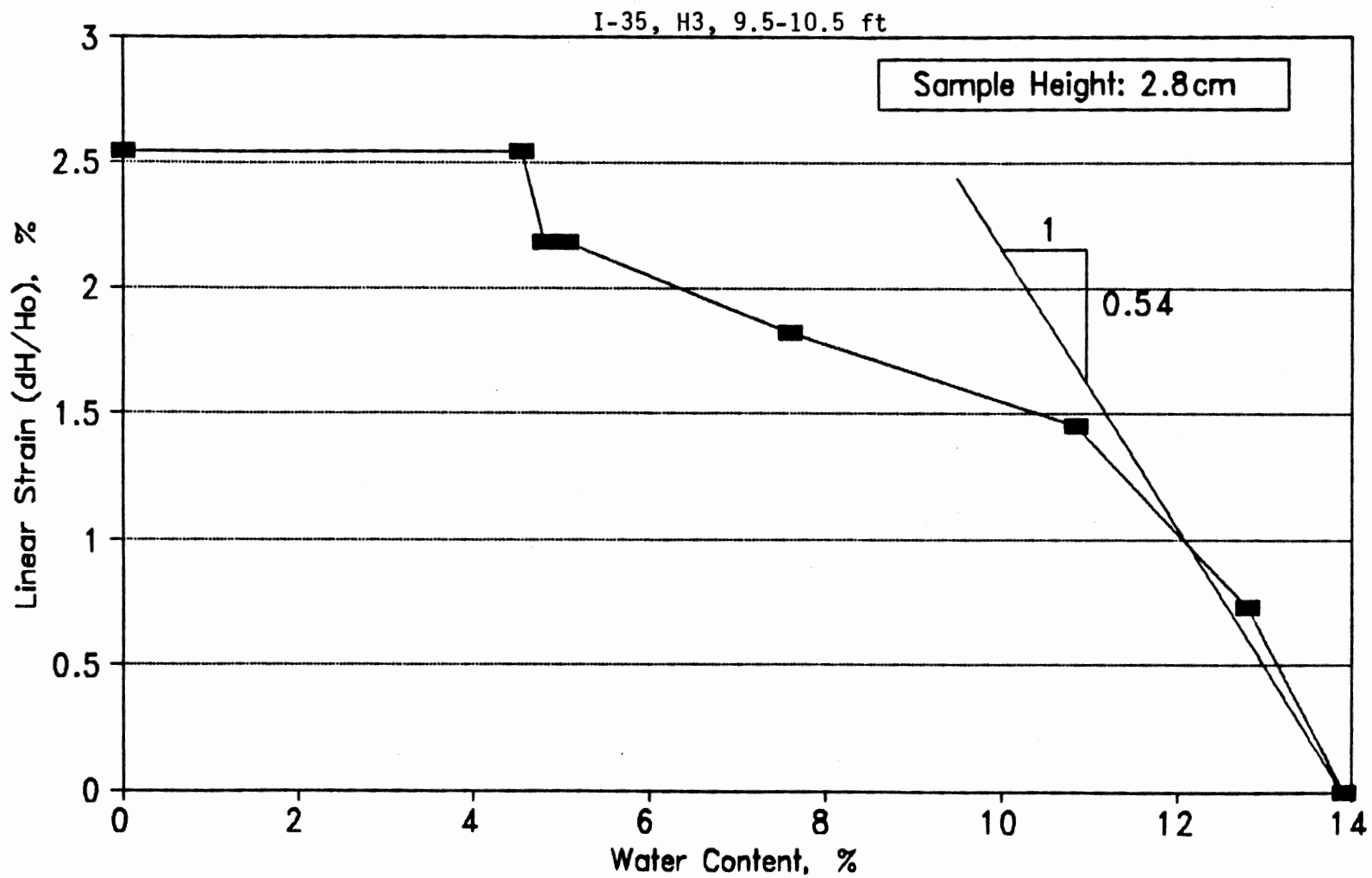
(b) Core Shrinkage Curve

Figure B-3. (Continued)



(b) Core Shrinkage Curve

Figure B-3. (Continued)



(b) Core Shrinkage Curve

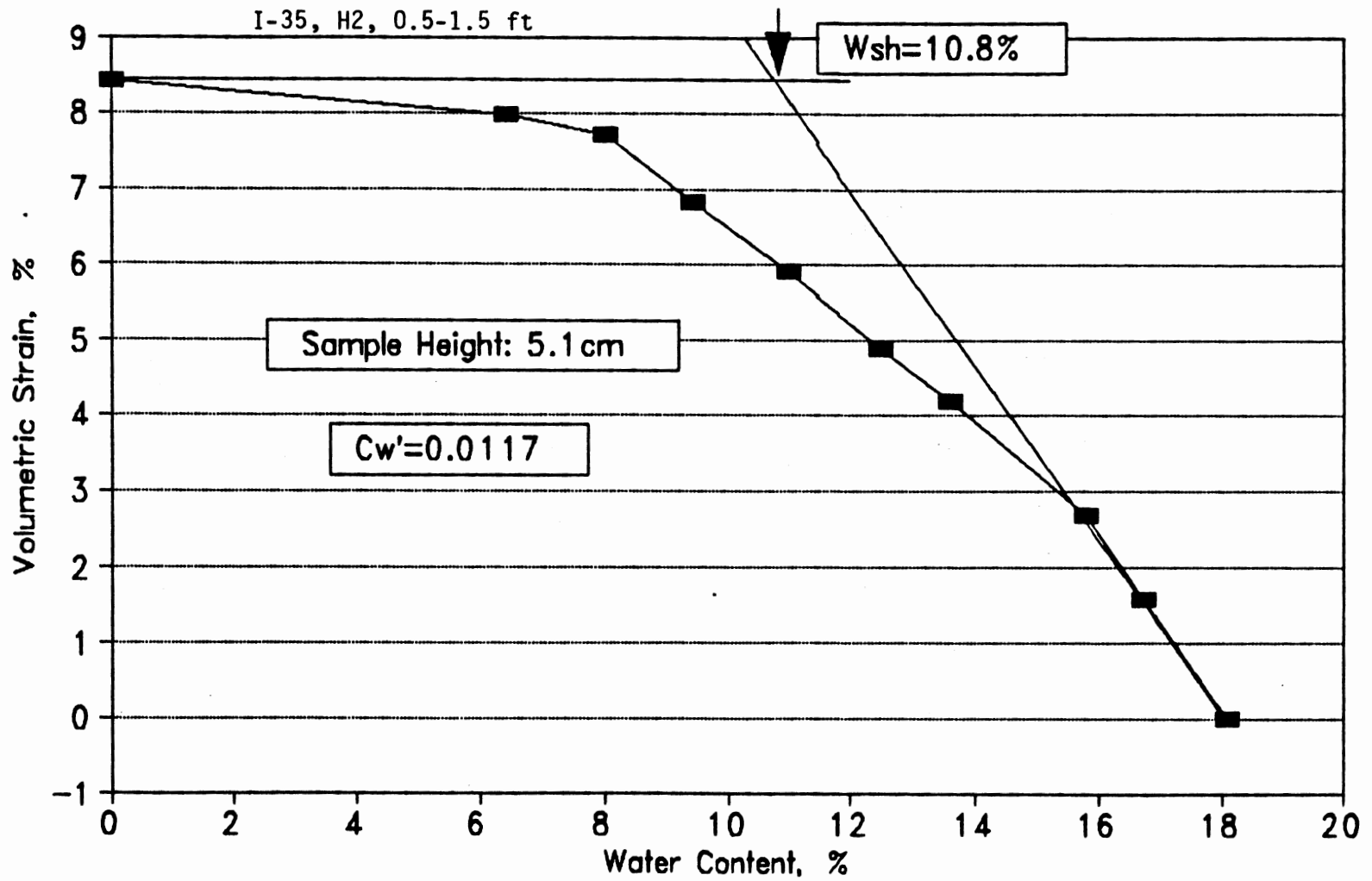
Figure B-3. (Continued)

TABLE B.2 (Continued)

W. Weight (grams)	Diameter (cm)	Height (cm)	w (%)	dD/D (%)	dH/H (%)	dV/V (%)
<u>Sample Dimension: Diameter = 7.3 cm, Height = 5.1 cm</u>						
<u>I-35, H2, 0.5-1.5 ft</u>						
435.7	7.30	5.09	18.1	0.00	0.00	0.00
430.7	7.25	5.08	16.7	0.68	0.20	1.56
427.3	7.23	5.05	15.8	0.96	0.79	2.68
419.2	7.21	5.00	13.6	1.23	1.77	4.18
415.1	7.19	4.99	12.5	1.51	1.96	4.90
409.5	7.18	4.95	11.0	1.64	2.75	5.92
403.7	7.16	4.93	9.4	1.92	3.14	6.82
398.5	7.14	4.91	8.0	2.19	3.54	7.72
392.7	7.13	4.91	6.4	2.33	3.54	7.98
369.0	7.12	4.90	0.0	2.47	3.73	8.42
<u>I-35, H2, 2.0-3.0 ft</u>						
443.5	7.25	5.10	19.3	0.00	0.00	0.00
439.1	7.20	5.04	18.1	0.69	1.18	2.53
436.0	7.15	5.01	17.2	1.38	1.76	4.46
429.3	7.09	4.95	15.4	2.21	2.94	7.18
426.1	7.07	4.93	14.6	2.48	3.33	8.07
421.4	7.02	4.89	13.3	3.17	4.12	10.10
416.2	6.99	4.86	11.9	3.59	4.71	11.42
411.4	6.94	4.84	10.6	4.28	5.10	13.04
404.6	6.91	4.81	8.8	4.69	5.69	14.32
371.9	6.89	4.80	0.0	4.97	5.88	15.00
<u>I-35, H2, 3.5-4.5 ft</u>						
463.1	7.33	5.10	16.2	0.00	0.00	0.00
458.9	7.27	5.05	15.1	0.82	0.98	2.59
455.9	7.24	5.02	14.3	1.23	1.57	3.97
449.7	7.22	4.98	12.8	1.50	2.35	5.26
446.7	7.20	4.96	12.0	1.77	2.75	6.16
442.5	7.16	4.92	11.0	2.32	3.53	7.95
438.2	7.14	4.91	9.9	2.59	3.73	8.65
434.2	7.12	4.90	8.9	2.86	3.92	9.35
428.9	7.09	4.90	7.6	3.27	3.92	10.11
398.7	7.09	4.89	0.0	3.27	4.12	10.29

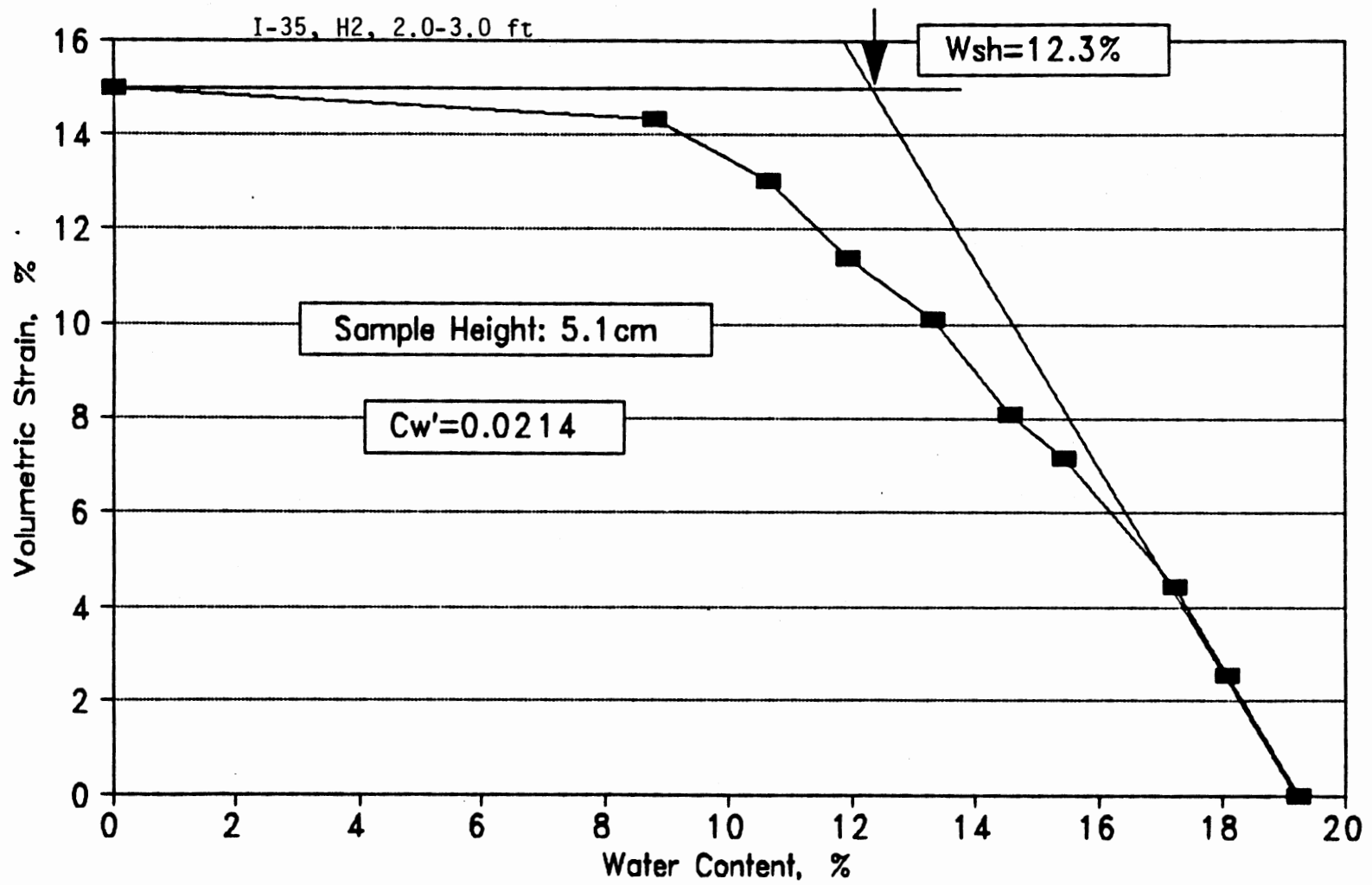
TABLE B.2 (Continued)

W. Weight (grams)	Diameter (cm)	Height (cm)	w (%)	dD/D (%)	dH/H (%)	dV/V (%)
<u>I-35. H2. 5.0-6.0 ft</u>						
461.7	7.30	5.10	14.6	0.00	0.00	0.00
457.8	7.28	5.08	13.7	0.27	0.39	0.94
454.6	7.27	5.06	12.9	0.41	0.78	1.60
448.3	7.24	5.02	11.3	0.82	1.57	3.18
445.2	7.23	5.02	10.5	0.96	1.57	3.45
440.8	7.21	5.02	9.4	1.23	1.57	3.98
436.3	7.20	5.01	8.3	1.37	1.76	4.44
432.1	7.19	5.01	7.3	1.51	1.76	4.70
426.9	7.18	5.00	6.0	1.64	1.96	5.16
402.8	7.18	5.00	0.0	1.64	1.96	5.16
<u>I-35. H2. 6.5-7.5 ft</u>						
466.3	7.31	5.10	14.1	0.00	0.00	0.00
462.6	7.27	5.09	13.2	0.55	0.20	1.29
459.5	7.25	5.06	12.4	0.82	0.78	2.41
453.4	7.23	5.03	10.9	1.09	1.37	3.52
450.3	7.21	5.03	10.2	1.37	1.37	4.05
446.0	7.19	5.01	9.1	1.64	1.76	4.96
441.6	7.18	5.01	8.0	1.78	1.76	5.23
437.4	7.16	5.00	7.0	2.05	1.96	5.94
432.1	7.15	4.99	5.7	2.19	2.16	6.39
408.7	7.14	4.99	0.0	2.33	2.16	6.65
<u>I-35. H2. 8.0-9.0 ft</u>						
463.6	7.30	5.10	14.7	0.00	0.00	0.00
460.0	7.29	5.09	13.8	0.14	0.20	0.47
456.7	7.27	5.08	13.0	0.41	0.39	1.21
450.0	7.25	5.04	11.3	0.68	1.18	2.53
446.5	7.24	5.03	10.5	0.82	1.37	2.99
441.8	7.24	5.01	9.3	0.82	1.76	3.37
436.4	7.23	5.00	8.0	0.96	1.96	3.83
431.1	7.21	4.99	6.7	1.23	2.16	4.55
424.9	7.20	4.95	5.1	1.37	2.94	5.58
404.2	7.20	4.95	0.0	1.37	2.94	5.58



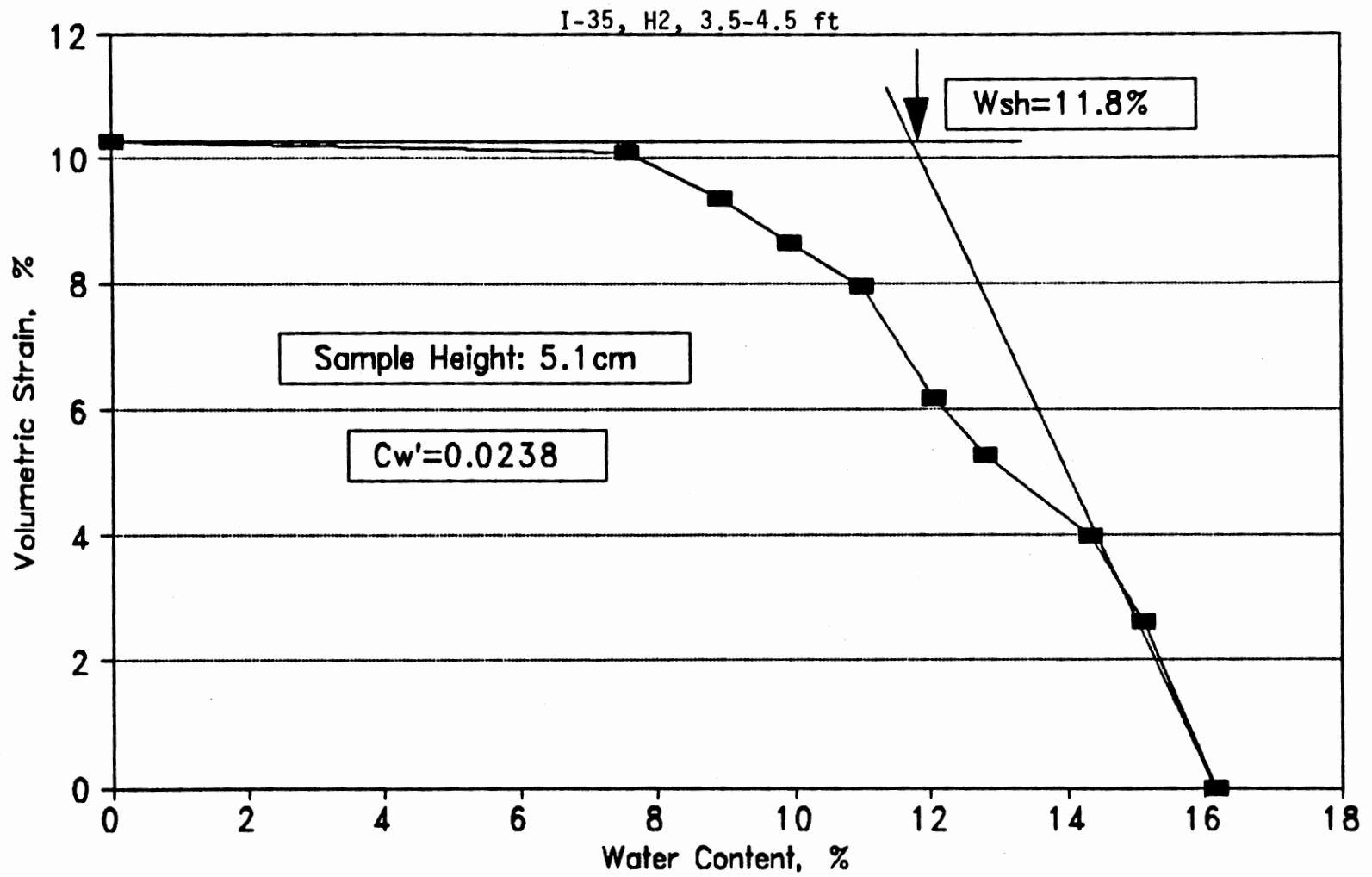
(a) Clod Shrinkage Curve

Figure B-3. (Continued)



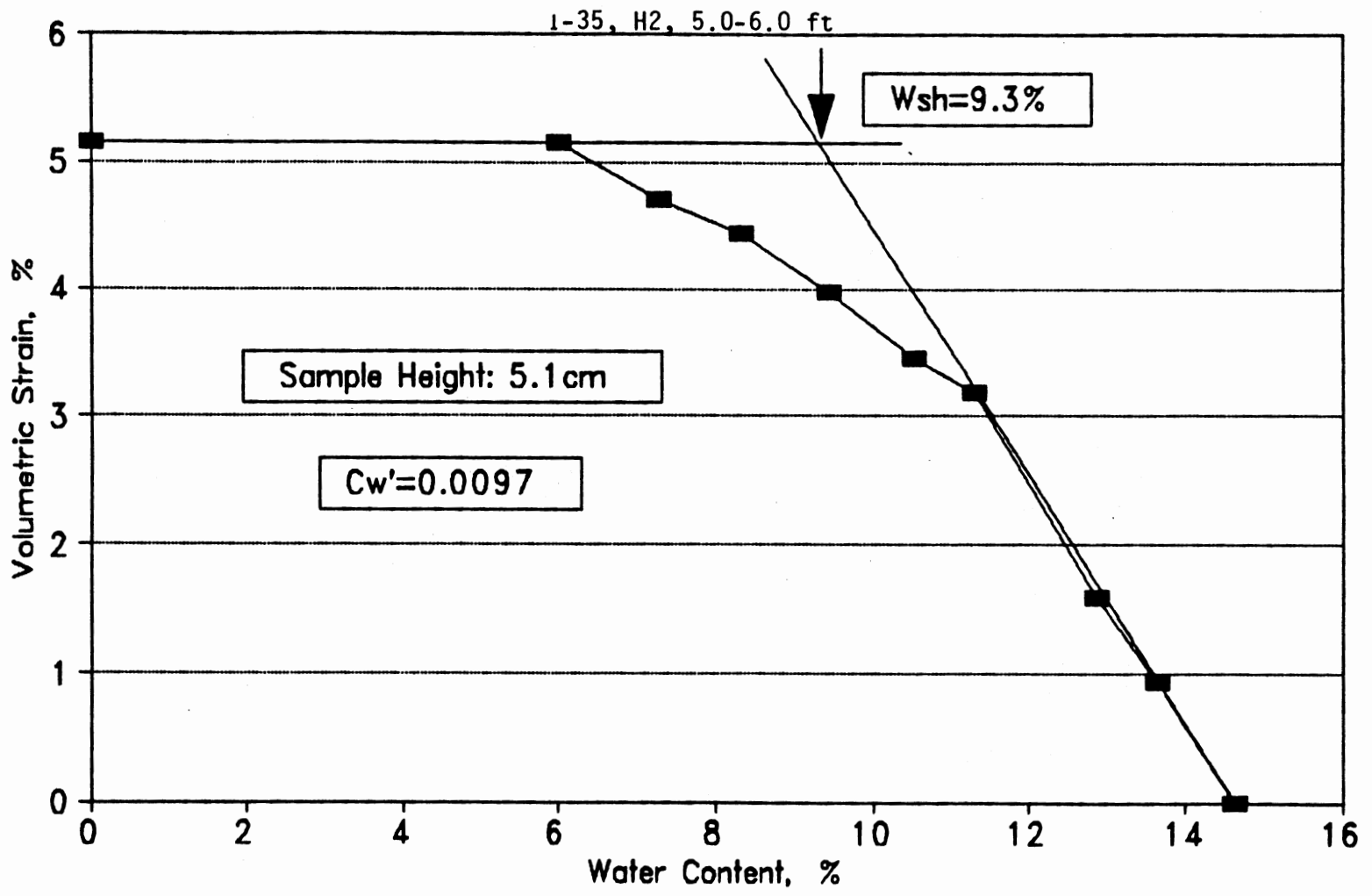
(a) Clod Shrinkage Curve

Figure B-3. (Continued)



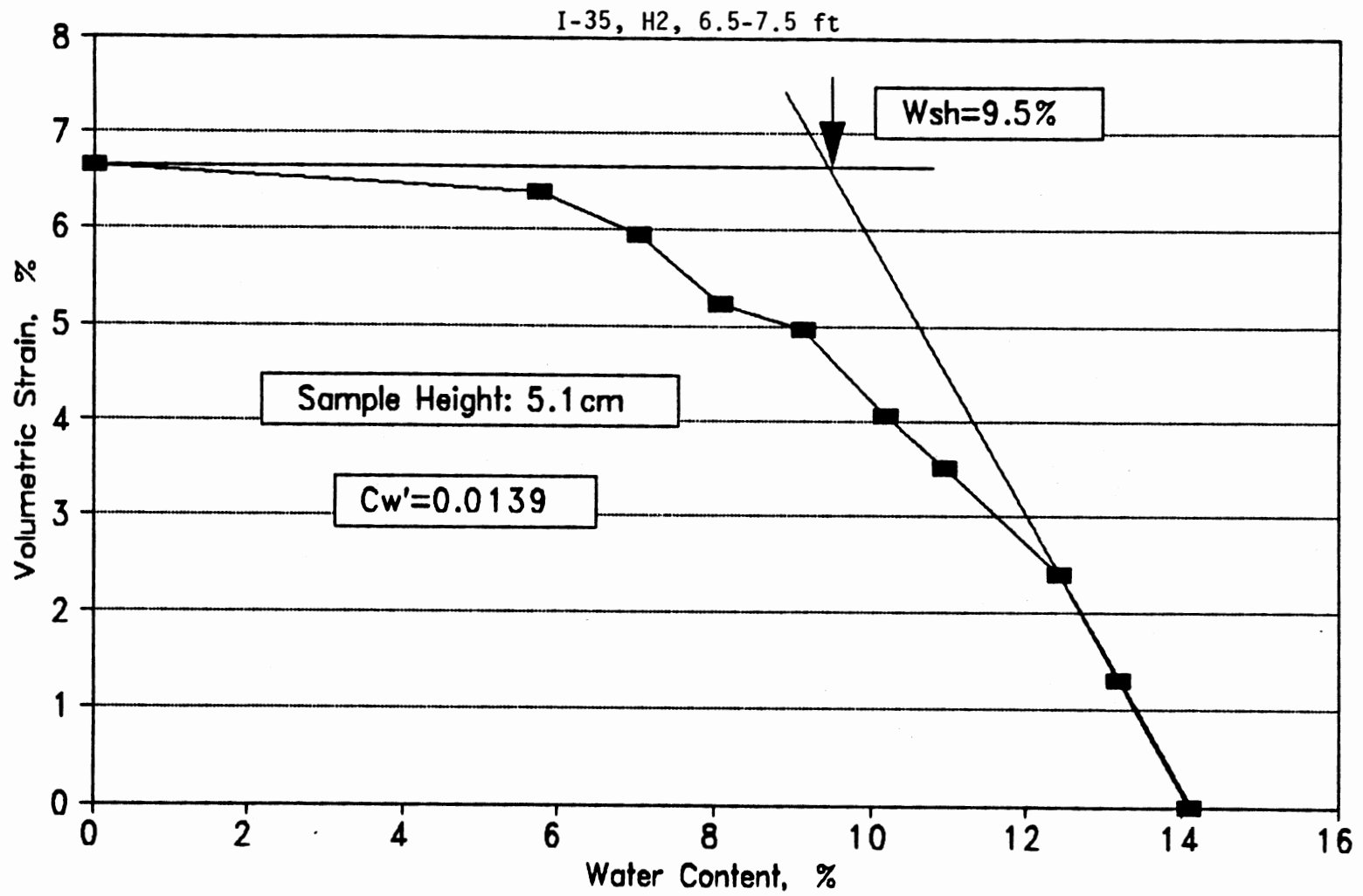
(a) Clod Shrinkage Curve

Figure B-3. (Continued)



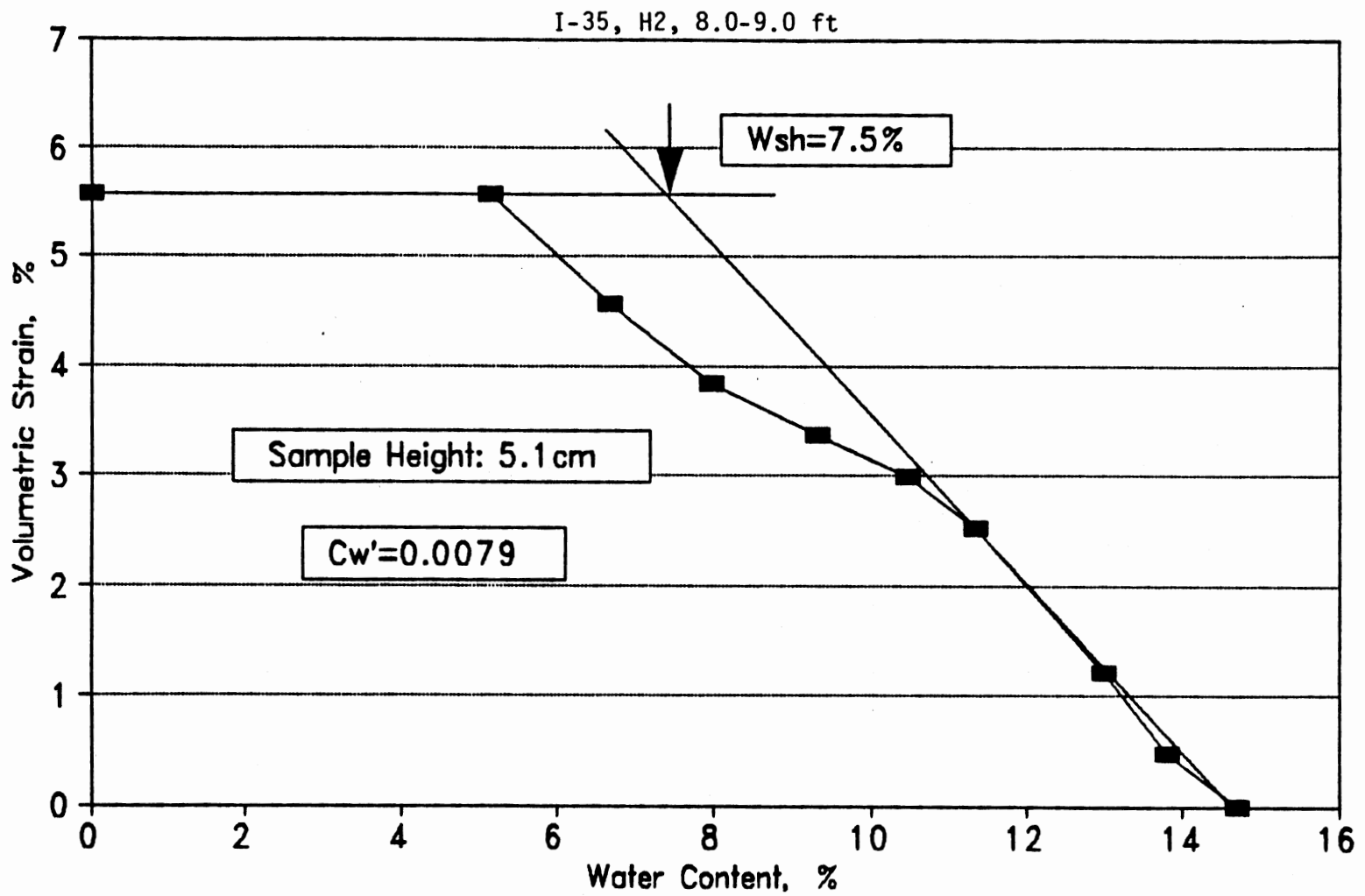
(a) Clod Shrinkage Curve

Figure B-3. (Continued)



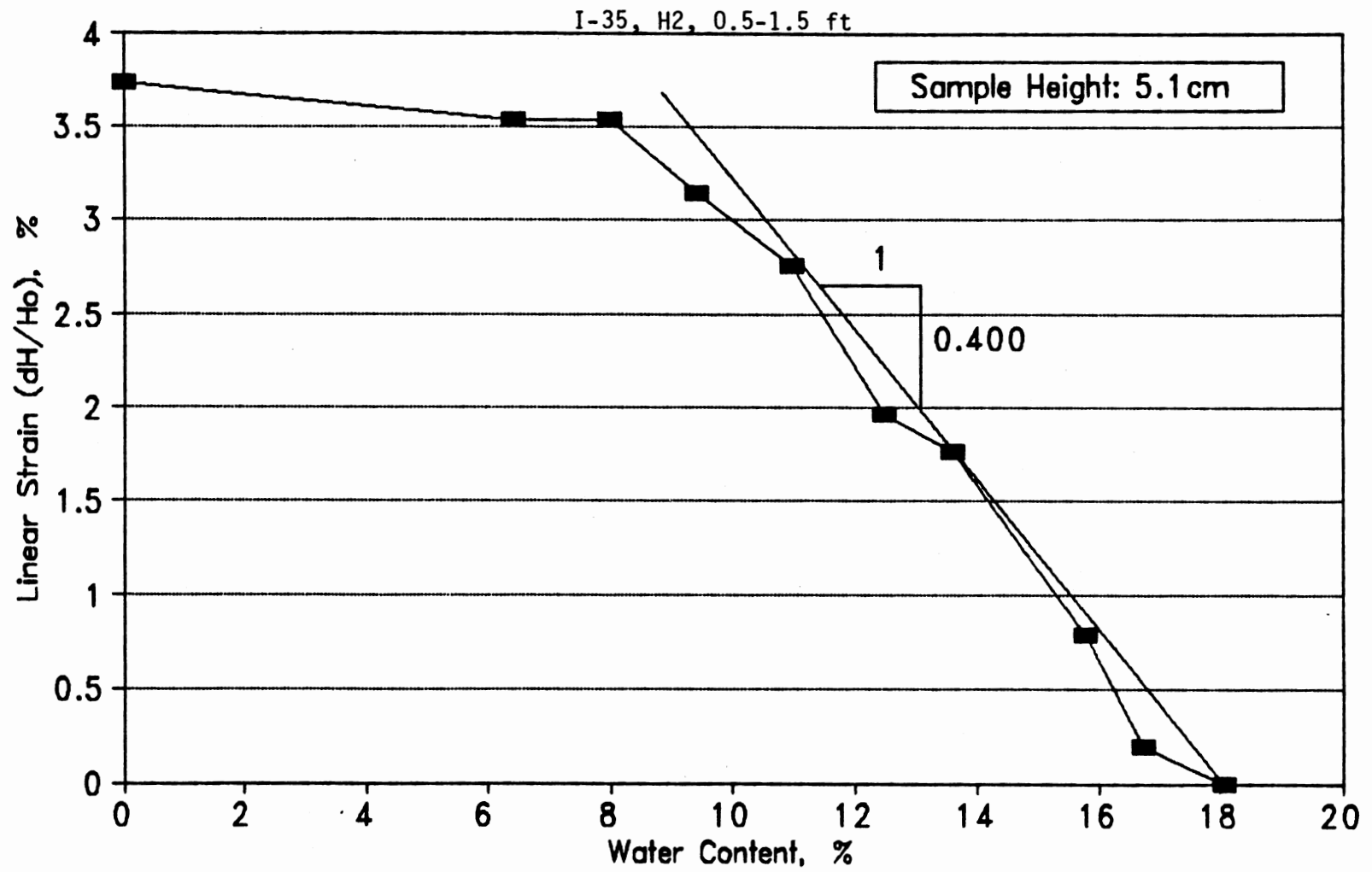
(a) Clod Shrinkage Curve

Figure B-3. (Continued)



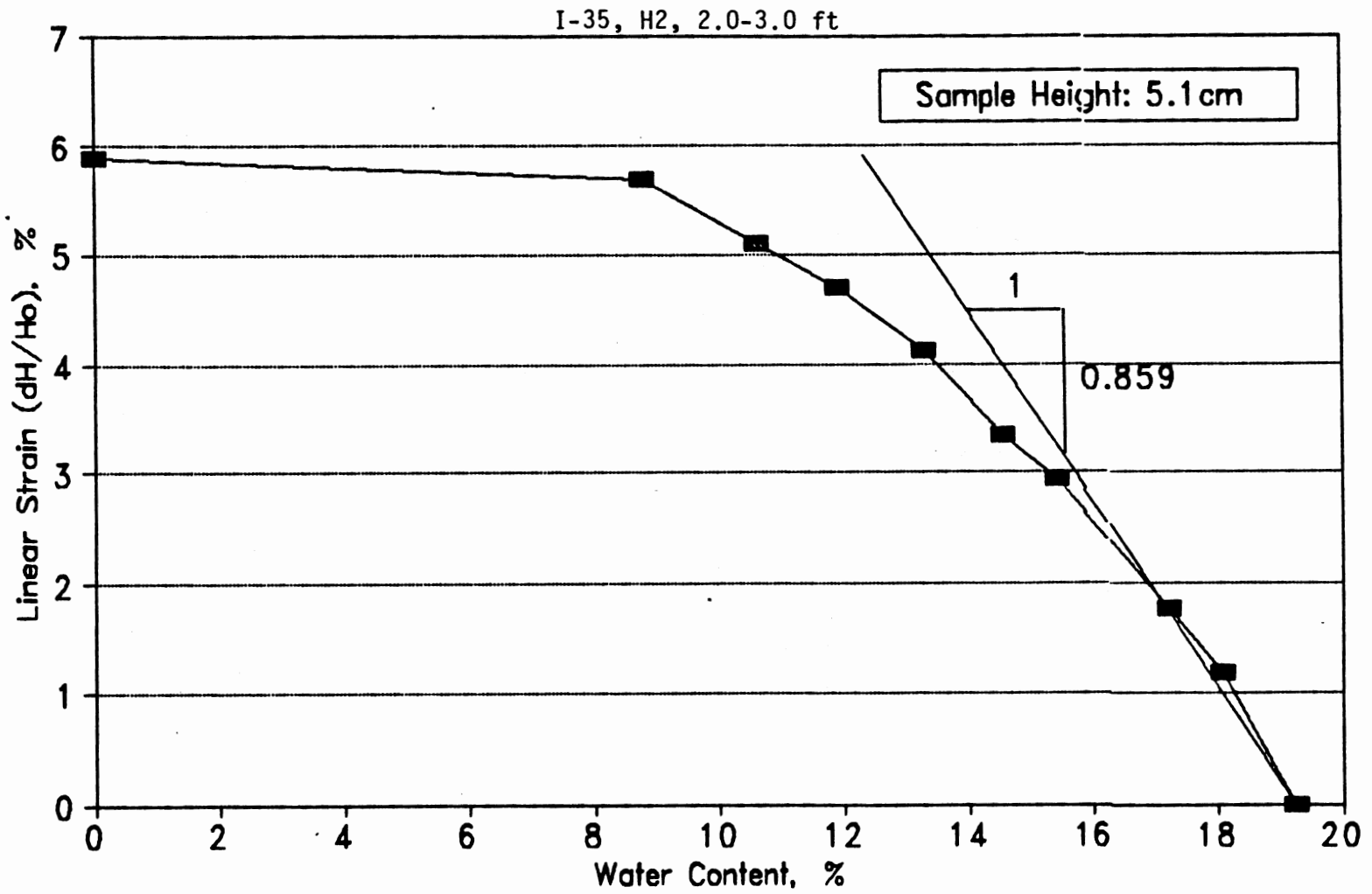
(a) Clod Shrinkage Curve

Figure B-3. (Continued)



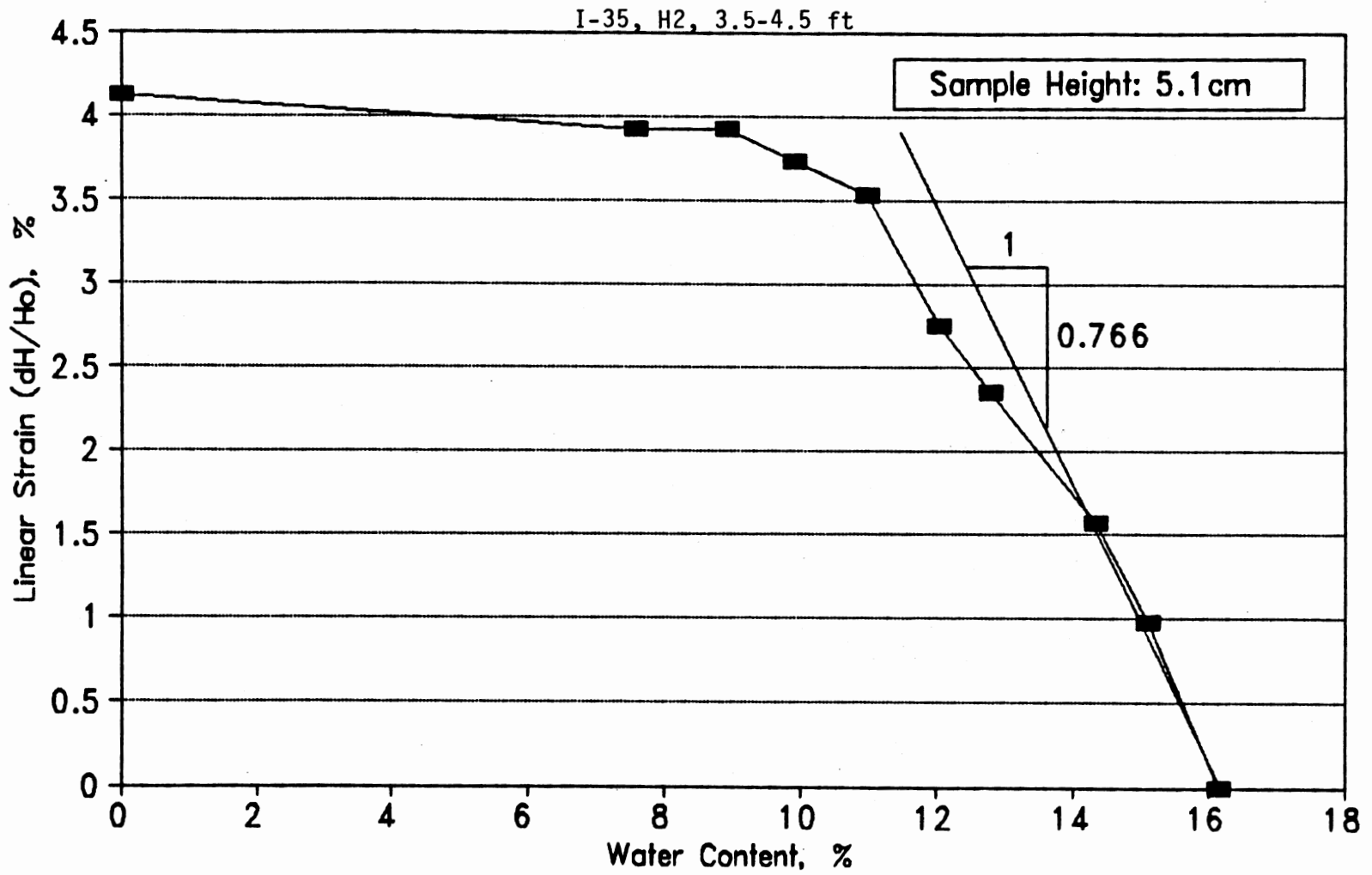
(b) Core Shrinkage Curve

Figure B-3. (Continued)



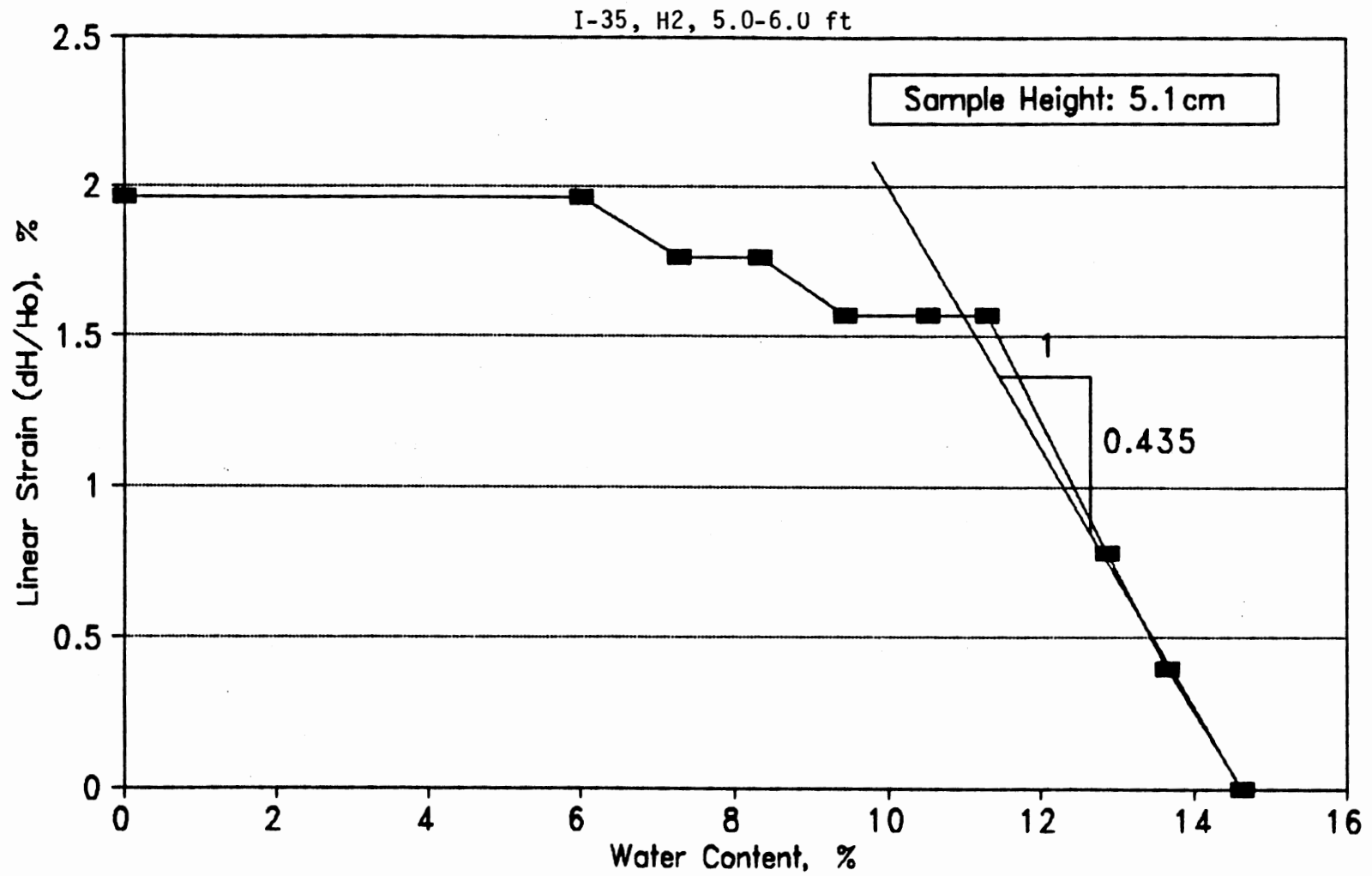
(b) Core Shrinkage Curve

Figure B-3. (Continued)



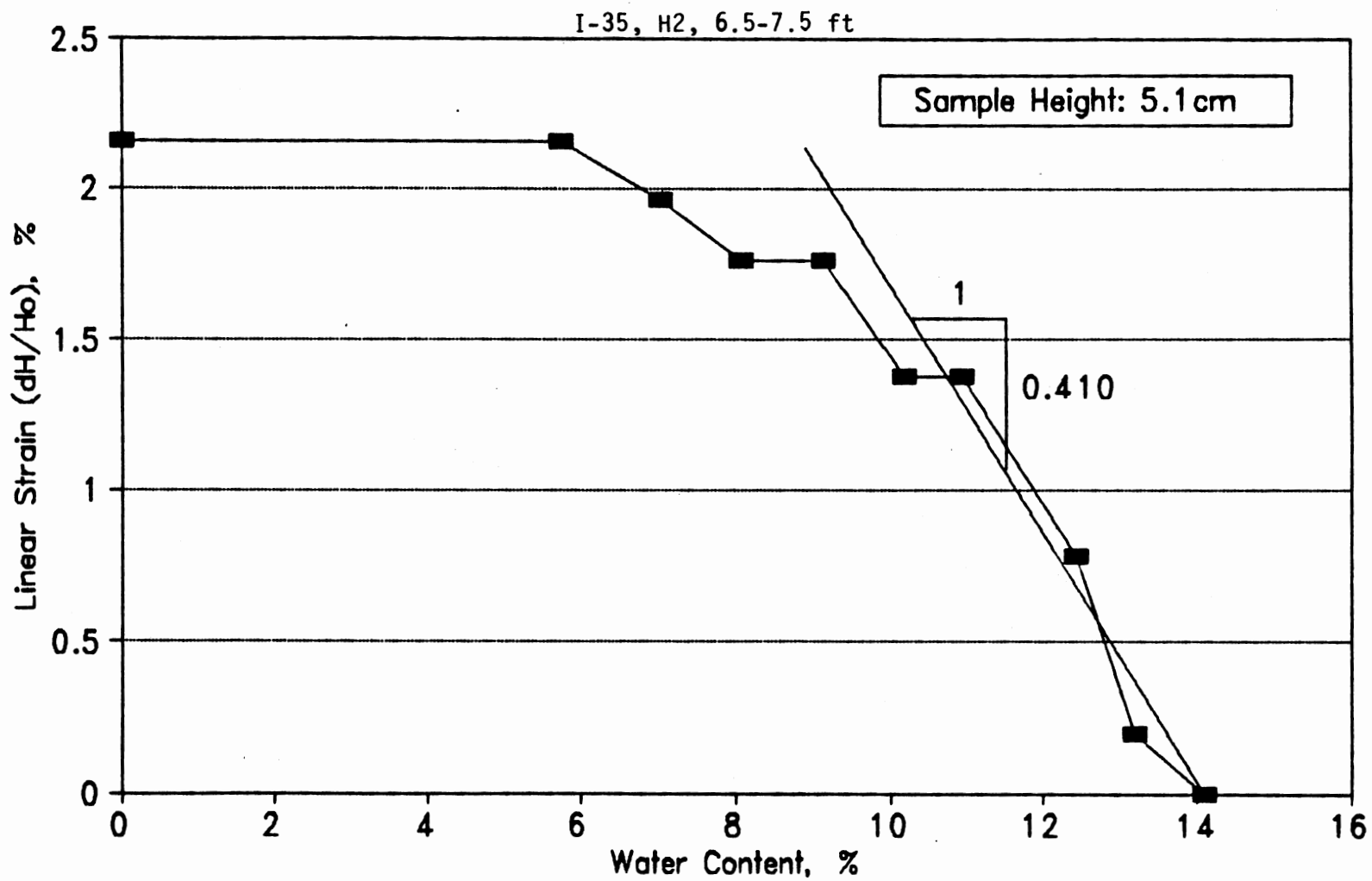
(b) Core Shrinkage Curve

Figure B-3. (Continued)



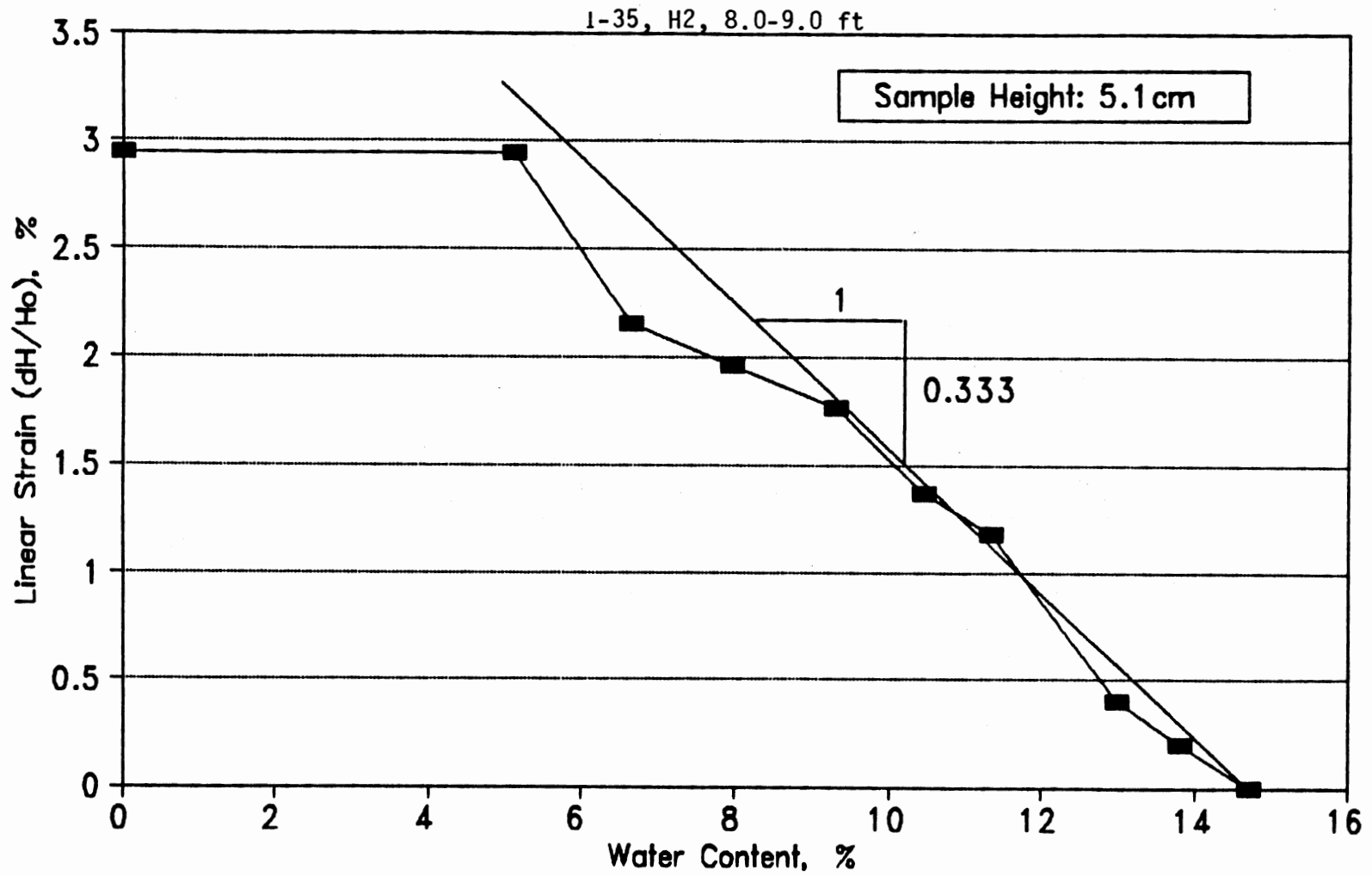
(b) Core Shrinkage Curve

Figure B-3. (Continued)



(b) Core Shrinkage Curve

Figure B-3. (Continued)



(b) Core Shrinkage Curve

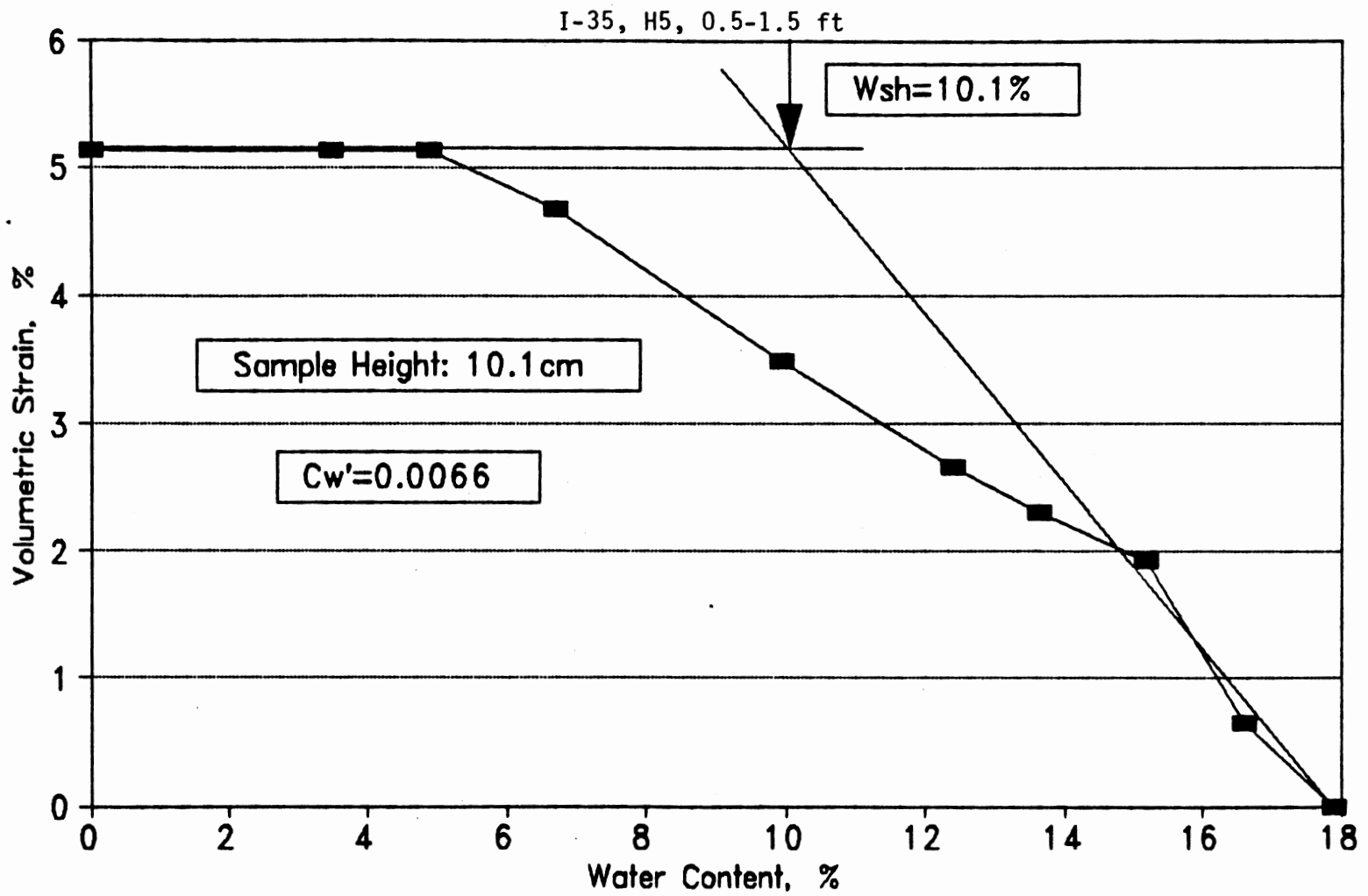
Figure B-3. (Continued)

TABLE B.2 (Continued)

W. Weight (grams)	Diameter (cm)	Height (cm)	w (%)	dD/D (%)	dH/H (%)	dV/V (%)
<u>Sample Dimension: Diameter = 7.3 cm. Height = 10.1 cm</u>						
<u>I-35. H2. 0.5-1.5 ft</u>						
856.2	7.30	10.13	17.9	0.00	0.00	0.00
846.8	7.28	10.12	16.6	0.27	0.10	0.65
836.5	7.24	10.10	15.2	0.82	0.30	1.93
825.3	7.23	10.09	13.6	0.96	0.39	2.30
816.3	7.22	10.08	12.4	1.10	0.49	2.66
798.3	7.20	10.05	9.9	1.37	0.79	3.49
774.9	7.17	10.01	6.7	1.78	1.18	4.67
761.7	7.16	9.99	4.9	1.92	1.38	5.13
751.4	7.16	9.99	3.5	1.92	1.38	5.13
726.2	7.16	9.99	0.0	1.92	1.38	5.13
<u>I-35. H2. 3.5-4.5 ft</u>						
907.2	7.28	10.06	16.2	0.00	0.00	0.00
899.2	7.24	10.00	15.2	0.55	0.60	1.69
890.2	7.22	9.97	14.0	0.82	0.89	2.52
880.7	7.21	9.95	12.8	0.96	1.09	2.99
873.8	7.19	9.92	11.9	1.24	1.39	3.81
859.9	7.18	9.89	10.1	1.37	1.69	4.37
841.5	7.15	9.84	7.8	1.79	2.19	5.65
828.3	7.14	9.83	6.1	1.92	2.29	6.01
817.5	7.13	9.82	4.7	2.06	2.39	6.37
780.8	7.12	9.81	0.0	2.20	2.49	6.72
<u>I-35. H4. 5.0-6.0 ft</u>						
913.3	7.30	10.10	14.5	0.00	0.00	0.00
903.5	7.28	10.05	13.2	0.27	0.50	1.04
893.7	7.23	10.00	12.0	0.96	0.99	2.88
883.7	7.21	10.00	10.8	1.23	0.99	3.42
876.2	7.21	10.00	9.8	1.23	0.99	3.42
861.6	7.20	9.99	8.0	1.37	1.09	3.78
843.7	7.20	9.99	5.7	1.37	1.09	3.78
833.3	7.20	9.99	4.4	1.37	1.09	3.78
824.4	7.20	9.98	3.3	1.37	1.19	3.88
797.9	7.19	9.98	0.0	1.51	1.19	4.14

TABLE B.2 (Continued)

W. Weight (grams)	Diameter (cm)	Height (cm)	w (%)	dD/D (%)	dH/H (%)	dV/V (%)
<u>I-35. H3. 6.5-7.5 ft</u>						
916.4	7.26	10.10	14.1	0.00	0.00	0.00
906.1	7.23	10.05	12.8	0.41	0.50	1.32
896.3	7.22	10.01	11.5	0.55	0.89	1.98
886.3	7.21	10.00	10.3	0.69	0.99	2.35
878.8	7.21	10.00	9.4	0.69	0.99	2.35
864.1	7.20	9.99	7.5	0.83	1.09	2.72
847.3	7.19	9.97	5.5	0.96	1.29	3.18
837.4	7.18	9.97	4.2	1.10	1.29	3.45
828.9	7.18	9.97	3.2	1.10	1.29	3.45
803.5	7.18	9.96	0.0	1.10	1.39	3.55
<u>I-35. H3. 8.0-9.0 ft</u>						
915.8	7.30	10.14	15.8	0.00	0.00	0.00
904.5	7.29	10.12	14.4	0.14	0.20	0.47
894.1	7.28	10.09	13.0	0.27	0.49	1.04
883.2	7.27	10.08	11.7	0.41	0.59	1.41
874.9	7.26	10.06	10.6	0.55	0.79	1.87
859.3	7.25	10.05	8.6	0.68	0.89	2.24
838.6	7.24	10.03	6.0	0.82	1.08	2.70
826.5	7.23	10.01	4.5	0.96	1.28	3.17
817.2	7.23	10.01	3.3	0.96	1.28	3.17
790.9	7.23	10.01	0.0	0.96	1.28	3.17



(a) Clod Shrinkage Curve

Figure B-3. (Continued)

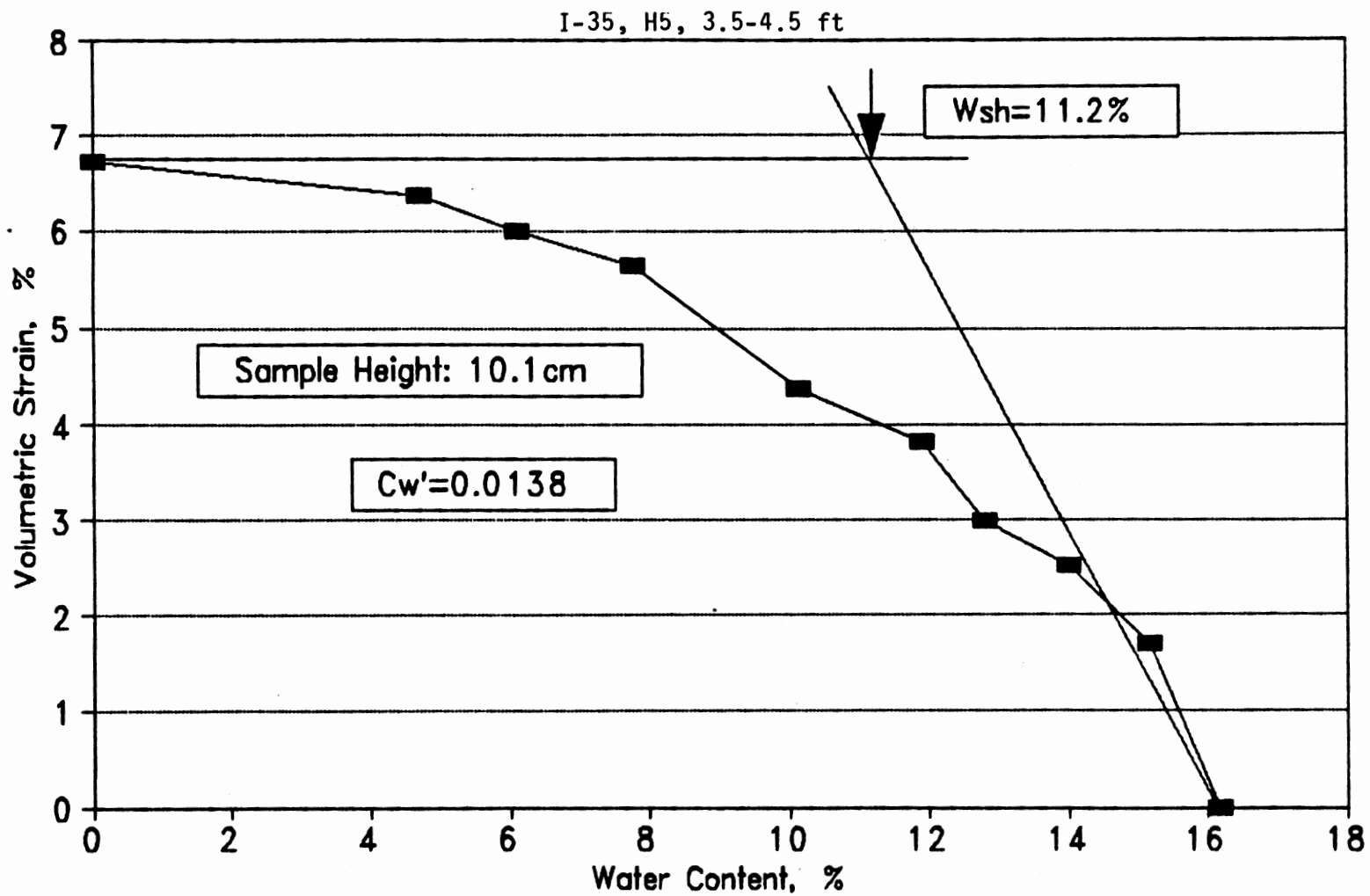
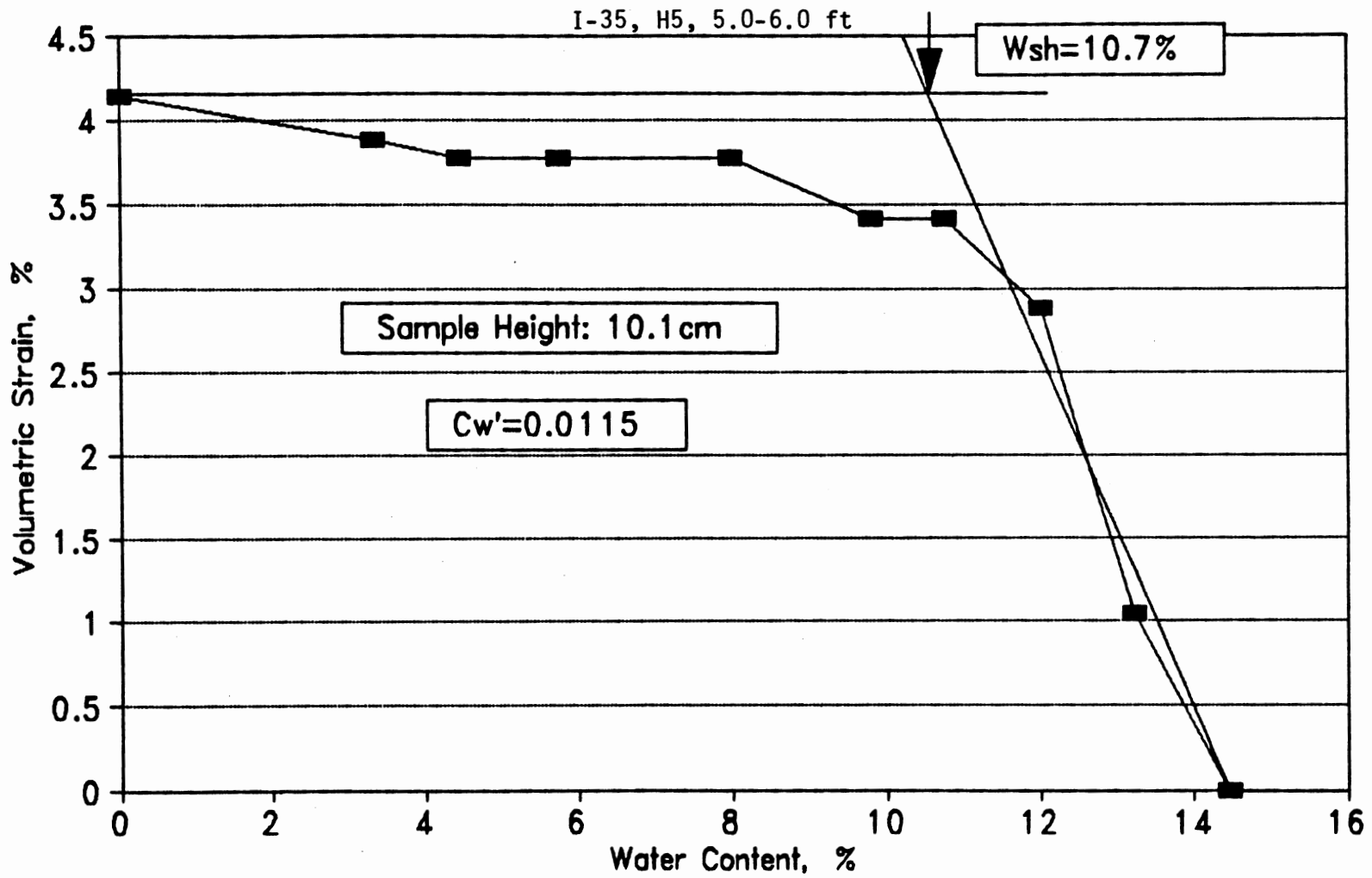
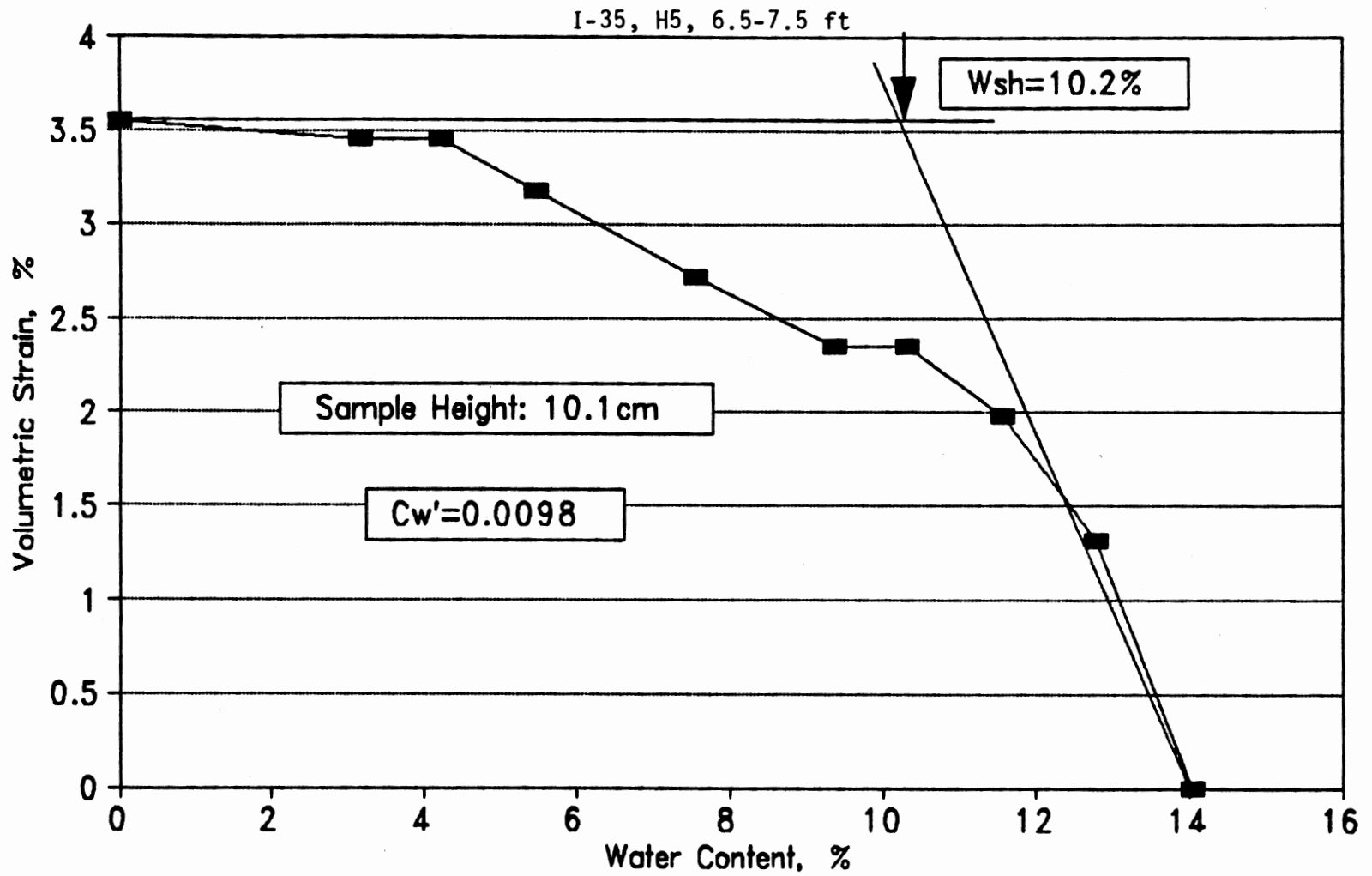


Figure B-3. (Continued)



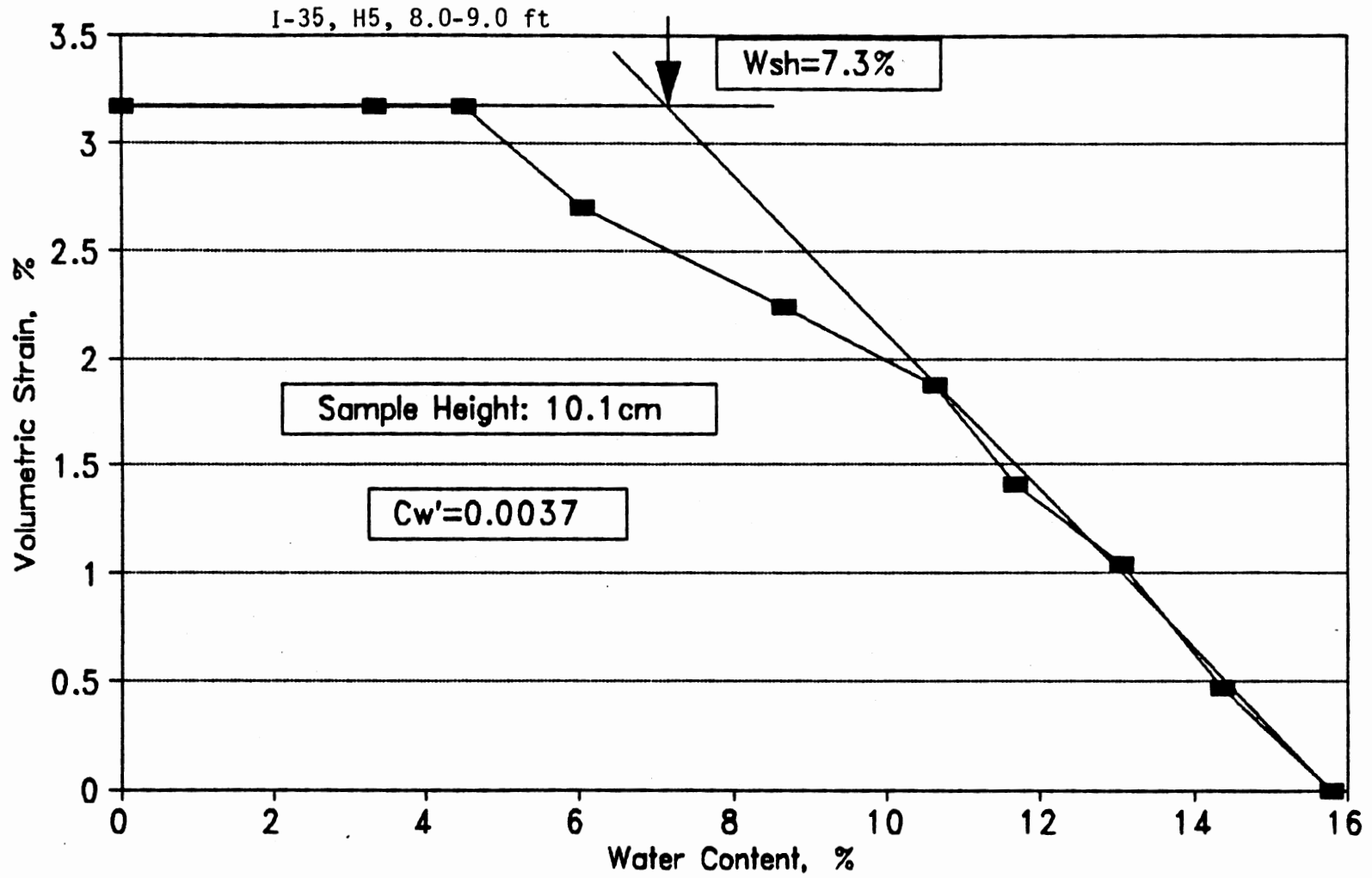
(a) Clod Shrinkage Curve

Figure B-3. (Continued)



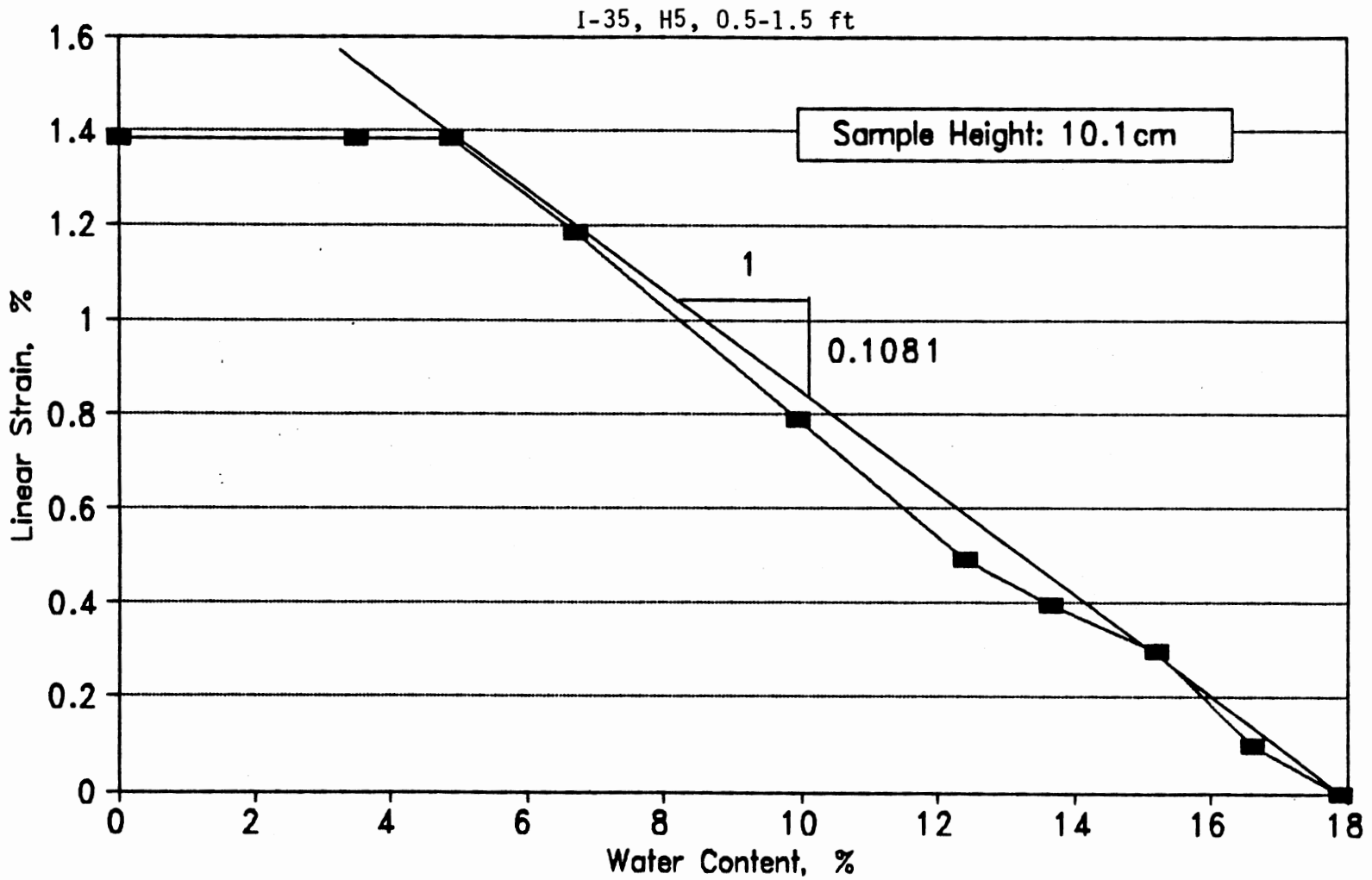
(a) Clod Shrinkage Curve

Figure B-3. (Continued)



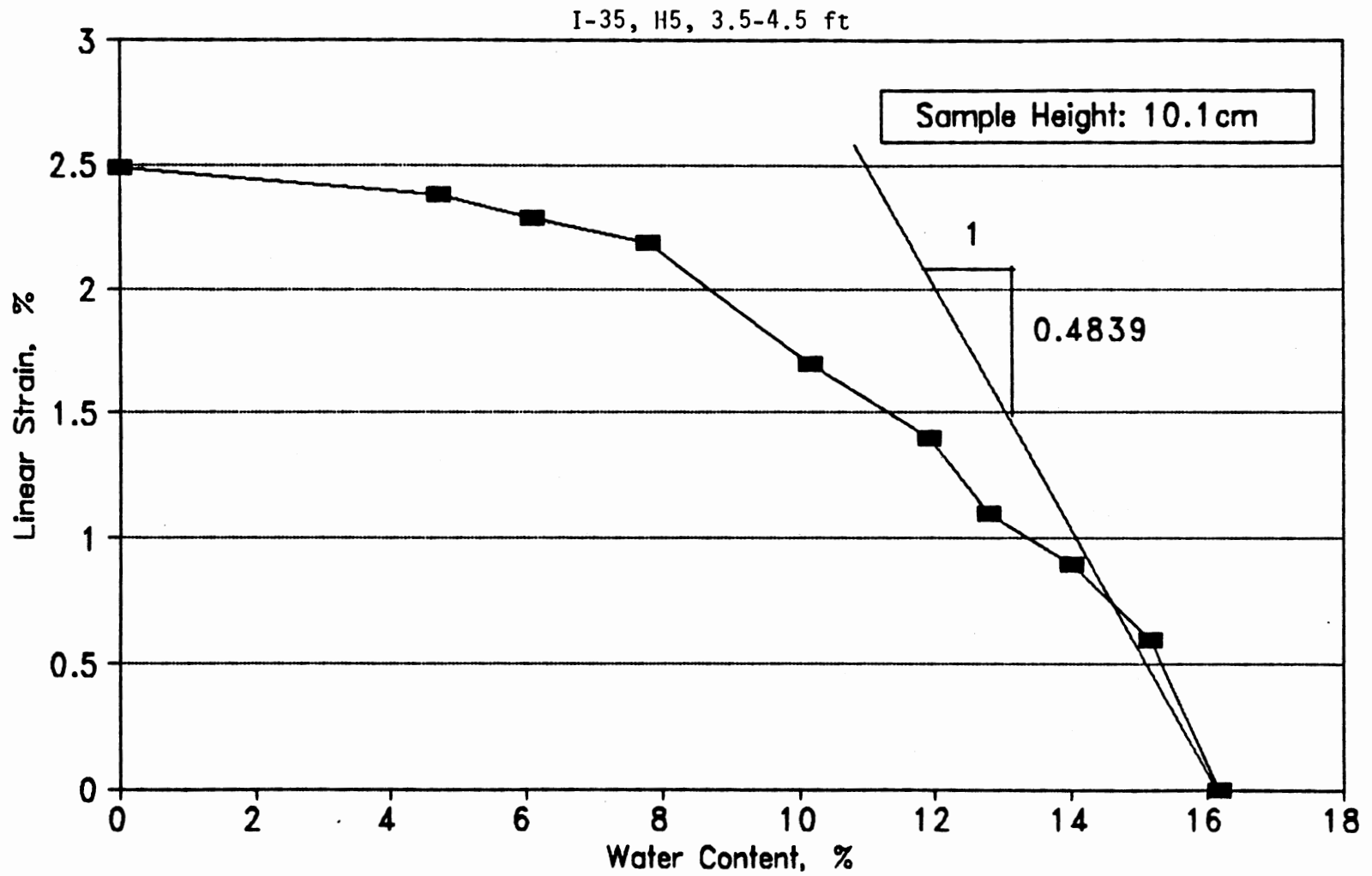
(a) Clod Shrinkage Curve

Figure B-3. (Continued)



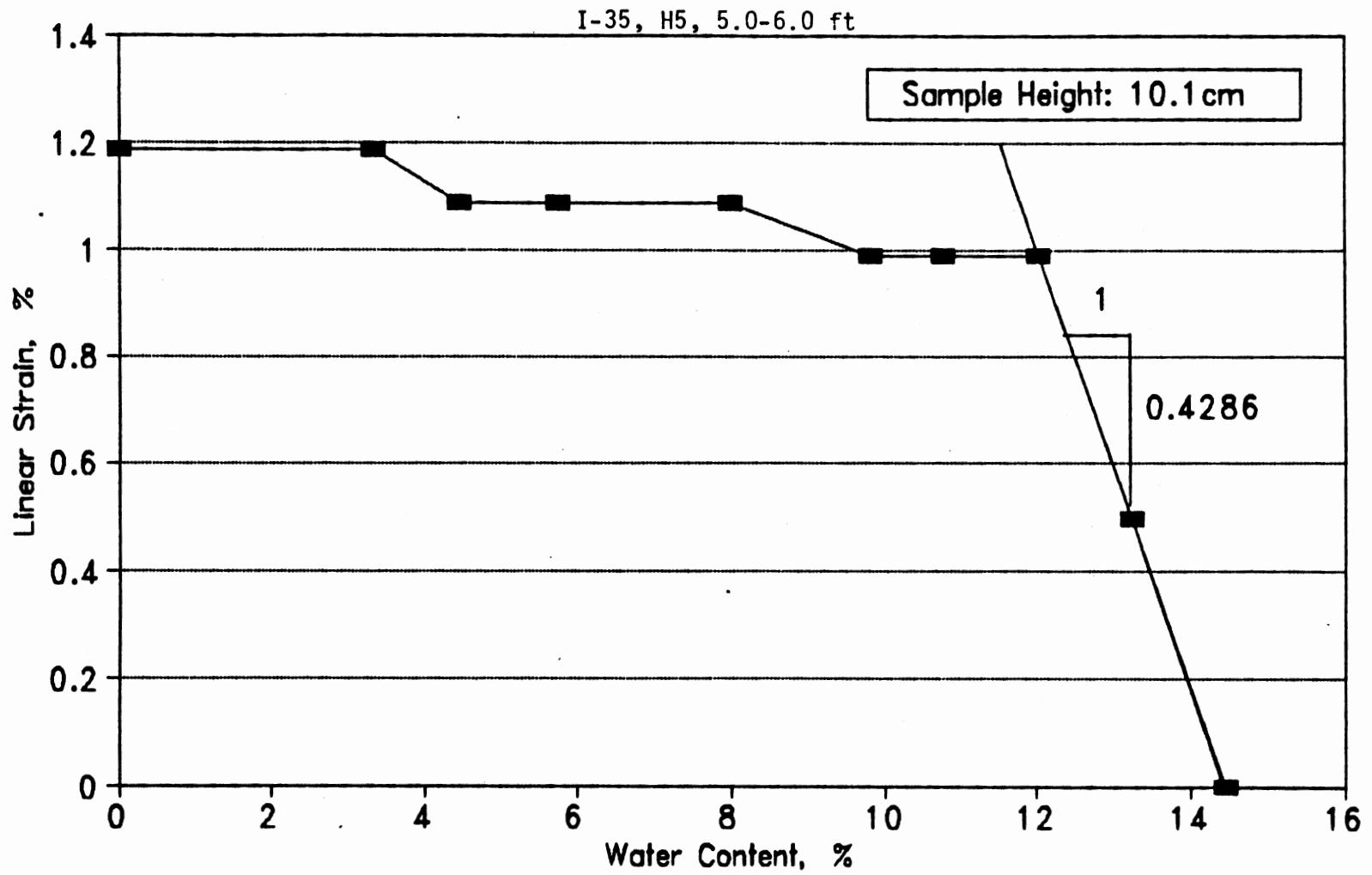
(b) Core Shrinkage Curve

Figure B-3. (Continued)



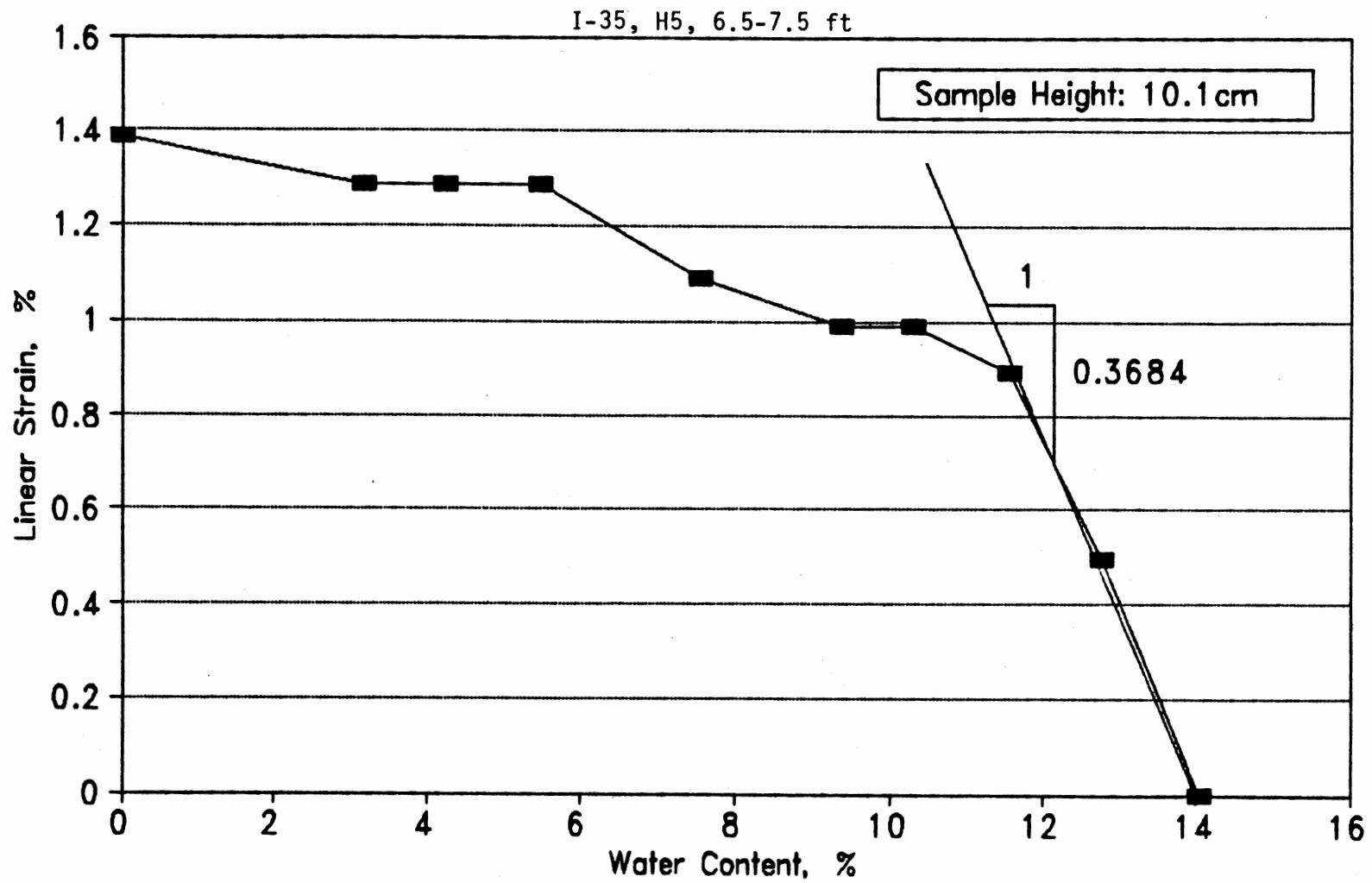
(b) Core Shrinkage Curve

Figure B-3. (Continued)



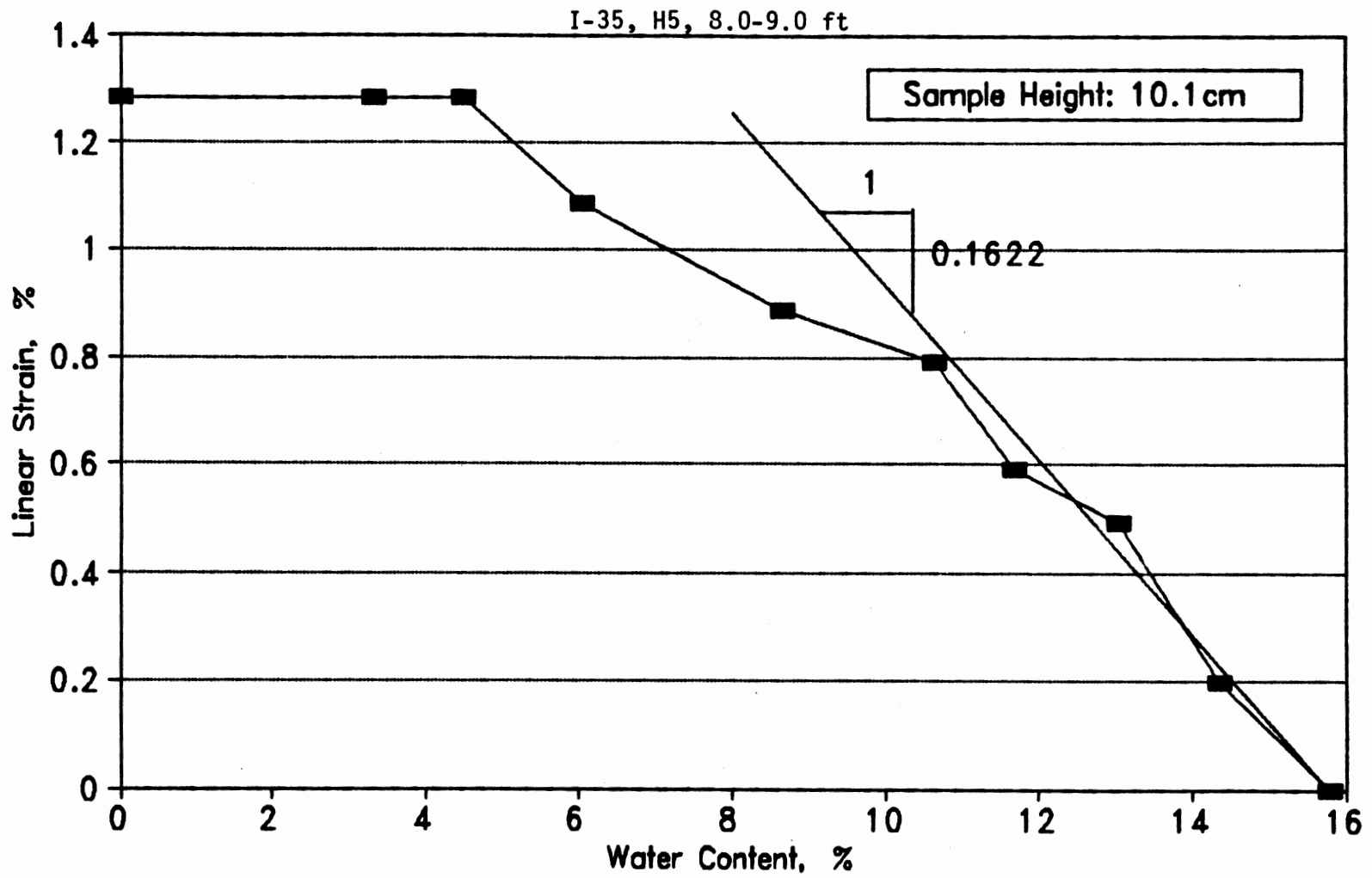
(b) Core Shrinkage Curve

Figure B-3. (Continued)



(b) Core Shrinkage Curve

Figure B-3. (Continued)



(b) Core Shrinkage Curve

Figure B-3. (Continued)

APPENDIX C

ELEVATION SURVEY DATA AND SITE PLAN

TABLE C.1
ELEVATION OF CENTER LINE FOR NORTHBOUND LANE

Station	Right E.O.P.		Left E.O.P.		Average	
	Planned	Measured	Planned	Measured	Planned	Measured
337986	948.97	949.30	949.34	949.38	949.16	949.34
337996	949.01	949.36	949.38	949.42	949.20	949.39
338006	949.05	949.35	949.42	949.39	949.24	949.37
338016	949.09	949.34	949.46	949.38	949.28	949.36
338026	949.13	949.26	949.50	949.33	949.32	949.30
338036	949.17	949.25	949.54	949.35	949.36	949.30
338046	949.21	949.22	949.58	949.43	949.40	949.33
338056	949.25	949.19	949.62	949.55	949.44	949.37
338066	949.29	949.24	949.66	949.62	949.48	949.43
338076	949.33	949.28	949.70	949.66	949.52	949.47
338086	949.37	949.30	949.74	949.69	949.56	949.50
338096	949.41	949.31	949.78	949.74	949.60	949.53
338106	949.45	949.31	949.82	949.79	949.64	949.55
338116	949.49	949.39	949.86	949.81	949.68	949.60
338126	949.53	949.44	949.90	949.87	949.72	949.66
338136	949.57	949.54	949.94	949.90	949.76	949.72
338146	949.61	949.66	949.98	949.94	949.80	949.80
338156	949.65	949.71	950.02	950.00	949.84	949.86
338166	949.69	949.76	950.06	950.10	949.88	949.93
338176	949.73	949.82	950.10	950.16	949.92	949.99
338186	949.77	949.84	950.14	950.25	949.96	950.05
338196	949.81	949.85	950.18	950.31	950.00	950.08
338206	949.85	949.91	950.22	950.35	950.04	950.13
338216	949.89	949.90	950.26	950.36	950.08	950.13
338226	949.93	949.81	950.30	950.37	950.12	950.09
338236	949.97	949.80	950.34	950.34	950.16	950.07
338246	950.01	949.80	950.38	950.30	950.20	950.05
338256	950.05	949.81	950.42	950.29	950.24	950.05
338266	950.09	949.88	950.46	950.28	950.28	950.08
338276	950.13	949.91	950.50	950.28	950.32	950.10
338286	950.17	949.98	950.54	950.31	950.36	950.15
338296	950.21	950.00	950.58	950.31	950.40	950.16
338306	950.25	949.95	950.62	950.35	950.44	950.15
338316	950.29	949.99	950.66	950.36	950.48	950.18
338326	950.33	950.07	950.70	950.40	950.52	950.24
338336	950.37	950.09	950.74	950.45	950.56	950.27
338346	950.41	950.11	950.78	950.49	950.60	950.30
338356	950.45	950.15	950.82	950.56	950.64	950.36
338366	950.49	950.16	950.86	950.58	950.68	950.37
338376	950.53	950.15	950.90	950.60	950.72	950.38
338386	950.57	950.15	950.94	950.65	950.76	950.40

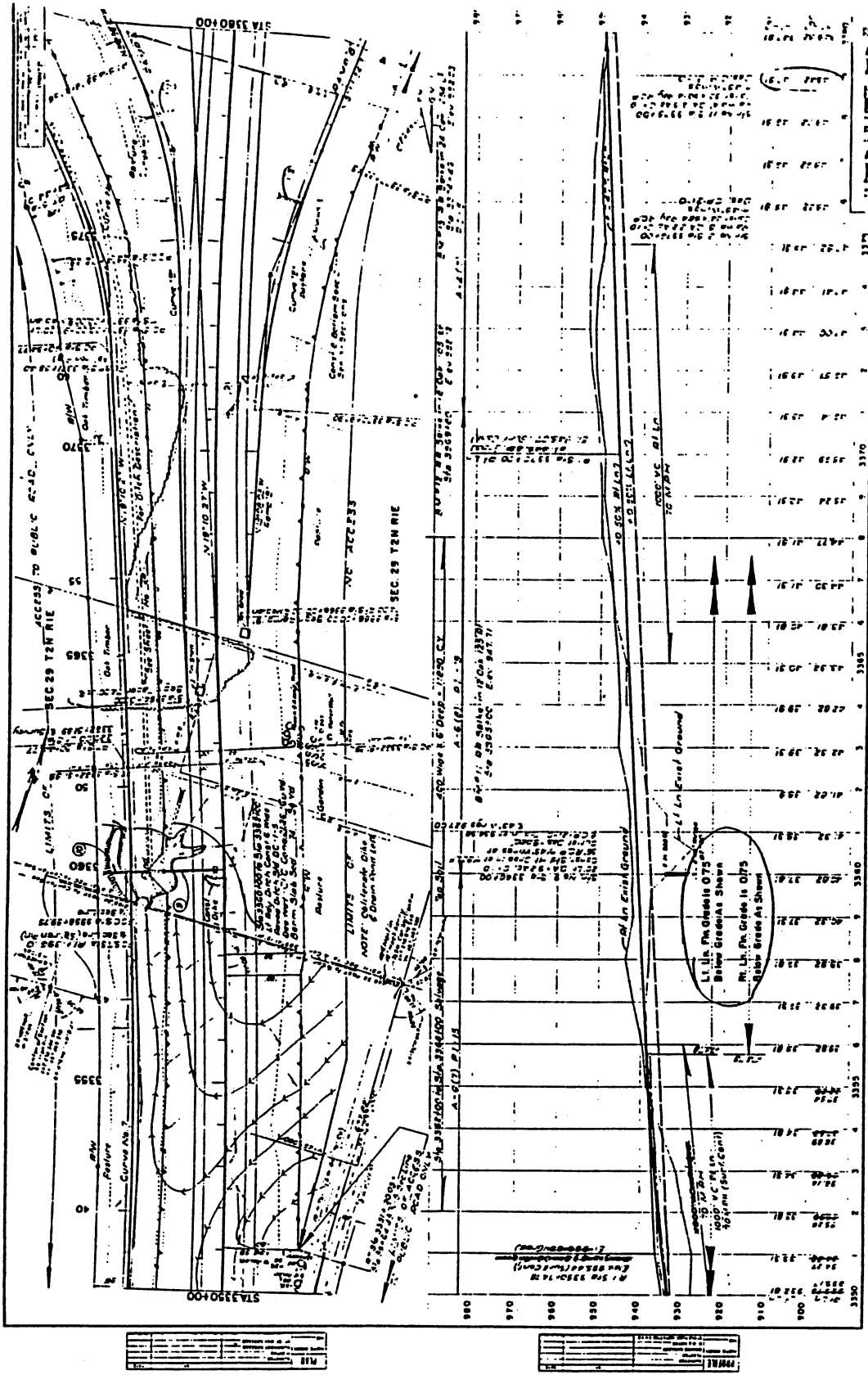


Figure C-1. Site Plan and Profile of Surveying Section

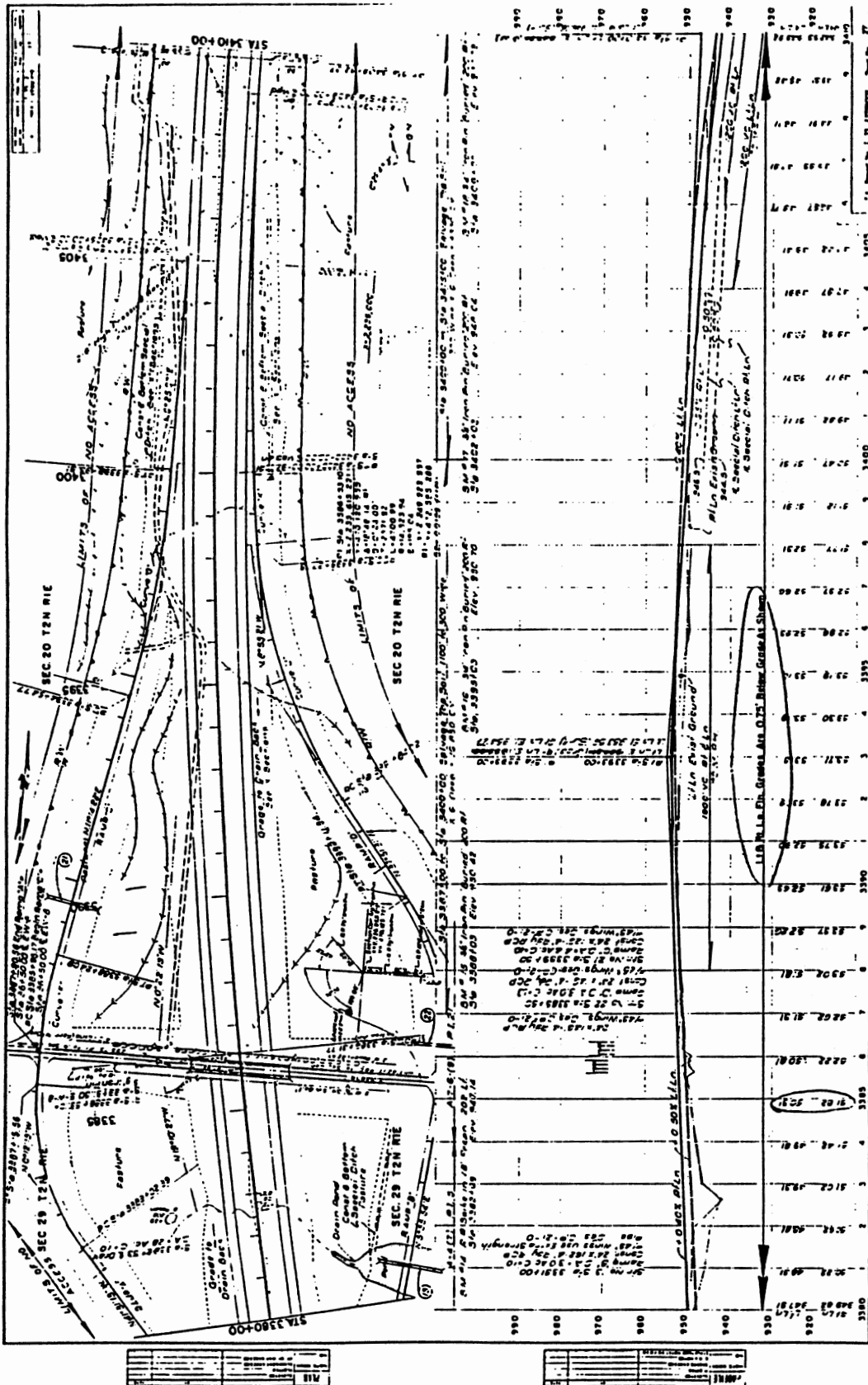


Figure C-1. (Continued)

VITA

Gang Huang

Candidate for the Degree of

Doctor of Philosophy

Thesis: EVALUATION OF GROUND HEAVE PREDICTION METHODS

Major Field: Civil Engineering

Biographical:

Personal Data: Born in Wuhan, People's Republic of China, June 30, 1959, the son of Mr. Shu-bin Huang and Mrs. Yi-min Tao.

Education: Graduated from Wuhan the 24th High School, Wuhan, P.R. China, in August, 1977; received the Bachelor of Science degree from Wuhan University of Hydraulic and Electric Engineering, Wuhan, P.R. China, in January, 1982, with a major in Civil Engineering; received the Master of Science degree from Wuhan University of Hydraulic and Electric Engineering in November, 1984, with a major in Civil Engineering; completed the requirements for the Doctor of Philosophy degree at Oklahoma State University in December, 1992.

Professional Experience: Graduate Research Assistant, Department of Civil Engineering, Wuhan University of Hydraulic and Electric Engineering, September, 1982, to November, 1984; Instructor, Department of Civil Engineering, Wuhan University of Hydraulic and Electric Engineering, November, 1984, to November, 1986; Research Associate and Research Assistant, Department of Civil Engineering, University of California at Los Angeles, November, 1986, to January, 1988; Graduate Teaching Assistant, Department of Civil Engineering, Oklahoma State University, August, 1988, to present.

Professional Societies: Student Member, American Society of Civil Engineering; Student Member, Chi Epsilon; E.I.T. (No.12005), Oklahoma.